INTERACTION OF ORGANOTIN MOIETIES WITH DNA AND NUCLEIC ACID CONSTITUENTS

Ph.D. THESIS

by
NAGAMANI KOMPELLI

**DEPARTMENT OF CHEMISTRY
INDIAN INSTITUTE OF TECHNOLOGY ROORKEE
ROORKEE - 247 667 (INDIA)
JUNE, 2015**

INTERACTION OF ORGANOTIN MOIETIES WITH DNA AND NUCLEIC ACID CONSTITUENTS

A THESIS

*Submitted in partial fulfilment of the
requirements for the award of the degree
of*

DOCTOR OF PHILOSOPHY
in
CHEMISTRY

by
NAGAMANI KOMPELLI

DEPARTMENT OF CHEMISTRY
INDIAN INSTITUTE OF TECHNOLOGY ROORKEE
ROORKEE-247 667 (INDIA)
JUNE, 2015

4.1. INTRODUCTION

In this chapter, synthesis, characterization, DNA binding studies along with the cleavage studies and cytotoxicity studies of mixed organotin complexes with guanosine (H_2GuO) (H represents proton; only used for clarity purpose) and 1,10-phenanthroline (phen), and enzyme assays of two selected complexes have been discussed. Synthesis and biological studies of titled complexes have not been reported till now. The literature reports on the organotin(IV) complexes of nucleotides have already been described in literature review of chapter **1**. The studied complexes are characterized *via* elemental analysis, molar conductance, and spectroscopic techniques such as IR, far-IR, NMR (^{1}H, ^{13}C, ^{119}Sn) spectroscopy. The binding affinity of the studied complexes with DNA has been investigated by using ultraviolet-visible (UV-Vis) and fluorescence spectroscopy. Results of cleavage experiments conducted using submarine agarose gel electrophoresis are also being discussed. Cytotoxicity profile of the titled complexes against human embryonic kidney (HEK293), mammary (MCF7), liver (HepG2), prostrate (DU145) and cervical (HeLa) cancer cell lines of human origin *via* MTT assay is screened and the IC_{50} values are determined. Only those organotin(IV) mixed ligand complexes having very high anti-tumor activity in MTT assay are selected, and *in vivo* DNA fragmentation studies, staining studies such as acridine orange/ethidium bromide (AO/EB) studies, comet assay, enzyme assays i.e., lipid peroxidase assay and lactate dehydrogenase assays have been carried out and discussed in detail in this chapter.

4.2. EXPERIMENTAL SECTION

4.2.1. Synthesis of Dimethyltin(IV) Derivative of Guanosine and 1,10-Phenanthroline (1)

An aqueous methanolic (20 mL, 1:1) solution of dimethyltin(IV) dichloride (0.220 g, 1.0 mmol) was stirred for half an hour. The resulting solution was added to the aqueous methanolic solution of guanosine (H_2GuO) (0.566 g, 2.0 mmol) (pH maintained at 2–3 by adding few drops of conc. HCl) and constantly stirred for ~ 20 h under nitrogen atmosphere. 1,10-phenanthroline (0.18 g, 1.0 mmol) in aqueous methanol (20 mL, 1:1) was added to the resulting solution and stirred for another ~ 3 h. The resulting product was chilled, filtered and washed with water-methanol or methanol-hexane mixture (1:3 v/v), and dried under vacuum.

4.2.2. Synthesis of Diphenyltin(IV) Derivative of Guanosine and 1,10-Phenanthroline (2)

Guanosine (0.566 g, 2.0 mmol) was dissolved in minimum amount (20 mL) of aqueous methanol (1:1 or 50%) under nitrogen. The pH of the solution was maintained at 2–3 by adding few drops of conc. HCl. To this was added an aqueous methanol (20 mL, 1:1) solution of diphenyltin(IV) dichloride (0.344 g, 1.0 mmol). The resulting solution was refluxed with constant stirring for ~ 20 h under nitrogen atmosphere. An aqueous methanolic (20 mL, 1:1) solution of 1,10-phenanthroline (0.18 g, 1.0 mmol) was added to the resulting solution and was refluxed for another ~ 3 h with constant stirring. After chilling, a pale red solid product thus obtained was washed with water and methanol-hexane or methanol-petroleum ether (b.p. 40–60 °C) mixture (1:3 v/v), and dried under vacuum.
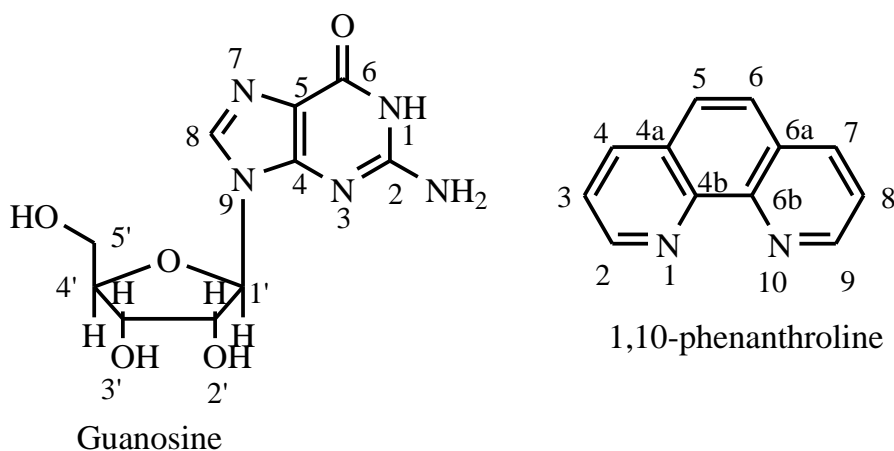

Fig. 4.1. Structure and numbering scheme of the ligands: guanosine (H$_2$GuO) and 1,10-phenanthroline.

4.2.3. Synthesis of Dibutyltin/Dioctyltin(IV) Derivatives of Guanosine and 1,10-Phenanthroline (3)/(4)

Dibutyltin/dioctyltin(IV) derivatives were prepared under nitrogen atmosphere by the drop-wise addition of aqueous methanolic (20 mL, 1:1) solution of dibutyltin (0.286 g, 1.0 mmol)/dioctyltin(IV) oxide (0.342 g, 1.0 mmol) to the aqueous methanolic (20 mL, 1:1) solution of guanosine (0.566 g, 2.0 mmol) at pH ~ 2–3. The reaction mixture obtained was refluxed with constant stirring for at least 20 h with simultaneous azeotropic removal of water. Further to this

solution, an aqueous methanolic (10 mL, 1:1) solution of 1,10-phenanthroline (0.18 g, 1.0 mmol) was added drop wise and refluxed for ~ 3 h with constant stirring. The solution was chilled, filtered and the solid product thus obtained was washed with water and methanol–hexane or methanol–petroleum ether (b.p. 40–60 °C) mixture (1:3 v/v), and dried under vacuum.

4.2.4. Synthesis of Triphenyltin(IV) Derivative of Guanosine and 1,10-Phenanthroline (5)

Similar procedure as described in section 4.2.2. has been adapted for the triphenyltin(IV) derivative, except triphenyltin chloride was used instead of diphenyltin dichloride, and varying the ratio of organotins and the ligands. Triphenyltin(IV) chloride (0.385 g, 1.0 mmol), guanosine (H_2GuO) (0.283 g, 1.0 mmol) and 1,10-phenanthroline (0.18 g, 1.0 mmol) were employed for the synthesis in the ratio of 1:1:1.

4.2.5. DNA Binding Studies

Absorption spectral titration experiments were performed in 10% DMSO/Tris–HCl buffer by diluting an appropriate amount of metal complex solution and DNA stock solutions while maintaining the total volume constant. The concentration of the complexes were maintained constant (2×10^{-5} M) and the DNA concentration ($2–20 \times 10^{-5}$ M) is varied, resulting in a series of solutions. Absorbance (A) was recorded with successive addition of CT DNA to both the compound solution and the reference solution to eliminate the absorbance of the DNA itself. The intrinsic binding constant K_b of the complex to CT DNA was determined from Eq. (4.3) through a plot of [DNA]/(e_a − e_f) vs [DNA], where [DNA] is the concentration of the DNA in base pairs; e_a, e_f and e_b, the apparent extinction coefficient (A_{obs}/M), the extinction coefficient for the free metal (M) and the extinction coefficient for the metal complex in the fully bound form, respectively [126–133]. In plots of [DNA]/(e_a − e_f) vs [DNA], K_b is given by the ratio of the slope to the intercept.

 Fluorescence spectral measurements were carried out by using Tris–HCl/NaCl buffer as a blank to make preliminary adjustments. The excitation wavelength was fixed and the emission range was adjusted before measurements. The fluorescence quenching constants 'K_{sv}' [126–131, 133] were obtained by titrating the fixed amount of ethidium bromide (EB)-bound CT DNA with increasing amount of metal complexes $(1 – 10) \times 10^{-5}$ M. An excitation wavelength of 263 nm was used and the total fluorescence emission was monitored at 603 nm. The measured

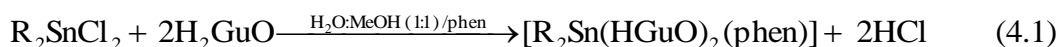fluorescence was normalized to 100% relative fluorescence.

4.2.6. Gel Electrophoresis

DNA cleavage experiments [126–133] executed using pBR322 plasmid DNA where the supercoiled DNA in buffer solution (5:50 mM Tris–HCl/NaCl, pH 7.2) was treated with different concentrations of complexes (5–50 μM, r = 1–20, where r = [complex]/[DNA]) and diluted with the buffer to a total volume of 10 μL. After incubating the samples at 37 °C for 2.5 h, loading buffer was added and were loaded onto agarose gel containing EB and run in 0.5X TBE buffer at 50 V/cm for 2 h. Bands were visualized and photographed.

4.3. RESULTS AND DISCUSSION

4.3.1. Synthetic Aspects

Reaction(s) of Me_2SnCl_2, Ph_2SnCl_2, Bu_2SnCl_2, Oct_2SnCl_2 (Eq. (4.1)) and Ph_3SnCl (Eq. (4.2)) with guanosine (H_2GuO) and 1,10-phenanthroline (phen) in aqueous methanol (50%) at 1:2:1/1:1:1, led to the formation of new mixed ligand complexes of general formulae, $[R_2Sn(HGuO)_2(phen)]$ and $[R_3Sn(HGuO)(phen)]$. All the complexes obtained are pale red solid and are stable towards air and moisture. In common organic solvents, they are insoluble but readily soluble in DMSO.

$$R_2SnCl_2 + 2H_2GuO \xrightarrow{\text{H}_2\text{O:MeOH (1:1)/phen}} [R_2Sn(HGuO)_2(phen)] + 2HCl \qquad (4.1)$$

(Where, R = Me, Ph, Bu, Oct; H_2GuO = Guanosine; phen = 1,10-phenanthroline)

$$R_3SnCl + H_2GuO \xrightarrow{\text{H}_2\text{O:MeOH (1:1)/phen}} [R_3Sn(HGuO)(phen)] + HCl \qquad (4.2)$$

(Where, R = Ph; H_2GuO = Guanosine; phen = 1,10-phenanthroline)

10^{-3} M solutions (in DMSO) of the synthesized complexes were used to measure the conductance, and the solvent's conductance values was deducted. The resultant values are in the range of 2–11 ohm^{-1} cm^2 mol^{-1}, which suggests that the complexes are non-electrolytic in nature.

Table 4.1. Characteristic Physical Properties and Analytical Data of Tri- and Diorganotin(IV) Derivatives of Guanosine and 1,10-Phenanthroline

Complex No.	Complex (Empirical Formula)	Color & Physical state	Yield (%)	Decomposition temperature (°C)	Analysis (%) Observed (Calculated)			
					C	H	N	Sn
1.	$[Me_2Sn(HGuO)_2(phen)]$ $(C_{34}H_{38}N_{12}O_{10}Sn)$	Pale red solid	42	210–212	44.95 (45.71)	4.62 (4.29)	18.26 (18.81)	13.43 (13.28)
2.	$[Ph_2Sn(HGuO)_2(phen)]$ $(C_{44}H_{42}N_{12}O_{10}Sn)$	Pale red solid	75	208–210	52.42 (51.94)	4.18 (4.16)	15.84 (16.52)	11.95 (11.66)
3.	$[Bu_2Sn(HGuO)_2(phen)]$ $(C_{40}H_{50}N_{12}O_{10}Sn)$	Pale reddish white solid	77	90–95 (sub.)	50.25 (49.14)	5.29 (5.16)	16.70 (17.19)	12.12 (12.14)
4.	$[Oct_2Sn(HGuO)_2(phen)]$ $(C_{48}H_{66}N_{12}O_{10}Sn)$	Pale reddish white solid	62	180–183	52.70 (52.90)	6.68 (6.10)	15.23 (15.42)	10.95 (10.89)
5.	$[Ph_3Sn(HGuO)(phen)]$ $(C_{50}H_{47}N_{12}O_{10}Sn)$	Pale red solid	94	150–152	54.56 (54.86)	4.26 (4.33)	15.48 (15.35)	10.59 (10.84)

Sub.: sublimation

4.3.2. IR and Far IR Spectroscopy

The characteristic IR and Far IR frequencies (cm^{-1}) of the titled complexes and ligands are presented in Table 4.2. In all the complexes, the ν(OH) (3465–3571 cm^{-1}) peaks are broadened. A negligible shift in ν(NH$_2$) (3115–3211 cm^{-1}) and ν(C=O) (1733 and 1694 cm^{-1}; except for complex (**1**), 1701and 1656 cm^{-1} are observed) frequencies of the nitrogen base unit is observed, indicating the non-involvement of base ring of guanosine moiety in complexation. A significant shift towards higher wave number for ν(C=N) at 1620 ± 6 cm^{-1} is observed. The C–H in plane deformation peaks corresponding to phenanthroline moiety are observed in the region 1250–1210 cm^{-1} and the ν(C–N) stretching frequency which is absent in phenanthroline spectrum is observed at 1226 ± 3 cm^{-1} attesting the ring deformation due to complex formation. The ν(C–O) stretching frequencies corresponding to ribose –OH of the guanosine moiety are observed in the range 1180–1046 cm^{-1}. A notable change in finger print region in comparison to the spectra of ligands is observed. Further, the ν(ring) characteristic of the ribose pucker (882–836 cm^{-1}) shows a considerable shift from that of the ligand suggesting that furanose –OH of guanosine may be involved in bonding with tin. The Sn–C bond frequencies in the ranges 584–560 cm^{-1} (ν_{as}(Sn–C)) and 549–524 cm^{-1} (ν_{s}(Sn–C)) for (**1**), (**3**) and (**4**) complexes and in the ranges 289–210 cm^{-1} (ν_{as}(Sn–C)) and 273–211 cm^{-1} (ν_{s}(Sn–C)) in far IR region of (**2**) and (**5**) complexes are observed. Further, the appearance of new ν(Sn–O) (510–446 cm^{-1}) and ν(Sn–N)/ ν(Sn←N) (366–335 cm^{-1}) bands indicate that the coordination occurs possibly *via* oxygen of guanosine moiety and nitrogen of phenanthroline moiety. The ring deformation peaks (427–409 and 262–239 cm^{-1}) of *o*-phenanthroline are appeared which clearly shows that a change in phenanthroline ring might have occurred due to bond formation.

4.3.3. NMR Spectroscopy

The ^{1}H, ^{13}C and ^{119}Sn NMR spectra of the complexes were recorded in DMSO-*d6* solvent and the data are presented in Tables 4.3, 4.4 and 4.5, respectively. Some representative ^{1}H, ^{13}C and ^{119}Sn NMR spectra of the titled complexes are presented in the Figs. 4.2, 4.3, 4.4, 4.5, 4.6 and 4.7. The chemical shift values of the protons and carbons of the ligands and the alkyl/phenyl groups attached to the tin atom are found to be consistent with the literature. The coupling of the alkyl protons with the tin nucleus results in the formation of satellites and the heteronuclear coupling constants ^2J [^{119}Sn-^1H] and ^1J [^{119}Sn-^{13}C] have been calculated from ^{1}H

and ^{13}C spectra, respectively. The $\angle C–Sn–C$ angles have been calculated with the help of ^2J $[^{119}Sn\text{-}^1H]$ and ^1J $[^{119}Sn\text{-}^{13}C]$ using Lockhart and Manders equation [123]. The N(1)H chemical shift of guanosine base moiety drifted downfield (δ 10.67–10.69 ppm) compared to that of the ligand. The H-8 (~ δ 7.95 ppm) and NH_2 (~ δ 6.45 ppm except for dibutyltin complex) showed almost negligible upfield shift, except a minor shift towards downfield is observed for complex **(5)** (δ 7.98 ppm, H-8). Similarly, a negligible shift is observed for H-1' proton, except for the splitting of the signal (J = ~ 6 Hz) due to the interaction of tin with the ribose sugar. One of the hydroxyl protons (OH-2') of furanose ring is absent in the complexes' spectra, which clearly indicates the coordination of tin to guanosine *via* the oxygen (O-2') of ribose sugar. The chemical shifts of (OH-3') and (OH-5') hydroxyl protons of the ribose sugar were broadened. All the furanose ring protons showed upfield shift along with the signals splitting due to the long-range heteronuclear coupling occurring due to the presence of the tin atom in the complexes, except the H-5' protons where a downfield shift is observed. The phenanthroline ring protons underwent downfield shift indicating that electron fluctuation might have occurred due to reorganisation to form new Sn-N (phen) bond. The alkyl/aryl-Sn resonances appeared in multiplet pattern, hence, ^2J $[^{119}Sn\text{-}^1H]$ could not be resolved except for complex **(1)** (dimethyltin(IV) complex) where the heteronuclear coupling constant ^2J $[^{119}Sn\text{-}^1H]$ is determined (111 Hz) and the C–Sn–C bond angle is calculated (θ = 163.16°). Similarly, in ^{13}C NMR, a negligible downfield shift is observed for all carbon atoms and ^1J $[^{119}Sn\text{-}^{13}C]$ value could not be determined, except the dimethyltin(IV) complex (^1J = 998.6 Hz, θ = 164.35°) which is also in accordance with the ^1H NMR data. In order to confirm the coordination and geometry around the tin nucleus, ^{119}Sn NMR spectrum is incumbent. All the complexes showed ^{119}Sn NMR chemical shifts in between δ −200 to −400 ppm, which may suggest an octahedral geometry around tin.

Table 4.2. IR and Far-IR Spectral Data of Tri- and Diorganotin(IV) Derivatives of Guanosine and 1,10-Phenanthroline in KBr (v/cm^{-1})

Ligand/ Complex	v(OH)/ v(NH$_2$)	v(C=O)/ v(C=N)	v(C=C)/ v(ring)	v(C–O)/ v(C–N)/ (C–H)$_{inplane}$	v outplane (ring)	v_{as}(Sn–C) /v_s(Sn–C)	v(Sn– O)/v(Sn– O– Sn)	v(Sn–N)/ v(Sn←N)	ring deform- ation
Guanosine[a]	3465 sbr, 3315 sbr, 3115 sbr	1733 s, 1688 s, 1638 s	1569 m, 1536 s, 1486 s, 1425 s, 1394 m, 1388 m	1130 s, 1085 m, 1045 w	838 w	–	–	–	–
1,10-phen- anthroline[c]	–	1618 s, 1589 s, 1560 s	1503 s, 1420 s	1250 br[*], 1125 br[*]	850 s	–	–	–	409 m, 259 w, 242 s
1,10-phen- anthroline[b]	–	1619 s, 1599 s	1502 s, 1416 s, 1345 sh	1210 w, 1137 w, 1090 w	849 s	–	–	–	–
1.	3483 sbr, 3371 sbr, 3144 sbr	1701 s, 1656 s, 1614 s	1482 s, 1371s	1252 m, 1166 s, 1004 mbr	836 w	580 sh, 530 m	475 m	364 w	412 m
2.	3564 sbr, 3466 sbr, 3328 sbr,	1731 s, 1694 s, 1624 s	1578 sh, 1537 s, 1484 s,	1250 sh, 1223 s, 1178 s,	850 s	289 s, 210 m	460 s	370 w	425 w, 262 s

Contd.

	3213 sbr		1427 s, 1393 m, 1344 m	1130 s, 1084 s, 1047 s					
3.	3571 sbr, 3465 sbr, 3324 sbr, 3207 sbr	1733 s, 1693 s, 1629 s	1573 s, 1537 s, 1487 s, 1426 s, 1397 s, 1342 s	1225 s, 1180 s, 1131 s, 1084s, 1046 s	855 s	581 s, 549 m	506 s	366 m	416 s
4.	3567 sbr, 3464 sbr, 3326 sbr, 3217 sbr	1730 s, 1693 s, 1627 s	1526 s, 1477 s, 1421 s, 1345 s	1227 s, 1180 s, 1132 s, 1036 s	861 s	584 s, 540 s	510 s	–	416 m
5.	3571 s, 3469sbr, 3323sbr, 3211 sbr	1733 s, 1694 s, 1627 m	1571 s, 1537 s, 1486 s, 1425 s, 1396 s, 1338 sh	1250 s, 1180 s, 1130 s, 1084 s, 1046 sh	883 s	273 s, 211 s	446 s	335 s	427 m, 260 sh, 243 s

[a] ref [37], [b] observed, [c] ref [28]; s = strong; br = broad; m = medium; sh = shoulder; w = weak. [*] both the bands merged together and appeared as a broad band.

Complex numbers as indicated in Table 4.1.

Table 4.3. ^{1}H NMR Spectral Data of Tri- and Diorganotin(IV) Derivatives of Guanosine and 1,10-Phenanthroline

Ligand/Complex	δ ppm (DMSO-*d6*)
Guanosine[a]	10.09 s, 1H (N1-H); 7.97 s, 1H (H-8); 6.50 s, 2H (NH$_2$); 5.70 s, 1H, (H-1'); 5.45 s, 1H (OH-2'); 5.20 s, 1H (OH-5'); 5.10 s, 1H (OH-3'); 4.40 s, 1H, (H-2'); 4.10 s, 1H, (H-3'); 3.90 s, 1H, (H-4'); 3.60, 3.48 s, 2H, (H-5').
1,10-phenanthroline[c]	8.81 s, 2H, (H-2, H-9); 8.00 s, 2H, (H-4, H-7); 7.55 s, 2H, (H-5, H-6) 7.26 s, 2H, (H-3, H-8).
1,10-phenanthroline[b]	9.17 s, 2H, (H-2, H-9); 8.76 s, 2H, (H-4, H-7); 8.44 s, 2H, (H-5, H-6) 7.26 s, 2H, (H-3, H-8).
1.	guanosine unit: 10.67 s, 2H (N1-H); 7.95s, 2H (H-8); 6.49 s, 4H (NH$_2$); 5.71 d, 2H, J = 6Hz (H-1'); 5.15 sbr, 5.07 sbr, 4H (OH-3',OH-5'); 4.40 q, 2H, J = 5.1 Hz (H-2'); 4.09 s, 2H, (H-3'); 3.87 q, 2H, J = 3.8 Hz (H-4'); 3.63–3.60 dd, 2H, J = 3.2 Hz and 3.54–3.51 dd, 2H, J = 9 Hz (H-5'); phenanthroline unit: 9.27 d, 2H, ^nJ = 3.5 Hz (H-2, H-9); 8.70 d, 2H, ^nJ = 8 Hz (H-4, H-7); 8.13 m, 2H (H-5, H-6); 7.98 m, 2H (H-3, H-8); Sn-methyl: 0.89 m, 6H, ^2J = 111 Hz, θ = 163.16°.
2.	guanosine unit: 10.64 s, 2H (N1-H); 7.94s, 2H (H-8); 6.40 s, 4H (NH$_2$); 5.69 d, 2H, J = 5.95 Hz (H-1'); 5.40 sbr, 2H (OH-3'); 5.09 sbr, 2H (OH-5'); 4.39 t, 2H, J = 5 Hz (H-2'); 4.08 t, 2H, J = 3.9 Hz (H-3'); 3.86 q, 2H, J = 3.7 Hz (H-4'); 3.62–3.59 dd, 2H, J = 3.9 Hz and 3.53–3.50 dd, 2H, J = 3.8 Hz (H-5'); phenanthroline unit: 9.32 d, 2H, ^nJ = 1.5 Hz (H-2, H-9); 8.70 s, 2H (H-4, H-7); 7.98 m, 2H (H-5, H-6); 7.84 s, 2H (H-3, H-8); Sn-phenyl: 8.15-8.58 m, 4H, (H-β); 7.27–7.50 m, 6H (H-γ, H-δ).
3.	guanosine unit: 10.67 s, 2H (N1-H); 7.96s, 2H (H-8); 6.48 sbr, 4H (NH$_2$); 5.69 d, 2H, J = 6Hz (H-1'); 5.42 d, 2H, J = 6Hz (OH-3'); 5.15 d, 2H, J = 4.6Hz (OH-5'); 4.40 dd, 2H, J = 5.7 Hz (H-2'); 4.08 dd, 2H, J = 4.5 Hz (H-3'); 3.87 dd, 2H, J = 3.6 Hz (H-4'); 3.61 dd, 2H, J = 4.65 Hz and 3.5 (H-5'); phenanthroline unit: 9.37 d, 2H, ^nJ = 3.5 Hz (H-2, H-9); 8.82 d, 2H, ^nJ = 7.4 Hz (H-4, H-7); 8.21 t, 2H, ^nJ = 11.5 Hz (H-5, H-6); 8.08 dd, 2H, ^nJ = 4.6 Hz (H-3, H-8); Sn-butyl: 1.52-1.40 m, 4H, (H-α); 1.35-1.29 m, 4H, (H-β); 1.10–1.03 m, 4H (H-γ); 0.66–0.33 t, 6H, J = 7.3 Hz (H-δ).

Contd.

4.	guanosine unit: 10.69 s, 2H (N1-H); 7.95s, 2H (H-8); 6.49 s, 4H (NH$_2$); 5.70 d, 2H, J = 6Hz (H-1'); 5.50–5.0 s br,4H, (OH-3',OH-5'); 4.40 t, 2H, J = 5.5 Hz (H-2'); 4.09 t, 2H, J = 4 Hz (H-3'); 3.87 q, 2H, J = 3.5 Hz (H-4'); 3.63–3.59 dd, 2H, J = 4 Hz and 3.54 d, 2H, J = 4 Hz (H-5'); phenanthroline unit: 9.4 d, 2H, ^nJ = 3.5 Hz (H-2, H-9); 8.9 d, 2H, ^nJ = 7 Hz (H-4, H-7); 8.26 s, 2H (H-5, H-6); 8.14 q, 2H, ^nJ = 3.7 Hz (H-3, H-8); Sn-octyl: 1.29-1.30 m, 4H, (H-α); 1.42-1.39 m, 4H, (H-β); 1.13–1.07 m, 4H (H-γ); 0.97 m, 16H (H-δ, H-f, H-g, H-h); 0.75–0.72 t, 6H, J = 15.5 Hz (H-i).
5.	guanosine unit: 10.69 s, 1H (N1-H); 7.98 s, 1H (H-8); 6.50 sbr, 2H (NH$_2$); 5.70 d, 1H, J = 5.95 Hz (H-1'); 5.60−4.90 br, 2H (OH-5' and OH-3'); 4.39 t, 1H, J = 5.4 Hz (H-2'); 4.08 t, 1H, J = 4.2 Hz (H-3'); 3.88–3.85 q, 1H, J = 3.75 Hz (H-4'); 3.62–3.59 dd, 1H, J = 4.0 Hz and 3.53–3.50 dd, 1H, J = 4.0 Hz (H-5'); phenanthroline unit: 9.21 d, 2H, ^nJ = 2.95 Hz (H-2, H-9); 8.8 d, 2H, ^nJ = 8.0 Hz (H-4, H-7); 8.22–8.13 m, 2H (H-5, H-6); 8.02–7.99 m, 2H (H-3, H-8); Sn-phenyl: 7.87–7.79 m, 6H (H-β); 7.44–7.38 m, 9H (H-γ, H-δ).

[a] ref [37], [b] observed data, [c] ref [28], [*] numberring of carbons and protons are as mentioned in Fig. 4.1.; s = singlet; d = doublet; t = triplet; m = multiplet; br = broad, angle θ calculated from Eq: $\angle$C–Sn–C = $0.0161|^2J|^2 - 1.32|^2J| + 133.4$.; $\overset{\alpha}{-}CH_3$; $\overset{\alpha}{-}CH_2\overset{\beta}{-}CH_2\overset{\gamma}{-}CH_2\overset{\delta}{-}CH_3$; $\overset{\alpha}{-}CH_2\overset{\beta}{-}CH_2\overset{\gamma}{-}CH_2\overset{\delta}{-}CH_2\overset{f}{-}CH_2\overset{g}{-}CH_2\overset{h}{-}CH_2\overset{i}{-}CH_3$;

Complex numbers as indicated in Table 4.1.

Table 4.4. ^{13}C NMR Spectral Data of Tri- and Diorganotin(IV) Derivatives of Guanosine and 1,10-Phenanthroline

Ligand/Complex	δ ppm (DMSO-*d6*)
Guanosine[a]	156.70 (C-6); 153.50 (C-2); 151.10 (C-4); 135.50 (C-8); 116.40 (C-5); 86.20 (C-1'); 85.10 (C-4'); 73.50 (C-2'); 70.20 (C-3'); 61.20 (C-5').
Guanosine[b]	156.36 (C-6); 149.25 (C-2); 140.45 (C-4); 135.00 (C-8); 113.43 (C-5); 83.78 (C-1'); 82.31 (C-4'); 71.39 (C-2'); 68.31 (C-3'); 60.87 (C-5').
1,10-phenanthroline[c]	149.20 (C-9, C-2); 136.75 (C-4, C-7); 125.95 (C-6, C-5); 123.20 (C-3, C-8); 129.10 (C-4a, C-6a/C-4b, C-6b).
1,10-phenanthroline[b]	149.20 (C-9, C-2); 136.75 (C-4, C-7); 125.95 (C-6, C-5); 123.23 (C-3, C-8); 132.74 (C-4a, C-6a/C-4b, C-6b).
1.	guanosine unit: 157.20 (C-6); 154.13 (C-2); 151.77 (C-4); 136.03 (C-8); 117.12 (C-5); 86.76 (C-1'); 85.64 (C-4'); 74.15 (C-2'); 70.82 (C-3'); 61.84 (C-5'); phenanthroline unit: 149.62 (C-9, C-2); 138.36 (C-4, C-7); 127.56 (C-6, C-5); 124.76 (C-3, C-8); 129.44 (C-4a, C-6a/C-4b, C-6b); Sn-methyl: 24.14 (C-α) ^1J = 998.6 Hz, θ = 164.35°.
2.	guanosine unit: 156.70 (C-6); 153.65 (C-2); 151.26 (C-4); 135.58 (C-8); 116.53 (C-5); 86.36 (C-1'); 85.17 (C-4'); 73.67 (C-2'); 70.32 (C-3'); 61.35 (C-5'); phenanthroline unit: 148.75 (C-9, C-2); 134.13, 133.91 (C-4, C-7); 127.70, 127.43 (C-6, C-5); 125.01, 124.90 (C-3, C-8); 129.00 (C-4a, C-6a/C-4b, C-6b); Sn-phenyl: 129.00 (C-α), 137.50 (C-β), 128.80 (C-γ, C-δ).
3.	guanosine unit: 156.75 (C-6); 153.62 (C-2); 151.28 (C-4); 135.59 (C-8); 116.60 (C-5); 86.29 (C-1'); 85.16 (C-4'); 73.65 (C-2'); 70.33 (C-3'); 61.35 (C-5'); phenanthroline unit: 148.93 (C-9, C-2); 139.09 (C-4, C-7); 127.35 (C-6, C-5); 124.89 (C-3, C-8); 129.23 (C-4a, C-6a/C-4b, C-6b); Sn-butyl: 17.41 (C-α), 27.59 (C-β), 25.32 (C-γ), 13.47 (C-δ).
4.	guanosine unit: 157.21 (C-6); 154.13 (C-2); 151.73 (C-4); 136.08 (C-8); 117.02 (C-5); 86.84 (C-1'); 85.66 (C-4'); 74.17 (C-2'); 70.82 (C-3'); 61.84 (C-5'); phenanthroline unit: 149.18 (C-9, C-2); 141.13, 140.21 (C-4, C-7); 127.94 (C-6, C-5); 125.68 (C-3, C-8); 129.87 (C-4a, C-6a/C-4b, C-6b); Sn-octyl: 41.14 (C-α) , 25.68 (C-β), 32.54 (C-γ), 28.78 (C-δ), 28.77 (C-f), 31.55 (C-g), 22.43 (C-h), 14.31 (C-i).

5.	guanosine unit: 156.59 (C-6); 153.68 (C-2); 151.20 (C-4); 135.54 (C-8); 116.32 (C-5); 86.38 (C-1'); 85.16 (C-4'); 73.67 (C-2'); 70.28 (C-3'); 61.30 (C-5'); phenanthroline unit: 148.59 (C-9, C-2); 136.05 (C-4, C-7); 127.13 (C-6, C-5); 124.56 (C-3, C-8); Sn-phenyl: 129.04 (C-α), 139.13 (C-β), 128.19 (C-γ), 128.81 (C-δ).

[a] ref [37], [b] observed data, [c] ref [28], [*] numberring of carbons and protons are as mentioned in Fig. 4.1. $-CH_3$; $-CH_2-CH_2-CH_2-CH_3$; $-CH_2-CH_2-CH_2-CH_2-CH_2-CH_2-CH_2-CH_3$; . Complex numbers as indicated in Table 4.1.

Table 4.5. ^{119}Sn NMR Spectral Data of Tri- and Diorganotin(IV) Derivatives of Guanosine and 1,10-Phenanthroline

Complex[a]	δ ppm (DMSO-*d6*)
1.	−224.83
2.	−362.28
3.	−237.46
4.	−251.63, −150.36
5.	−253.11

[a] Complex number as indicated in Table 4.1.
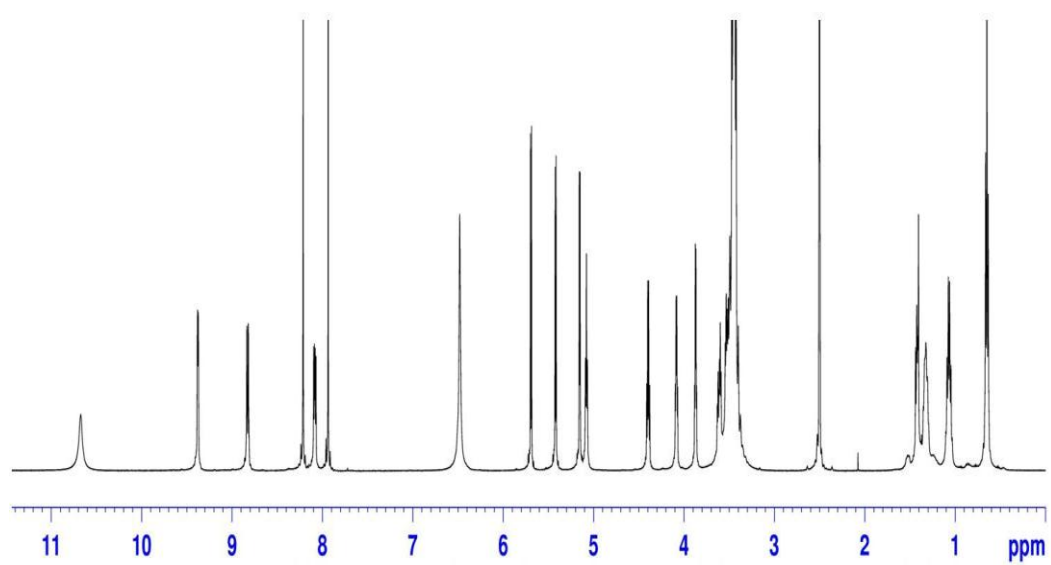
Fig. 4.2. ^{1}H NMR spectrum of [Bu$_2$Sn(HGuO)$_2$(phen)].
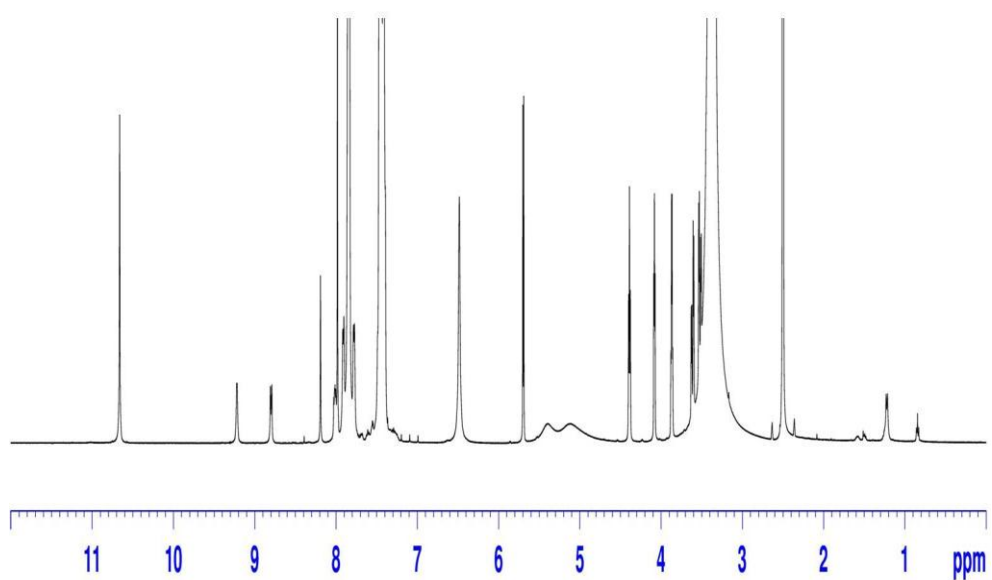
Fig. 4.3. ^{1}H NMR spectrum of [Ph$_3$Sn(HGuO)(phen)].
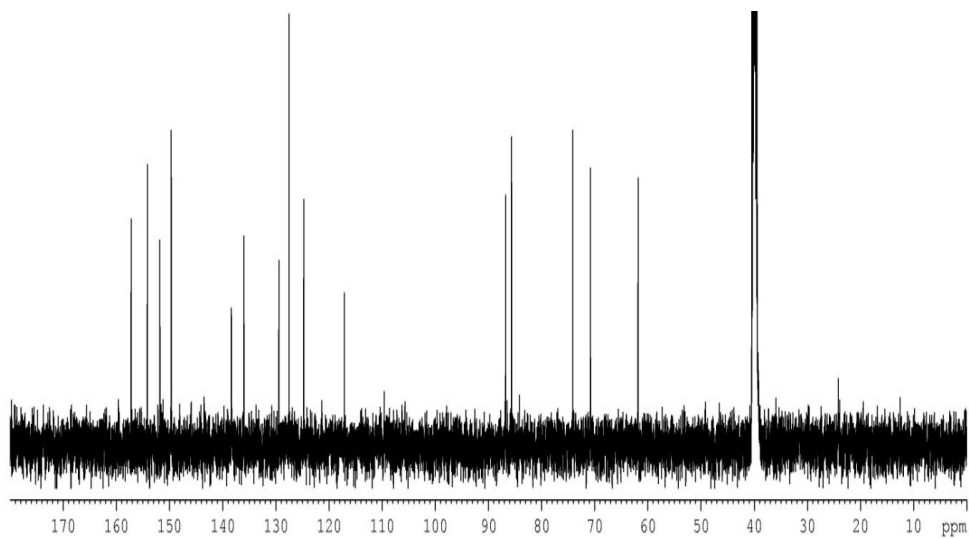
Fig. 4.4. ^{13}C NMR spectrum of [Me$_2$Sn(HGuO)$_2$(phen)].
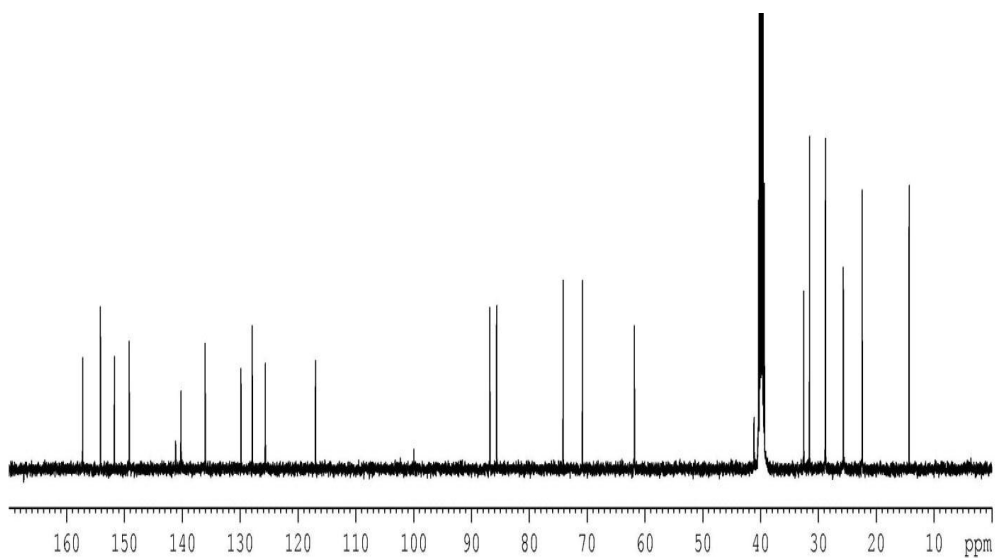
Fig. 4.5. ^{13}C NMR spectrum of [Oct$_2$Sn(HGuO)$_2$(phen)].
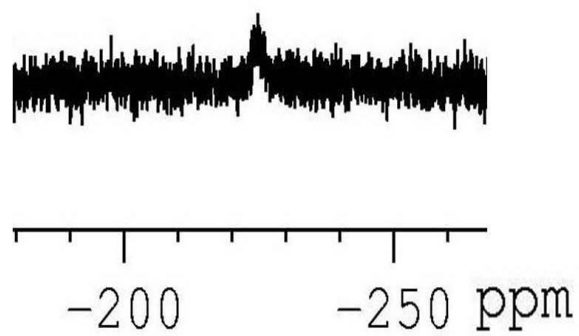
Fig. 4.6. ^{119}Sn NMR spectrum of [Me$_2$Sn(HGuO)$_2$(phen)].
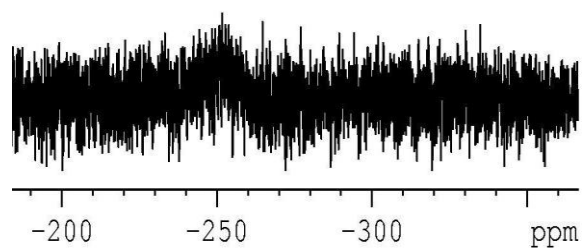
Fig. 4.7. ^{119}Sn NMR spectrum of [Oct$_2$Sn(HGuO)$_2$(phen)].
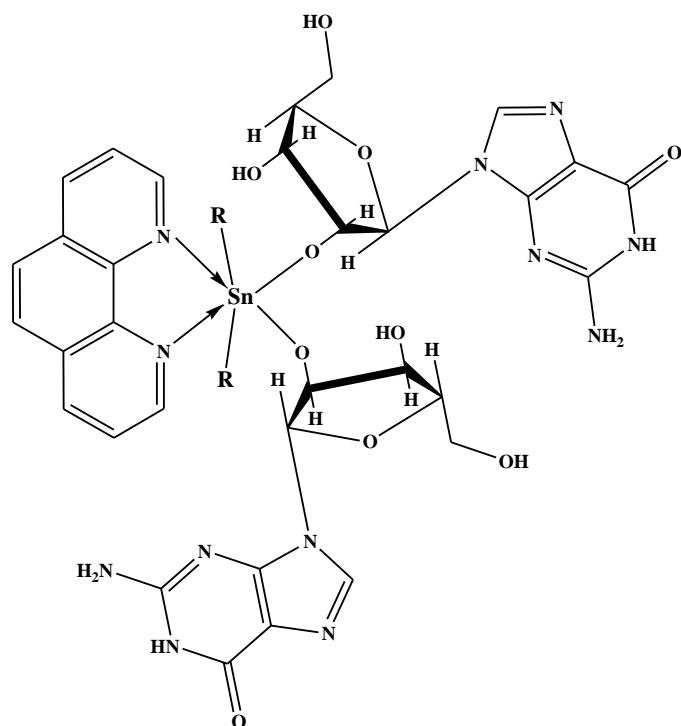
Fig. 4.8. Proposed structure of [R₂Sn(HGuO)₂(phen)].
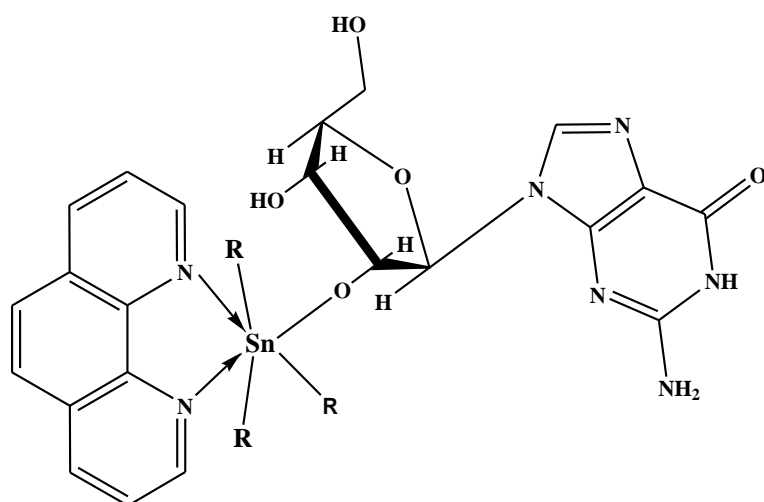
Fig. 4.9. Proposed structure of [R₃Sn(HGuO)(phen)].

4.3.4. *In Vitro* Cytotoxicity Studies

4.3.4.1. MTT assay

The studied diorgano- and triphenyltin(IV) complexes of guanosine and 1,10-phenanthroline have been screened for *in vitro* anti-tumor activity against HEK293 (human embryonic kidney) and a panel of four cancer cell lines of human origin, *viz*, MCF7 (mammary), HepG2 (liver), DU145 (prostrate) and HeLa (cervical). The inhibitory concentration (IC_{50}) values are calculated for the titled complexes using the best fit linear regression model [35, 57, 58]. Table 4.6 presents the IC_{50} values of the studied complexes along with standard reference drugs, *cis*-platin (CPT) and 5-fluorouracil (5-FU). The IC_{50} values of complexes (1) and (4) against all cell lines are found to be above 40 μg/mL, therefore, they are considered to be inactive [35, 57, 58]. From the table 4.6, it can be inferred that the complexes (2) and (3) are more active against all cell lines compared to that of *cis*-platin, but less active than 5-fluorouracil against HepG2 cell line. The complexes (2), (3) and (5) against DU145 cell line exhibit comparable cytotoxicity with *cis*-platin, but their activity is lower than that of 5-fluorouracil. Complex (5) displayed less activity than *cis*-platin against HEK293, MCF7 and DU145 cell lines, but more active against HepG2 cell line. Furthermore, it is much less active than 5-fluorouracil against all cell lines. Finally, complex (3) (dibutyltin(IV) complex) is more active out of all the complexes, but also adversely affect normal cell lines, hence, complexes (2) and (5) are selected for the further studies.

Table 4.6. Screening of Di- and Triorganotin(IV) Derivatives of Guanosine and 1,10-Phenanthroline for Their Cytotoxic Properties (MTT assay). The Results are Expressed as IC_{50} (μg/mL ± SEM) Values

Complex/Drug	HEK293	MCF7	HepG2	DU145	HeLa
1.	> 40.0	> 40.0	> 40.0	> 40.0	> 40.0
2.	7.29 ± 0.05	38.23 ± 0.01	4.65 ± 0.05	20.73 ± 0.05	8.71 ± 0.12
3.	3.45 ± 0.02	21.99 ± 0.03	2.88 ± 0.06	20.85 ± 0.06	1.28 ± 0.04
4.	> 40.0	> 40.0	> 40.0	> 40.0	> 40.0
5.	27.53 ± 0.02	> 40.0	11.61 ± 0.03	21.27 ± 0.10	6.63 ± 0.03
CPT[a]	15.44 ± 5.12	29.79 ± 0.10	19.83 ± 0.10	19.89 ± 0.05	
5-FU[a]	2.06 ± 0.23	< 4.97	< 4.97	10.78 ± 0.05	

[a] ref [35]

4.3.4.2. Enzyme assays

There are two ways by which the cell death can occur; necrosis and apoptosis. Apoptosis is a programmed cell death (PCD), while necrosis is premature cell death (PMCD) [35, 57, 58]. Usually antitumor compounds arrest the cell growth *via* apoptosis [35, 57, 58]. A common method to ensure the apoptosis is through enzyme assays [35, 57, 58]. Lipid peroxidase and lactate dehydrogenase assays were performed in order to determine whether the cell death occur *via* apoptosis or necrosis. In lipid peroxidase assay, a series of oxidative reactions (free radical chain mechanism) trigger the oxidative degradation of lipid membrane, which leads to the generation of reactive oxygen species (ROS) upon the treatment of the drug with the cancer cells [134]. This excessive generation of reactive oxygen species disrupt the cell membrane causing cell damage. The end products of the lipid peroxidase assay are malondialdehyde (MDA) and 4-hydroxynonenal (HNE). Malondialdehyde (MDA) quantification can be done by utilizing thiobarbituric reactive substances assay (TBARS), in which the OD of the fluorescent end product is measured [134] and thus, the IC_{50} values are calculated. The complexes **(2)** and **(5)** showed a slight decrease in lipid peroxidase (one-fold) (Table 4.7 and Table 4.8), which shows that the cell membrane remained intact throughout the apoptosis process. Hence forth, it can be concluded that the cell death is *via* apoptosis. However, a possibility of very small amount necrosis could not be ignored. A sudden and marginal increment in lactate dehydrogenase (LDH) concentration results during the necrosis process. Both the complexes **(2)** and **(5)** showed a very small increment (0.7 to 0.9-fold) in LDH concentration, hence can be said that the apoptosis is the major cause but necrosis also plays vital role in cell death.

Table 4.7. Enzyme Assays of Complex (2) Against HepG2 (liver) Cancer Cell Line

Enzymes	Control/Untreated	Treated	IF
Lipid peroxidase[a]	7.2×10^{-2}	6.7×10^{-2}	1.07
Lactate dehydrogenase[b]	3.2×10^{-1}	4.52×10^{-1}	0.708

[a] μM/μg protein; [b] IU/mg protein; Induction fold (IF): mean of treated/mean of untreated; the experiment was performed in triplicate and mean values are shown here.
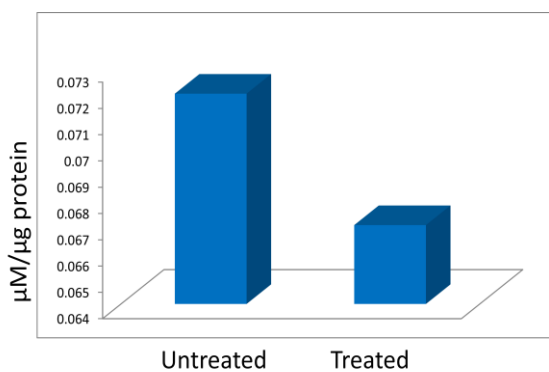
Table 4.8. Enzyme Assays of Complex (5) Against HeLa (cervical) Cancer Cell Line

Enzymes	Control/Untreated	Treated	IF
Lipid peroxidase[a]	6.4×10^{-2}	5.7×10^{-2}	1.12
Lactate dehydrogenase[b]	4.3×10^{-1}	4.73×10^{-1}	0.91

[a] μM/μg protein; [b] IU/mg protein; Induction fold (IF): mean of treated/mean of untreated; the experiment was performed in triplicate and mean values are shown here.

Fig. 4.10. Lipid peroxidase assay of Complex (2) against HepG2 (liver) cancer cell line.
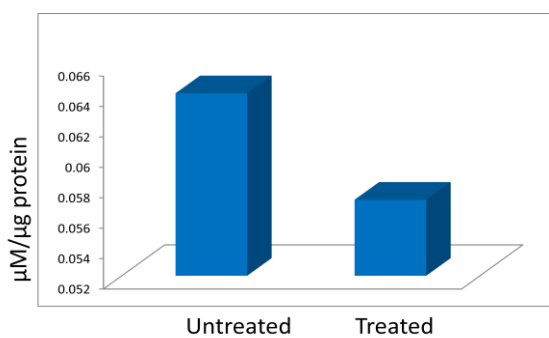
Fig. 4.11. Lipid peroxidase assay of Complex (5) against HeLa cancer cell line.
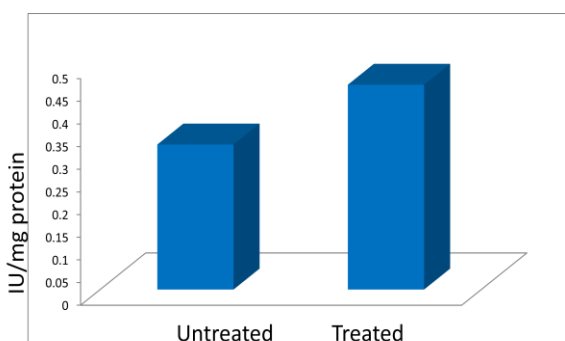
Fig. 4.12. Lactate dehydrogenase assay of Complex (2) against HepG2 (liver) cancer cell line.
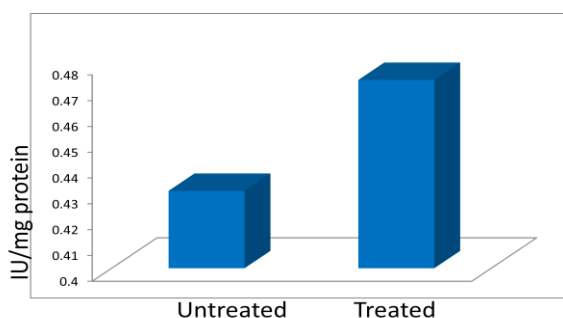
Fig. 4.13. Lactate dehydrogenase assay of Complex (5) against HeLa cancer cell line.

4. 3.4.3. Acridine orange assay

Acridine orange assay is a fluorescent staining assay by which the morphological changes can be visualized. Depending upon the percentage intake of Acridine orange AO/Ethidium bromide EB stains, the live and apoptotic cells can be distinguished. AO permeates all the live cells hence appear green; where as the EB is taken up only by the cells which have lost their cytoplasmic membrane integrity, therefore appear red [35, 57, 58]. The cancer (HepG2 and HeLa) cells were incubated with the IC_{50} value of the test compound and the vehicle control. After the nuclear staining, they were visualized under fluorescent microscope (Ziess, Axiovert 25, Germany). From Figs. 4.14 (a) and 4.115 (a), it can be clearly observed that the live cells with green nucleus were predominant in the control compared to that of the test compound (Figs. 4.14 (b) and 4.15 (b)). The apoptotic cells with orange nucleus were substantial in the test compound treated cells. Along with the apoptosis, small amount of necrosis is also observed.

4.3.4.4. Comet assay

Cytotoxicity leading to DNA damage can be validated by single cell gel electrophoresis. A simple yet sensitive technique like comet assay or single cell gel electrophoresis detects the DNA damage at cellular level [35, 57, 58]. The nuclei of HepG2 and HeLa cells treated with the test compound alongside the control were stained with EB and visualized under fluorescent microscope. Figs. 4.16 and 4.17 represent the single cell gel (alkaline) electrophoresis showing DNA fragmentation in test compounds treated HepG2 and HeLa cells, respectively. The fragmentation or DNA disintegration in an individual cell is observed as comet tails [35, 57, 58]. However, vehicle treated cells (control) do not show any fragmentation.

(a)   **(b)**
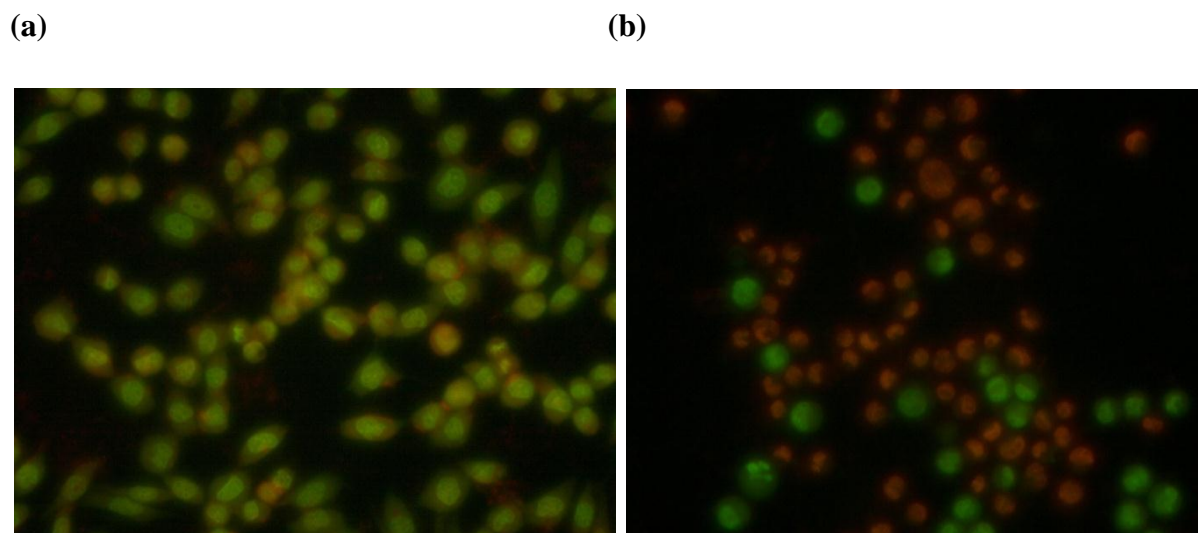
Fig. 4.14. Acridine orange assay for: (a) control, (b) complex (2) treated HepG2 cells. Green and orange colors indicate live and apoptotic cells, respectively.
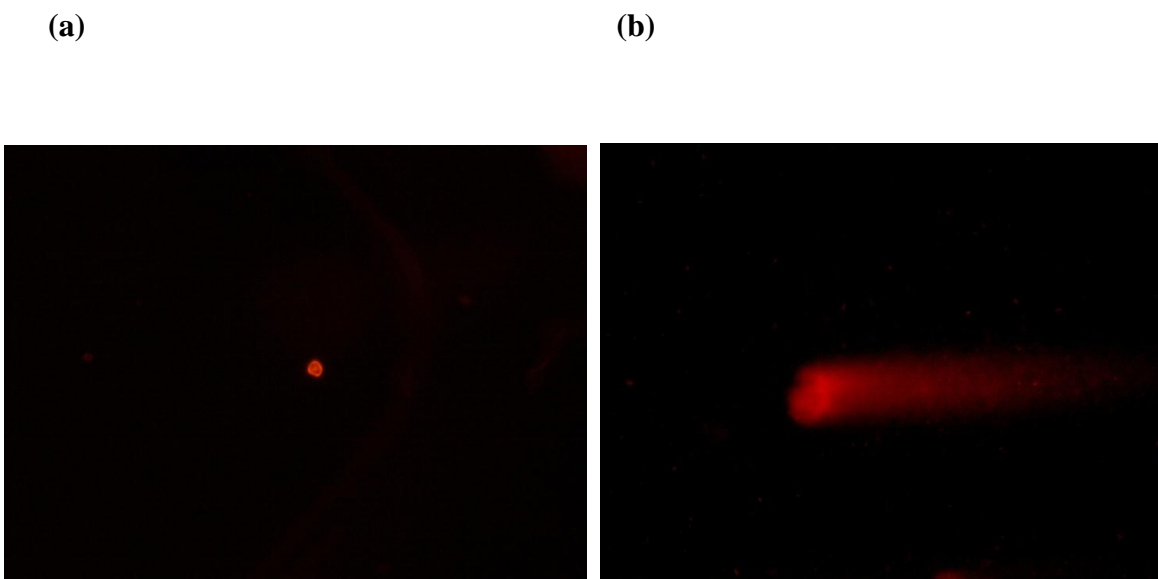
(a)   **(b)**
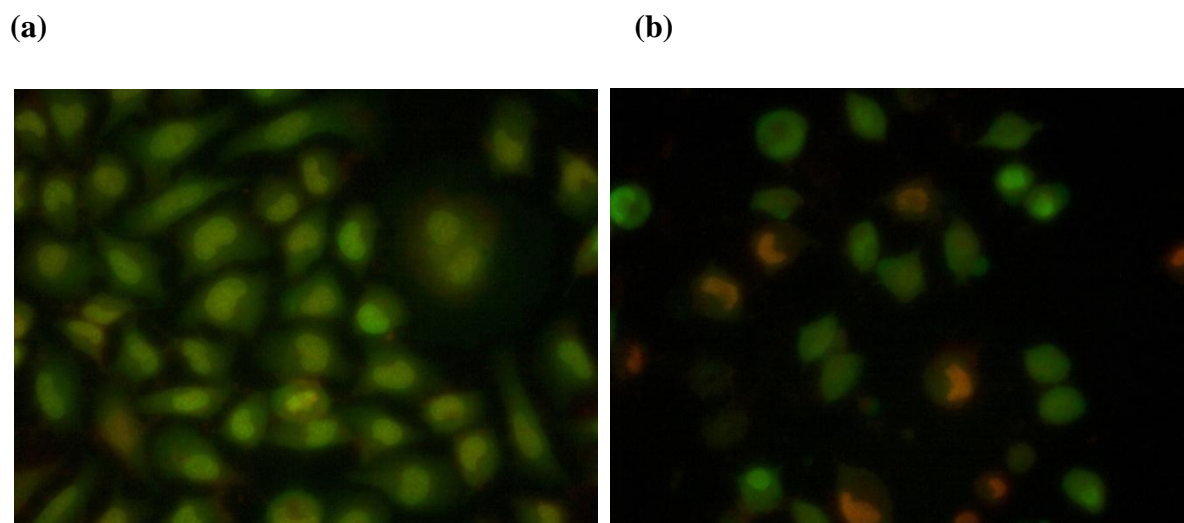
Fig. 4.15. Acridine orange assay for: (a) control, (b) complex (5), treated HeLa cells. Green and orange colors indicate live and apoptotic cells, respectively.

(a) (b)

Fig. 4.16. Comet assay for: (a) control, (b) complex (2), treated HepG2 cells.

(a) (b)
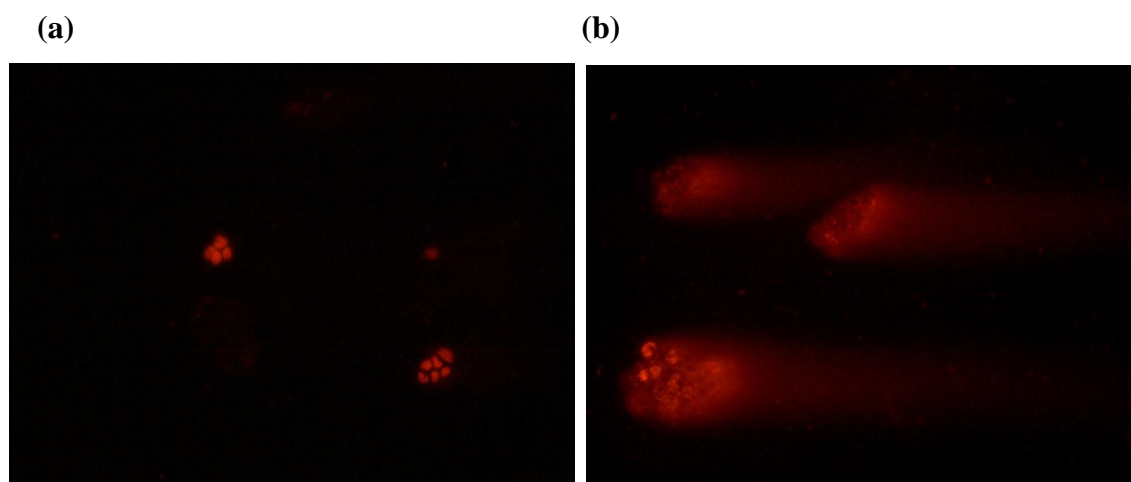
Fig. 4.17. Comet assay for: (a) control, (b) complex (5) treated HeLa cells.

4.4.5. DNA Binding Studies by UV-Visible Absorption Spectrometry

The absorption spectra of the complexes show intense absorption bands arising from the intraligand transitions [41, 88, 89, 91, 133] located in the range 250–260 nm and 330 nm. Upon increasing the concentration of DNA, a considerable change in the absorptivity with apparent red or blue shift (~ 2 nm) was observed (as shown in Fig. 4.18). The hyperchromism in the spectra of the complex **(2)** was found to be correlated with the non-classical electrostatic binding mode with DNA and may arise due to the preferential binding of the Sn(IV) to dinegative phosphate group of DNA backbone because of its hard Lewis acidic property [41, 88, 89, 91, 133]. The complex does not exhibit any pronounced sequence or base preference while interacting with DNA which elicits electrostatic binding of the complex. For complexes **(1)**, **(3)**, **(4)** and **(5)**, a decrease in the intensity suggests that the complex can unwind DNA helix and leads to the loss of helicity, perturbing the secondary structure of DNA [41, 88, 89, 91, 133]. As complexes **(2)** and **(5)** are non-planar, the presence of two/three phenyl groups induces steric effects which also promote partial intercalative binding of complexes to DNA. The intrinsic binding constant determined according to Eq. 4.3 for the complex **(2)** (Fig. 4.18 (b)) and **(5)** (Fig. 4.22 (b)) were found to be 2.33×10^5 M^{-1} and 2.46×10^5 M^{-1}, respectively, while for the complexes **(1)** , **(3)** and **(4)** (Figs. 4.19 (a), 4.19 (c) and Fig. 4.19 (d)), it is 1.13×10^5 M^{-1}, 2.78×10^5 M^{-1} and 2.51×10^5 M^{-1}, respectively indicating pronounced binding with DNA.

$$\frac{[DNA]}{|e_a - e_f|} = \frac{[DNA]}{|e_b - e_f|} + \frac{1}{|e_b - e_f|K_b} \qquad (4.3)$$

(a)

(b)

(c)

(d)
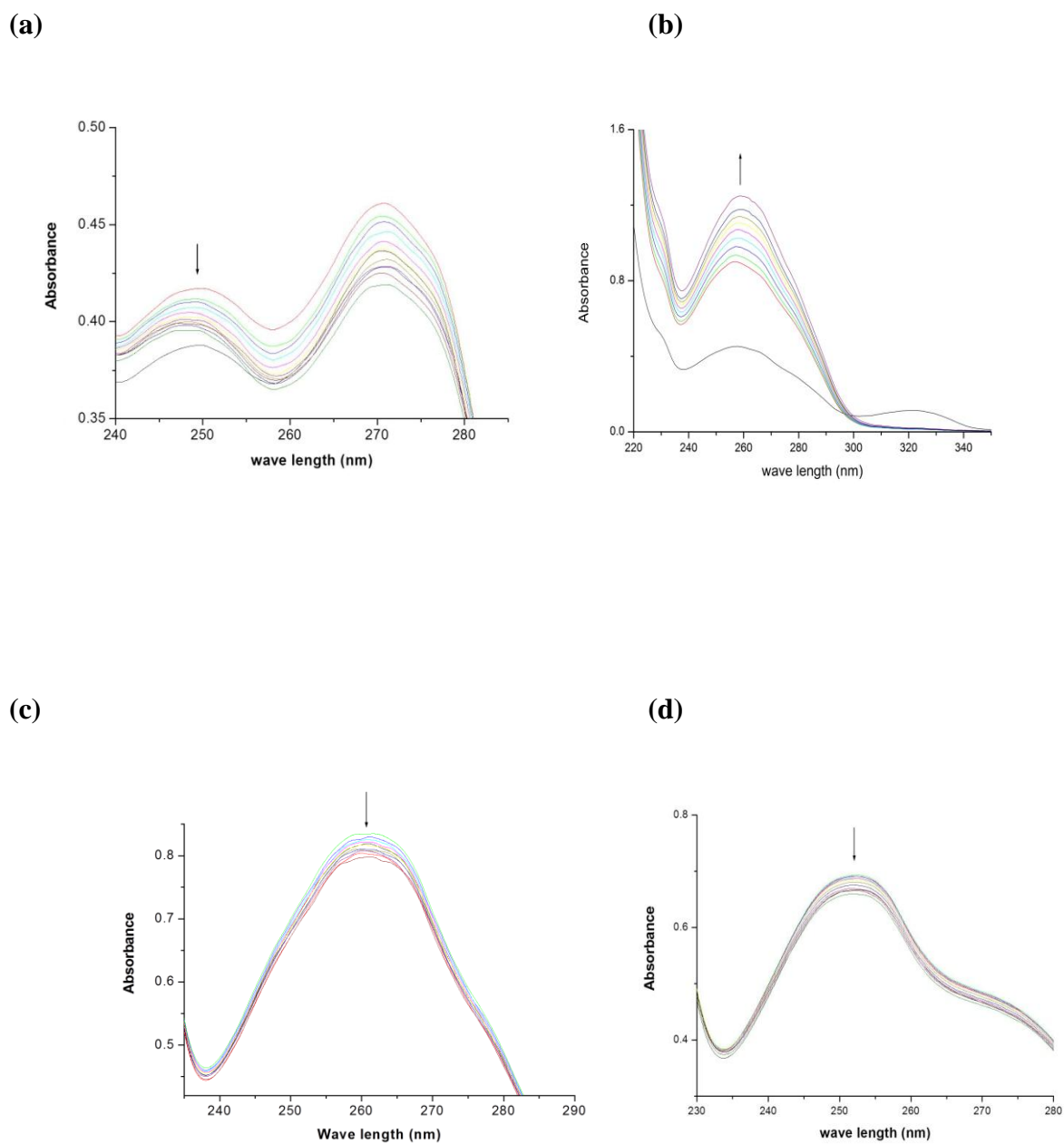
Fig. 4.18. Variation of UV-Visible absorption for complexes (1): (a), (2): (b), (3): (c), and (4): (d), respectively, with increase in the concentration of CT DNA (2–20 $\times$ 10^{-5} M) in buffer (5 mM Tris–HCl/50 mM NaCl, pH = 7.2) at room temperature. [Complex] = 2 $\times$ 10^{-5} M. Arrows indicate increment or decrement in absorbance.
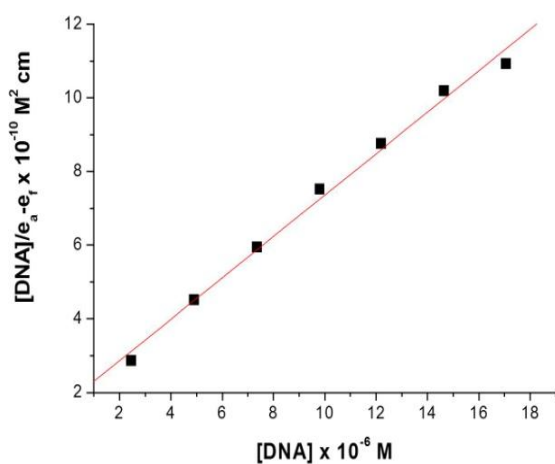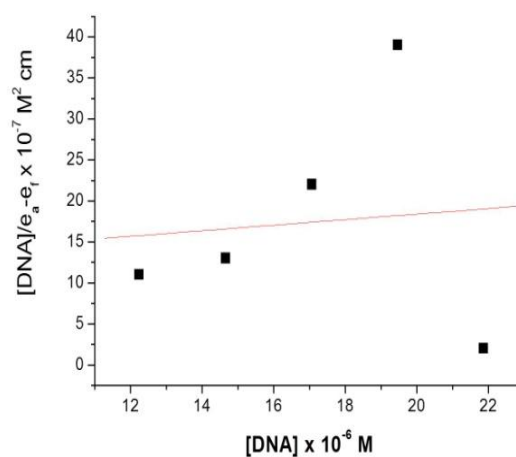
(a)
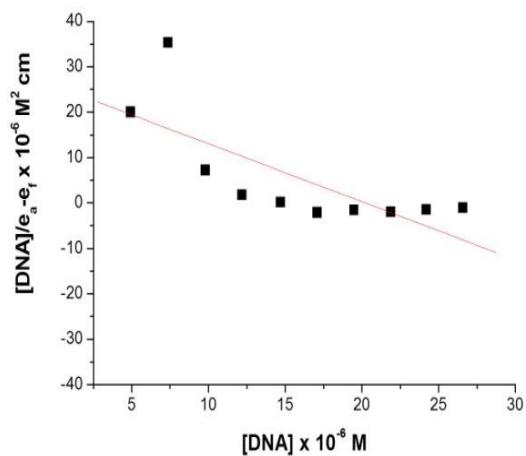
(b)
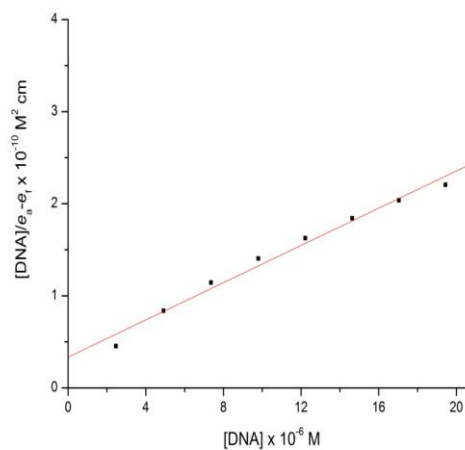
(c)

(d)

Fig. 4.19. Plots of [DNA]/(e_a − e_f) vs [DNA] for the titration of CT DNA complexes (1): (a), (2): (b), (3): (c), and (4): (d), respectively.

4.3.6. Fluorescence Studies

The binding of the complexes to CT DNA was studied by evaluating the fluorescence emission intensity of the ethidium bromide (EB)–DNA system upon the addition of series of concentrations of the complexes [41, 88, 89, 91, 133]. The emission spectra of (2) and (5) in the absence of DNA and presence of DNA and Stern-volmer plots are presented in Fig. 4.20, Fig. 4.21 and Fig. 4.22 (c), when excited at 263 nm and the emission wave length is 603 nm. As evident from the spectra, the intensity of the emission (λ = 603 nm) decreases for (2) because it replaces the EB. Emission intensity increases in case of (5) appreciably in presence of DNA indicative of the binding of the complex (2) to the hydrophobic pockets of DNA. This is due to the fact that the metal complex is bound in a relatively non-polar environment compared to water [41, 88, 89, 91, 133]. Although the emission enhancement could not be regarded as criterion for binding mode, they are related to the extent to which the complex gets into the hydrophobic environment inside the DNA and avoid or reduce the accessibility of solvent molecules to the complex.

Furthermore, the relative binding propensity of the complexes to CT DNA was determined by the classical Stern-Volmer equation (Eq. 4.4) where, I and I_0 are fluorescence intensities in absence and presence of quencher, respectively; K_{sv} is the linear Stern-Volmer quenching constant, dependent on r_{bE} (the bound concentration of EB to the [DNA]) and r is the ratio of [quencher] to that of [DNA].

$$\frac{I_0}{I} = 1 + K_{sv}r \tag{4.4}$$

The Stern-Volmer quenching constants can be used to evaluate the nature of DNA-binding modes; a value above 10^6 M^{-1} is an indication of intercalation, while values in the range 10^4–10^5 M^{-1} imply the groove binding mode [129]. The Stern-Volmer quenching constant (K_{sv}) of complex (2) (Fig. 4.21 (b)) and (5) (Fig. 4.22 (d)) is 9.74×10^5 M^{-1} and 2.9×10^6 M^{-1}, respectively, while for the complexes (1), (3) and (4) (Figs. 4.21 (a), 4.21 (c) and 4.21 (d), respectively), it is 6.38×10^4 M^{-1}, 1.50×10^5 M^{-1} and 1.86×10^6 M^{-1}, respectively. Therefore, from K_{sv} values, the DNA-binding mode of (2) might be by the groove binding and that of (5) by intercalation.
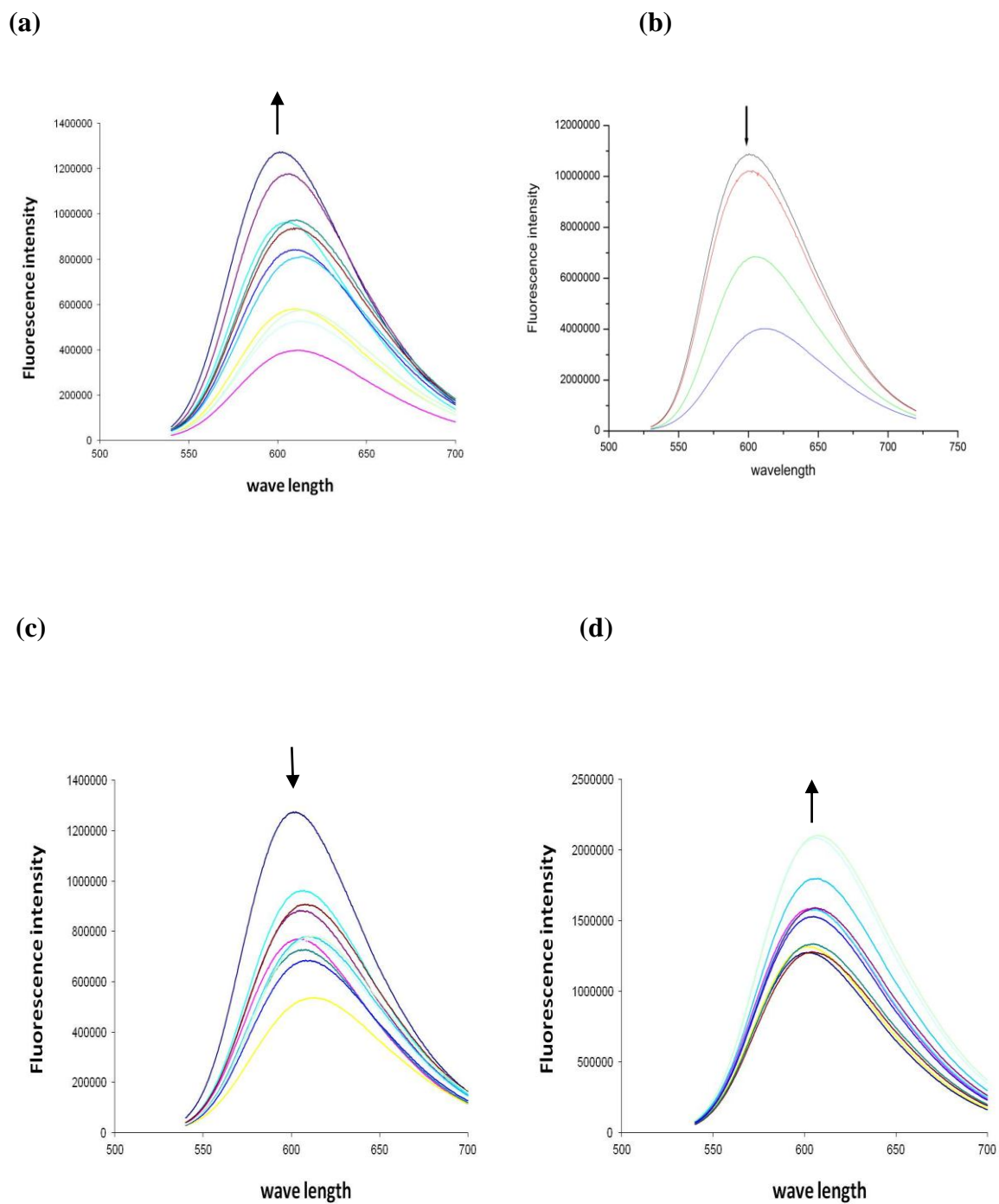
(a)

(b)

(c)

(d)

Fig. 4.20. Emission spectra of complexes (1): (a), (2): (b), (3): (c), and (4): (d), in Tris–HCl buffer (pH = 7.2) in the absence and presence of CT DNA. [Complex] = $1\text{–}10 \times 10^{-5}\,\text{M}$, [DNA] = $10^{-5}\,\text{M}$.
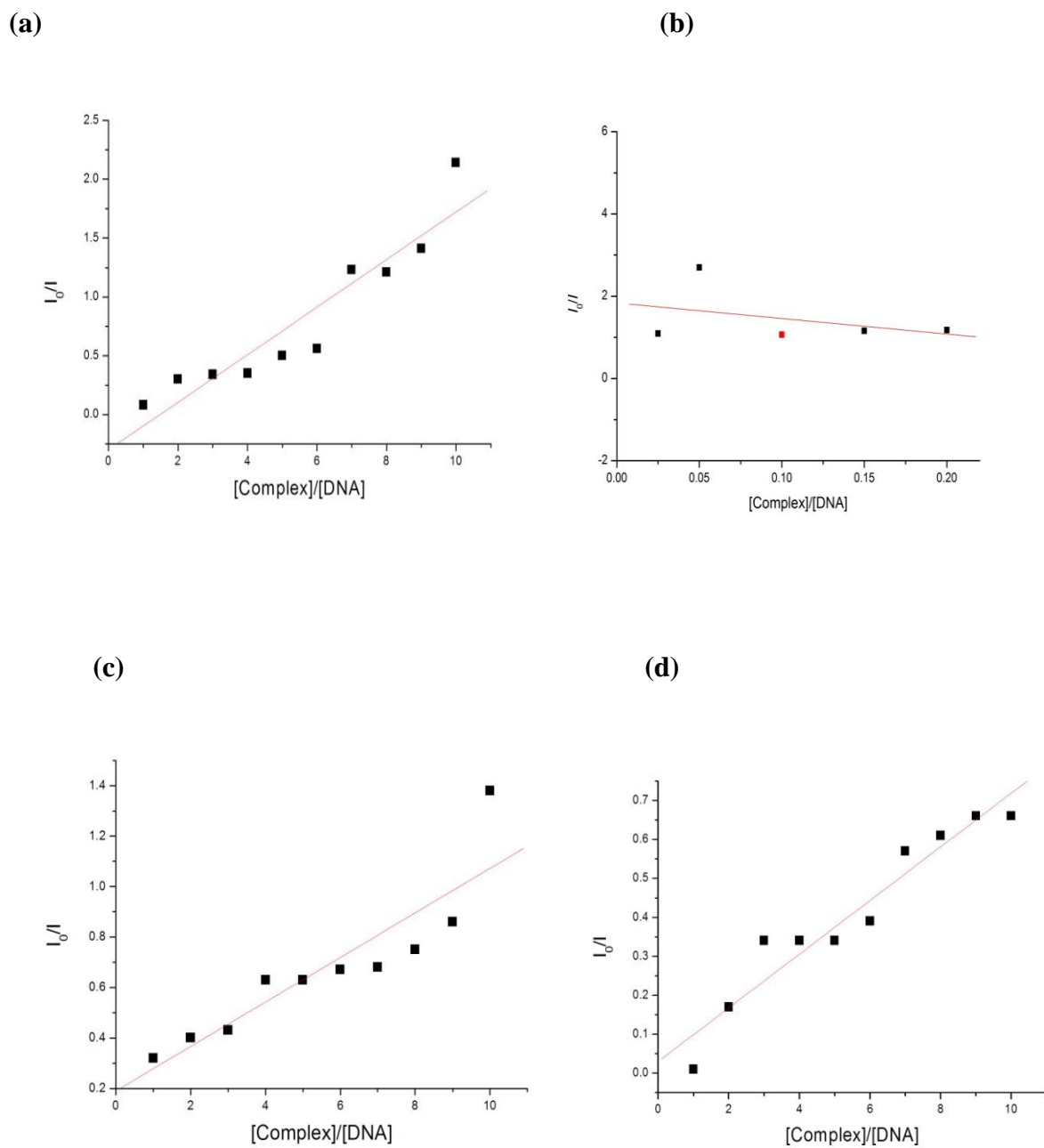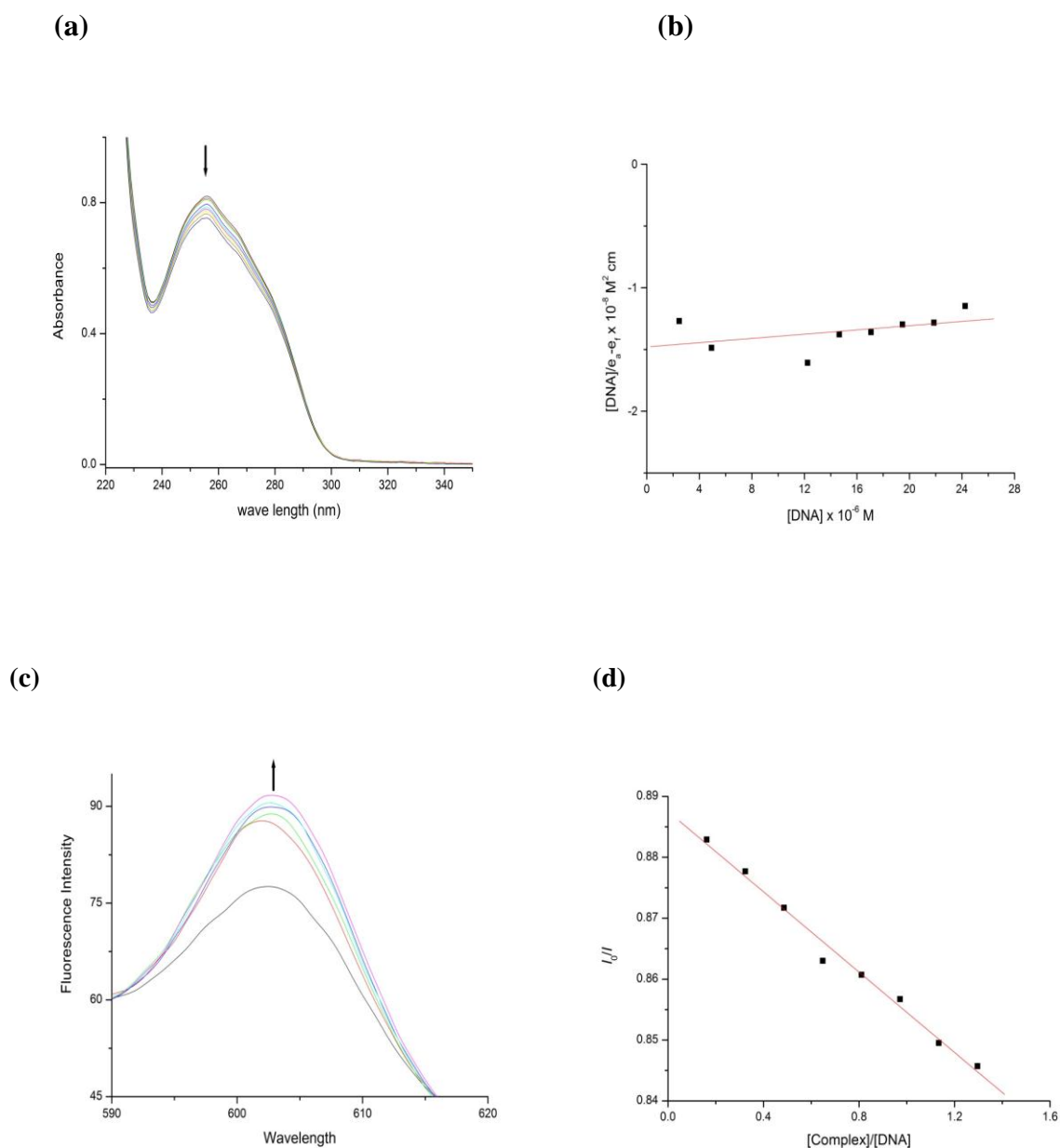
(a)

(b)

(c)

(d)

Fig. 4.21. Stern-Volmer quenching plots of EB bound to DNA with complexes (1): (a), (2): (b), (3): (c), and (4): (d), in Tris–HCl buffer (pH = 7.2) in the absence and presence of CT DNA.

(a)

(b)

(c)

(d)

Fig. 4.22. (a) Variation of UV-visible absorption for complex (5) with increase in the concentration of CT DNA (2–20×10^{-5} M) in buffer (5 mM Tris–HCl/50 mM NaCl, pH = 7.2) at room temperature. [complex] = 2×10^{-5} M. Arrows indicate increment or decrement in absorbance; (b) Plot of [DNA]/(e_a – e_f) vs [DNA] for the titration of CT DNA with complex; (c) Emission spectra of complex (5) in Tris–HCl buffer (pH = 7.2) in the absence and presence of CT DNA. [Complex] = 1–10×10^{-5} M, [DNA] = 10^{-5} M; and (d) Stern-Volmer quenching plot of EB bound to DNA with complex (5).

4.3.7. Gel Electrophoresis

To assess the DNA cleavage ability of the **(2)** and **(5)**, pBR322 DNA was incubated with different concentrations of the complexes (5–50 µM) in 5 mM Tris–HCl/50 mM NaCl buffer at pH 7.2, for 2.5 h. When circular plasmid DNA was subjected to gel electrophoretic mobility assays, relatively fast migration was observed for intact supercoiled form I. However, if scission of DNA occurs at one strand, the supercoiled DNA converted in to a slower moving open/nicked circular form II. If both strands are cleaved, a linear form III was generated [130]. In all the complexes, upon gel electrophoresis, there is an enhancement of the intensity of form II upon increasing concentration from $r = 1$ to $r = 20$, where $r =$ [complex]/[DNA]), a slight increase in form II is observed as depicted from Fig. 4.23. This indicates that these complexes promotes the conversion of DNA from supercoiled form I to nicked circular form II, which clearly implicates the role of organotin in the process of DNA cleavage.
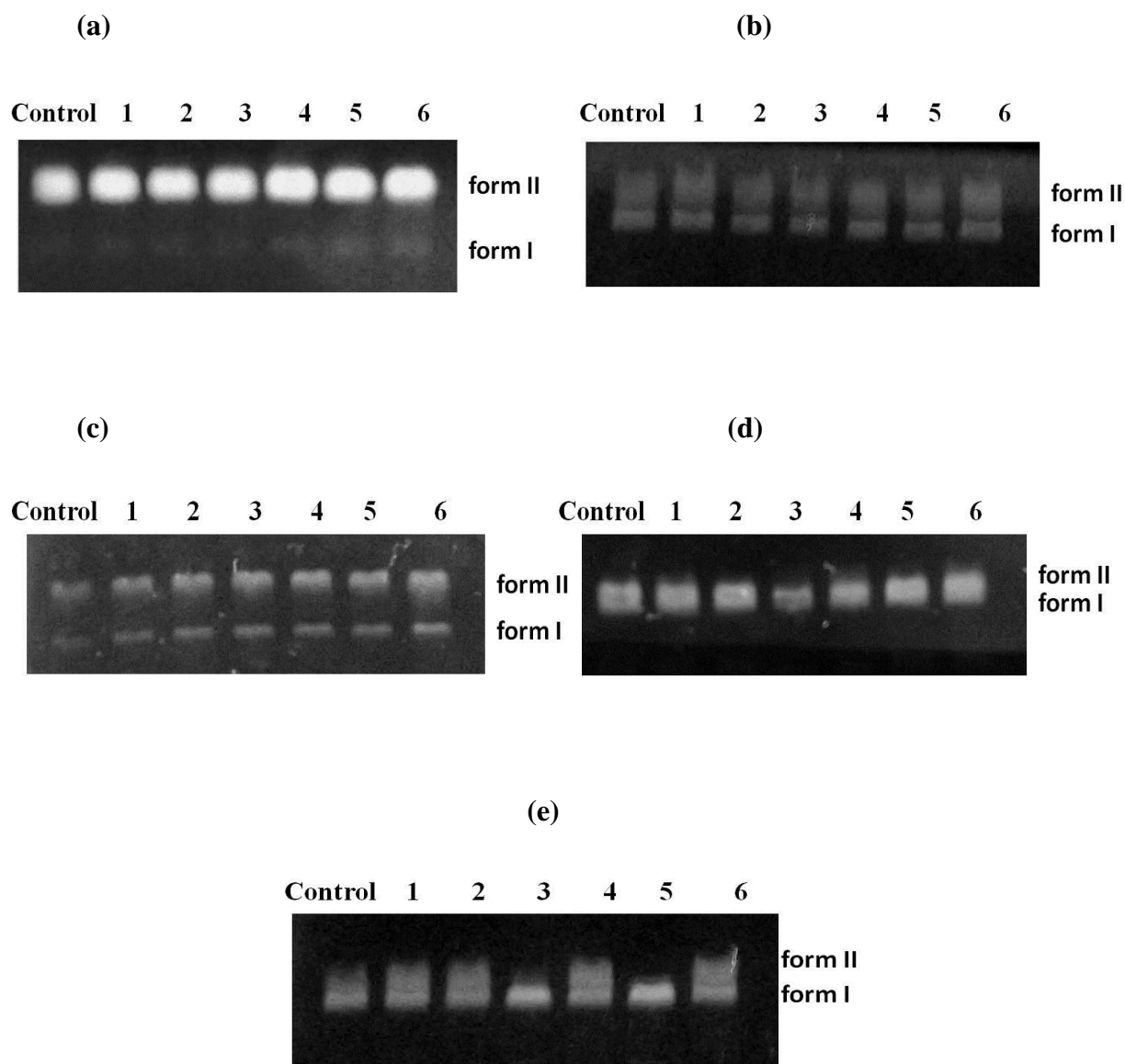
Fig. 4.23. Agarose gel (0.8%) electrophoretograms of cleavage of pBR322 DNA plasmid with complexes (1): (a), (2): (b), (3): (c), (4): (d), and (5): (e), respectively, incubated for 2.5 h at 37 °C in 5:50 mM Tris–HCl/NaCl buffer, pH 7.2. From left to right: DNA control; lane 1, $r = 1$; lane 2, $r = 2$; lane 3, $r = 5$; lane 4, $r = 10$; lane 5, $r = 15$; lane 6, $r = 20$; $r = $ [Complex]/[DNA].

5.1. INTRODUCTION

Inosine monophosphate (5'-IMP) or inosinic acid is a ribonucleoside monophosphate of hypoxanthine [135, 136]. Derivatives of 5'-IMP are found in nucleic acids, muscle and other tissues [135, 136]. Inosinate ($(5'\text{-}IMP)^{2-}$) is the first intermediate formed in the synthesis of purines, AMP and GMP. Replacement of carbonyl group at C6 position with an amino group results in AMP, whereas, GMP is formed by the inosinate oxidation to xanthylate (XMP) followed by the addition of an amino group at C2 [135, 136]. Inosine monophosphate dehydrogenase (IMPDH) enzyme catalyses this step, thus it is a key enzyme in *de novo* GMP biosynthesis. The diseases and physiological processes could be affected with the expression and activity of IMPDH [137]. Prevention of this step inhibits cancer cell proliferation and induction of apoptosis, hence could be a possible target for cancer chemotherapy [137]. 5'-IMP and its salts (e.g. disodium inosinate) are also used as flavor enhancers in food industry [136]. Organotin(IV) complexes of 5'-IMP and their biological activities have not been reported till now, however, their solution studies are available in literature. Chapter 1 literature review gives a brief report on 5'-IMP and its organotin(IV) solution studies. Synthesis and characterization of diorganotin complexes with $(5'\text{-}IMP)^{2-}$ have been discussed in the current chapter. It has been reported that the disodium-5'-inosinate consists of ~ 7.5 molecules of water of crystallization [136], however, it varies depending upon the source and purification method. The disodium-5'-inosinate ligand utilized in the present study is procured from Sigma-Aldrich with water not more than 25% (approximately 5.5 H_2O molecules). The presence of phenanthroline moiety may have pronounced influence (increase/decrease) on the biological activities of organotin–(5'-IMP) complexes, therefore, mixed diorganotin(IV) complexes of $(5'\text{-}IMP)^{2-}$ and 1,10-phenanthroline (phen) were also synthesized and characterized by using spectroscopic techniques such as IR, far-IR, NMR (^{1}H, ^{13}C, ^{119}Sn). *In vitro* anti-tumor activity (by MTT assay) against mammary (MCF7), liver (HepG2) cancer cell lines of human origin have been screened and IC_{50} values of the titled complexes have been determined. Furthermore, to view the insight on the mode of action of the studied complexes, acridine orange and comet assays have been done. DNA binding affinity studies of the complexes by using ultraviolet-visible (UV-Vis), fluorescence spectroscopy and cleavage experiments by submarine agarose gel electrophoresis have been carried out and the results are discussed in detail in this chapter.

5.2. EXPERIMENTAL SECTION

5.2.1. Synthesis of Dimethyltin(IV) Derivative of (5'-IMP)$^{2-}$ (1)

An aqueous methanolic (20 mL, 1:1 or 50%) solution of dimethyltin(IV) dichloride (0.220 g, 1.0 mmol) was stirred for half an hour. An aqueous methanolic solution of 5'-inosine monophosphate disodium salt hydrate (5'-IMP-Na$_2$.xH$_2$O, also referred as 5'-IMP-Na$_2$) (0.392 g, 1.0 mmol) was added to the resulting solution and constantly stirred for ~ 5 h under nitrogen atmosphere. The resultant was centrifuged and filtered to remove the NaCl formed during the reaction. Excess solvent was removed under reduced pressure and allowed to chill. The fluffy white solid product obtained was washed with methanol-water mixture (1:1 v/v) followed by methanol-hexane mixture (1:3 v/v), and dried under vacuum.

5.2.2. Synthesis of Diphenyltin(IV) Derivative of (5'-IMP)$^{2-}$ (2)

5'-IMP-Na$_2$ (0.392 g, 1.0 mmol) was dissolved in minimum amount (20 mL) of hot aqueous methanol (1:1) under nitrogen. An aqueous hot methanolic (20 mL, 1:1) solution of diphenyltin(IV) dichloride (0.344 g, 1.0 mmol) was added and the resultant was further refluxed with constant stirring for at least ~ 24–26 h under nitrogen atmosphere. The resulting solution was centrifuged and filtered to remove the NaCl formed during the reaction. The excess of solvent was removed under reduced pressure and chilled. The solid cream product obtained was washed with methanol-hexane or methanol-petroleum ether (b.p. 40–60 °C) mixture (1:3 v/v), and dried under vacuum.

5.2.3. Synthesis of Dibutyltin (IV) Derivative of (5'-IMP)$^{2-}$ (3)

Dibutyltin(IV) derivative was prepared under nitrogen atmosphere by the drop-wise addition of aqueous hot methanolic (20 mL, 1:1) solution of dibutyltin dichloride (0.304 g, 1.0 mmol) to the aqueous hot methanolic (20 mL, 1:1) solution of 5'-IMP-Na$_2$ (0.392 g, 1.0 mmol). The reaction mixture was further refluxed with constant stirring for at least 24–26 h. Centrifugation of the resultant and the removal of NaCl was carried out by filtration. Excess solvent was reduced and chilled, and the white solid product thus obtained was washed with water followed by methanol–hexane or methanol–petroleum ether (b.p. 40–60 °C) mixture (1:3 v/v), and dried under vacuum.

5.2.4. Synthesis of Mixed Dimethyl/Diphenyl/Dibutyltin(IV) Derivatives of (5'-IMP)$^{2-}$ and 1,10-Phenanthroline (4)/(5) and (6)

Similar procedures discussed in subsections 5.2.1., 5.2.2 and 5.2.3., respectively, were adapted initially to synthesize the dimethyl/diphenyl/dibutyltin(IV) derivatives of 5'-IMP in 1:1 ratio. I*n situ* addition of 1,10-phenanthroline (0.18 g, 1.0 mmol) in aqueous methanol (20 mL, 1:1) to the above mixtures was carried out. Dimethyltin(IV) derivative was stirred for ~ 3 h, whereas the diphenyl/dibutyltin(IV) derivatives were refluxed for another ~ 20 h. The products were centrifuged and the NaCl was removed by filtration. The filtrate was reduced and allowed to cool followed by washing with water-methanol (1:1 v/v) and methanol-hexane (1:3 v/v) mixtures, and dried under vacuum.
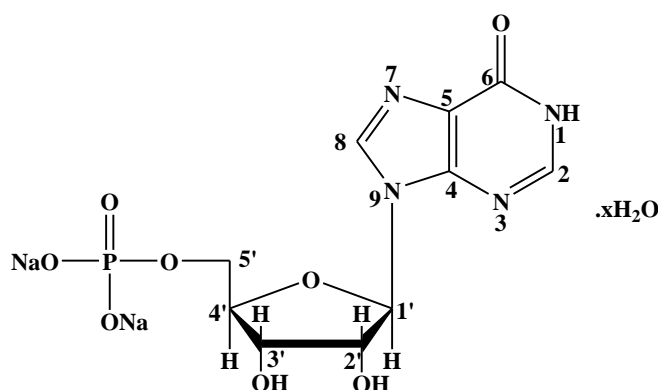
Fig. 5.1. Structure and numbering scheme of sodium salt of inosine monophosphate (5'-IMP-Na$_2$.xH$_2$O).

5.3. RESULTS AND DISCUSSION

5.3.1. Synthetic Aspects

Reaction(s) of Me$_2$SnCl$_2$, Ph$_2$SnCl$_2$, Bu$_2$SnCl$_2$ with 5'-IMP-Na$_2$.xH$_2$O (x ~ 5.5) (Eq. (5.1)) in aqueous methanol (50%) in 1:1 ratio led to the formation of new diorganotin(IV) inosinates ((**1**), (**2**) and (**3**), respectively) of general formulae, [R$_2$Sn(5'-IMP.4H$_2$O).H$_2$O]$_n$ and the *in situ* reaction(s) of Me$_2$SnCl$_2$, Ph$_2$SnCl$_2$, Bu$_2$SnCl$_2$ with 5'-IMP-Na$_2$.xH$_2$O (x ~ 5.5)

and 1,10-phenanthroline (phen) (Eq. (5.2)) in aqueous methanol (50%) in 1:1:1 ratio led to the formation of new ligand complexes ((**4**), (**5**) and (**6**), respectively) of general formulae, [R$_2$Sn(5'-IMP.5H$_2$O)(phen)]. All the complexes obtained are white or cream solids (Table 5.1) and are stable towards air and moisture. Dimethyltin(IV) inosinate complex (**1**) is sparingly soluble in hot DMSO and insoluble in all organic solvents. Mixed dimethyltin(IV) derivative of inosinate and 1,10-phenanthroline (**4**) is insoluble in all organic solvents. Complexes (**2**), (**3**), (**5**) and (**6**) are readily soluble in hot DMSO, but insoluble in other organic solvents.

$$R_2SnCl_2 + 5'\text{-IMP-}Na_2 . xH_2O \xrightarrow{\text{H}_2\text{O:MeOH (1:1)}} [R_2Sn(5'\text{-IMP}.4H_2O).H_2O]_n + 2NaCl \quad (5.1)$$
(Where, R = Me, Ph, Bu; 5'-IMP-Na$_2$.xH$_2$O = 5'-Inosine monophosphate disodium salt hydrate, x ~ 5.5; n > 2)

$$R_2SnCl_2 + 5'\text{-IMP-}Na_2 . xH_2O \xrightarrow{\text{H}_2\text{O:MeOH (1:1) /phen}} [R_2Sn(5'\text{-IMP}.5H_2O)(phen)] + 2NaCl \quad (5.2)$$
(Where, R = Me, Ph, Bu; 5'-IMP-Na$_2$.xH$_2$O = 5'-Inosine monophosphate disodium salt hydrate, x ~ 5.5; phen = 1,10-phenanthroline)
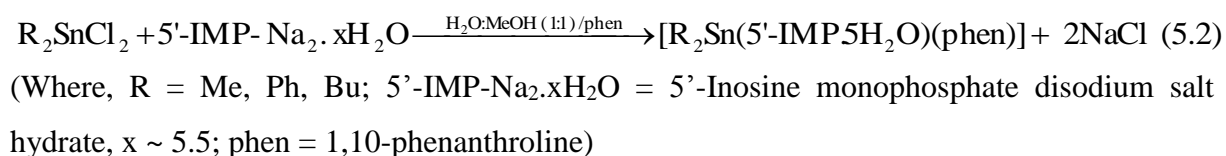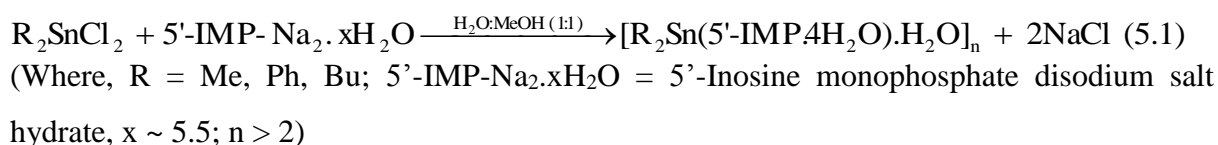
All the complexes were decomposed instead of melting, indicating their polymeric nature. The analytical data of all the synthesized derivatives suggests that the diorganotin inosinate complexes (**1**), (**2**) and (**3**) are crystallized in 1:1 stoichiometry (Table 5.1) with 5 H$_2$O molecules. It has been proposed that one water molecule is involved in coordination with the tin atom and four water molecules of the ligand (5'-IMP.xH$_2$O; x ~ 5.5) staying intact (on the basis of spectral studies discussed in the later sections), whereas the mixed diorganotin(IV) derivatives of inosinate and 1,10-phenanthroline (**4**), (**5**) and (**6**) were observed in 1:1:1 stoichiometry (Table 5.1) with five ligand water molecules remaining intact.

Table 5.1. Characteristic Physical Properties and Analytical Data of Diorganotin(IV) Derivatives of (5'-IMP)$^{2-}$ and Their Mixed 1,10-Phenanthroline Complexes

Complex No.	Complex (Empirical Formula)	Color & Physical state	Yield (%)	Decomposition temperature (°C)	Analysis (%) Observed (Calculated)			
					C	H	N	Sn
1.	[Me$_2$Sn(5'-IMP.4H$_2$O).H$_2$O]$_n$ (C$_{12}$H$_{27}$N$_4$O$_{13}$PSn)$_n$	White solid	85	178–180	23.95 (24.64)	4.62 (4.65)	9.26 (9.58)	19.43 (20.29)
2.	[Ph$_2$Sn(5'-IMP.4H$_2$O).H$_2$O]$_n$ (C$_{22}$H$_{31}$N$_4$O$_{13}$PSn)$_n$	Cream solid	75	170–175	36.42 (37.26)	4.58 (4.41)	7.98 (7.90)	15.95 (16.74)
3.	[Bu$_2$Sn(5'-IMP.4H$_2$O).H$_2$O]$_n$ (C$_{18}$H$_{39}$N$_4$O$_{13}$PSn)$_n$	White solid	77	280–282	31.25 (32.31)	5.29 (5.87)	8.70 (8.37)	18.50 (17.74)
4.	[Me$_2$Sn(5'-IMP.5H$_2$O)(phen)] (C$_{24}$H$_{35}$N$_6$O$_{13}$PSn)	White solid	31	180–182	37.70 (38.37)	4.68 (4.70)	9.23 (9.32)	16.95 (15.80)
5.	[Ph$_2$Sn(5'-IMP.5H$_2$O)(phen)] (C$_{34}$H$_{39}$N$_6$O$_{13}$PSn)	White solid	48	238–240	45.56 (46.65)	4.26 (4.49)	8.48 (8.00)	14.59 (13.56)
6.	[Bu$_2$Sn(5'-IMP.5H$_2$O)(phen)] (C$_{30}$H$_{47}$N$_6$O$_{13}$PSn)	White solid	33	240–242	44.37 (43.13)	6.40 (5.67)	9.45 (8.38)	15.92 (14.21)

5.3.2. IR and Far IR Spectroscopy

Table 5.2 presents the characteristic infrared and far-infrared frequencies (cm^{-1}) of the titled complexes and ligands. Some representative IR spectra of the studied complexes are presented in Figs. 5.2 and 5.3. In the IR spectra of all the complexes, the $\nu(OH)$ in 3414–3321 cm^{-1} region are broadened due to the presence of water molecules which may result in various degrees of hydrogen bonding. In all the complexes, a sharp band at 1685 ± 5 cm^{-1} corresponding to $\nu(C=O)$ of hypoxanthine unit of $(IMP)^{2-}$ is shifted towards higher frequencies (0–10 cm^{-1}) as compared to that of the ligand (1680 cm^{-1}). The high frequency shift is attributed to the intermolecular hydrogen bonding of water molecules with the carboxyl oxygen group ($(C=O)\cdots H–O$). The $\nu(CO)$ of ribose of $(IMP)^{2-}$ unit shows significant shifts in the range 1259–1209 cm^{-1} in all the complexes, attributed to the change in ribose conformation. The in plane C–H vibrations of phenanthroline ring in the mixed diorganotin(IV) derivatives (**(4), (5)** and **(6)**) show significant shifts in the region 1217–1127 cm^{-1}, which can be attributed to phenanthroline ring deformation. Further, the $\nu(ring)$ characteristic of the ribose pucker (~ 850 cm^{-1} [38]) shows a considerable shift in the range 896–826 cm^{-1}, suggesting that the ribofuranose of $(IMP)^{2-}$ is involved in complexation with tin. The shifts in the asymmetric and symmetric stretching frequencies of phosphate group ($\nu_{as}(PO_3)^{2-}/\nu_{s}(PO_3)^{2-}$) of ribofuranose at 1090–900 cm^{-1} indicate the bonding of phosphate group with the organotin moiety. Further, the appearance of the new $\nu(Sn–O– Sn)/\nu(Sn–O)$ bands at 551–508 cm^{-1} in all the complexes and $\nu(Sn–N)/\nu(Sn\leftarrow N)$ at 508–453 cm^{-1} in complexes **(4), (5)** and **(6)**, indicate that the coordination occurs possibly *via* oxygen of $(PO_3)^{2-}$ of $(IMP)^{2-}$ moiety and nitrogen of phenanthroline moiety, respectively. Very weak to medium Sn–C bond frequencies in the ranges 695–603 cm^{-1} ($\nu_{as}(Sn–C)$) and 607–558 cm^{-1} ($\nu_{s}(Sn–C)$) for **(1), (3), (4)** and **(6)** complexes, and in the ranges 289–210 cm^{-1} ($\nu_{as}(Sn–C)$) and 273–211 cm^{-1} ($\nu_{s}(Sn–C)$) in far IR region for **(2)** and **(5)** demonstrate a modest prospect of *cis*-disposition of alkyl/aryl groups around tin. The ring deformation peaks in ranges 427–416 cm^{-1} for complexes **(4), (5)** and **(6)** clearly shows the conformational changes in the phenanthroline ring moiety.

5.3.3. NMR Spectroscopy

The ^{1}H, ^{13}C and ^{119}Sn NMR spectra of the studied complexes were recorded in DMSO-*d6* solvent and the data are presented in Tables 5.3, 5.4 and 5.5, respectively. Some

Table 5.2. IR and Far-IR Spectral Data of Diorganotin(IV) Derivatives of (5'-IMP)$^{2-}$ and Their Mixed 1,10-Phenanthroline Complexes in KBr (v/cm^{-1})
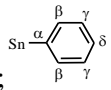
Ligand/Complex[a]	v(OH)	v(C=O)	v(C=N)/ v(C=C)/ v(ring)	v(C–O)/ v(C–N)/ $v_{inplane}$(C–H)/ v_{as}(PO$_3$)^{2}/ v_s(PO$_3$)$^{2-}$	$v_{outplane}$ (ring)	v_{as}(Sn–C)/ v_s(Sn–C)	v(Sn–O)/ v(Sn–O–Sn)	v(Sn–N)/ v(Sn←N)	ring deform-ation
5'-IMP-Na$_2$	3355 sbr	1680 s	1592 s, 1549 s, 1477 s, 1422 s, 1374 m, 1337 m	1218 s, 1069 br	827 m, 704 m	–	–	–	–
phen	–	–	1619 s, 1599 s, 1502 s, 1416 s, 1345 sh	1210 m, 1137 m	849 s	–	–	–	409 m
1.	3406 br	1688 s	1590 s, 1547 s, 1516 s, 1418 s, 1380 m,	1206 m, 1128 mbr, 1001sbr	896 m, 792 s	633 s, 558 s	524 m, 492 w	–	–

117

Contd.

			1345 m						
2.	3414 br	1690 s	1537m, 1515m, 1459 m, 1421m, 1377 m, 1348 m	1209 w, 1127 s, 1020 s, 903 w	826 m, 741 m	289 s, 210 m	508 m, 455 w	–	–
3.	3411 br	1693 s	1533 sh, 1483s, 1401 s	1231m, 1177m, 1129 m, 1075m, 1045 m, 1008 m	825 w, 777 m	603 w, 585 w	508 w, 446 m	–	–
4.	3335 br	1681 sbr	1591 s, 1548 s, 1519 s, 1478 s, 1422 s, 1374 s	1259 sh , 1217 s, 1060 mbr, 979 w	828 s	635 w, 594 w	515 s	490 w	416 s

Contd.

5.	3424 br	1685 s	1630 m, 1588 s, 1516sh, 1405 s, 1341 sh	1209 m, 1126 s, 1012 s, 900 w	833 m, 726 m	273 m, 211 m	509 m	453 m	416 m
6.	3339 br	1688 s	1627 sh, 1558 s, 1427 s, 1376 s, 1338 sh	1218 m, 1176s, 1126 s, 1090 mbr	882 mbr, 787 m	695 m, 607 m	551 m	508 s	427 m

ᵃ Complex number as indicated in Table 5.1; phen = 1,10-phenanthroline; s: strong; br: broad; m: medium; sh: shoulder; w: weak

Table 5.3. ^{1}H NMR Spectral Data of Diorganotin(IV) Derivatives of (5'-IMP)$^{2-}$ and Their Mixed 1,10-Phenanthroline Complexes

Ligand/ Complex[a]	δ ppm (DMSO-*d6*)
5'-IMP-Na$_2$	10.64 s, 1H (N1-H); 8.27 s, 1H (H-2); 7.94 s, 1H (H-8); 5.87 s, 1H (H-1'); 5.45 s, 1H (OH-2'); 5.10 s, 1H (OH-3'); 4.50 s, 1H, (H-2'); 4.18 s, 1H, (H-3'); 4.00 s, 1H, (H-4'); 3.92, 3.79 s, 2H, (H-5').
phen	9.17 s, 2H, (H-2, H-9); 8.76 s, 2H, (H-4, H-7); 8.44 s, 2H, (H-5, H-6) 7.26 s, 2H, (H-3, H-8).
1.	IMP unit: 12.44 s, 1H (N1-H); 8.31 s, 1H (H-2); 7.95s, 1H (H-8); 5.89 s, 1H (H-1'); 5.56–5.07 sbr, 2H (OH-2', OH-3'); 4.60 s, 1H (H-2'); 4.19 s, 1H, (H-3'); 4.10 s, 1H, (H-4'); 4.00, 3.41 s, 2H (H-5');) 3.16 s, 10H (H$_2$O); Sn-methyl: 0.93 m, 6H, ^2J = 106.02 Hz, θ = 175.53°.
2.	IMP unit: 12.38 s, 1H (N1-H); 8.28 s, 1H (H-2); 7.98 s, 1H (H-8); 5.90 s, 1H, (H-1'); 5.54– 5.46 sbr, 2H (OH-2', OH-3'); 4.57 s, 1H, (H-2'); 4.13 s, 1H, (H-3'); 4.00 s, 1H, (H-4'); 3.36–3.59 m, 2H (H-5'); 3.35 s, 10H (H$_2$O); Sn-phenyl: 7.19-8.25 m, 10H (H-β, H-γ, H-δ).
3.	IMP unit: 12.35 s, 1H (N1-H); 8.27 s, 1H (H-2); 8.00 s, 1H (H-8); 5.87 s, 1H, (H-1'); 5.66– 5.14 sbr, 2H (OH-2', OH-3'); 4.55 s, 1H, (H-2'); 4.15 s, 1H, (H-3'); 4.08 s, 1H, (H-4'); 3.98 m, 2H (H-5'); 3.30 s, 10H (H$_2$O); Sn-butyl: 0.53-1.72 m, 18H (H-α, H-β, H-γ, H-δ).
5.	IMP unit: 12.37 s, 1H (N1-H); 8.05 s, 1H (H-2); 7.92 s, 1H (H-8); 5.89 s, 1H, (H-1'); 5.56, 5.52 sbr, 2H (OH-2', OH-3'); 4.57 s, 1H, (H-2'); 4.11 s, 1H, (H-3'); 4.09 s, 1H, (H-4'); 4.04, 4.03 s, 2H (H-5'); 3.34 s, 10H (H$_2$O); phenanthroline unit: 9.10 s, 2H, (H-2, H-9); 8.51, 8.49 s, 2H (H-4, H-7); 8.00 m, 2H (H-5, H-6); 7.84, 7.78 s, 2H (H-3, H-8); Sn-phenyl: 7.21-7.44 m, 10H (H-β, H-γ, H-δ).

Contd.

6. IMP unit: 12.34 s, 1H (N1-H); 8.14 s, 1H (H-2); 7.83 s, 1H (H-8); 5.87 s, 1H, (H-1'); 5.66, 5.12 s, 2H (OH-2', OH-3',); 4.48 s, 1H, (H-2'); 4.15 s, 1H, (H-3'); 4.08 s, 1H, (H-4'); 3.99, 3.31 2H (H-5'); 3.30 s, 10H (H$_2$O); phenanthroline unit: 9.15 s, 2H (H-2, H-9); 8.56, 8.54 s, 2H, (H-4, H-7); 8.27 s, 2H (H-5, H-6); 8.02, 8.00 s, 2H (H-3, H-8); Sn-butyl: 0.53-1.73 m, 18H (H-α, H-β, H-γ, H-δ).

Table 5.4. ^{13}C NMR Spectral Data of Diorganotin(IV) Derivatives of (5'-IMP)$^{2-}$ and Their Mixed 1,10-Phenanthroline Complexes

Ligand/ Complex[a]	δ ppm (DMSO-*d6*)
5'-IMP-Na$_2$	156.90 (C-6); 150.80 (C-2); 145.60 (C-4); 144.80 (C-8); 117.60 (C-5); 80.90 (C-4'); 79.10 (C-1'); 75.30 (C-3'); 74.80 (C-5'); 74.00 (C-2').
phen	149.20 (C-9, C-2); 136.75 (C-4, C-7); 125.95 (C-6, C-5); 123.23 (C-3, C-8); 132.74 (C-4a, C-6a/C-4b, C-6b).
1[b].	IMP unit: 157.83 (C-6); 155.78 (C-2); 147.67 (C-4); 137.12 (C-8); 122.07 (C-5); 86.51 (C-4'); 84.76 (C-1'); 82.12 (C-3'); 76.36 (C-2'); 71.18 (C-5'); Sn-methyl: 12.27 (C-α).
2.	IMP unit: 156.06 (C-6); 152.73 (C-2); 149.39 (C-4); 141.96 (C-8); 116.15 (C-5); 89.48 (C-4'); 84.70 (C-1'); 78.29 (C-3'); 74.27 (C-2'); 71.37 (C-5'); Sn-phenyl: 126.66 (C-α); 131.94 (C-β); 123.07, 125.72 (C-γ, C-δ).
3.	IMP unit: 155.63 (C-6); 152.90 (C-2); 147.09 (C-4); 146.06 (C-8); 113.59 (C-5); 81.11 (C-4'); 76.58 (C-1'); 75.04 (C-3'); 72.74 (C-2'); 70.00 (C-5'); Sn-butyl: 12.97 (C-α); 37.96 (C-β); 31.21, 32.91 (C-γ, C-δ).
4[b].	IMP unit: 157.21 (C-6); 154.13 (C-2); 151.73 (C-4); 136.08 (C-8); 117.02 (C-5); 86.84 (C-4'); 85.66 (C-1'); 74.17 (C-3'); 70.82 (C-2'); 61.84 (C-5'); phenanthroline unit: 149.18 (C-9, C-2); 141.13, 140.21 (C-4, C-7); 127.94 (C-6, C-5); 125.68 (C-3, C-8); 129.87 (C-4a, C-6a/C-4b, C-6b); Sn-methyl: 14.14 (C-α)
5.	IMP unit: 157.67 (C-6); 153.68 (C-2); 146.35 (C-4); 135.49 (C-8); 115.16 (C-5); 87.13 (C-4'); 86.24 (C-1'); 74.90 (C-3'); 70.98 (C-2'); 65.81 (C-5'); phenanthroline unit: 147.19 (C-9, C-2); 138.38 (C-4, C-7); 135.38 (C-6, C-5); 135.19 (C-3, C-8); 128.02 (C-4a, C-6a/C-4b, C-6b); Sn-phenyl: 128.24 (C-α),

Contd.

130.06 (C-β), [c]129.06 (C-γ, C-δ).

6. IMP unit: 158.45 (C-6); 152.64 (C-2); 148.02 (C-4); 144.60 (C-8); 119.14 (C-5); 89.83 (C-4'); 86.07 (C-1'); 77.18 (C-3'); 76.41 (C-2'); 72.48 (C-5'); phenanthroline unit: 141.44 (C-9, C-2); 136.06[c] (C-4, C-7, C-6, C-5); 129.05[c] (C-3, C-8, C-4a, C-6a/C-4b, C-6b); Sn-butyl: 3.26 (C-α), 37.01(C-β, C-γ), 31.38 (C-δ).

---

[a] Complex number as indicated in Table 5.1. [b] determined through solid state ^{13}C NMR at 10 KHz; [c] merged; [*]numberring of carbons are as mentioned in Fig. 5.1.; $\overset{\alpha}{-CH_3}$; $\overset{\alpha}{-}CH_2\overset{\beta}{-}CH_2\overset{\gamma}{-}CH_2\overset{\delta}{-}CH_3$; ; phen = 1,10-phenanthroline
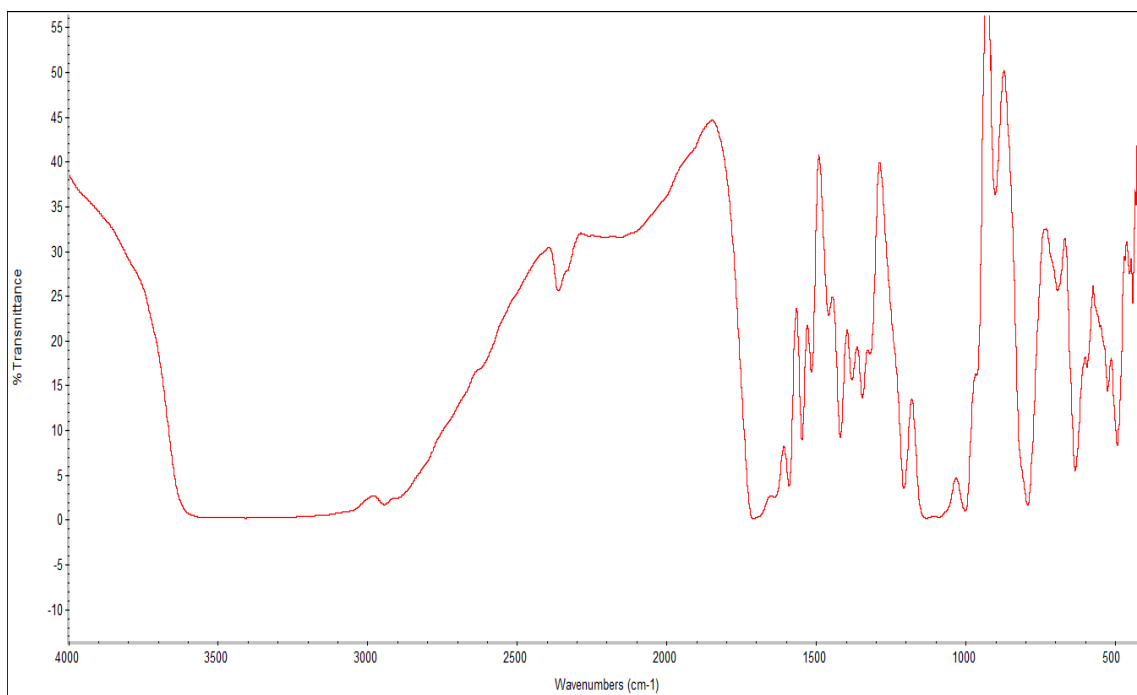
Fig. 5.2. IR spectrum of dimethyltin(IV) inosinate.
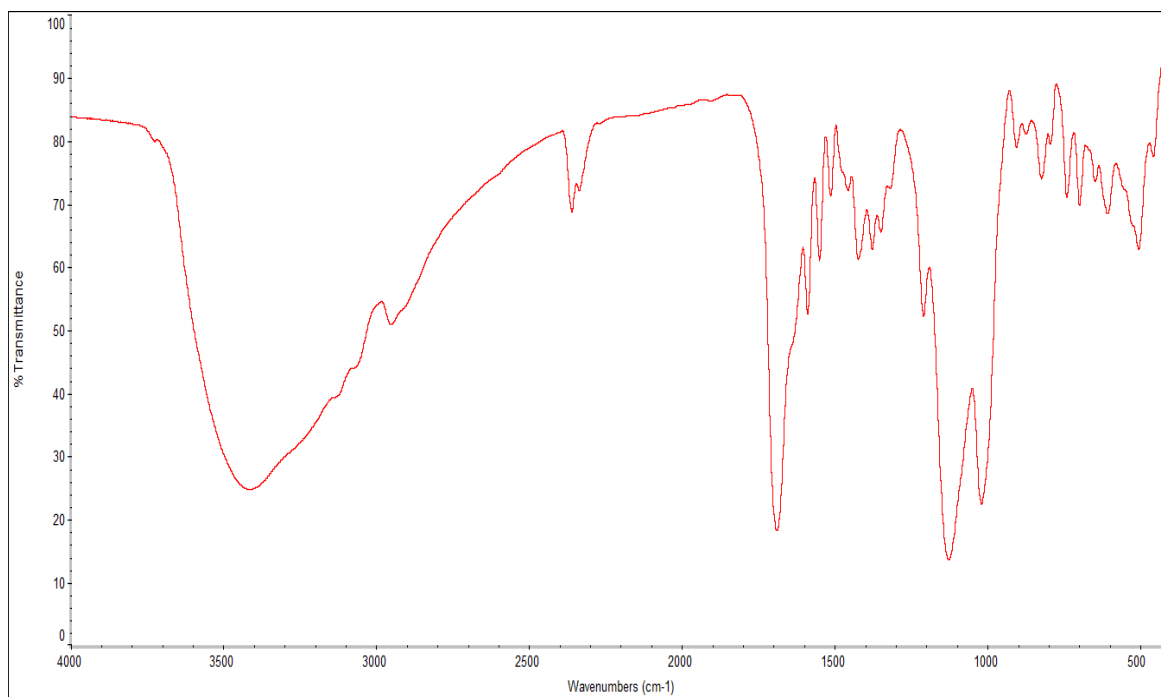
Fig. 5.3. IR spectrum of diphenyltin(IV) inosinate.
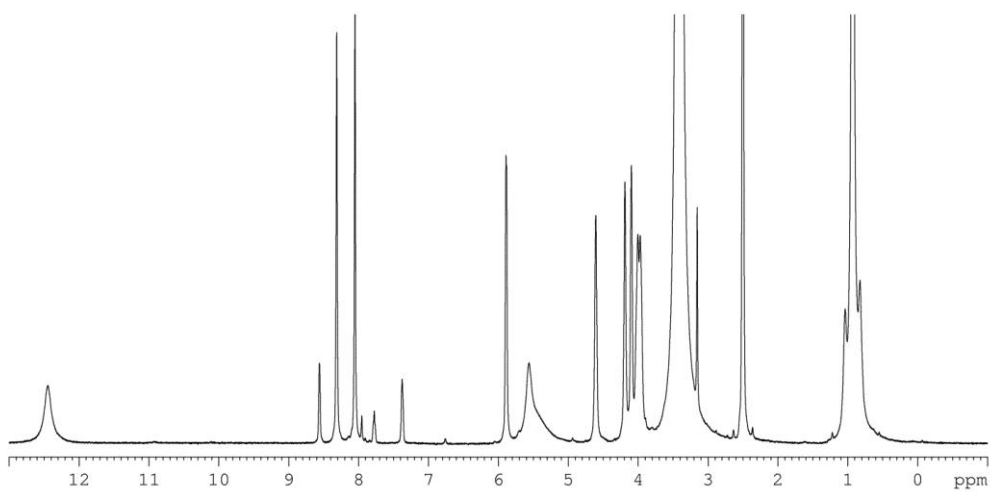
Fig. 5.4. ¹H NMR spectrum of dimethyltin(IV) inosinate.
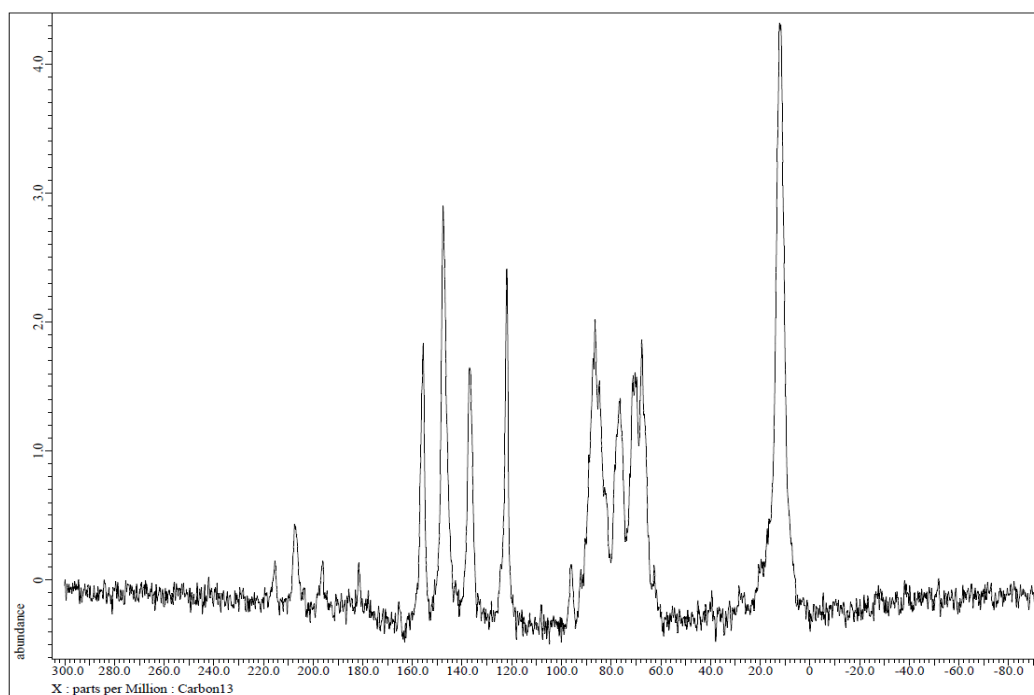
Fig. 5.5. Solid state ¹³C NMR spectrum of dimethyltin(IV) inosinate.

125
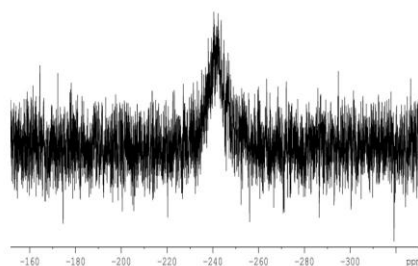
Fig. 5.6. ^{119}Sn NMR spectrum of mixed diphenyltin(IV) derivative of $(5'\text{-}IMP)^{2-}$ and 1,10-phenanthroline.

representative ^{1}H, ^{13}C and ^{119}Sn NMR spectra of the titled complexes are presented in the Figs. 5.4, 5.5 and 5.6. Complex **(1)** is sparingly soluble in DMSO-*d6*, therefore, only the solution state ^{1}H NMR could be recorded. Complex **(4)** is insoluble in all the organic solvents, therefore, acquisition of ^{1}H NMR spectra could not be obtained. The chemical shifts of the protons are observed at the expected position as compared to the ligands, 5'-IMP-Na$_2$ and 1,10-phenanthroline. The N(1)H chemical shift of (5'-IMP) base moiety drifted downfield (δ 12.34 –12.44 ppm) indicating the hydrogen bonding with water molecules. The H-2 ($\sim \delta$ 8.31 ppm) and H-8 ($\sim \delta$ 7.95 ppm) showed almost negligible downfield shift for diorganotin(IV) inosinate derivatives, where as a minor upfield shift is observed for the mixed diorganotin(IV) derivatives of $(5'\text{-}IMP)^{2-}$ and phenanthroline. Similarly, a negligible downfield shift for H-1' proton ($\sim \delta$ 5.87 ppm) is observed indicating the non-involvement of base unit in complex formation. The (OH-2') and (OH-3') hydroxyl protons chemical shifts of the ribose sugar were broadened. All the furanose ring protons are observed at respective chemical shifts, but the H-5' resonances are shifted considerably indicating the involvement of $(PO_3)^{2-}$ group in bonding with organotin moiety. The phenanthroline ring proton resonances in complexes **(4)**, **(5)** and **(6)** underwent upfield shift indicating that electron fluctuation might have occurred due to reorganization to form new Sn–N (phen) bond. The alkyl/aryl-Sn resonances are appeared in multiplet pattern for all the complexes, hence, ^2J $[^{119}Sn\text{-}^1H]$ could not be resolved except for the complex **(1)** (dimethyltin(IV) inosinate), where the heteronuclear coupling constant ^2J $[^{119}Sn\text{-}^1H]$ is determined to be 106.02 Hz and the C–Sn–C bond angle is calculated ($\theta = 175.53°$) using Lockhart and Manders equation [123].

126

(a)
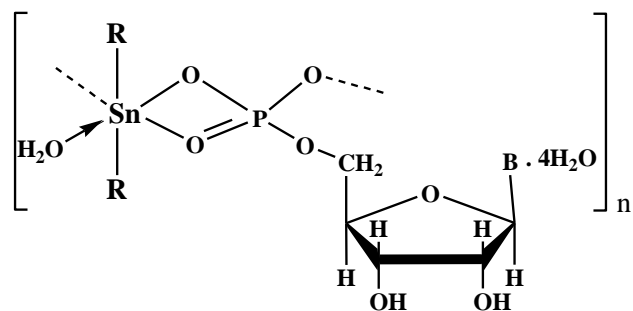
B = Hypoxanthine

(i)
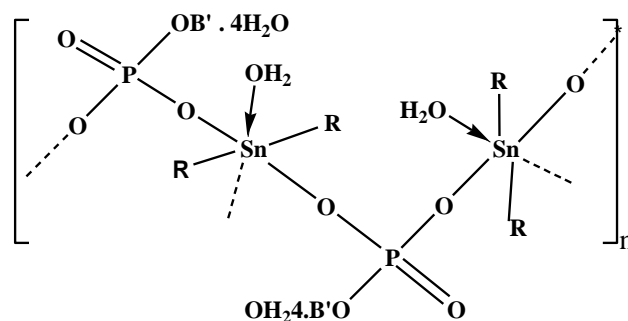
B' = inosine

(ii)

(b)
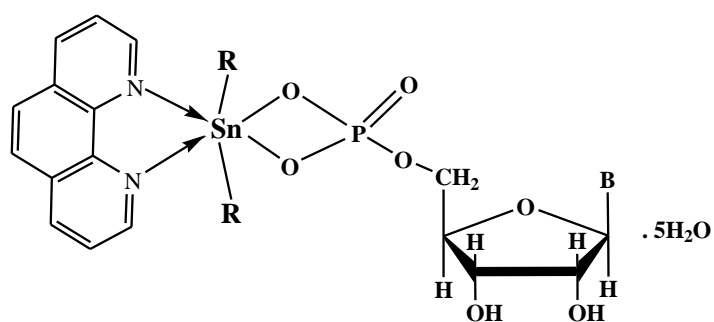
B = Hypoxanthine

Fig. 5.7. Proposed structures of: (a) (i) and (ii) diorganotin(IV) inosinate derivative, (b) mixed diorganotin(IV) derivative of (5'-IMP)$^{2-}$ and 1,10-phenanthroline.

127

Due to low solubility, the ^{13}C NMR spectra of complexes **(1)** and **(4)** are obtained by using solid state NMR spectroscopy at 10 KHz in a 4 mm diameter tube. The ^{13}C NMR spectral data suggests that a negligible shift is observed for all base carbon atoms but, a considerable shift is observed for the ribose carbon atoms especially for C-5', further confirms the involvement of phosphate group of furanose ring in bonding with the tin. The ^{119}Sn NMR spectra of complexes **(1)** and **(4)** could not be recorded owing to their poor solubility in all the solvents. The ^{119}Sn NMR chemical shifts of complexes **(2)**, **(3)**, **(5)** and **(6)** are observed at δ –240.49, –270.02, –219.62 and –284.76 ppm, respectively, suggesting a distorted octahedral geometry around tin [32].

5.3.4. *In Vitro* Cytotoxicity Studies

5.3.4.1. MTT assay

Owing to the poor solubility of complexes **(1)** and **(4)**, only complexes **(2)**, **(3)**, **(5)** and **(6)** have been screened for *in vitro* anti-tumor activity against two cancer cell lines of human origin, *viz*. MCF7 (mammary), HepG2 (liver). The inhibitory concentration (IC$_{50}$) values are calculated for the titled complexes using best fit linear regression model [35]. Table 5.6 presents the IC$_{50}$ values of the studied complexes along with the standard reference drugs, *cis*-platin (CPT) and 5-fluorouracil (5-FU). From the table 5.6, it can be inferred that the test compounds **(3)**, **(5)** and **(6)**) are found to be much more active against MCF7 cell lines compared to that of *cis*-platin, in fact their activities are comparable to that of 5-fluorouracil. The complex **(2)** is slightly more active against MCF7 as compared to that of *cis*-patin but it shows very less activity in comparison to 5-fluorouracil. The dibutyltin(IV) complexes **(3)** and **(6)** are found to be very active against HepG2 cell lines in comparison to that of *cis*-platin but they show comparable activity with respect to 5-fluorouracil. The IC$_{50}$ values of the diphenyltin(IV) complexes **(2)** and **(5)** against HepG2 cell line are found to be above 40 µg/mL, hence considered to be inactive for the reason unknown. The presence of phenanthroline moiety induces the cytotoxicity, hence, the mixed complexes **(5)** and **(6)** are more active compared to that of respective diorganotin(IV) inosinates. However, the dibutyltin(IV) inosinate **(3)** is found to be the most active complex against both (MCF7 and HepG2) cell lines.

Table 5.5. ^{119}Sn NMR Spectral Data of Diorganotin(IV) Derivatives of (5'-IMP)$^{2-}$ and Their Mixed 1,10-Phenanthroline Complexes

Complex[a]	δ ppm (DMSO-*d6*)
2.	−240.49
3.	−270.02
5.	−219.62
6.	−284.76

[a] Complex number as indicated in Table 5.1; ^{119}Sn NMR complexes **(1)** and **(4)** could not be determined due to low solubility.

Table 5.6. Screening of Diorganotin(IV) Derivatives of (5'-IMP)$^{2-}$ and Their Mixed 1,10-Phenanthroline Complexes for their *In Vitro* Cytotoxic Properties (MTT assay). The Results are Expressed as IC$_{50}$ (μg/mL ± SEM) Values

Complex[a]/Drug	MCF7	HepG2
2.	23.31 ± 9.19	> 40.0
3.	1.05 ± 0.70	5.45 ± 1.88
5.	2.62 ± 1.89	> 40.0
6.	1.15 ± 0.79	6.80 ± 2.49
cis-**platin**	15.79 ± 0.10	12.83 ± 0.10
5-Fluorouracil	< 4.97	< 4.97

[a] Complex number as indicated in Table 5.1. IC$_{50}$ < 4 μg/mL: most active; IC$_{50}$ in between 4 – 40 μg/mL moderately active; IC$_{50}$ > 40 μg/mL: inactive [35].

5.3.4.2. Acridine orange assay

The cancer MCF7 cells were incubated with the IC_{50} value of the test compounds (**3**) and (**6**) and the vehicle control (DMSO). As already mentioned in chapter **4**, depending upon the percentage intake of Acridine orange AO/Ethidium bromide EB stains, the live and apoptotic cells can be distinguished [35]. AO permeates all the live cells hence appear green; where as the EB is taken up only by the cells which have lost their cytoplasmic membrane integrity, therefore appear red [35]. The acridine orange assay results of the control, complexes (**3**) and (**6**) are represented in the Figs. 5.8 (a), 5.8 (b) and 5.8 (c), respectively. From the Figs. 5.8 (a), 5.8 (b) and 5.8 (c), it can be clearly observed that the live cells with green nucleus were predominant in the control compared to that of the test compounds. Out of both the test compounds, it has been observed that the apoptotic cells are substantial for complex (**3**) (dibutyltin(IV) inosinate) compared to that of mixed complex (**6**) ($Bu_2Sn(5'$-$IMP.5H_2O)(phen)$). Therefore, apoptosis is the main cause for the cytotoxicity of the test compounds. Along with the apoptosis, a small amount of necrosis can also be considered.

5.3.4.3. Comet assay

The nuclei of MCF7 cells treated with the test compounds ((**3**) and (**6**)) alongside the control were stained with EB and visualized under fluorescent microscope. Figs. 5.9 (a), 5.9 (b) and 5.9 (c) represents the single cell gel (alkaline) electrophoresis showing DNA fragmentation in MCF7 cell treated with the control, test compounds (**3**) and (**6**), respectively. The fragmentation or DNA disintegration in an individual cell is observed as comet tails [35]. However, vehicle (control) treated cells do not show any fragmentation. This also confirms that the cytotoxicity of complexes (**3**) and (**6**) is mainly due to apoptosis.

(a)   **(b)**
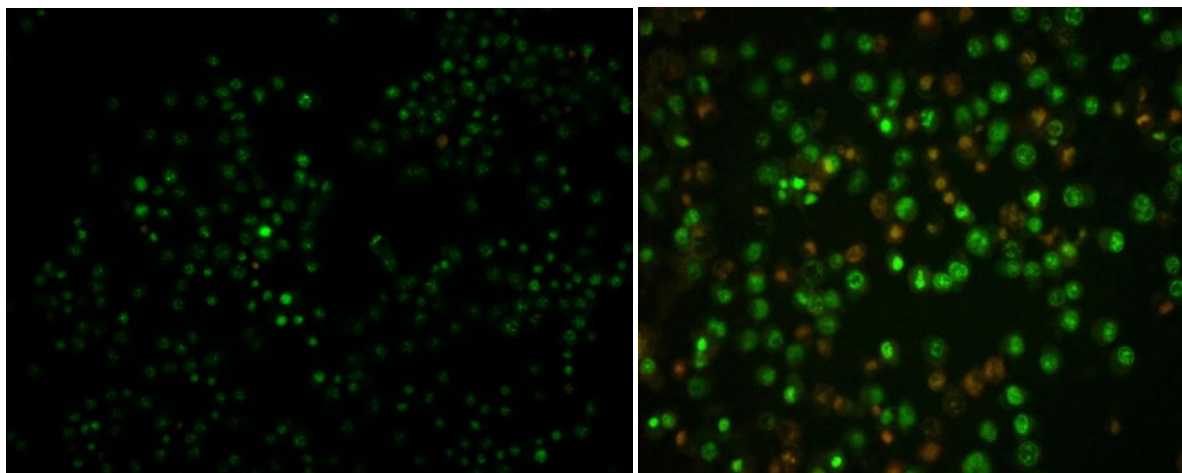
(c)
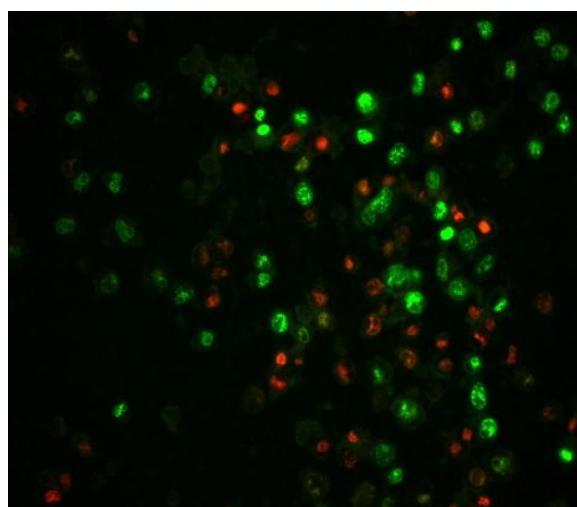
Fig. 5.8. Acridine orange assay for: (a) control, (b) complex (3), and (c) complex (6), treated MCF7 cells. Green and orange colors indicate live and apoptotic cells, respectively.

(a)   **(b)**
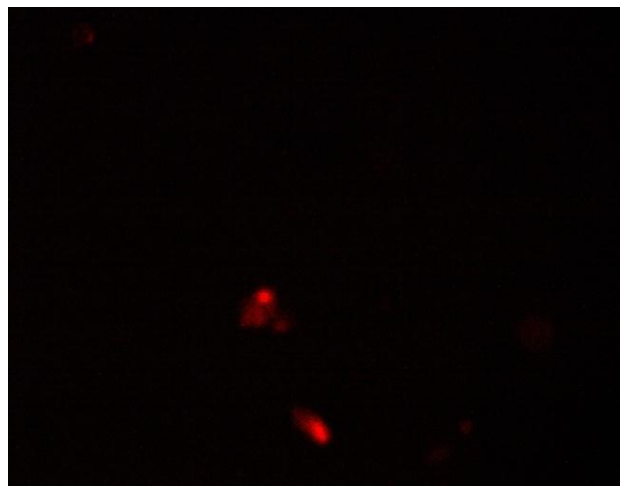
(c)
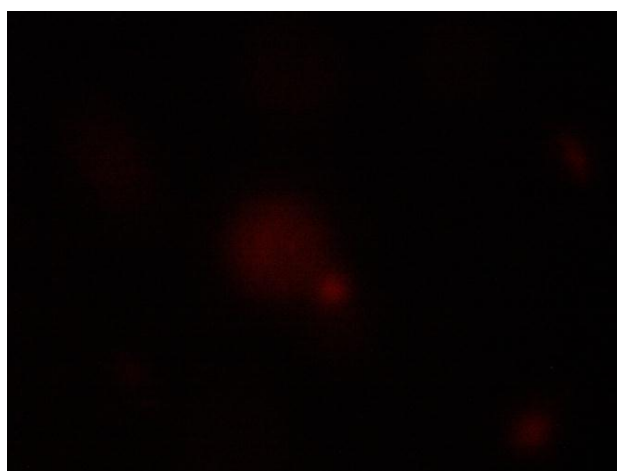
Fig. 5.9. Comet assay for: (a) control, (b) complex (3), and (c) complex (6), treated MCF7 cells.
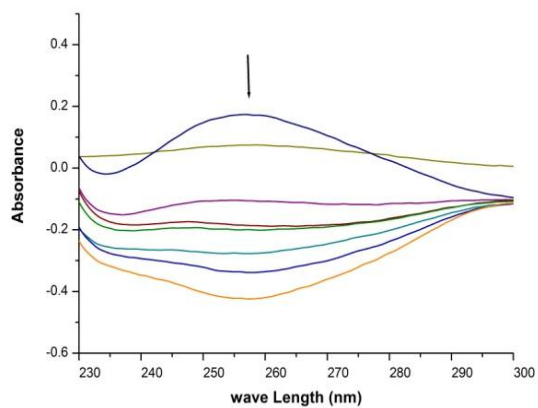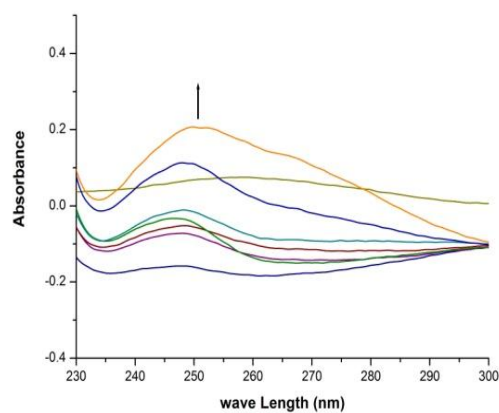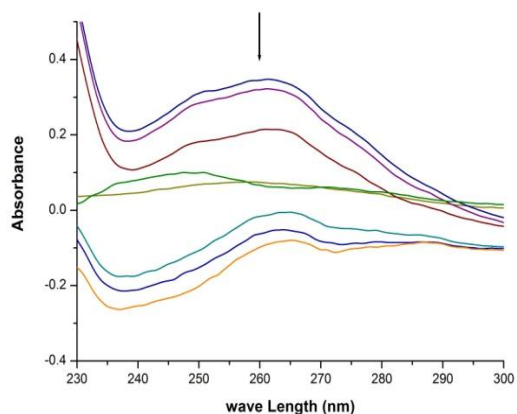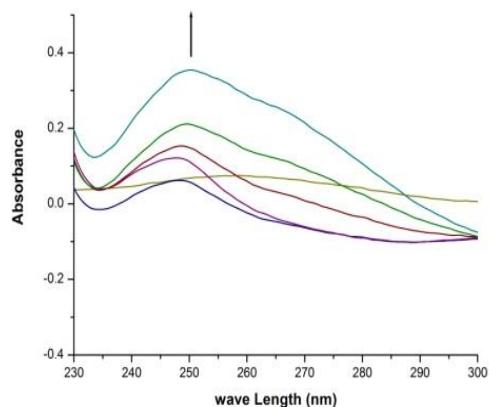
Fig. 5.10. Variation of UV-visible absorption for complexes (2): (a), (3): (b), (5): (c), and (6): (d), with increase in the concentration of CT DNA (2–20 × 10^{-5} M) in buffer (5 mM Tris–HCl/50 mM NaCl, pH = 7.2) at room temperature; [Complex] = 2 × 10^{-5} M. Arrows indicate increment or decrement in absorbance.

(a)
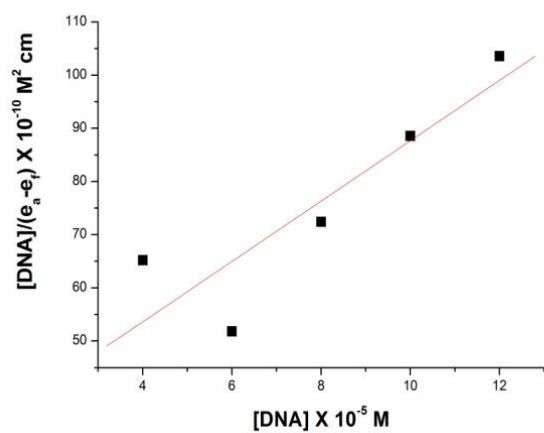
(b)
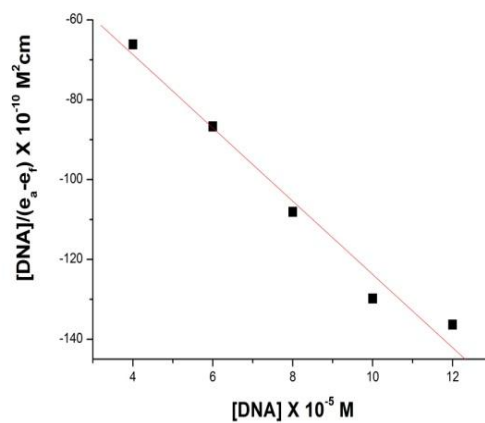
(c)
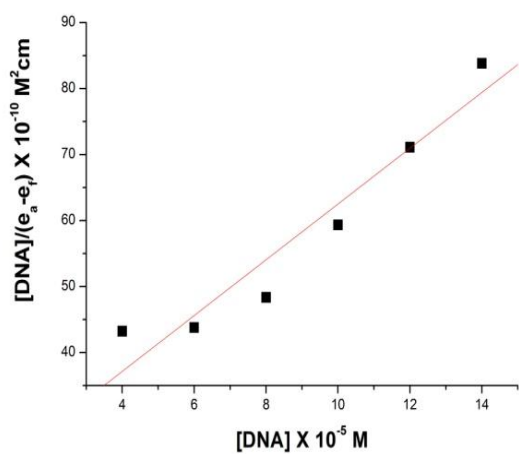
(d)
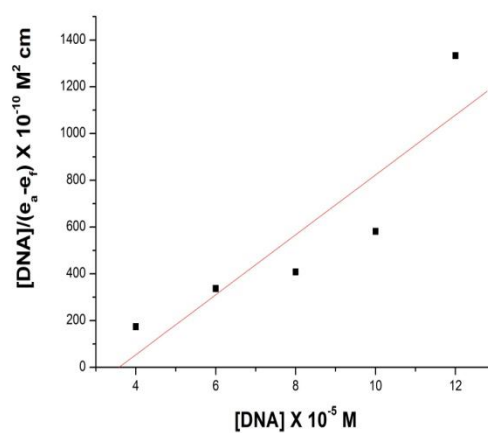
Fig. 5.11. Plots of [DNA]/(e_a – e_f) vs [DNA] for the titration of CT DNA with complex (2): (a), complex (3): (b), complex (5): (c), and complex (6): (d).

134

5.3.5. DNA Binding Studies by UV-Visible Absorption Spectrometry

The stock solutions of the complexes and the CT DNA have been prepared as mentioned in chapter **4**. The Eq. 4.3, presented in chapter **4**, is mentioned here for clarity purpose.

$$\frac{[DNA]}{|e_a - e_f|} = \frac{[DNA]}{|e_b - e_f|} + \frac{1}{|e_b - e_f|K_b} \qquad (4.3)$$

The UV-Visible absorption spectra of the complexes show intense absorption bands located at 245–275 nm and 200–210 nm which corresponds to n–π^* and π–π^* transitions, respectively [41, 88, 89, 91, 133]. Upon increasing the concentration of CT DNA, a significant decrease in the absorptivity (hypochromic effect) with apparent red shift (~ 2 nm) was observed (as shown in Fig. 5.10) for complexes (**2**) and (**5**) suggests that the complex can unwind DNA helix and leads to the loss of helicity, perturbing the secondary structure of DNA [41, 88, 89, 91, 133]. The presence of two planar phenyl groups in complexes (**2**) and (**5**) induces steric effects which also promote partial intercalative binding of complexes to DNA. The hyperchromic effect and strong perturbations in the absorption peaks of the complexes (**3**) and (**6**) indicate the electrostatic binding with DNA and may arise due to the preferential binding of the Sn(IV) to dinegative phosphate group of DNA backbone due of its hard Lewis acidic property [41, 88, 89, 91, 133]. The presence of planar 1,10-phenanthroline moiety in complexes (**5**) and (**6**) also accounts for the intercalation of the complex with DNA. The intrinsic binding constant determined according to Eq. 4.3 for the complex (**2**) and (**3**) were found to be 4.46 ×10^5 M^{-1} and 2.88 ×10^5 M^{-1}, respectively, while for the complexes (**5**) and (**6**), it is 2.94 ×10^4 M^{-1} and 6.47 ×10^4 M^{-1}, respectively, indicating pronounced binding with DNA.

5.3.6. Fluorescence Studies

The binding of the complexes to CT DNA was studied by evaluating the fluorescence emission intensity of the ethidium bromide (EB)–DNA system upon the addition of series of concentrations of the complexes [41, 88, 89, 91, 133] from the stock solutions (preparation as mentioned in chapter **4**). The emission spectra of complexes (**2**), (**3**), (**5**) and (**6**) in the absence of DNA and presence of DNA are presented in Fig. 5.12. The excitation is done at

(a)

(b)

(c)

(d)
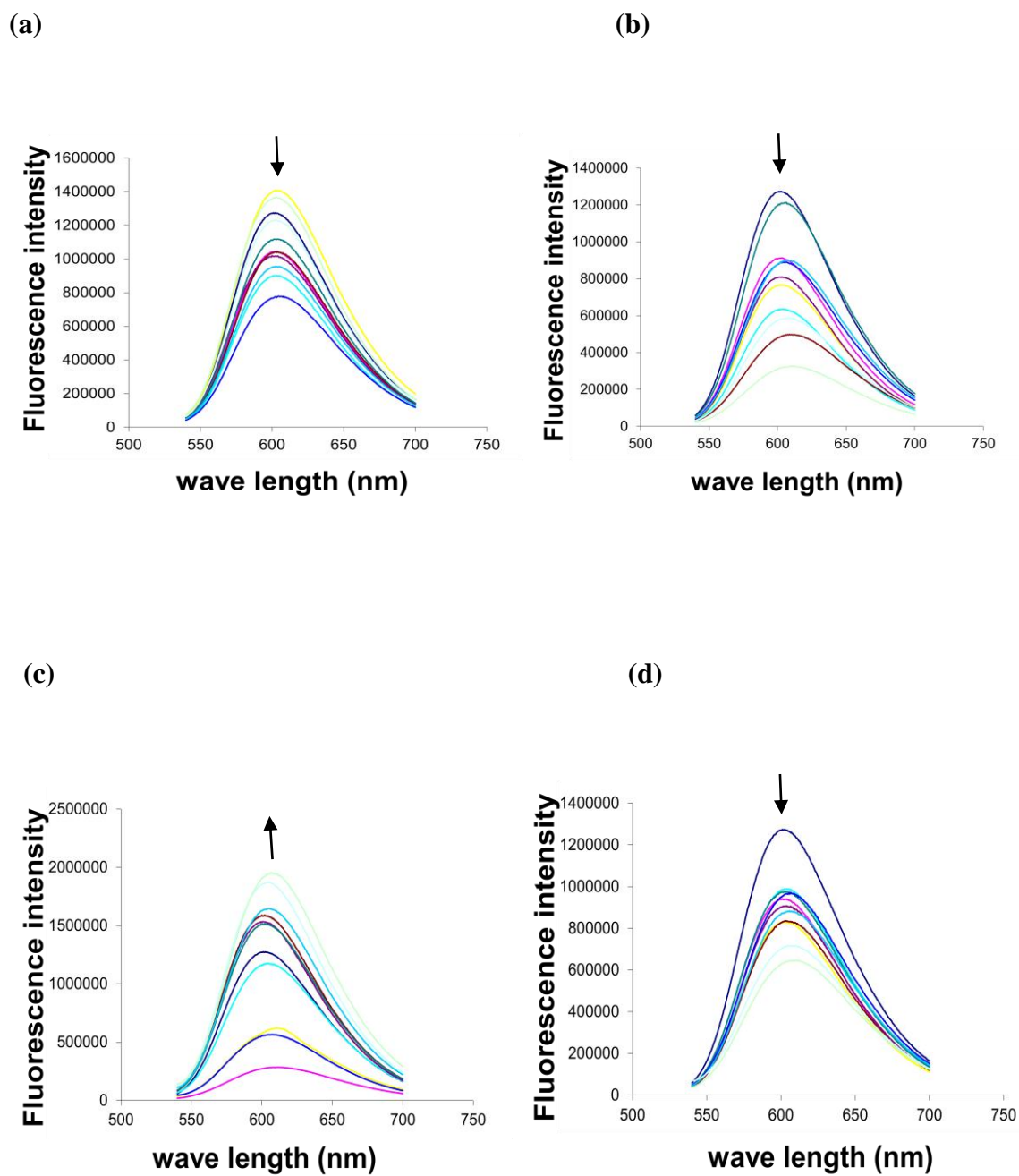
Fig. 5.12. Emission spectra of complexes (2): (a), (3): (b), (5): (c), and (6): (d), in Tris–HCl buffer (pH = 7.2) in the absence and presence of CT DNA. [Complex] = 1–10 × 10^{-5} M, [DNA] = 10^{-5} M.
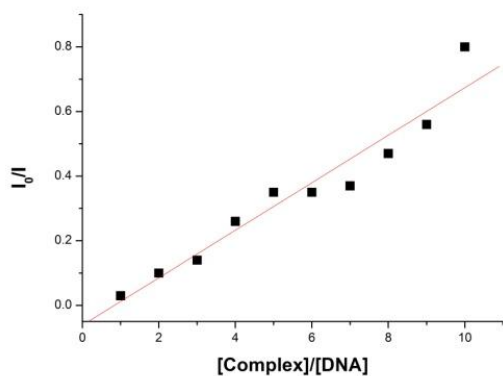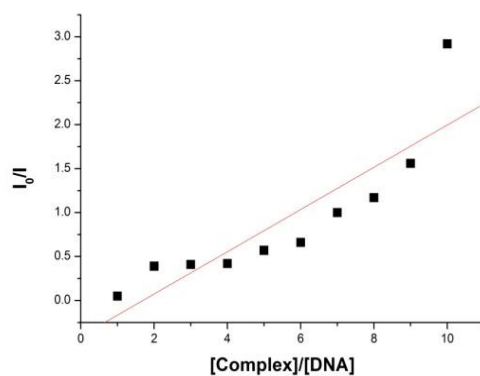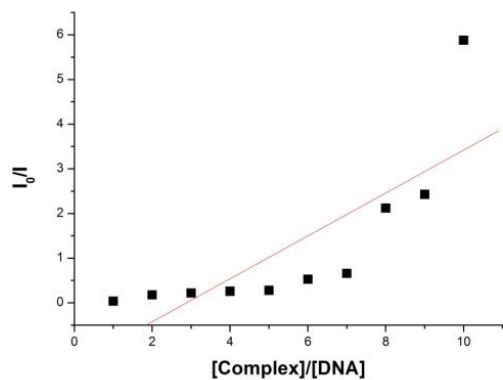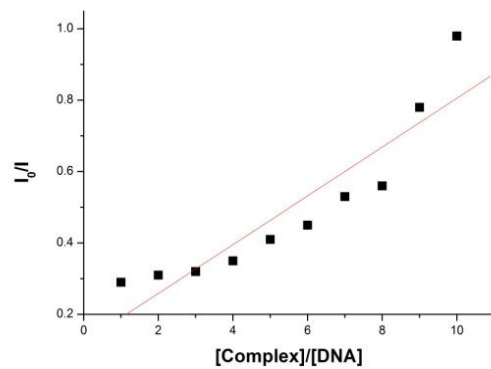
Fig. 5.13. Stern-Volmer quenching plots of EB bound to DNA with complexes (2): (a), (3): (b), (5): (c), and (6): (d), in Tris–HCl buffer (pH = 7.2) in the absence and presence of CT DNA.

430 nm and the emission wave length is 603 nm. The relative binding propensity of the complexes to CT DNA was determined by the classical Stern-Volmer equation (Eq. 4.4, from chapter **4**) [129] where, I and I_0 are fluorescence intensities in absence and presence of quencher, respectively; K_{sv} is the linear Stern-Volmer quenching constant, dependent on r_{bE} (the bound concentration of EB to the [DNA]) and r is the ratio of [quencher] to that of [DNA].

$$\frac{I_0}{I} = 1 + K_{sv}r \tag{4.4}$$

The Stern-Volmer quenching constants can be used to evaluate the nature of DNA-binding modes; a value above 10^6 M^{-1} is an indication of intercalation, while values in the range 10^4–10^5 M^{-1} imply the groove binding mode [41, 88, 89, 91, 133]. The Stern-Volmer quenching constant (K_{sv}) of complex (**2**) and (**3**) is 1.84 $\times$ 10^5 and 5.58$\times$ 10^4 M^{-1}, respectively, where as for complex (**5**) and (**6**), it is 2.70 $\times$ 10^4 M^{-1} and 1.69 $\times$ 10^5 M^{-1}. Therefore, from K_{sv} values the DNA-binding mode of all the complexes might be *via* the groove binding, however, intercalation mode is also observed slightly.

5.3.7. Gel Electrophoresis

To assess the DNA cleavage ability of the complexes (**2**), (**3**), (**5**) and (**6**), pBR322 DNA was incubated with different concentrations of the complexes (5–50 µM) in 5 mM Tris–HCl/50 mM NaCl buffer at pH 7.2, for 2.5 h. In all the complexes, upon gel electrophoresis, there is an enhancement of the intensity of form II upon increasing concentration from $r = 1$ to $r = 20$, where r = [complex]/[DNA]), a slight increase in form II is observed as depicted from Fig. 5.14. This indicates that these complexes promotes the conversion of DNA from super coiled form I to nicked circular form II [41, 88, 89, 91, 133], which clearly implicates the role of organotin(IV)s in the process of DNA cleavage.

(a)

(b)

(c)

(d)
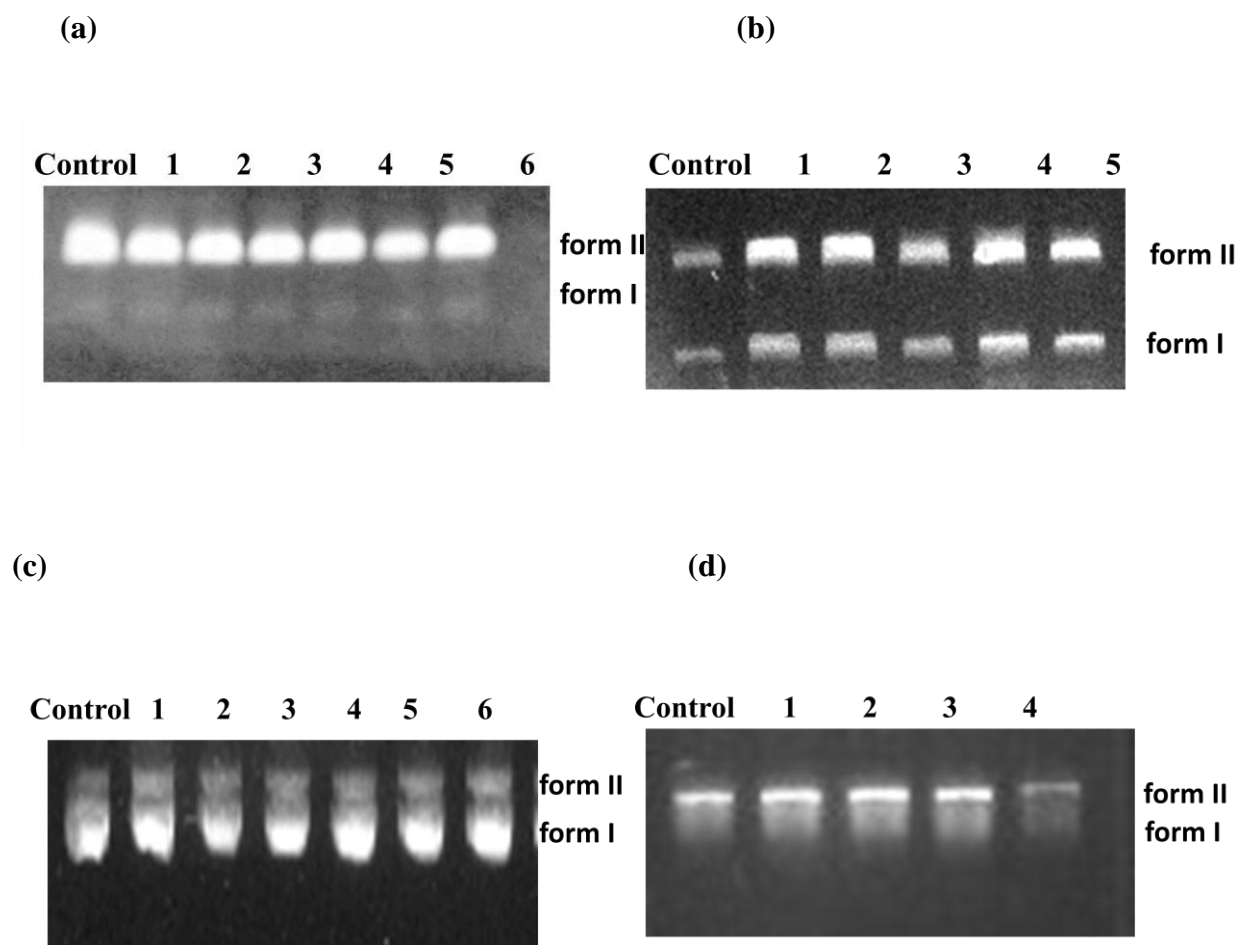
Fig. 5.14. Agarose gel (0.8%) electrophoretograms of cleavage of pBR322 DNA plasmid with complexes (2): (a), (3): (b), (5): (c), and (6): (d), respectively, incubated for 2.5 h at 37 °C in 5:50 mM Tris–HCl/NaCl buffer, pH 7.2. From left to right: DNA control; lane 1, r = 1; lane 2, r = 2; lane 3, r = 5; lane 4, r = 10; lane 5, r = 15; lane 6, r = 20; r = [Complex]/[DNA].

6.1. CONCLUSIONS

Organotin(IV)$^{n+}$ complex formation equilibria with nucleic acid constituents give information on the species formed at the physiological pH and their coordination chemistry in solution. Due to their wide distribution, biological activities and toxicity point of view, the potentiometric studies of Me$_n$Sn$^{(4-n)+}$ (where n = 2 or 3) with 5'-guanosine monophosphate (5'-HGMP)$^{2-}$ and guanosine (HGUO) in aqueous solution at 298.15 ± 0.1 K and at an ionic strength of 0.1 M of KNO$_3$ in 1:1 and 1:2 ratios have been performed. The calculated protonation constants of the ligands ((5'-HGMP)$^{2-}$ and (HGUO)) and the hydrolysis constants of di-/trimethyltin(IV) chloride(s) using the SCOGS program are found to be consistent with the literature values. The formation constants of the complex species formed in aqueous solution at different pHs are determined and the output results with a minimum standard deviation have been used to draw the speciation curves. The speciation diagram results indicate that for both1:1 Me$_2$Sn(IV)-ligand and Me$_3$Sn(IV)- ligand systems (where ligand = (5'-HGMP)$^{2-}$ and (HGUO)), M(HL) species is the major species (87 − 100%) existing between pH ~ 6.0 − 7.0 along with traces of M(HL)H$_{-1}$ (4 − 10%), M(HL)(OH) (0.2 − 3%) and M(OH)$_2$ (0.4 − 0.5%). From the multinuclear (^{1}H, ^{13}C, ^{119}Sn) NMR studies of solutions of 1:1 and 1:2 systems at different pHs, the chemical shifts, hetero nuclear coupling constants (^2J(^{1}H−$^{117/119}$Sn) and ^1J(^{13}C−$^{117/119}$Sn)), ∠C–Sn–C bond angles (calculated by using the Lockhart and Manders equation) and the possible geometries of various species are proposed. On the basis of multinuclear NMR data, M(HL) species has a distorted octahedral geometry in case of Me$_2$Sn (IV)-ligand system and a distorted trigonal bipyramidal/distorted tetrahedral geometry in case of Me$_3$Sn(IV)-ligand system. However, with the increase in the pH beyond 8.0, concentration of hydrolyzed species increases with the release of the ligand. Same results are obtained for 1:2 systems except the formation of hydrolyzed species starts before 5.0 pH.

The synthesis of new mixed diorganotin(IV)/triphenyltin(IV) derivatives of guanosine and 1,10-phenanthroline resulted in the formation of complexes of general formulae, [R$_2$Sn(HGuO)$_2$(phen)] (R = Me, Ph, Bu and Oct; H$_2$GuO = guanosine; phen = 1,10-phenanthroline) and [Ph$_3$Sn(HGuO)(phen)] in 1:2:1 and 1:1:1 ratio, respectively. The synthesized derivatives show low molar conductance, suggesting their non-electrolytic nature. The IR and far-IR spectral results indicate the involvement of oxygen of ribose unit of guanosine and nitrogen of phenanthroline in bond formation with the tin atom. The multinuclear (^{1}H, ^{13}C, ^{119}Sn) magnetic resonance spectral studies suggests a distorted

octahedral geometry around tin for both the diorganotin(IV) and triphenyltin(IV) derivatives. The *in vitro* cytotoxicity (MTT assay) behavior against HEK293 (human embryonic kidney) and a panel of four cancer cell lines of human origin, *viz.* MCF7 (mammary), HepG2 (liver), DU145 (prostrate) and HeLa (cervical) and the inhibitory concentration (IC_{50}) values for the studied complexes along with standard reference drugs, *cis*-platin (CPT) and 5-fluorouracil (5-FU), indicate that the dialkyltin(IV) (R = Me and Oct) derivatives are found to be inactive, where as di- and triphenyltin(IV) derivatives show good activity (higher than *cis*-platin). Dibutyltin(IV) derivative is the most active complex and shows comparable activity to that of the standard drugs against all the cell lines. Enzyme assay results of lipid peroxidase and lactate dehydrogenase assays on two selected complexes *viz.* diphenyltin(IV) and triphenyltin(IV) derivatives show that both the complexes cause apoptosis along with a small amount of necrosis. Acridine orange and comet assays are in support of their mode of cytotoxicity *via* mainly apoptosis. DNA binding studies performed by using UV-Visible spectroscopy and fluorescence and the binding constants determined show that the complexes have good affinity to bind with CT DNA, suggesting that the synthesized derivatives binding to DNA lead to the DNA damage, one of the causes for apoptosis. Gel electrophoresis results of all the complexes indicates the promotion of the conversion of DNA from super coiled form I to nicked circular form II, which clearly implicates the important role of organotin(IV) moieties in the process of DNA cleavage.

The synthesis of new diorganotin (R = Me, Ph and Bu) inosinate derivatives and mixed diorganotin (R = Me, Ph and Bu) derivatives of 5'-inosine monophosphate $(5'-IMP)^{2-}$ and 1,10-phenanthroline resulted in the complexes with general formula ($[R_2Sn(5'-IMP.4H_2O).H_2O]_n$) and ($[R_2Sn(5'-IMP.5H_2O)(phen)]$), respectively. The analytical data along with the spectral studies of diorganotin(IV) inosinate complexes indicate 1:1 stoichiometry involving one water molecule in coordination with the tin atom while the four ligand water molecules remaining intact, whereas the mixed diorganotin(IV) derivatives of inosinate and 1,10-phenanthroline are observed in 1:1:1 stoichiometry with five ligand water molecules remaining intact. The IR and far-IR spectral results suggest the phosphate group of ribofuranose of $(5'-IMP)^{2-}$ is bonded with the organotin moiety. Further, the appearance of the new $\nu(Sn–O–Sn)/\nu(Sn–O)$ bands at 551–508 cm^{-1} in all diorganotin(IV) inosinate derivatives and $\nu(Sn–N)/\nu(Sn{\leftarrow}N)$ at 508 – 453 cm^{-1} in mixed diorganotin(IV) derivatives of $(5'-IMP)^{2-}$, indicate that the coordination occurs possibly *via* oxygen of $(PO_3)^{2-}$ of $(5'-IMP)^{2-}$ and nitrogen of 1,10-phenanthroline moieties, respectively. The ^1H, ^{13}C, ^{119}Sn NMR of the synthesized derivatives shows a distorted octahedral geometry around tin. Due to the

poor solubility of dimethyltin derivatives, biological studies could not be performed. The diphenyltin(IV) inosinate is slightly more active against MCF7 as compared to that of *cis*-platin but it shows very less activity in comparison to 5-fluorouracil. The compounds dibutyltin(IV) inosinate and the mixed diphenyltin(IV) and dibutyltin(IV) derivatives are found to be much more active against MCF7 cell lines compared to that of *cis*-platin and the activity is comparable to that of 5-fluorouracil. The dibutyltin(IV) derivatives are found to be very active against HepG2 cell lines in comparison to that of *cis*-platin but they show comparable activity with respect to 5-fluorouracil. The IC_{50} values of the diphenyltin(IV) derivatives against HepG2 cell line suggests that the compounds inactive for the reason unknown. The presence of phenanthroline moiety induces the cytotoxicity, hence, the mixed diphenyltin(IV) and dibutyltin(IV) derivatives are more active compared to that of respective diorganotin(IV) inosinates. However, the dibutyltin(IV) inosinate is found to be the most active complex against both (MCF7 and HepG2) cell lines. Acridine orange and comet assay results of the test compounds indicate that apoptosis is the main cause of cytotoxicity. UV-Visible spectral and fluorescence binding studies shows that the diphenyltin(IV) and dibutyltin(IV) derivatives have moderate binding affinity with DNA indicating that organotin(IV) binding with DNA is one of the causes for apoptosis. Gel electrophoresis results of the complexes shows the interaction of the complexes with DNA but no cleavage is observed.

6.2. FUTURE PROSPECTS AND UTILITY OF ORGANOTIN(IV) COMPOUNDS IN CANCER CHEMOTHERAPY

• From the above conclusions, it can be inferred that the organotin(IV) compounds can be used as future possible antitumor drugs. However, other factors such as low solubility and systemic toxicity *in vivo* have to be determined. The problem with the solubility can be solved by introducing the polar groups (such as fluorine) in the pharmacophore which may enhance their water solubility at room temperature.

• Large number of organotin(IV) compounds were screened for antitumor activity, however, very less amount of work has been done on mode of action studies.

• More detailed experimental studies such as *in vivo* cytotoxicity, anti-inflammatory, toxicity studies, enzyme assays, DNA fragmentation assay, flow-cytometric analysis, analysis of caspase-9, Bcl-2 and Bax expression are required to determine and confirm the other possible modes of action.

[1]   Riordan, J. F.; "The Role of Metals in Enzyme Activity," Ann. Clin. Lab Sci., 7, 119–129 (1977).

[2]   Berg, J. M.; "Metal Ions in proteins: Structural and Functional roles," Cold Spring Harb. Symp. Quant. Biol., 52, 579–585 (1987).

[3]   Müller, J.; "Functional Metal Ions in Nucleic Acids," Metallomics, 2, 318–327 (2010).

[4]   Glusker, J. P.; Katz, A. K.; Bock, C. W.; "Metal ions in Biological Systems," The Rigaku J., 17, 1–17 (2000).

[5]   Martin, R. B.; "Metal Ion Toxicity," Ency. Inorg. Chem., 1– 5 (2006).

[6]   Huang, R.; Wallqvist, A.; Covell, D. G.; "Anticancer Metal Compounds in NCI's Tumor-Screening Database: Putative Mode of Action," Biochem. Pharmacol., 69, 1009–1039 (2005); and references cited therein.

[7]   Desoize, B.; "Cancer and Metals and Metal Compounds. Part II. Cancer Treatment," Crit. Rev. Oncol. Hematol., 42(3), 213–5, (2002).

[8]   Hartinger, C. G.; Dyson, P. J.; "Bioorganometallic Chemistry–From Teaching paradigms to Medicinal Applications," Chem. Soc. Rev., 38, 391–401 (2009).

[9]   Chavain, N.; Biot, C.; "Organometallic Complexes: New Tools for Chemotherapy," Curr. Med. Chem., 17(25), 2729–2745 (2010).

[10]   Singh, V. P.; Singh, H. B.; Butcher, R. J.; "Stable Selenenium Cations;Unusual Reactivity and Excellent Glutathione Peroxidase-Like Activity," Eur. J. Inorg. Chem., 637-647 (2010).

[11]   Selvakumar, K.; Singh, H. B.; Goyal, N.; Singh, U. P.; Butcher, R. J.; "Synthesis and Structures of Anionic Hypervalent Cyclic Selenenate Esters: Relevance to the Hypervalent Intermediates in Nucleophilic Substitution Reactions at Selenium(II) Center," Chem. Eur. J. (2011).

[12]   Chakraborty, T.; Srivastava, K.; Singh, H. B.; Butcher, R. J.; "Palladium Selenolates via Oxidative Addition of Organylselenenyl Halides to Palladium(0) Precursor   and via Cleavage Reaction of Diselenides: Synthesis, Structure and Spectroscopic Investigation," J. Organomet. Chem. (2011).

[13]   Pettinari, C.; Marchetti, F.; Pettinari, R.; Martini, D.; Drozdov, A.; Troyanov, S.; "The Interaction of Organotin(IV) Acceptors with a Benzoic Acid Containing Two Pyrazolone Groups," J. Chem. Soc., Dalton Trans., 1790–1797 (2001).

[14]   Marchetti, F.; Pettinari, C.; Cingolani, A.; Pettinari, R.; Rossi, M.; Caruso, F.; Organotin(IV) Derivatives of Novel β-Diketones Part V. Synthesis and

Characterization of Di- and Triorganotin(IV) Derivatives of 4-acyl-5-pyrazolones Modified in position 3 of the Pyrazole.Crystal Structure of (1,3-diphenyl-4-benzoyl-pyrazolon-5-ato)triphenyltin(IV)," J. Organomet. Chem., 645, 134–145 (2002).

[15] Davies, A. G.; "Organotin Compounds in Technology and Industry," J. Chem. Res., 34, 181–190 (2010); and references cited therein.

[16] Kroschwitz, J. I.; Howe-Grant, M. (eds.); "Tin Compounds," Kirk-Othmer Ency. Chem. Tech., Wiley, New York, 24, 122–161 (1997).

[17] Smith, P. J.; "Chemistry of Tin," 2nd Edition, Blackie Academic & professional, London, United Kingdom, 1–578 (1998).

[18] Penninks, A. H.; Bol-Schoenmakers, M.; Seinen, W.; "Cellular Interaction of Organotin Compounds in Relation to Their Antitumour Activity," In: Gielen, M. (ed.) Tin-Based Antitumour Drugs. NATO ASI Series, H37, 169, Springer, Berlin (1990); and references cited therein.

[19] Crowe, A. J.; "Tin Compounds and Their Potential as Pharmaceutical Agents," In: Gielen, M. (ed.) Tin-Based Antitumour Drugs. NATO ASI Series, H37, 69, Springer, Berlin (1990).

[20] Tsangaris, J. M.; Williams, D. R.; "Tin in Pharmacy and Nutrition," Appl. Organomet. Chem., 6, 3–18 (1992).

[21] Clarke, M. J.; Zhu, F. Fransca, D. R.; " Non-Platinum Chemotherapeutic Metallopharmaceuticals," Chem. Rev., 99, 2511–2534 (1999); and references cited there in.

[22] Pruchnik, F. P.; Banbula, M.; Ciunik, Z., Latocha, M; Skop, B.; Wilczok, T.; "Structure, Properties and Cytostatic Activity of Tributyltin Aminoaryl-carboxylates," Inorg. Chim. Acta, 356, 62–68 (2003).

[23] Carraher, C. E.; Bleicher, R. E.; " Organotin Oligomeric Drugs Containing the Antiviral Agent Acyclovir," In: Macromolecules Containing Metal and Metal-Like Elements: Biomedical Applications, Abd-El-Aziz, A. S.; Carraher, C. E.; Pittman, C. U.; Sheats, J. E.; Zeldin, M (eds), John Wiley & Sons, Inc., Hoboken, N. J., USA, 3 (2004).

[24] Jankovics, H.; Pettinari, C.; Marchetti, F.; Kamu, E.; Nagy, L.; Tryanov, S.; Pellerito, L.; "Characterization of Diorganotin(IV) Complexes with Captopril. The First Crystallographically Authenticated Metal Complex of this Anti-hypertensive Agent," J. Inorg. Biochem., 97, 370–376 (2003); and references cited therein.

[25]   Molloy, K. C.; Purcel, T. G.; Hahn, E.; Schumann, H.; Zuckerman, J. J.; "Organotin Biocides. 4. Crystal and Molecular Structure of Tricyclohexylstannyl 3-Indolylacetate, Incorporating the First Monodentate Carboxylate Group Bonded to a Triorganotin(IV)," Organomet., 5, 85–89 (1986).

[26]   Sam, N.; Affan, M. A.; Salam, M. A.; Ahmad, F. B.; Asaruddin, M. R.; "Synthesis, Spectral Characterization and Biological Activities of Organotin(IV) Complexes with Ortho-vanillin-2-hydrazinopyridine (VHP)," Open J. Inorg. Chem., 2, 22–27 (2012).

[27]   Salam, M. A.; Affan, M. A.; Ahmad, F. B.; Arafath, M. A.; "Organotin(IV) Complexes with Pyruvic Acid Phenylhydrazone (HPAPD): Synthesis, Spectral, Characterization, and *In Vitro* Antibacterial Activity," J. Coord. Chem., 65, 1999–2007 (2012).

[28]   Rehman, W.; Baloch, M. K.; Badshah, A.; "Synthesis, Spectral Characterization and Bio-analysis of Some Organotin(IV) Complexes," Eur. J. Med. Chem., 43, 2380–2385 (2008).

[29]   Sedaghat, T.; Yousefi, M.; Bruno, G.; Rudbari, H. A.; Motamedi, H.; Nobakht, V.; "Synthesis, Spectral Characterization, Crystal Structure and Antibacterial Studies of Diorganotin(IV) Complexes With Isonicotinoyl Hydrazone Derivatives," Polyhedron, 79, 88–96 (2014); and the references cited therein.

[30]   Qureshi, Q.-u. A. H.; Nadhman, A.; Sirajuddin, M.; Shahnaz, G.; Ali, S.; Shah, A.; Yasinzai, M. M.; "Organotin(IV) Complexes of Carboxylate Derivative as Potential Chemotherapeutic Agents Against *Leishmania*," Inorg. Chim. Acta, 423, 220–228 (2014).

[31]   Ferreira, I. P.; de Lima, G. M.; Paniago, E. B.; Rocha, W. R.; Takahashi, J. A.; Pinheiro, C. B.; Ardisson, J. D.; "Design, Structural and Spectroscopic Elucidation, and the *In Vitro* Biological Activities of New Triorganotin Dithiocarbamates − Part II," Polyhedron, 79, 161−169 (2014).

[32]   Nath, M.; Sulaxna; Song, X.; Eng, G.; Kumar, A.; "Synthesis and Spectral Studies of Organotin(IV) 4-amino-3-alkyl-1,2,4-triazole-5-thionates: *In Vitro* Antimicrobial Activity," Spectrochim. Acta Part A, 70, 766–774 (2008); and references cited therein.

[33]   Nath, M.; Saini, P. K.; Kumar, janA.; "New Di- and Triorganotin(IV) Complexes of Tripodal Schiff Base Ligand Containing Three Imidazole Arms: Synthesis, Structural Characterization, Anti-inflammatory Activity and Thermal Studies," J. Organomet. Chem., 695, 1353–1362 (2010); and references cited therein.

[34]   Nath, M.; Saini, P. K.; and Kumar, A.; "Synthesis, Structural Characterization, Biological Activity and Thermal Study of Tri and Diorganotin(IV) Complexes of Schiff Base Derived from 2-aminomethyl-benzimidazole," Appl. Organometal. Chem., 23, 434–445 (2009); and references cited therein.

[35]   Nath, M.; Vats, M.; Roy, P.; "Di- and Triorganotin(IV) Complexes of Biologically Important Orotic Acid: Synthesis, Spectroscopic Studies, *In Vitro* Anti-cancer, DNA Fragmentation, Enzymes Assays, and *In Vivo* Anti-inflammatory Activities," Eur. J. Med. Chem., 59, 310–321 (2013); and references cited therein.

[36]   Nath, M.; Singh, H.; Eng, G.; Song, X.; "Synthesis, Structure–activity Relationship of Some New Triorganotin(IV) Derivatives of Dipeptides as Anti-inflammatory Agents," Phosphorus, Sulfur, and Silicon and the Related Elements, 188, 755–767 (2013); and references cited therein.

[37]   Nath, M.; Singh, H.; Eng, G.; Song, X.; "Interaction of Organotin(IV) Moieties With Nucleic Acid Constituent: Synthesis, Structural Characterization and Anti-inflammatory Activity of Tri-*n*-propyltin(IV) and Diorganotin(IV) Derivatives of Guanosine," Inorg. Chem. Commun., 14, 1381–1385 (2011); and references cited therein.

[38]   Nath, M.; Singh, H.; Eng, G.; Song, X.; "Interaction of 5'-Guanosine Monophosphate with Organotin(IV) Moieties: Synthesis, Structural Characterization, and Anti-inflammatory Activity," ISRN Org. Chem., 1–9 (2012); and references cited therein.

[39]   Nath, M.; Singh, H.; Eng, G.; Song, X.; Kumar, A.; "Syntheses, Characterization and Biological Activity of Diorganotin(IV) Derivatives of 2-amino-6-hydroxypurine (guanine)," Inorg. Chem. Commun., 12, 1049–1052 (2009); and references cited therein.

[40]   American Cancer Society. Global Cancer Facts & Figures 2nd Edition. Atlanta: American Cancer Society, (2011).

[41]   Tabassum, S.; Yadav, S.; Arjmand, F.; "Exploration of Glycosylated–Organotin(IV) Complexes as Anticancer Drug Candidates," Inorg. Chim. Acta, 423, 38–45 (2014); and references cited therein.

[42]   Tabassum, S.; Pettinari, C.; "Chemical and Biotechnological Developments in Organotin Cancer Chemotherapy," J. Organomet. Chem., 691, 1761–1766 (2006); and references cited therein.

[43]   Pellerito, C.; D'Agati, P.; Fiore, T.; Mansueto, C.; Mansueto, V.; Stocco, G.; Nagy, L.; Pellerito, L.; "Synthesis, Structural Investigations on Organotin(IV) Chlorine-6

Complexes, Their Effect on Sea Urchin Embryonic Development and Induced Apoptosis," J. Inorg. Biochem., 99, 1294–1305 (2005); and references cited therein.

[44] Atsushi, A.; Hisada, K.; Ando, I.; "Radioactive Tin Compound as New Bone Scanning Agent," Radioisotopes 22, 7, 297–394 (1973).

[45] Crowe, A.; Smith, P.; Atassi, G.; "Investigations into the Antitumour Activity of Organotin Compounds. I. Diorganotin dihalide and Di-pseudohalide Complexes," Chem. Biol. Interact. 32, 171 (1980).

[46] Saxena, A.; Huber, F.; "Organotin Compounds and Cancer Chemotherapy," Coord. Chem. Rev., 95, 109 (1989).

[47] Gielen, M.; "Tin–based Antitumour Drugs," Coord. Chem. Rev., 151, 41 (1996); and references cited therein.

[48] Gielen, M.; Tiekink, E. R. T. (eds); "Metallotherapeutic Drugs and Metal–based Diagnostic Agents," The Use of Metals in Medicine, J Wiley & Sons, 421 (2005); and references cited therein.

[49] Tiekink, E. R.T.; Gielen, M.; Bouhdid, A.; de Vos, D.; Biesemans, M.; Verbruggen, I.; Willem, R.: " Synthesis, Chracterization and In vitro Antitimour Activity of Dibutyltin Carboxylates Involving the Perfluorephenyl Moiety: Crystal Struture of the Dimeric Bix[(4-fluoro and pentafluoro- benzoate)di-n-butyltin]oxides," Appl. Organomet. Chem., 9, 639–648 (1995).

[50] Kemmer, M.; Dalil, H.; Biesemans, M.; Martins, J. C.; Mahieu, B.; Horn, E.; de Vos, D.; Tiekink, E. R.T.; Willem, R.; Gielen, M.: "Dibutyltin perfluoroalkanecarboxylates: Synthesis, Chracterization and In vitro Antitimour Activity," J. Organomet. Chem., 608, 63–70 (2000).

[51] Mancilla, T.; Carrillo, L.; Zamudio R., Luis S.; Camacho C. C.; de Vos, D.; Kiss, R.; Darro, F.; Mahieu, B.; Tiekink, E. R. T.; Rahier, H.; Gielen, M.; Kemmer, M.; Biesemans, M.; Willem, R.; "Di-n-butyltin(IV) Derivatives of Bis(carboxymethyl)benzylamines: Synthesis, NMR and X-ray Structure Characterization and In Vitro Antitumour Properties," Appl. Organomet. Chem., 15, 593–603, (2001).

[52] Li, Y.; Li, Y.; Niu, X.; Jie, L.; Shang, X.; Guo, J.; Li, Q.; "Synthesis and Antitumor Activity of a New Mixed-Ligand Complex Di-*n*-butyl-(4-chlorobenzohydroxamato)tin(IV) Chloride," J. Inorg. Biochem., 102, 1731–1735 (2008).

[53]   Han, G.; Yang, P.; "Synthesis and Characterization of Water-insoluble and Water-soluble Dibutyltin(IV) porphinate Complexes Based on the Tris(pyridinyl)porphyrin Moiety, Their Anti-tumor Activity In vitro and Interaction with DNA," J. Inorg. Biochem., 91, 230–236 (2002).

[54]   Falcioni, M. L.; Pellei, M.; Gabbianelli, R.; "Interaction of Tributyltin(IV) Chloride and a Related Complex [Bu3Sn(LSM)] with Rat Leukocytes and Erythrocytes: Effect on DNA and on Plasma Membrane," Mutat. Res., 653, 57–62 (2008).

[55]   Khan, N; Farina , Y; Mun, L. K.; Rajab, N. F.; Awang, N.; "Syntheses, Spectral Characterization, X-ray Studies and *In Vitro* Cytotoxic Activities of Triorganotin(IV) Derivatives of *p*-substituted *N*-methylbenzylaminedithiocarbamates," J. Mol. Struct., 1076, 403–410 (2014).

[56]   Girasolo, M. A.; Attanzio, A.; Sabatino, P.; Tesoriere, L.; Rubino, S.; Stocco, G.; "Organotin(IV) Derivatives with 5,7-disubstituted-1,2,4-triazolo[1,5-*a*]pyrimidine and Their Cytotoxic Activities: The Importance of Being Conformers," Inorg. Chim. Acta, 423, 168–176 (2014).

[57]   Nath, M.; Vats, M.; Roy, P.; "Design, Spectral Characterization, Anti tumor and Anti-inflammatory Activity of Triorganotin(IV) hydroxycarboxylates, Apoptosis Inducers: *In Vitro* Assessment of Induction of Apoptosis by Enzyme, DNA-Fragmentation, Acridine Orange and Comet Assays," Inorg. Chim. Acta, 423, 70–82 (2014); and references cited therein.

[58]   Nath, M.; Vats, M.; Roy, P.; "Design and Microwave-assisted Synthesis of Tri- and Dialkyltin(IV) Hippurates, Characterization, *In Vitro* Anti-cancer and *In Vivo* Anti-inflammatory Activities," Med. Chem. Res., 24, (2014); and references cited therein.

[59]   Ferancová, A.; Adamovski, M.; Gründler, P.; Zima, J.; Barek, J.; Mattusch, J.; Wennrich, R.; Labuda, J.; "Interaction of Tin(II) and Arsenic(III) with DNA at the Nanostructure Film Modified Electrodes," Bioelectrochemistry, 71, 33–37 (2007).

[60]   Atkinson, A.; Rodriguez, M. D.; Shewmaker, T. E.; and Walmsley, J. A.; "Synthesis and Characterization of Compounds of Di- and Tributyltin Chloride with Adenine and Guanine Mononucleotides," Inorg. Chim. Acta, 285, 60–69 (1999); and references cited therein.

[61]   Samuel, P. M.; Roy, S.; Diwan, P. V.; "Process for the Preparation of Organotin Compounds Useful as Cytotoxic Agents," patent Ref. No.: US 5877320 A, (1999).

[62]   Ohhira, S.; Enomoto, M.; Matsui, H.; "In Vitro Metabolism of Tributyltin and Triphenyltin by Human Cytochrome P-450 Isoforms," Toxicology, 228, 171–177 (2006).

[63]   Shpakovsky, D. B.; Banti, C. N.; Mukhatova, E. M.; Gracheva, Yu. A.; Osipova, V. P.; Berberova, N. T.; Albov, D. V.; Antonenko, T. A.; Aslanov, L. A.; Milaeva, E. R.; and Hadjikakou, S. K.; "Synthesis, Antiradical Activity and In Vitro Cytotoxicity of Novel Organotin Complexes Based on 2,6-di-tert-butyl-4-mercaptophenol," Dalton Trans., 43, 6880–6890 (2014).

[64]   Samuel, P. M.; Roy, S.; Jaiswal, K. A.; Rao, J. V.; "Differential Effects of Organometallic Tin Compounds on Na^+/K^+-ATPasr Activity," J. Appl. Toxicol., 18, 383 (1998).

[65]   Moosavi-Movahedi, A. A.; Golchin, A. R.; Nazari, K. ; Chamani, J.; A.A. Saboury, S.Z. Bathaie, S. Tangestani-Nejad, Microcalorimetry, energetics and binding studies of DNA–dimethyltin dichloride complexes, Thermochimica Acta 414 (2004) 233–241.

[66]   Ravera, M.; Bagni, G.; Mascini, M.; and Osella, D.; "DNA-Metallodrugs Interactions Signaled by Electrochemical Biosensors: An Overview," Bioinorg. Chem. Appl., 2007, 1–11 (2007) and references cited therein.

[67]   Zhang, N.; Tai, Y.; Li, M.; Ma, P.; Zhao, J.; and Niu, J.; "Main Group Bismuth(III), Gallium(III) and Diorganotin(IV) Complexes Derived from Bis(2-acetylpyrazine)thiocarbonohydrazone: Synthesis, Crystal Structures and Biological Evaluation," Dalton Trans., The Royal Society of Chemistry, 43, 5182–5189 (2014).

[68]   El-Sherif, A. A.; "Solution Coordination Chemistry of Organotin(IV) Cations with Bio-relevant Ligands," J. Solution Chem. 41, 1522–1554 (2012).

[69]   Penninks, A. H.; Seinen, W.; "Mechanisms of Dialkyltin Induced Immunopathology," Vet. Q. 6, 209–215 (1984).

[70]   Li, Q.; Yang, P.; Wang, H.; Guo, M.; "Diorganotin(IV) Antitumor Agent. $C_2H_5SnCl_2$ (phen)/nucleotides Aqueous and Solid-State Coordination Chemistry and Its DNA Binding Studies," J. Inorg. Biochem., 64, 181–195 (1996).

[71]   Nafisi, S.; Sobhanmanesh, A.; Esm-Hosseini, M.; Alimoghaddam, K.; Tajmir-Riahi, H. A.; "Interaction of Antitumor Drug $Sn(CH_3)_2Cl_2$ with DNA and RNA," J. Molecular Struct., 750, 22–27 (2005).

[72]   Rehman, Z.; Shah, A.; Muhammad, N.; Ali, S.; Qureshi, R.; Meetsma, A.; Butler, I.S.; "Synthesis, spectroscopic characterization, X-ray structure and evaluation of binding

parameters of new triorganotin(IV) dithiocarboxylates with DNA," Eur. J. Med. Chem., 1–8 (2009).

[73] Snoeij, N. J.; Penninks, A. H.; Seinen, W.; "Dibutyltin and Tributyltin Compounds Induce Thymus Atrophy in Rats Due to a Selective Action on Thymic Lymphoblasts," Int. J. Immunopharmacol., 10, 891–9 (1988).

[74] Abdellah, M. A.; Hadjikakou, S. K.; Hadjiliadis, N.; Kubicki, M. ; Bakas, T.; Kourkoumelis, N.; Simos, Y. V.; Karkabounas, S.; Barsan, M. M.; Butler, I. S.; "Synthesis, Characterization, and Biological Studies of Organotin(IV) Derivatives with o- or p-hydroxybenzoic Acids," Bioinorg. Chem. Appl., 2009 (2009).

[75] Hadjikakou, S. K.; Hadjiliadis, N.; "Antiproliferative and Anti-tumor Activity of Organotin Compounds," Coord. Chem. Rev., 253, 235–249 (2009).

[76] Unno, T.; Iida, R.; Okawa, M.; Matsuyama, H.; Hossain, M. M.; Kobayashi, H.; Komori, S.; "Tributyltin-Induced Ca^{2+} Mobilization via L-type Voltage-dependent Ca^{2+} Channels in $PC1_2$ Cells," Environ. Toxicol. Pharmacol., 28, 70–77 (2009).

[77] Legraverend, M.; "Recent Advances in the Synthesis of Purine Derivatives and their Precursors," Tetrahedron, 64, 8585–8603 (2008) and referenced cited therein.

[78] Mukherjee, G. N.; Ghosh, T.: "Metal-Ion Interactions with Some Antibiotic Drugs of Pencillin Family. 4. Equilibrium Study on the Complex-Formation of Cobalt(II), Nickel(II), and Zinc(II) with Ampicillin," J. Indian. Chem. Soc., 71, 169–173, 1994

[79] Mukherjee, G. N.; Chattopadhyay, S. K.; Sarkar, S.: "Metal-Complexes of Some Model Peptide Derivatives. 11. Mixed-Ligand Complex-Formation of Copper(II) with Salicyloyglycine and Typical Ligands," J. Indian. Chem. Soc., 71, 45–48, 1994.

[80] Mukherjee, G. N.; Basu S.; Ghosh, T.: "Studies on the Interactions of Biological Metal-Ions with Some Sulfonamide Drugs. 1. Equilibrium Study on the Complex-Formation of Cobalt(II), Nickel(II), Copper(II) and Zinc(II) with Sulfapyridine, Sulfadiazine and Sulfathiazole," J. Indian. Chem. Soc., 70, 1043–1049, 1993.

[81] Mohamed, M. M. A. and Shoukry M. M.; "Interaction of Diphenyltin(IV) Dichloride with Some Selected Bioligands," Chem. Pharm. Bull. 49(3), 253–257 (2001); and references cited there in.

[82] Shoukry, M. M.; "Equilibrium Studies of the Diorganotin(IV) Complexes with Some Amino acids and Related Compounds," Talanta, 43, 177–183 (1996).

[83] Al-Najjar, A. A.; Shehata, M. R.; Mohamed, M. M. A.; Shoukry, M. M.; "Equilibrium Studies of Organotin(IV) Complexes of Peptides," Main Group Metal Chem., 22, 253–261 (1999).

[84]   Jankovics, H.; Nagy, L.; Buzás, N.; Pellerito, L.; and Barbieri, R.; "Coordination Properties of Adenosine-5'-monophosphate and Related Ligands Towards $Me_2Sn(IV)^{2+}$ in Aqueous Solution," J. Inorg. Biochem., 92, 55–64 (2002).

[85]   Nagy, L.; Szorcsik, A.; Jankovics, H.; Yamaguchi, T.; Yoshida, K.; Scopelliti, M.; Pellerito, L. and Sletten, E.; "Preparation and XAFS Studies of Organotin(IV) Complexes with Adenosine and Related Compounds and Calf Thymus DNA," J. Radioanal. Nucl. Chem., 275(1), 193–200 (2008).

[86]   Jancsó, A.; Nagy, L.; Moldrheim, E.; and Sletten, E.; "Potentiometric and Spectroscopic Evidence for Co-ordination of Dimethyltin(IV) to Phosphate Groups of DNA Fragments and Related Ligands," J. Chem. Soc., Dalton Trans., 1587–1594 (1999).

[87]   Barbieri, R.; Silvestri, A. and Piro, V.; "Tin- 119 'Mössbauer Titration' of Dimethyl- and Trimethyl-tin(IV) Hydroxides with Model Ligands Mimicking Nucleic Acid Phosphate Sites, and with Deoxyribonucleic Acid," J. Chem. Soc. Dalton Trans., 3605–3609 (1990).

[88]   Tabassum , S.; Khan , R. A.; Arjmand , F.; Juvekar , A. S.; Zingde, S. M.; "Synthesis of Carbohydrate-Conjugate Heterobimetallic Cu^{II}–Sn_2^{IV} and Zn^{II}–Sn_2^{IV} Complexes; Their Interactions with CT DNA and Nucleotides; DNA Cleavage, *in vitro* Cytotoxicity," E. J. Med. Chem., 45, 4797–4806 (2010).

[89]   Tabassum , S.; Khan , R. A.; Arjmand , F.; Sen, S.; Kayal, J.; Juvekar , A. S.; Zingde, S. M.; "Synthesis and Characterization of Glycoconjugate Tin(IV) Complexes: *In Vitro* DNA Binding Studies, Cytotoxicity, and Cell Death," J. Organomet. Chem., 696, 1600–1608 (2011).

[90]   Prasad, K. S.; Kumar, L. S.; Prasad, M.; Revanasiddappa H. D.; "Novel Organotin(IV)-Schiff Base Complexes: Synthesis, Characterization, Antimicrobial Activity, and DNA Interaction Studies," Bioinorg. Chem. Appl., 1–9 (2010).

[91]   Arjmand, F.; Sharma, G. C.; Sayeed, F.; Muddassir, M.; Tabassum, S.; "*De novo* Design of Chiral Organotin Cancer Drug Candidates: Validation of Enantiopreferential Binding to Molecular Target DNA and 5'-GMP by UV–visible, Fluorescence, ^{1}H and ^{31}P NMR," J. Photochem. Photobiol. B: Biology, 105, 167–174 (2011).

[92]   Poller, R. C.; "The Chemistry of Organotin Compounds," Logos Press Limited, London, pp. 1–315 (1970); and references cited therein.

[93]   Reicmann, M. E.; Rice, S. A.; Thomas, C. A.; Doty, P.; "A Further Examination of the Molecular Weight and Size of Desoxypentose Nucleic Acid," J. Am. Chem. Soc., 76, 3047–3053 (1954).

[94]   Sayce, I. G.; "Computer Calculation of Equilibrium Constants of Species Present in Mixtures of Metal Ions and Complexing Agents," Talanta, 15, 1397–1411 (1968).

[95]   Sayce, I. G.; "Computer Calculation of Equilibrium Constants by Use of the Program SCOGS; A Correction," Talanta, 18, 653–654 (1971).

[96]   Sayce I. G.; Sharma, V. S.; "Computer Calculation of Equilibrium Constants Using Programme SCOGS: A Further Modification," Talanta, 19, 831 (1972).

[97]   Cima, F.; Craig, P. J.; Harrington, C.; "Organotin Compounds in the Environment," In: Craig, P. J. (ed.) Organometallic Compounds in the Environment, 2nd edn., 101–157. John Wiley & Sons, Chicester, U.K. (2003).

[98]   Byrd, J. T.; Andreae, M. O.; "Tin and Methyltin Species in Seawater:Concentrations and Fluxes," Science, 218, 565–569 (1982).

[99]   Mizukawa, H.; Takahashi, S.; Nakayama, K.; Sudo, A.; Tanabe, S.; "Contamination and Accumulation Feature of Organotin Compounds in Common Cormorants (Phalacrocorax carbo) from Lake Biwa, Japan," Interdiscip. Stud. Environ. Chem.−Environ. Res. Asia, 153–161 (2009).

[100]   Meng-Pei, H.; Shiu-Mei, L.; "Accumulation of Organotin Compounds in Pacific Oysters, Crassostrea Gigas, Collected from Aquaculture Sites in Taiwan," Sci. Total Environ., 313, 41–48 (2003).

[101]   El Hassani, L. H.; Frenich, A. G.; Martinez Vidal, J. L.; Muros, M. J. S.; Benajiba, M. H.; "Study of the Accumulation of Tributyltin and Triphenyltin Compounds and Their Main Metabolites in the Sea Bass, Dicentrachus Labrax, Under Laboratory Conditions," Sci. Total Environ., 348, 191–198 (2005).

[102]   Strand, J.; Jacobsen, J. A.; "Accumulation and Trophic Transfer of Organotins in a Marine Food Web from the Danish Coastal Waters," Sci. Total Environ., 350, 72–85 (2005).

[103]   Al-Najjar, A. A.; Mohamed, M. M. A.; Shehata, M. R.; Shoukry, M. M.; "Tripropyltin(IV) Complexes with Some Selected Bioligands in 50% V/V Dioxane/Water Mixture," Annali di Chimica, Societa Chimica Italiana, 96 (2006).

[104]   Gianguzza, A.; Giuffrè, O.; Piazzese, D.; Sammartano, S.; "Aqueous Solution Chemistry of Alkyltin(IV) Compounds for Speciation Studies in Biological Fluids and Natural Waters," Coord. Chem. Rev., 256, 222–239 (2012).

[105]   Hynes, M. J.; Keely, J. M.; McManus, J.; "Investigation of the Hydrolysis of $[Sn(CH_3)_3(H_2O)_2]^+$ in Aqueous Aolution by Tin-119 Nuclear Magnetic Resonance Spectroscopy," J. Chem. Soc., Dalton Trans., 3427–3429 (1991).

[106]   Barbieri, R.; Silvestri, A.; "The Hydrolysis of Me_2Sn^{IV} and Me_3Sn^{IV} Moieties Monitored Through ^{119}Sn Mössbauer Spectroscopy," Inorg. Chim. Acta, 188, 95–98 (1991).

[107]   Natsume, T.; Aizawa, S.; Hatano, K.; Funahashi, S.; Hydrolysis, Polymerization, and Structure of Dimethyltin(IV) in Aqueous Solution. Molecular Structure of the Polymer $[(SnMe_2)_2(OH)_3]ClO_4$," J. Chem. Soc., Dalton Trans., 2749–2753 (1994).

[108]   Takahashi, A.; Natsume, T.; Koshino, N.; Funahashi, S.; Inada, Y.; Takagi, H.D.; "Speciation of Trimethyltin(IV): Hydrolysis, Complexation Equilibria, and Structures of Trimethyltin(IV) Ion in Aqueous Solution," Can. J. Chem., 75, 1084–1092 (1997).

[109]   Pellerito, L.; Nagy, L.; "Organotin(IV)$^{n+}$ Complexes Formed with Biologically Active Ligands: Equilibrium and Structural Studies, and Some Biological Aspects," Coord. Chem. Rev., 224, 111–150 (2002).

[110]   Nath, M.; Jairath, R.; Mukherjee, G. N.; Das, A.; "Speciation of Dimethyltin(IV) and Trimethyltin(IV) Cations with Some Biologically Important Ligands in Aqueous Medium: A Potentiometric Investigation," Indian J. Chem., 44A, 1602–1607 (2005).

[111]   Arena, G.; Gianguzza, A.; Pellerito, L.; Musumeci, S.; Purrello, R.; Rízzarelli, E.; "Coordination Properties of Dialkyltin(IV) in Aqueous Solution. Thermodynamics of Complex Formation with Carboxylic Acids," J. Chem. Soc., Dalton Trans.: Inorg.Chem., 8, 2603–2608 (1990).

[112]   Gielen, M.; "Cytotoxic, Mutagenic and Carcinogenic Potential of Heavy Metals Related to Human Environment," Tin-based antitumor drugs, NATO ASI Series, vol. 26, pp. 445–455. Springer, Netherlands (1997) and references cited therein.

[113]   Yang, P.; Guo, M.; "Interactions of Organometallic Anticancer Agents with Nucleotides and DNA," Coord. Chem. Rev., 185–186, 189–211 (1999).

[114]   Al-Najjar, A. A.; Mohamed, M. M. A.; Shoukry, M. M.; "Interaction of Dipropyltin(IV) Amino acids, Peptides, Dicarboxylic Acids and DNA Constituents," J. Coord. Chem., 59, 193–206 (2006).

[115]   De Moraes Silva, A.; Mercê, A. L. R.; Mangrich, A. S.; Souto, C. A. T.; Felcman, J.; "Potentiometric and Spectroscopic Study of Mixed Copper(II) Complexes with Amino Acids and Either Adenosine 5' Triphosphate or Phosphocreatine," Polyhedron, 25, 1319–1326 (2006).

[116]   De Stefano, C.; Gianguzza, A.; Giuffrè, O.; Piazzese, D.; Orecchio, S.; Sammartano, S.; "Speciation of Organotin Compounds in NaCl Aqueous Solution: Interaction of Mono-, Di- and Tri-organotin (IV) Cations with Nucleotide 5' Monophosphates," Appl. Organomet. Chem., 18, 653–661 (2004).

[117]   Arena, G.; Cali, R.; Contino, A.; Loretta, N.; Musumeci, S.; Purrello, R.; "Thermodynamic Study of Dimethyltin(IV) Complexes with Nucleoside 5'– Triphosphates," J. Chem. Soc., Dalton Trans., 2039–2043 (1992).

[118]   Roberts, J. J.; Pascoe, J. M.; "Cross-linking of Complementary Strands of DNA in Mammalian Cells by Antitumor Platinum Compounds," Nature, 235, 282–284 (1972).

[119]   Izatt, R. M.; Christensen, J. J.; Rytting, J. H.; "Sites and Thermodynamic Quantities Associated with Proton and Metal Ion Interaction with Ribonucleic Acid, Deoxyribonucleic Acid, and Their Constituent Bases, Nucleosides, and Nucleotides," Chem. Rev., 71, 439–481 (1971).

[120]   Shoukry, M.; van Eldik, R.; "Correlation Between Kinetic and Thermodynamic Complex-Formation Constants for the Interaction of Bis(amine)palladium(II) with Inosine, Inosine 5'-monophosphate and Guanosine 5'-monophosphate," J. Chem. Soc., Dalton Trans., 2673–2678 (1996).

[121]   Cigala, M. R.; De Stefano, C.; Giacalone, A.; Gianguzza, A.; Sammartano, S.; "Hydrolysis of Monomethyl-, Dimethyl-, and Trimethyltin(IV) Cations in Fairly Concentrated Aqueous Solutions at $I = 1$ mol·L^{-1} (NaNO$_3$) and T = 298.15 K. Evidence for the Predominance of Polynuclear Species," J. Chem. Eng. Data, 56, 1108–1115 (2011).

[122]   Al-Najjar, A. A.; Shehate, M. R.; Mohamed, M. M. A.; Shoukry, M. M.; "Equilibrium Studies of Organotin(IV) Complexes of Peptides," Main Group Met. Chem., 22, 253–261 (1999).

[123]   Lockhart, T. P.; Manders, W. F.; "Structure Determination by NMR Spectroscopy. Correlation of [^{2}J(^{119}Sn, ^{1}H) and the Me-Sn-Me Angle in Methyltin(IV) Compounds," Inorg. Chem., 25, 892–895 (1986).

[124]   Surdy, P.; Rubini, P.; Buzás, N.; Henry, B.; Pellerito, L.; Gajda, T.; "Interaction of Dimethyltin(IV)$^{2+}$ Cation with Gly-Gly, Gly-His, and Some Related Ligands. A New Case of a Metal Ion Able to Promote Peptide Nitrogen Deprotonation in Aqueous Solution," Inorg. Chem., 38, 346–352 (1999).

[125]   Holeček, J.; Nádvorník, M.; Handlíř, K.; Lyčka, A.; "^{13}C and ^{119}Sn NMR Spectra of Di-*n*-butyltin(IV) Compounds," J. Organomet. Chem., 315, 299–308 (1986).

[126]   Tan, L. F.; Chao, H.; Zhen, K. C.; Fei, J. J.; Wang, F.; Zhou, Y. F.; Liang, N. J.; "Co(III) Complexes of Me-salpn and Me-salbn and the Ring Size Effect on the Coordination Modes and Electrochemical Properties: The Crystal Structures of Trans-[CoIII(Me-salpn)(py)$_2$]PF$_6$ and cis-α-[CoIII(Me-salbn)(4-Mepy)$_2$]BPh$_4$ 4-Mepy," Polyhedron, 26, 5448–5457 (2007).

[127]   Childs, L. J.; Malina, J.; Rolfsnes, B. E.; Pascu, M.; Prieto, M. J.; Broome, M. J.; Rodger, P. M.; Sletten, E.; Moreno, V.; Rodger, A.; Hannon, M. J.; "A DNA-binding Copper(I) Metallosupramolecular Cylinder That Acts as an Artificial Nuclease," Chem..Eur. J., 12, 4919 – 4927 (2006).

[128]   Yellappa, S.; Seetharamappa, J.; Rogers, L. M.; Chitta, R.; Singhal, R. P.; D'Souza, F.; "Binding, Electrochemical Activation, and Cleavage of DNA by Cobalt(II) Tetrakis-*N*-methylpyridyl Porphyrin and Its β-Pyrrole brominated Derivative," Bioconjugate Chem., 17, 1418 – 1425 (2006).

[129]   Satyanarayana, S.; Dabrowiak, J. C.; Chaires, J. B.; "Neither DELTA- nor LAMBDA -Tris(phenanthroline)ruthenium(II) Binds to DNA by Classical Intercalation," Biochemistry, 31, 9319 – 9324 (1992).

[130]   Ma, D. -L.; Che, C. -M.; "A Bifunctional Platinum(II) Complex Capable of Intercalation and Hydrogen-bonding Interactions with DNA: Binding Studies and Cytotoxicity," Chem. Eur. J., 9, 6133 – 6144 (2003).

[131]   Ma, D. -L.; Che, C. -M.; Siu, F. -M.; Yang, M.; Wong, K. -Y.; "DNA Binding and Cytotoxicity of Ruthenium(II) and Rhenium(I) Complexes of 2-Amino-4-phenylamino-6-(2-pyridyl)-1,3,5-triazine," Inorg. Chem., 46, 740 – 749 (2007).

[132]   Wang, S.; Cosstick, R.; Gardner, J. F.; Gumport, R. I.; "The Specific Binding of Escherichia coli Integration Host Factor Involves Both Major and Minor Grooves of DNA," Biochemistry, 34, 13082 –13090 (1995).

[133]   Tabassum, S.; Khan, R. A.; Arjmand, F.; Aziz, M.; Juvekar, A. S.; Zingde, S. M.; "Carbohydrate-conjugate Heterobimetallic Complexes: Synthesis, DNA Binding Studies, Artificial Nuclease Activity and *In vitro* Cytotoxicity," Carbohydr. Res., 346, 2886–2895 (2011).

[134]   Marnett, L. J. "Lipid Peroxidation-DNA damage by Malondialdehyde," Mutation Res., 424, 83–95 (1999).

[135]   Davies, O.; Mendes, P.; Smallbone, K.; Malys, N.; "Charaterization of Multiple Substrate-Specific (d)ITP/(d)XTPase and Modelling of Deaminated Purine Nucleotide Metabolism," BMB Reports, 45, 259–264 (2012).

[136]   Voet, D.; Voet, J. G.,(Eds.); "Biochemistry" John Wiley & Sons, Inc., 3rd Ed.,1095 (2004); and the references cited there in.

[137]   Zhang, Y.-W.; Zhang, Dan; Sun, Hua.; "The Basic Functions of Inosine5'-monophosphate Dehydrogenase and Its Application in Drug Discovery," Am. Chem. Soc., 49, 285–292 (2014).

INDIAN INSTITUTE OF TECHNOLOGY ROORKEE
ROORKEE

<u>CANDIDATE'S DECLARATION</u>

I hereby certify that the work which is being presented in the thesis entitled **"INTERACTION OF ORGANOTIN MOIETIES WITH DNA AND NUCLEIC ACID CONSTITUENTS",** in partial fulfilment of the requirements for the award of the Degree of **DOCTOR OF PHILOSOPHY** and submitted in the **Department of Chemistry** of the **Indian Institute of Technology Roorkee, Roorkee,** is an authentic record of my own work carried out during a period from January, 2009 to June, 2015 under the supervision of Dr. (Mrs.) Mala Nath, Professor, Department of Chemistry, Indian Institute of Technology Roorkee, Roorkee.

The matter presented in the thesis has not been submitted by me for the award of any other degree of this or any other Institute.

(NAGAMANI KOMPELLI)

This is to certify that the above statement made by the candidate is correct to the best of my knowledge.

Date: ………………., 2015   (Prof. Mala Nath)
                                                                                       Supervisor

The Ph.D. Viva-Voce examination of **Ms. Nagamani Kompelli**, Research Scholar, has been held on ………………………… .

Signature of Supervisor   Chairman, SRC   External Examiner

Head of the Department/Chairman, ODC

ABSTRACT

Due to tremendous contribution in agricultural, industrial, nanotechnology and pharmaceutical fields, the significance of organometallic compounds escalated rapidly in recent years. Organotin(IV) compounds have extensive industrial applications *viz.* stabilizers for poly(vinyl chloride), homogeneous catalysts, disinfectants, antifouling paints, timber preservatives, anti-wear agents, recycling agents, flame retardants and corrosive inhibitors. They are renowned for their practical applications in agriculture as pesticides, fungicides, bactericides and biocides, and are also well known to exhibit potential biological properties such as antimicrobial, antibacterial, antifungal, antiviral, antiherpes, antituberculosis, anti-inflammatory, antitumor and antihypertensive activities. Amongst metal-based non-platinum chemotherapeutics, organotin(IV) compounds lie forefront for their potential application in cancer therapy. Several organotin(IV) derivatives with ligands having donor atoms *viz.* N, O or S, are reported to exhibit antitumor activity comparable to that of standard antitumor drug, *cis*-platin. The biological activity of these compounds may be due to the presence of vulnerable Sn–X (X = N, O, S or halogen) bonds (due to longer covalent bonds, high polarizability and less thermodynamic stability) yielding $R_nSn^{(4-n)+}$ (*n* = 2 or 3) species, which have high affinity for negatively charged cellular moieties such as amino acids, proteins, nucleic acids and DNA. These species also play key role in delivering the active species to the site(s) of action.

DNA (deoxyribonucleic acid) and RNA (ribonucleic acid) are the biopolymers of nucleic acids (nucleotides) which are essential to store, transmit and express the genetic information in living organisms. The nucleic acid constituents are the precursors of obligatory metabolites and main energy donors for all cellular processes. Purines are the most ubiquitous nitrogen-containing heterocycles, which are involved in many metabolic processes, such as cofactors associated with a great number of enzymes and receptors, notably ATP, GTP, GDP, cAMP, cGMP, AcCoA, NAD, NADP, FAD, PAPS and SAM; playing vital roles at various cell cycle phases, in cell signalling and many other fundamental biological processes. The antitumor platinum-based drug, *cis*-platin binds at N7 position of two successive guanines (purine base) of same strand or two different strands of DNA, thereby, hinders transcription and replication. Guanosine (a purine nucleoside) comprises of guanine attached with ribofuranose ring, whereas 5'-guanosine monophosphate (5'-GMP) (nucleotide) consists of a phosphate group attached at C'5 of ribose of guanosine. 5'-Inosine

monophosphate (5'-IMP) or inosinic acid is a ribonucleotide of hypoxanthine. It has been reported that 1,10-phenanthroline, a bidentate chelate ligand, is effective for cancer treatment when used in combination with other antitumor drugs. Keeping in view of their extensive bioavailability in cellular fluids, important roles in biochemical processes and non-toxicity in low amounts, the selected ligands are ideal for the present studies.

In order to maintain the clarity in the presentation, the work in the thesis is systematically divided into the following chapters.

First chapter presents the general introduction and an overview of some important applications of organotin(IV) compounds, nucleic acid derivatives and DNA. A critical and comprehensive review on the antitumor activity and possible modes of action of organotin(IV) derivatives has also been presented. A brief literature survey on solution studies of organotin(IV) compounds with biologically important ligands and DNA binding studies of organotin(IV) complexes has also been presented.

Second chapter features the details of make, purity and other specifications of the materials used in the present study. The specifications of the instruments used to carry out the potentiometric studies, elemental analyses, spectroscopic studies *viz.* IR, far-IR, multinuclear (^{1}H, ^{13}C, ^{119}Sn) NMR, UV-Visible and fluorescence have been mentioned. The details of the procedures of various biological studies (gel electrophoresis, cytotoxicity (MTT assay) studies, enzyme (lipid peroxidase, lactate dehydrogenase) assays, acridine orange assay, comet assay of the synthesized compounds have also been described.

Third chapter includes the solution studies of organotin(IV) compounds with 5'-guanosine monophosphate (5'-HGMP)$^{2-}$ and guanosine (HGUO) (H indicate the N1 site of nitrogen base is protonated; used only in chapter **3** for clarity purpose). The potentiometric studies of Me$_n$Sn$^{(4-n)+}$ (where n = 2 or 3) with (5'-HGMP)$^{2-}$ and guanosine in aqueous solution at 298.15 ± 0.1 K and ionic strength 0.1 M of KNO$_3$ in 1:1 and 1:2 ratios have been performed. The protonation constants of ligands, hydrolysis constants of Me$_n$Sn(IV)$^{(4-n)+}$ (where n = 2 or 3) species and formation constants of complex species formed in aqueous solution at different pHs have been calculated by using computer program, SCOGS (Stability Constants of Generalized Species). The output files obtained from the SCOGS program for a given system have been employed in Origin 6.1 software to draw speciation curves. From speciation diagrams, the formation of various species at different pHs have been discussed. The results indicate that for both 1:1 Me$_2$Sn(IV)-ligand and Me$_3$Sn(IV)-ligand systems (where ligand = (5'-HGMP)$^{2-}$ and (HGUO)), M(HL) species is the major species (87–100%) existing between pH ~ 6.0–7.0 (physiological pH) along with traces of M(HL)H$_{-1}$ (4–10%),

M(HL)(OH) (0.2–3%) and M(OH)$_2$ (0.4–0.5%) (M = Me$_n$Sn(IV)$^{(4-n)+}$; n = 2 or 3). Multinuclear (^{1}H, ^{13}C, ^{119}Sn) NMR studies of the solutions of both 1:1 and 1:2 systems at different pHs were recorded. From the chemical shifts, coupling constants $^2J(^1$H$-^{117/119}$Sn) and $^1J(^{13}$C$-^{117/119}$Sn), and ∠C–Sn–C bond angles, the possible geometries of various species have been proposed. M(HL) species adopt a distorted octahedral geometry in case of Me$_2$Sn (IV)-ligand system and a distorted trigonal bipyramidal/distorted tetrahedral geometry in case of Me$_3$Sn(IV)-ligand system. As the pH increases beyond 8.0, concentration of hydrolyzed species increases with the release of the ligand. Same results are obtained for 1:2 systems except the formation of hydrolyzed species starts before 5.0 pH.

Fourth chapter deals with the synthesis and characterization of some new mixed diorganotin(IV) (R = Me, Ph, Bu and Oct) and triphenyltin(IV) derivatives of guanosine and 1,10-phenanthroline in 1:2:1 and 1:1:1 ratio, respectively. The probable structure for the synthesized derivatives on the basis of spectral studies *viz*. IR, far-IR and multinuclear (^{1}H, ^{13}C, ^{119}Sn) NMR has been proposed to be a distorted octahedral geometry around tin. The *in vitro* cytotoxicity activities against HEK293 (human embryonic kidney) and a panel of four cancer cell lines of human origin, *viz*. MCF7 (mammary), HepG2 (liver), DU145 (prostrate) and HeLa (cervical) have been screened and the IC$_{50}$ values indicate that the dimethyltin(IV) and dioctyltin(IV) derivatives are found to be inactive against all cell lines, where as the di-/triphenyltin(IV) derivatives show good activity (higher than *cis*-platin in few cases). Dibutyltin(IV) derivative exhibits the highest activity against all cell lines, except DU145. Enzyme assays *viz*. lipid peroxidase and lactate dehydrogenase assays, performed on two selected complexes (diphenyltin(IV) and triphenyltin(IV) derivatives) indicate that both the complexes cause apoptosis along with a minor necrosis. Acridine orange and comet assays on HepG2 and HeLa cell lines also support that apoptosis is the main cause for cell death. DNA binding studies have been performed by using UV-Visible and fluorescence spectroscopy, and the determined binding constants showed that the complexes have good binding affinity with CT DNA, suggesting that the synthesized derivatives binding to DNA led DNA damage, one of the causes for apoptosis. Further, the interaction of organotin(IV) moieties might takes place *via* electrostatical binding or groove insertion of DNA. Gel electrophoresis results of all the complexes indicate the promotion of the conversion of DNA from super coiled form I to nicked circular form II, implicating the role of organotin(IV) compounds in the process of DNA cleavage.

Fifth chapter deals with the synthesis and characterization of some new diorganotin(IV) (R = Me, Ph and Bu) derivatives of 5'-inosine monophosphate (5'-IMP)$^{2-}$ (1:1) and mixed diorganotin(IV) (R = Me, Ph and Bu) derivatives of (5'-IMP)$^{2-}$ and 1,10-phenanthroline (1:1:1). On the basis of spectral studies (IR, far-IR, and ^{1}H, ^{13}C, ^{119}Sn NMR) of the synthesized derivatives, a distorted octahedral geometry around tin is proposed. Owing to the poor solubility, biological studies of dimethyltin(IV) derivatives could not be performed. The diphenyltin(IV) inosinate is slightly more active against MCF7 as compared to that of *cis*-platin but it shows very less activity in comparison to 5-fluorouracil. The compounds dibutyltin(IV) inosinate and the mixed diphenyltin(IV) and dibutyltin(IV) derivatives are found to be much more active against MCF7 cell lines. The dibutyltin(IV) derivatives are found to be very active against HepG2 cell lines. The IC$_{50}$ values of the diphenyltin(IV) derivatives against HepG2 cell line suggests that the compounds are inactive for the reason unknown. The presence of phenanthroline moiety induces the cytotoxicity, hence, the mixed diphenyltin(IV) and dibutyltin(IV) derivatives a more active compared to that of respective diorganotin(IV) inosinates. However, the dibutyltin(IV) inosinate is found to be the most active complex against both MCF7 and HepG2 cell lines. Acridine orange and comet assays on MCF7 cell line support that the main cause for cell death is *via* apoptosis. UV-Visible spectral and fluorescence binding studies shows that the diphenyltin(IV) and dibutyltin(IV) derivatives have moderate binding affinity with DNA and the interaction might takes place *via* electrostatical binding or groove insertion of DNA, thus indicating that organotin(IV) binding with DNA is one of the causes for apoptosis. Gel electrophoresis results show the interaction of the complexes with DNA, but no cleavage has been observed.

Chapter 6 concludes the results from the solution studies of organotin(IV) moieties with nucleic acid constituents and the studies of newly synthesized organotin(IV) derivatives. The solution studies and various biological studies have been performed in order to understand their mechanism of action. However, more detailed experimental studies are required to throw light upon their cytotoxic activities and possible modes of action. The future prospects of utility of organotin(IV) moieties in anticancer chemotherapy have also been discussed.

ACKNOWLEDGEMENTS

LIST OF ABBREVIATIONS

AcCoA	Acetyl co-enzyme A
AMP	Adenosine monophosphate
ATP	Adenosine triphosphate
AO	Acridine Orange
cAMP	Cyclic adenosine monophosphate
cGMP	Cyclic guanosine monophosphate
CsI	Cesium iodide
CPT	*cis*-platin
DMSO	Dimethyl sulfoxide
DNA	Deoxyribonucleic acid
EB	Ethidium bromide
EDTA	Ethylenediamminetetraacetic acid
FAD	Flavin adenine dinucleotide
5-FU	5-Fluorouracil
GDP	Guanosine diphosphate
GMP	Guanosine monophosphate
GTP	Guanosine triphosphate
H_2GuO	Guanosine
IMP	Inosine monophosphate
KBr	Potassium bromide
NAD	Nicotinamide adenine dinucleotide
NADPH	β-nicotinamide adenine dinucleotide phosphoric acid
PAPS	3'-Phosphoadenosine-5'-phosphosulfate
PVC	Poly(vinyl chloride)
RNA	Ribonucleic acid
SAM	S-Adenosyl methionine
XMP	Xanthylate
Miscellaneous	
as	Asymmetric stretching
b.p.	Boiling point
Bu	Butyl (prefix *n*, refers to normal butyl)
Bz	Benzyl

cm	Centimeter
$CDCl_3$	Deuterated chloroform
CD_3OD	Deuterated methanol
DMSO	Dimethyl sulfoxide
DMSO-d_6	Hexadeuteriodimethyl sulfoxide
D_2O	Deuterium oxide
e.g.	Example
Eq.	Equation
Et	Ethyl
Fig.	Figure
FTIR	Fourier transform infrared
g	Gram
h	Hour
Hz	Hertz
IC_{50}	Drug concentration at 50% growth inhibition
IR	Infrared
L	Litre
LD_{50}	Lethal dose at 50% survival
M	Molar
M.P.	Melting point
Me	Methyl
min	Minute
mol	Mole
NMR	Nuclear magnetic resonance
Oct	Octyl (Prefix *n*, normal octyl)
OD	Optical density
ppm	Parts per million
Ph	Phenyl
phen	1,10-phenanthroline
pqs	Partial nuclear quadrupole splitting
Pr	Propyl (Prefix *n*, normal propyl)
s	Symmetric stretching
SEM	Standard error of mean

TAE	Buffer containing tris base, acetic acid and EDTA
TBE	Buffer containing tris base, boric acid and EDTA
U	Unit
UV	Ultra Violet
V	Volt
viz.	Videcilet
v/v	Volume/Volume

$[Me_3Sn(H_2O)_2]^+$, (g) $[Me_3Sn(HL-2)]^+$, and (h1/h2/h3) isomers of $[Me_3Sn(HL-2)]^+/Me_3Sn(HL-2)(OH)$ (For the sake of simplicity, the charges on the species are omitted).

LIST OF PUBLICATIONS

IN THE REFERRED JOURNALS

1. "Speciation and NMR Spectrometric Studies of Interaction of Di- and Triorganotin(IV) Moieties with 5'-Guanosine Monophosphate and Guanosine in Aqueous Solution"
    Mala Nath*, **Nagamani Kompelli**.
    J. Sol. Chem., 43, 1184–1204 (2014).

2. "Metal-based Anticancer Agents: *In Vitro* DNA Binding, Cleavage and Cytotoxicity"
    Mala Nath*, **Nagamani Kompelli**, Partha Roy, Snehasish Das.
    Int. J. Med. Health Pharm. Biomed. Eng., World Academy of Science, Engineering and Technology, 8 (No. 8), 403–409 (2014).

IN CONFERENCES

1. "Speciation and NMR spectrometric studies of interaction of di- and triorganotin(IV) moieties with 5'-guanosine monophosphate and guanosine in aqueous solution"
    Mala Nath, <u>**Nagamani Kompelli**</u>[*] and Hitendra Singh.
    4th conference on "Recent Trends in Instrumental Methods of Analysis" (2011) held at Department of Chemistry, IIT Roorkee, Roorkee.

2. "Metal-based Anticancer Agents: *In Vitro* DNA Binding, Cleavage and Cytotoxicity"
    <u>Mala Nath</u>*, **Nagamani Kompelli**, Partha Roy, Snehasish Das.
    International Conference on Metallurgy, Materials Science and Engineering (ICMMSE 2014) during 14-15, August-2015 at Venice, Italy.

    This paper is also published in the proceedings of the conference:
    "Metal-based Anticancer Agents: *In Vitro* DNA Binding, Cleavage and Cytotoxicity,"
    In: International Science Index, Vol. 8, No. 8, Part IV, pp. 538–544 (2014).
    (Underlined authors presented the paper)

<div align="center">

CONTENTS

</div>

REFERENCES

Dedicated

to

My Parents

&

Beloved Husband

Chapter-1

INTRODUCTION

Chapter-2

MATERIALS & METHODS

Chapter-3

SOLUTION STUDIES OF ORGANOTIN(IV) WITH GUANOSINE AND GUANOSINE MONOPHOSPHATE

Chapter-4

TRI- AND DIORGANOTIN(IV) DERIVATIVES OF GUANOSINE AND PHENANTHROLINE

Chapter-5

DIORGANOTIN(IV) DERIVATIVES OF INOSINE MONOPHOSPHATE AND PHENANTHROLINE

Chapter-6

CONCLUSIONS AND FUTURE PROSPECTS

1.1. GENERAL INTRODUCTION

All essential life processes require the role of metals in enzymatic, structural or chemical reactions [1–3]. About 12% of enzymes catalytic activities are attributed to metal centers in which metals act to bridge substrate to enzyme lowering the free energy of activation, while structurally they are involved in the tertiary folding of proteins [4]. Some transition metals generate the functional reactive intermediates whereas the others turn out to be adversely toxic [5]. Few typical examples include: iron (Fe) and manganese (Mn) act as enzyme cofactors and catalyze redox reactions; zinc (Zn) and calcium (Ca) providing structural integrity and flexibility of proteins; iron (Fe) in oxygen transportation; sodium (Na) and potassium (K) serving as charge carriers and, magnesium (Mg) and manganese (Mn) function in hydrolysis and group-transfer [6]. Metal compounds significance in medicine date back to the 16th century [7]. Presently, the therapeutically prescribed metal containing compounds catalouge features platinum (anticancer), silver (antimicrobial), gold (antiarthritic), bismuth (antiulcer), antimony (antiprotozoal), vanadium (antidiabetic) and iron (antimalarial) [6]. Most biological molecules (proteins and DNA) are electron rich whereas metal ions are electron deficient; hence, the disposition of metal ions to bind to/interact with many important biological molecules is fairly possible [4]. Prior to 1960s, organometallic complexes were considered to be unstable in aqueous media, therefore, they were not recommended to be used in biological systems [8]. Serendipitous discovery of tumor suppressing properties of *cis*-platin (a platinum-based drug) by rosenberg et al. (1969) motivated to design, screen new metallodrugs and allow for biological applications, especially in the field of oncology. After the discovery of new types of metal-carbon bonds *viz.* metallocenes, metal carbonyls and metal carbenes, titanocene dichloride (structurally similar to *cis*-platin) was the first organometallic anticancer molecule which exhibited medium anti-proliferative activity *in vitro*, but displayed potential performance *in vivo* [9]. Thus, organometallic compound's significance rapidly escalated in recent years along with their tremendous contribution in agricultural, industrial, nanotechnological and pharmaceutical fields [10–12]. Organometallic complexes were known to have distinctive properties including: variation in coordination numbers and geometries, their predictable ligand exchange reactions, kinetic stability, lipophilic nature, metal-specific mode of action towards biomolecules. The design of new pharmacophore with intriguing featues which are

not often groomed by classical synthetic approach, can be easily obtained by using organometals. An emerging branch, bioorganometallic chemistry emphasize on the synthesis and study of organometallic complexes of biological and medicinal interest. Currently, bioorganometallic chemistry includes five main domains: organometallic therapeuticals, toxicology and environment, molecular recognition in aqueous phases, enzymes, proteins and peptides, and bioanalysis and pharmaceutical sensors [9, 13, 14].

1.2. ORGANOTIN COMPOUNDS – A BRIEF REVIEW

Organotin(IV) compounds are characterized by the presence of at least one covalent C–Sn bond with a general formula R_nSnX_{4-n} (n = 1 to 4; R = alkyl or aryl group; X = hydrogen or a metal or halogen or O, S, N containing groups) [15]. Depending upon the number of alkyl (R) or aryl (Ar) moieties attached to the tetravalent Sn, organotin(IV) compounds are classified as mono-, di-, tri- or tetraorganotin(IV), with Chloride, fluoride, oxide, hydroxide, carboxylate or thiolate group(s) as the common anions. The skeleton of organotin framework usually involve tetrahedrally–oriented bonds resulted from the hybridization of 5s and 5p orbitals of tin atom with a coordination number four, however, it can be stretched beyond sp^3 featuring extended coordination geometries, giving advantage in designing complexes with biological motifs such as amino acids, proteins, carbohydrates, nucleic acids etc [16]. While elucidating the structure–activity relationship of organotin(IV) derivatives (usually represented as $R_nSnX_{4-n}(L)_x$) [17], three primary factors are considered: the nature of the organic group (R), halide or pseudohalide (X), and finally the donor ligand (L) attached to tin. A diligent choice of the ligand scaffold coordinated to the organotin(IV) moiety can modulate the activity, impart desirable features to achieve the specific targeting site and minimize its drawbacks [18]. Few examples are cited here to explain the significance of organotins in day-to-day life, however, emphasis on biological applications are focussed in detail.

1.2.1. Agricultural, Industrial and Synthetic Applications of Organotin Compounds

Organotin compounds are well known for their practical applications in agriculture as pesticides, fungicides, bactericides and biocides [15]. A large array of biocidal properties was

shown by tributyltin-halides, oxides and acetates, thereby used extensively in wood preservatives and in marine antifouling paints.

Organotin(IV) compounds have extensive applications as industrial commodities which include stabilizers for chlorine (poly(vinyl chloride)) and non-chlorine (polyethylene) based compounds, industrial catalysts (homogeneous catalysts in synthesis), disinfectants, antifouling paints, anti-mold agents, timber preservatives, anti-wear agents, recycling agents, flame retardants, smoke suppressants, corrosive inhibitors in chlorinated lubricating oils, transformer oils and solvents, and industrial biocides [15]. Many organotin compounds have been used in polymer and plastic industry as stabilizers against heat, light, oxygen, decomposition during hot fabrication for chlorinated polymers such as PVC, chlorinated rubbers, modified plastics such as neoprene, transformer oils, paraffin and non-chlorine based compounds such as lubricating oils, cellulose acetate, polyethylene, polypropylene, polycarbonates, polyamides (nylon), hydrogen peroxide and as biocides e.g. disinfectants, slime control for paper pulp mills and cooling towers [15]. Tin(II) octoate, tin(II) oxalate and dibutyltin(IV) diacetate have been used as homogeneous catalysts for polyurethane foam production. Organotin carboxylates have been used as curing agents in silicone rubber production and as catalyst in the production of dental prosthetic devices [16].

Organotin chemistry exploits the weakness of Sn–C bonds (longer covalent bond, high polarizability and less thermodynamic stability) to deliver whatever is attached to the tin to another reagent or compound *via* radical mechanism as well as by polar mechanism, thus making them good synthetic reagents and/or catalysts for either selective reactions or multistep synthesis. Organotin complexes have been employed as homogeneous catalysts in plastic and polymer industry, for various reactions such as esterification, polymerization, C–C bond formation, ester hydrolysis, reduction reactions, addition reactions, dehydrogenation reactions, palladium catalysed cross-coupling reactions, transmetallation reactions, synthesis of higher homologues of hydrocarbons from the lower ones, stereo selective synthesis of alcohol and ketone derivatives, synthesis of derivatives of enantiomerically pure α-amino acid, tetracycline and azulene, and catalysis of Reformatsky type reactions [15, 16, 17].

1.2.2. Biological Applications

Organotin compounds display a wide spectrum of biological effects. They are renowned to exhibit potential biological activities such as antimicrobial, antibacterial, antifungal, antiviral, antiherpes, antituberculosis, anti-inflammatory, antitumor and antihypertensive activities [18–31]. Few examples from the recent past are collected and are given in detail along with their predicted mechanistic studies in the following subsections, based on their activity.

1.2.1.1. Antimicrobial activity

The antimicrobial activity studies of organotins against the microorganisms (i.e., bacterial, fungal, and protozoal) collected from the last five years are summarized as follows: Antibacterial activity of triorganotin(IV) derivatives of Schiff base derived from salicylaldehyde and adenine (Fig. 1.1), at low concentrations towards gram-positive (*Bacillus subtilis* and *Staphylococcus aureus*) and gram-negative bacteria (*Escherichia coli*, *Salmonella typhi* and *Pseudomonas aeruginosa*) is quite significant (show moderate to high activities and increases with concentration) as compared to that of the standard drug (imipenem), and the antimicrobial activity was suggested either due to the killing of microbes or inhibition of their multiplication by blocking the active sites [28]. The diorganotin(IV) complexes, R_2SnL (L = L^a: R = Me , Ph ; L = L^b: R = Me , Ph , L = L^c: R = Me, Ph, Bu) of hydrazone ligands (*N*'-(5-bromo-2-hydroxybenzylidene) isonicotinohydrazide (H_2L^a), *N*'-((2-hydroxynaphthalen-1-yl)methylene) isonicotinohydrazide (H_2L^b) and *N*'-(2,4-dihydroxybenzylidene)-isonicotinohydrazide (H_2L^c)) (Fig. 1.2) were evaluated *in vitro* against gram-positive (*Bacillus subtilis* and *Staphylococcus aureus*) and gram-negative (*Escherichia coli* and *Pseudomonas aeruginosa*) bacteria and were compared with standard antibacterial drugs (vancomycin, streptomycin, penicillin, nalidixic acid and gentamicin). It is reported that R_2SnL^c complexes exhibit greater inhibitory effects than both the parent ligand and other complexes towards *Bacillus subtilis*, *Staphylococcus aureus* and *Pseudomonas aeruginosa*. The presence of the OH group inside the ligand perhaps may increase the lipophilic character and efficient diffusion into bacterial cells upon complexation. The hydrogen bonding ability of the ligands in these three complexes will enhance their interaction with active biological
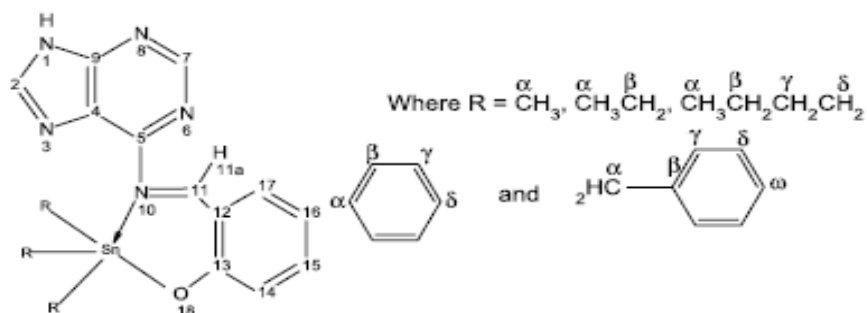
Fig. 1.1. Trialkyltin(IV) complexes of Schiff base derived from salicylaldehyde and adenine [28].

H_2L^a H_2L^b H_2L^c
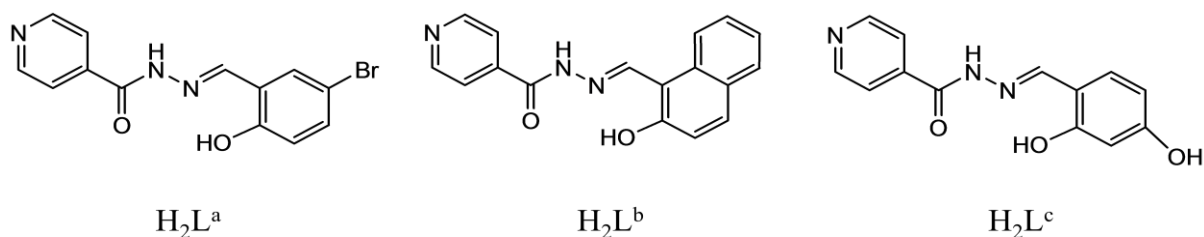
Fig. 1.2. Structures of ligands: (*N'*-(5-bromo-2-hydroxybenzylidene) isonicotino-hydrazide (H₂Lᵃ), *N'*-((2-hydroxynaphthalen-1-yl)methylene) isonicotino-hydrazide (H₂Lᵇ) and *N'*-(2,4-dihydroxybenzylidene) isonicotinohydrazide) (H₂Lᶜ) [29].
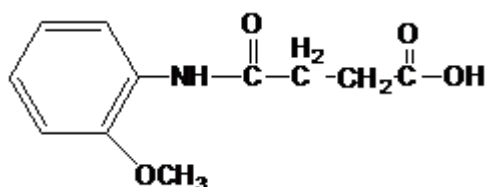
Fig. 1.3. Structure of (4-(2-methoxyphenylamino)-4-oxobutanoic acid) moiety [30].

centers impairing normal cellular processes, and also the intrinsic biocidal effects and lipophilicity of organotin moiety facilitate permeability across the bacterial cells. Many standard drugs were inactive towards *Pseudomonas* bacteria genus, but organotin derivatives of H_2L^c exhibit greater activities than the other compounds [29].

Leishmaniasis is a vector (insect phlebotomine sand fly)-borne endemic disease caused by an obligate protozoan parasite of genus *Leishmania*. Twelve organotin(IV) based peptide derivatives of carboxylate ligand (Fig 1.3) (R_3MS_{20}, where R = Me, Et, Bu, Ph, Cy, $R_2(MS_{20})_2$, R = Bu, Ph, Bz, di-*t*-Bu, Oct, and Me_3(1,10-ph)MS_{20}, MS_{20} = 4-(2-methoxyphenylamino)-4-oxobutanoic acid), against *Leishmania tropica* KWH23 strain showed significant *antileishmanial* activity and high biocompatibility. From the *in-silico* studies, the organotin derivatives were found to be bound to leishmanolysin (GP63) receptor, probably resulting in a receptor mediated inlet of these derived compounds inside the *Leishmania* cells, where they were further bound to the DNA (confirmed by DNA interaction study). This interaction caused a redox reaction between the DNA and the compounds, leading to the degradation of DNA and causing apoptotic death of *L. tropica* [30].

Triorganotin dithiocarbamates, *viz.* $[SnPh_3\{S_2CNR(R^1)\}]$, $[SnCy_3\{S_2CNR(R^1)\}]$, $[SnMe_3\{S_2CNR(R^2)\}]$, $[SnPh_3\{S_2CNR(R^2)\}]$ and $[SnCy_3\{S_2CNR(R^2)\}]$, [R = methyl, R^1 = $CH_2CH(OMe)_2$, and R^2 = 2-methyl-1,3-dioxolane] (Fig. 1.4), were screened against *Aspergillus flavus*, *Aspergillus niger*, *Aspergillus parasiticus* and *Penicillium citrinum*. The structure–activity relationship (SAR) indicate that the complexes $[SnPh_3\{S_2CNR(R^1)\}]$ and $[SnPh_3\{S_2CNR(R^2)\}]$ showed nanomolar inhibition concentration in terms of IC_{50} [31]. *In vitro* antimicrobial screening (by filter paper disc method) of di- and triorganotin(IV) ($R_{(4-n)}SnL_n$; where *n* = 2; R = Me, *n*-Bu and Ph; *n* = 1; R = Me, *n*-Pr, *n*-Bu and Ph) derivatives of 4-amino-3-methyl-1,2,4-triazole-5-thiol (HL-1), 4-amino-3-ethyl-1,2,4-triazole-5-thiol (HL-2), 3-amino-1,2,4-triazole-5-thiol (HL-3) and 5-amino-3H-1,3,4-thiadiazole-2-thiol (HL-4) along with two standard drugs such as fluconazole and ciprofloxacin was reported against the bacteria, *viz. Staphylococcus aureus* and *Escherichia coli*, and against some fungi, viz. *Aspergillus fumigatus, Candida albicans, Candida albicans* (ATCC 10231), *Candida krusei* (GO₃) and *Candida glabrata* (HO₅). Mild antifungal activity comparable to fluconazole was reported, but almost insignificant activity was shown against the gram-positive (*Staphylococcus aureas*) and gram-negative (*Escherichia coli*) bacteria as compared to that of standard drug, ciprofloxacin [32].

(a)
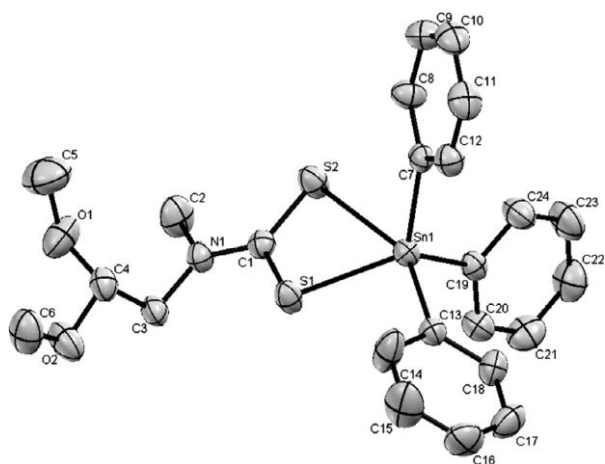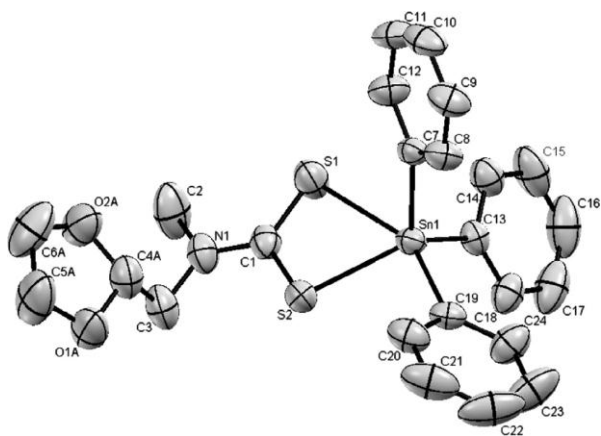
(b)   **(c)**
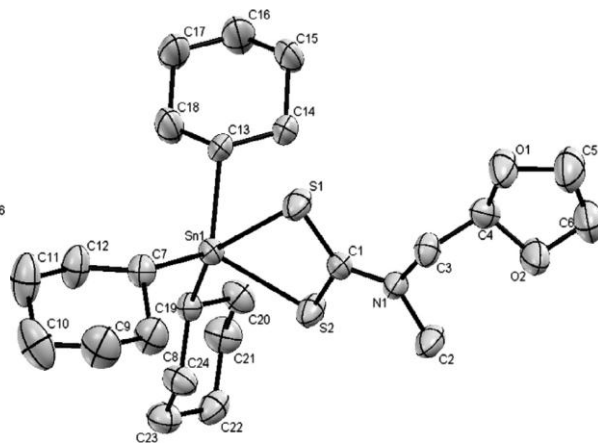
Fig. 1.4. Structure of complexes: (a) [SnPh₃{S₂CNMe(R¹)}] [R¹ = CH₂CH(OMe)₂], (b) [SnPh₃{S₂CNMe(R²)}] and [SnCy₃{S₂CNMe(R²)}] [R² = 2-methyl-1,3-dioxolane], and (c) [SnCy₃{S₂CNMe(R²)}] [R² = 2-methyl-1,3-dioxolane] [32].

1.2.2.2. Anti-inflammatory activity

Novel tri- and diorganotin(IV) derivatives with various ligands e.g. Schiff bases [33, 34], orotates [35], dipeptides [36], nucleic acid derivatives [37, 38, 39] (Figs. 1.5 to 1.9) were tested for anti-inflammatory activity by using the carrageenan-induced paw edema bioassay in albino rats and few of the compounds were reported to exhibit potent anti-inflammatory activity with no appreciable side effects on blood pressure (as evidenced by cardiovascular activity) with significantly low toxicity levels.

1.2.2.3. Antitumor activity

A brief note on cancer and antitumor activity of organotins and few selected examples availed in the literature are mentioned in this section.

Malignancy is the result from a multiple process by accumulation of mutations and other genetic alteration leading to cancer. Cancer is one of the principal causes of death worldwide, causing more deaths than AIDS, tuberculosis, and malaria combined. According to the International Agency for Research on Cancer (IARC), 12.7 million new cancer cases were estimated worldwide in 2008 and approximately 7.6 million deaths were documented. This burden is expected to escalate upto 21.4 million new cancer cases and anticipated to claim the lives of ~ 13 million people by 2030. Globally, one eighth deaths are due to cancer [40]. Changes or mutations, in the genetic material of normal cells can disrupt the balance of factors governing cell survival and division, causing the uncontrolled and pathological proliferation of abnormal cells resulting cancer [40]. Currently, surgery, radiation, chemotherapy, hormones or targeted biologic therapy, and immunotherapy–two or more methods in combination are usually used for treating cancer. Chemotherapy is an important weapon for combating cancers. Development of numerous compounds as potential candidates for anticancer drugs has progressed in last few decades, but only a handful of them strode effectively through clinical protocols. Primarily entered in the chemotherapeutic regime was *cis*-platin (by Barnet Rosenberg (1969)), a metal based—to be precise a platinum-based antitumor drug, showed optimistic results for treating solid malignancies [41].

The utility of *cis*-platin as anticancer agents is a phenomenal success. The mechanism of action of *cis*-platin primarily include hydrolysis where the two Cl^- s get replaced with H_2O molecules, forming highly reactive monoaquated $[Pt(NH_3)Cl(OH)_2]^+$ and diaquated
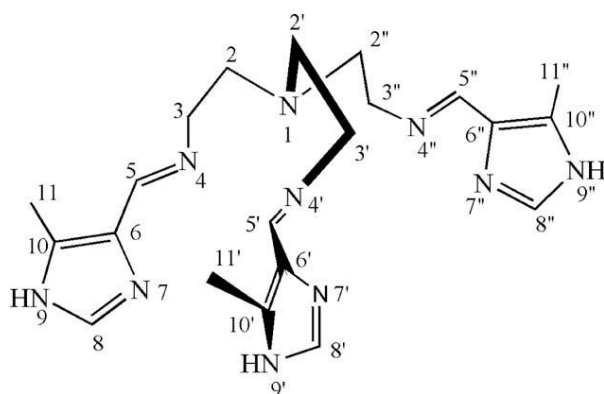
Fig. 1.5. Chemical structure of Schiff base ligand (tren(4-Me-5-ImH)₃) [33].
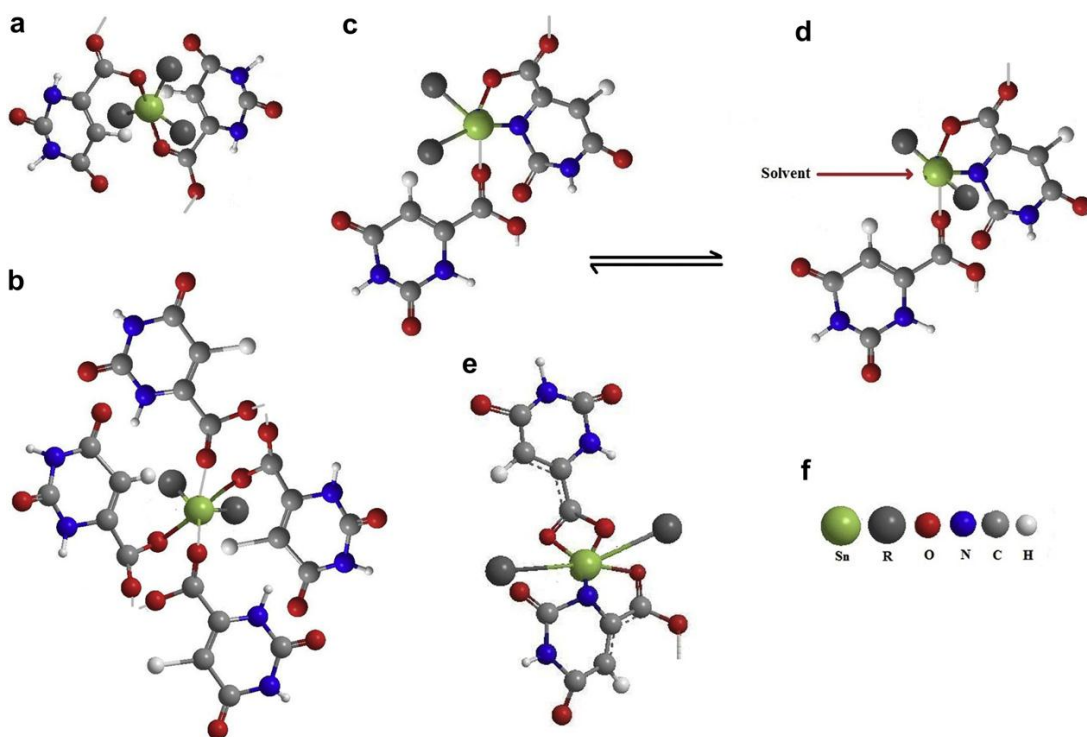
Fig. 1.6. Structures of: (a) R₃Sn(H₂Or),(R = Ph, *n*-Bu and Me), (b) R₂Sn(H₂Or)₂ (R = Ph, Me and *n*-Oct), (c) *n*-Bu₂Sn(HOr), (d) *n*-Bu₂Sn(HOr)·solvent, and (e) *n*-Bu₂Sn(H₂Or)₂ [35].

(i)

(a)   **(b)**   **(c)**

R = Me; R' = H_2C [indole structure] ; R" = H

R = -C_6H_5; R' = H_2C [imidazole structure] ; R" = -$CH_2CH(CH_3)_2$

R = -C_6H_5; R' = -$CH_2C_6H_4OH$; R" = -$CH_2C_6H_5$

(ii)

R = CH_3 or C_6H_5; R' = H_2C [imidazole structure] ; R" = -CH_3

R = -CH_3; R' = -$CH_2C_6H_4OH$; R" = -$CH_2C_6H_5$

R = -C_6H_5; R' = H_2C [indole structure] ; R" = H

(iii)
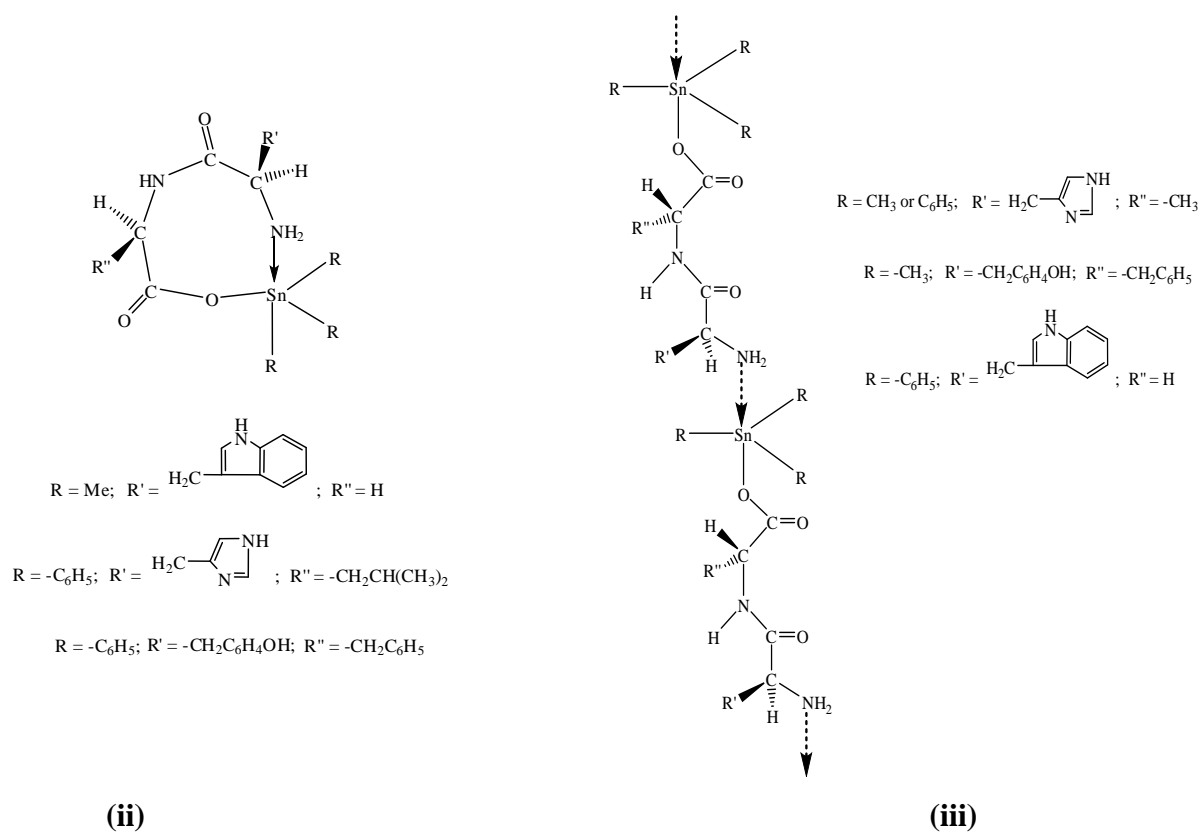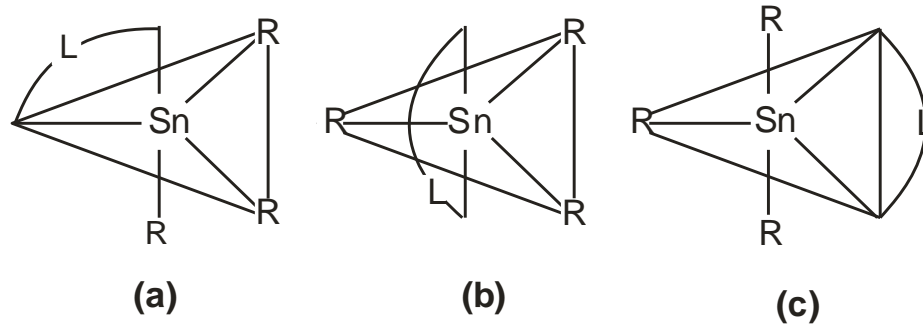
Fig. 1.7. (i) (a)/(b)/(c) are structural isomers of Me₃Sn(HHis-Ala) and Ph₃Sn(HHis-Leu), (ii) and (iii) are structures of Me₃Sn(HHis-Ala/HTyr-Phe) and Ph₃Sn(HHis-Ala/HTrp-Gly) [36].

(a)

(b)

B = Guanine Base

B = Guanine Base
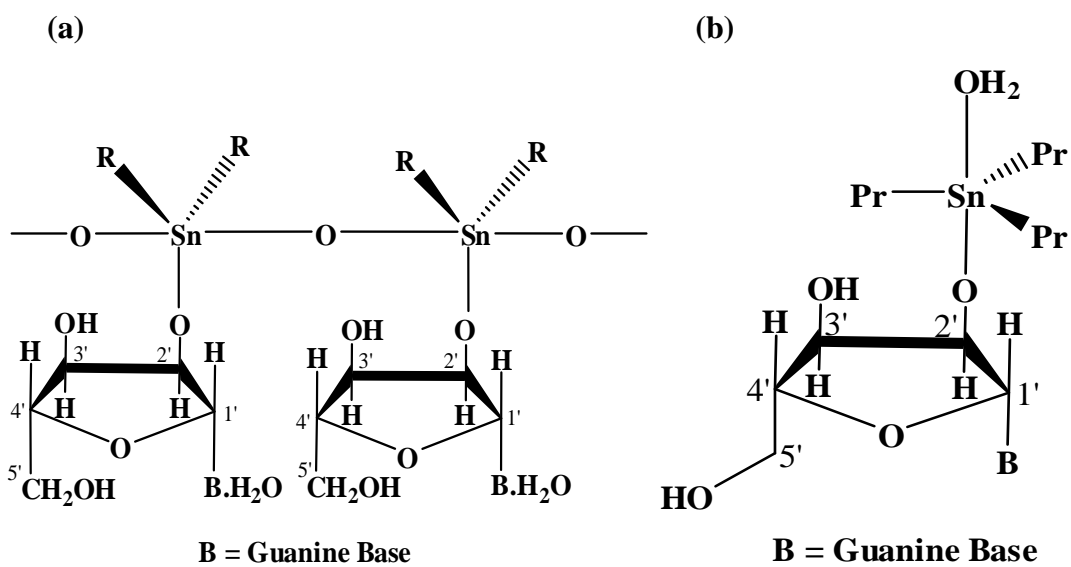
Fig. 1.8. Structures of: (a) diorganotin(IV) derivatives of guanosine, (b) tri-iso-propyltin(IV) derivative of guanosine [38].
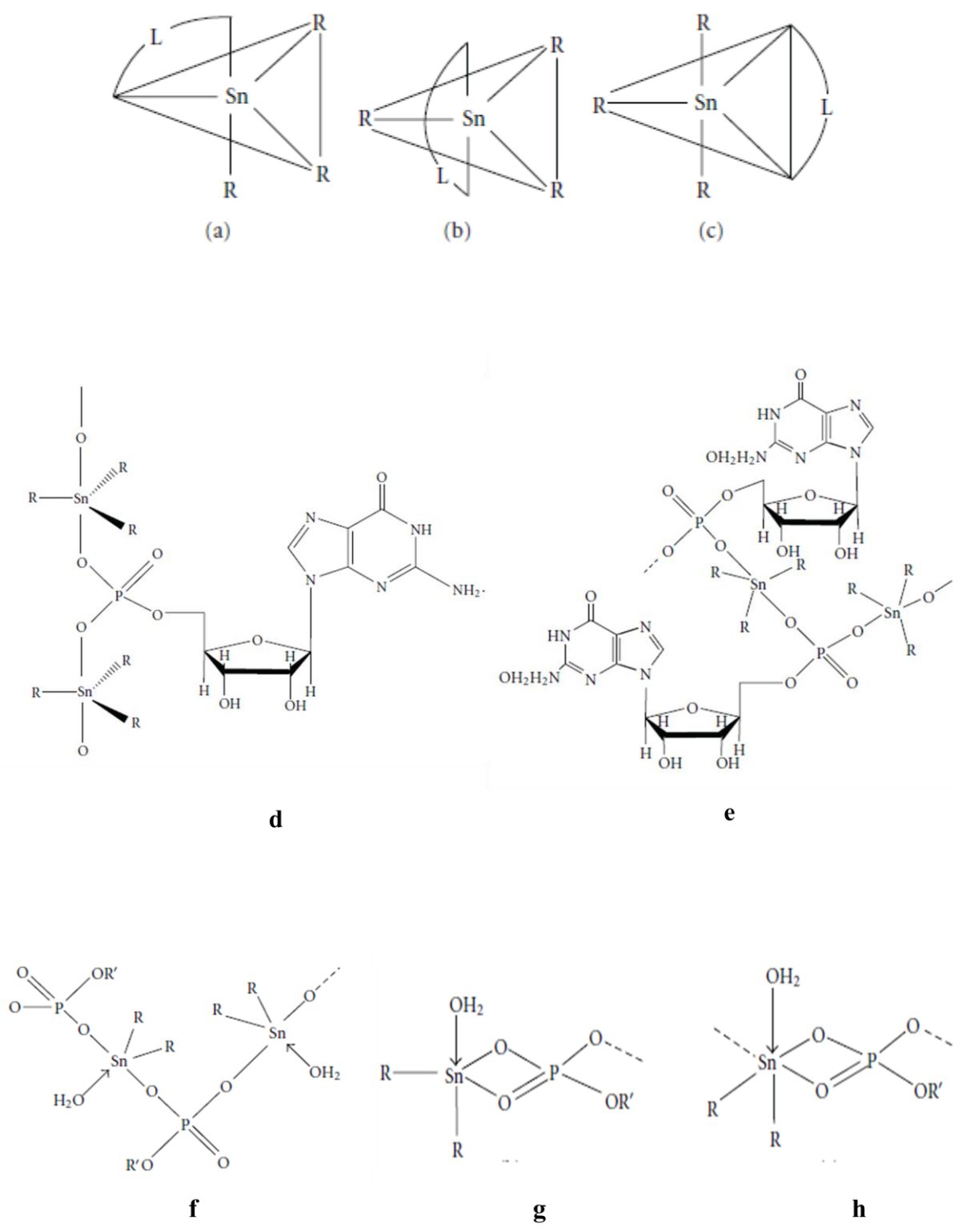
Fig. 1.9. (a)/(b)/(c) are isomers of R₃SnL (L = bidentate ligand), (d)/(e) are structures of triorganotin (IV) derivatives of (5'-GMP)$^{2-}$, (f)/(g)/(h) are structures of diorganotin(IV) derivatives of (5'-GMP)$^{2-}$ [39].

$[Pt(NH_3)_2(OH_2)_2]^{2+}$ moieties which further target towards nucleophilic centres of biological molecules of cellular fluid. Evidences suggest that the most important target is DNA where it binds to N7 sites of two successive guanines of the same strand of DNA *via* intra cross linkage and thus inhibiting its replication. Several second, third and contemporarily fourth generation of platinum analogues (notably carboplatin, oxaliplatin, iproplatin, picoplatin etc) were subsequently designed and screened against a variety of cancer cell lines of varied histological origins and some of these complexes exhibit a broad anti-neoplastic spectrum and in combination with other chemotherapeutic agents displayed incredibly good results. Regardless of their clinical and commercial success, one could not ignore their downsides such as systemic toxicity (accumulation of platinum in cells), development of cellular resistance associated with them and limited activity against certain types of cancers. In this context, organometallic chemistry seems to be a better platform to invent such molecules with lesser side-effects.

Though *cis*-platin and its analogues are efficient drugs, the Pt-resistance and severe side-effects compelled researchers to develop other alternatives to effectively treat various types of cancer and to comprehend their mode of action to understand the underlying mechanism of action at cellular and molecular levels. Among non-platinum chemotherapeutics, gold and organotin derivatives gained utmost attention due to their potential apoptotic inducing character, high therapeutic index with minimum toxicity and apparently negative platinum-induced resistance [41– 43]. Ando et al. was the pioneer to synthesize and test the bioactivity of a number of organotin derivatives *in vitro* and *in vivo* against murine leukemia cell lines (P388 and L1210) and different panels of human cancer cell lines [44], followed by Crowe et al. (1980) [45], Saxena et al. (1989) [46] but in fact, their biostudies ascented after the demonstration of cytotoxic profiles by M. Gielen [47, 48] against WiDr (colon cancer) and MCF7 (mammary cancer) cell lines. Thus, a new chapter began in the field of organotin chemistry, to adopt the potential drug candidates in medicine alongside the pre-existing commerical, agricultural, industrial and other biological applications (mainly as bactericides, fungicides, biocides and pesticides).

Organotin(IV)s are racing forward alongside with their competitors in terms of generation of novel complexes and evaluation of their activity against cancer [49–51], amongst non-platinum metal-based anticancer therapeutics. Few examples include:

Strong *in vitro* cytotoxic activity was exhibited by di-*n*-butyl-(4-chlorobenzo-hydroxamato)tin(IV) chloride (DBDCT) towards human immature granulocyte leukemia (HL60), human salivary-gland carcinoma (SGC7901), human Henrietta carcinoma (Hela) and human urinary bladder (T24) cell lines, which were equal to or even higher than that of *cis*-platin. Further, *in vivo* intraperitoneal injection of this compound on mice along with *cis*-platin as positive contrast drug, against the transplantation tumor models of sarcoma carcinoma (S_{180}), hepatocellular carcinoma (H_{22}) and Ehrlich's ascites carcinoma (EAC) displayed antitumor activity close to that of *cis*-platin against the hepatocellular carcinoma H_{22} and sarcoma carcinoma S_{180}, meanwhile, the survival extending rates at middle dose and high dose of DBDCT against Ehrlich's ascites tumor (EAC) were higher than those of *cis*-platin, signifying a good dose-effect relationship [52].
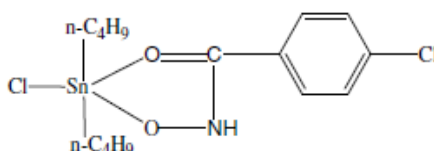
Fig. 1.10. Chemical structure of di-*n*-butyl-(4-chlorobenzo-hydroxamato)tin(IV) chloride (DBDCT) [52].

The antitumor activity results of few water-insoluble and water-soluble tris-(4-pyridinyl)porphyrin and tris(*N*-methyl-4-pyridiniumyl)porphyrin based dibutyltin(IV) porphinate complexes against P388 leukemia and A549 tumor cells were displayed and the activities are dependent on solubility of the compounds in aqueous medium and the central metal ion in the porphyrin ring. Further, the DNA hypochromism (A_{260}) and a slight increment in the viscosity and melting point of DNA with water-soluble dibutyltin(IV) porphinate complexes indicated their high affinity with DNA, but, no cleavage of DNA was detected in electrophoresis test. Hence, it was reported that the cytotoxic activity may be resulted from the interaction of cationic porphyrin with DNA by electrostatic and van der Waals forces, and binding of the pre-dissociated dibutyltin(IV) to nucleotides *via* phosphate group without destructing the duplex structure of DNA or DNA cleavage [53].
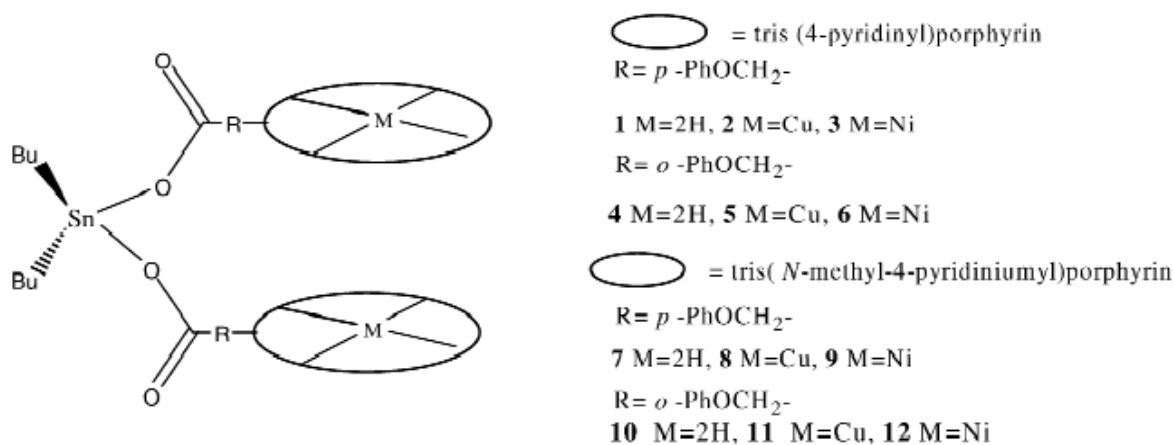
Fig. 1.11. Structure of dibutyltin(IV) porphinate complexes [53].

The comet assay results of tributyltin(IV) complex [Bu$_3$Sn(LSM)] (LSM= bis(1-methyl-1*H*-imidazol-2-ylthio)acetate) and its analogous tributyltin(IV) chloride (TBTC) on rat blood cells i*n vitro* was observed by Falcioni et al. When compared, both the complex and TBTC revealed an inducing of DNA damage in leukocytes, but effective potency was witnessed for tributyltin(IV) complex. Also, lipid hydroperoxide formation increased in leukocyte plasma membranes for [Bu$_3$Sn(LSM)] compared to that of TBTC, however, in presence of TBTC a change in the lipid order and packing of leukocytes (partially erythrocyte plasma membranes) was observed. When whole blood was treated with these two compounds, a preferential oxidative effect of TBTC on erythrocyte plasma membranes and erythrocyte oxidative processes, influencing the induction of DNA damage in leukocytes was observed. Further, the difference in hydrophobicity and extents of steric hindrance of TBTC and [Bu$_3$Sn(LSM)] also affected the capacity of the both to cross the plasma membrane and DNA damaging pathways [54].
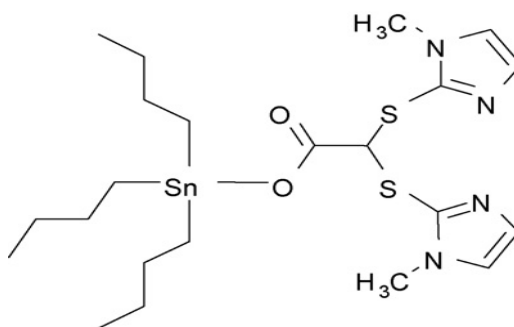
Fig. 1.12. Chemical structure of [Bu₃Sn(LSM)] complex, (LSM= bis(1-methyl-1*H*-imidazol-2-ylthio)acetate) [54].

The *in vitro* anti-proliferative tests of the two derivatives of organotin(IV) complexes of the type R₃SnL, where (L = *p*-bromo-*N*-methylbenzylaminedithiocarbamate and *p*-fluoro-*N*-methylbenzylaminedithiocarbamate, and R = phenyl) on three human cell lines, leukemic lymphoblastoma Jurkat cells, lymphoblastoma K562 cells, hepatoblastoma HepG2 cells and one mouse fibroblast cells L929 (cells with two species of origin (human and mouse), different morphology (lymphoblast, epithelial and fibroblast), diverse form of growth (adherent and suspension), and tissue origin (bone marrow, lymphoid, liver and subcutaneous connective tissue were selected) showed dose-dependent decrease of cell proliferation in all cell lines and the IC$_{50}$ values are comparable with the standard drug–doxorubicin. Tin was attached with the dithiocarbamato ligand in monodentate fashion resulting in distorted tetrahedron geometry and the same was illustrated by the spectral investigations and single crystal X-ray diffraction data [55].

Organotin(IV) compounds, *viz.* Me₂SnCl₂(dbtp), Me₂SnCl₂(dbtp)₂, Et₂SnCl₂(dbtp), Et₂SnCl₂(dbtp)₂, Et₂SnCl₂(dptp), *n*-Bu₂SnCl₂(dbtp)₂, *n*-Bu₂SnCl₂(dptp), Ph₂SnCl₂(dbtp), Ph₂SnCl₂(EtOH)₂ (dptp)₂ , where dbtp = 5,7-di-tert-butyl-1,2,4-triazolo[1,5-*a*]pyrimidine and dptp = 5,7-diphenyl- 1,2,4-triazolo [1,5-*a*]pyrimidine, were screened for their anticancer activity against three tumor cell lines, HepG2 (human hepatocellular carcinoma), HeLa (human cervix adenocarcinoma) and MCF7 (human breast cancer). All of them showed significant dose dependent anti-proliferative effect and followed the order (IC$_{50}$) *n*-Bu>Ph >Et >Me, except for Me₂SnCl₂(dbtp) and Me₂SnCl₂(dbtp)₂, which were ineffective against all cell lines. By measuring the exposure of phosphatidylserine to the outer membrane, the cell

death of HepG2 and observing the typical apoptotic morphological change by acridine orange/ethidium bromide staining induced by n-Bu$_2$SnCl$_2$(dbtp)$_2$, n-Bu$_2$SnCl$_2$(dptp), Ph$_2$SnCl$_2$(dbtp) and Ph$_2$SnCl$_2$(EtOH)$_2$ (dptp)$_2$, cell death was considered to be apoptotic. Flow cytometric analysis of propidium iodide stained cells also showed that organotin(IV) complexes caused apoptosis of HepG2 cells through cell arrest at G0–G1 phase [56].

In vitro anticancer screening of tri-and diorganotin(IV) orotates of formula, R$_n$Sn(H$_2$Or)$_m$ [n = 3/2, m = 1/2, R = Me, n-Bu, n-Oct and Ph; H$_2$Or$^-$ = monoanion of orotic acid (H$_3$Or)] (n-Bu$_2$Sn(HOr) as an exception) against MCF7(mammary), HEK293 (kidney), PC3 (prostate), HCT15 (colon) and HepG2 (liver) cancer cell lines suggest that n-Oct$_2$Sn(H$_2$Or)$_2$ is the most active complex amongst all the complexes. The cytotoxic effect of the complexes is suggested to be *via* selectively mediated induction of apoptosis [35].

Triorganotin(IV) hydroxycarboxylates of formula, R$_3$Sn(L) [R = Me, n-Bu and Ph; L = anion of glucuronic (HGlu), gallic (HGal) and mandelic (HMal) acid], were screened *in vitro* against five cancer cell lines of human origin *viz.* MCF7, HEK293, PC3, HCT15 and HepG2 and the complexes were found to be cytotoxic to mildly cytotoxic. The enzyme assays *viz.* glutathione reductase, glutathione peroxidase, total glutathione content and lipid peroxidase assay on MCF7 cells indicated that the reactive oxygen species generated in the cancer cells by triorganotin(IV) hydroxycarboxylates was responsible for cell death. Marginal increase of lactate dehydrogenase suggests that necrosis was also occurring to a small extent. DNA (deoxyribonucleic acid) fragmentation assay, acridine orange assay and comet assay suggested that the cell death is predominantly due to apoptosis [57].

Microwave-assistedly synthesized triorganotin(IV)/diorganotin(IV) hippurates, R$_3$Sn(HA) (R = Ph, n-Bu, and Me)/R$_2$Sn(HA)$_2$ (R = n-Oct, n-Bu, and Me); (HA = anion of hippuric acid), were screened *in vitro* against five cancer cell lines of human origin, *viz.* MCF7 (mammary cancer), HEK293 (kidney cancer), PC3 (prostate cancer), HCT15 (colon cancer), and HepG2 (liver cancer). R$_3$Sn(HA) with R = Ph and Me, exhibited good anticancer activity against MCF7, HEK293, and PC3 cell lines, while R$_2$Sn(HA)$_2$ with R = Me, showed better activity against PC3 and HepG2 cell lines [58].

1.2.3. Environmental Effects

Tin is a very common metal applied in day–to–day life. The reported low toxicity of tin made its wide consumption in food industry to conserve soft drinks as well as for metallic packing of food. Inorganic tin normally is considered harm less; albeit in some cases (especially tin chloride) induces DNA lesions, therefore, may act as potential genotoxic agent [59]. But most organotin compounds are quite harmful to the environment. Due to their enormous consumption, wide distribution, high hydrophobicity and persistence alarmed the concern about their adverse effects to the human health and environment. Especially, the leachate of tin compounds from the antifouling paints contaminate water bodies resulting in adverse effects in various small marine organisms such as shell thickening in pacific oysters and masculinisation of female gastropods, drew considerable environmental concern about their usage [60]. Nevertheless, organotin compounds have not displayed neurotoxicity, mutagenicity, teratogenicity, or carcinogenicity in humans.

1.2.4. Toxicity

Along with the potential application of organotin compounds, considerable attention has also been focused on their toxicity. Inorganic tin salts usually have low toxicity but their solutions often show acidic or alkaline properties. Organotin compounds toxicology depends upon the number of C–Sn bonds in a molecule, nature of group(s) directly attached to the tin atom and length of the carbon side chain. Generally, triorganotins are reported to have maximum biological activities. With the increase in the number of carbon atoms in the side chain, the toxicity increases to a maximum and then steadily reduces. The phenomena of toxicity may arise due to the inhibition of mitochondrial oxidative phosphorylation or interaction with amino acids or most likely binding to imidazole N–H of a histidine residue and/or a S–H group. Selective and irreversible neuronal destruction in the brain can be caused by trimethyltin compounds. The diorganotins tend to be less toxic than triorganotins and may effect by inhibiting α–keto acid oxidation, likely by combining with enzymes or coenzymes which bear vicinal dithiol groups [61].

Ohhira et al. proposed that tributyltin and triphenyltin compounds are embryotoxic, myotoxic, genotoxic and immunotoxic in mammals, and have been associated with occupational poisoning, hepatic injury, acute nephropathy, mucous membrane irritation.

Derivatives of these compounds are known to induce imposex (the superimposition of male sex organs, penis and vas deferens, in females) in marine neogastropods and to cause developmental and reproductive toxicity in mammals by disrupting endocrine systems [62]. Use of antioxidants like hindered 2,6-dialkylphenols derivatives and models of vitamin E can reduce the toxicity caused by organotin compounds in living organisms due to the induced oxidative stress and the binding of Sn atoms with protein SH-groups [63].

1.3. POSSIBLE MODES OF ACTION OF ORGANOTIN COMPOUNDS

Few mechanistic approaches of anticancer activity and interaction of organotin complexes with biological entities are mentioned in this section.

The anticancer drugs may fundamentally target four potential sites: nucleic acids, specific enzymes, microtubules, and hormone or growth factor receptors [64]. If the drugs were aimed to affect the nucleic acids (cytotoxic and genotoxic drugs), the cell death is caused due to DNA damage, therefore, DNA is identified as the primary molecular target. All forms of DNA have negative charge on their surface, hence; readily interact with positive charged molecules (such as proteins (histones), peptides, polyamines, metals, cationic lipids and liposomes, as well as monovalent cationic surfactants). Metal ions (Mg, Co, Ni, Mn, Zn, Cd and Cu) involve in binding to nucleic acids, are responsible for DNA replication, transcription and messenger RNA translation. However, few of them may cause destabilizing effect on DNA double–helical structure if they interact with the nitrogen bases instead of phosphate groups [65]. The interaction of drug with DNA results in chemical and conformational modifications. Drugs may bind to DNA *via* various mechanisms, mainly: electrostatic interaction with anionic phosphate of DNA backbone, intercalation into the stacked base pairs of DNA and groove binding. The alkylation of nucleophilic sites (electrostatic interaction) within the double helix outweigh among these three modes. Most therapeutic effectual alkylating agents have two moieties capable of developing transient carbocations which bind covalently to the electron-rich sites of DNA, for instance, the N7 position of guanine. In addition, the bifunctional alkylating ligands cross-link the two strands of DNA preventing the usage of DNA as a template for replication and transcription, thus, steering the inhibition of DNA and RNA synthesis, and further to cell death. *Cis*-platin and its congeners traditionally, although improperly, are considered as alkylating drugs. The other mechanism of binding to nucleic acids is that of intercalation which involve the insertion of a

planar (usually aromatic) ring molecule in between the two adjacent nucleotides of DNA. Intercalation of compound induces the unwinding of local structure of DNA, which in course causes DNA damage (distortion of double helix), further, affecting transcription and genetic transformation mechanism. Daunorubicin and doxorubicin, a class of antitumor antibiotics show this characteristic approach. Thirdly, the DNA damage mechanistic pathway is displayed by a category of glycopeptide antibiotic/anticancer agents called bleomycins, where the incorporation of glycopeptide motifs in between guanine-cytosine basepairs of DNA is involved. Bleomycin chelates metal ions (primarily Fe(II)) producing a pseudoenzyme which catalyze the reduction of molecular oxygen to superoxide or hydroxide free radicals, resulting in DNA strand scission by oxidative stress [66].

Few cancer chemotherapeutic drugs targeting certain proteins which participate in cell cycle progression were found to be effective. Microtubules are dynamic cytoskeletal proteins which form the mitotic spindle and are responsible for maintaining cell shape, polarity and intracellular transport of vesicles and organelles. The chemical compounds inhibiting the function of the mitotic spindle (thus, disturbing the spindle microtubule dynamics) are the ones with most prospects. 'Tubulin' of microtubules is one of the validated targets. "Vinca" or "colchicine" domains are the binding sites in the microtubule-targeted antimitotic drugs. The vinca site binds the vinca alkaloids (vinblastine, vincristine, etc.) and the colchicine site binds its colchicine analogues (podophyllotoxin, etc.). At high drug concentrations, microtubule polymerization is enhanced by the "microtubule-stabilizing" agents (e.g. paclitaxel (Taxol™), docetaxel (Taxotere™) and certain steroids). Trialkyltin compounds demonstrated colchicine-binding activity which prevents the assembly of tubulin into neurotubules [63].

Apart from this, mitochondria is also considered to be one of the major targeted sites for antitumor agents, where electron leakage from the electron transport chain occurs, thereby, the decreased MMP may open the mitochondrial permeability transition (MPT) and trigger the release of cytochrome c, which activates the caspase cascade, causing cell apoptosis [67].

Organotin(IV) compounds are considered to be Lewis acids, hence, upon hydrolysis generate the dissociated organotin(IV) species of varying acidic strengths, depending upon the groups surrounding the Sn(IV) atom. Among organotins, the dialkyl derivatives exhibit better antitumor activity than the corresponding mono-, tri-, and tetra alkyl derivatives. An

explanation that the activity of tri- or tetra-alkyl derivatives *in vivo* might be caused due to the dealkylation, yielding the corresponding active dialkyl derivatives is plausible. Further, it is hypothesised that R_2Sn^{2+} is the active species responsible for the antitumor action of diorganotins. Weak bonds between tin and the donor atom of the coordinated organic compounds are required to produce readily hydrolysable dissociated species. If the compound is hydrolytically unstable, the R_2Sn^{2+} moiety will be released too soon before reaching the target site, and if it is too stable, it may be released too slowly, consequently lowering the activity [68]. Simple diorganotin (IV) oxides and hydroxides, which either contain Sn–O bond or are capable of forming such a bond upon hydrolysis, were reported to display potential antitumor activity. Few organotin(IV) compounds containing N-donor atom tested for antitumor activity, revealed that the active Sn complex's structure showed the average Sn–N bond length > 2.39 Å, whereas the inactive complexes < 2.39 Å. These studies add weight to propose that relatively long Sn–N bonds are required for the activity of $R_2SnX_2L_2$ adducts, and the pre-dissociation of the ligand is also crucial for its mode of action. The coordinated ligand may favour the transport of the active species to the site of action in the cells, where upon the active species are released *via* hydrolysis.

Sn atom's tendency towards the interaction with free sulfhydryl groups of proteins is a well known fact. Previously, it was proposed that the effect of organotin(IV) compounds was due to their binding to thiol groups of protein [69], which further leads to the distortion of protein structure. Tubulin, a sulfhydryl rich protein with 20 cysteine residues distributed across both subunits of microtubule, can easily react with sulfhydryl-directed reagents like methyl-, phenyl- and tributyltin chlorides and dichlorides, thus preventing its polymerization. The interaction of tributyltin chloride with SH-groups results in depolymerisation of F-actin, a linear filamentous polymer which forms the microfilament [66].

In contrast to this view, accommodating the analogy of mechanism of several antitumor metal complexes, few researchers suggested that organotin compounds presumably target DNA [70]. But unlike *cis*-platin, which binds strongly to nitrogen atoms of DNA bases, simple dimethyltin(IV) dichloride showed no affinity towards base binding [71]. Few studies revealed the Sn atom's disposition towards sugar-phosphate backbone, while the others showed the insertion in to the groove (examples in detail are mentioned in the following section). The covalent binding metal-based drugs to nucleobase moieties of DNA have less selectivity, whereas non-covalent DNA binding complexes are known to strongly influence

the DNA properties [72]. Di-*n*-butyltin dichloride and tri-*n*-butyltin chloride are thymotoxic, thus, may influence the macromolecular DNA synthesis [73]. Organotin complexes with heterocyclic thioamides showed lipoxygenase inhibitory activity [74]. Lipid peroxidation in cellular membranes promoted by organotins may cause oxidative stress in living organisms [75]. Few suggested the organotin action may be *via* one of the biomolecular modes called metal-induced apoptosis. Increase in $[Ca^{2+}]_c$ *via* activating L-type voltage-dependent Ca^{2+} channel (VDCC)s was caused by tributyltin (TBT), which support the idea that the organotin-induced cell death arises through Ca^{2+} mobilization *via* L-type VDCCs [76].

Hence, from the above, there were no conclusive studies to explain the mechanism of action, so it is still open for debate. Further, specified experiments are required to ascertain the other possible modes of action.

1.4. LITERATURE REVIEW ON SOLUTION STUDIES OF ORGANOTIN COMPOUNDS AND THEIR DNA BINDING STUDIES

A comprehensive literature review on equilibrium studies of organotins with biorelevant ligands and their DNA binding action is presented in this section. A brief introduction about the DNA constituents is also included in this section.

1.4.1. Nucleic Acid Constituents

Nucleic acid constituents (nitrogenous bases mainly classified in to two parent compounds purines and pyrimidines, further nucleosides and nucleotides of DNA and RNA) and their precursors are obligatory metabolites in all organisms and main energy donors for all the cellular processes. Purines include adenine (A), guanine (G) and pyrimidines include cytosine (C), uracil (U) and thymine (T) (Fig. 1.14). They serve as building blocks for RNA and DNA synthesis and some nucleotides are constituents of coenzymes, while the others are engaged in the activation of precursors in polysaccharide and lipid synthesis. Additionally, nucleotides play an important role in the regulation of numerous cellular processes from the metabolic level to gene expression level. Out of both, purines are the most ubiquitous nitrogen-containing heterocycles and are involved in many metabolic processes, as cofactors associated with a great number of enzymes and receptors, notably ATP, GTP, GDP, cAMP,

cGMP, AcCoA, NAD, NADP, FAD, PAPS and SAM playing key roles at various cell cycle phases, in cell signalling and many other fundamental biological processes [77].

Purines
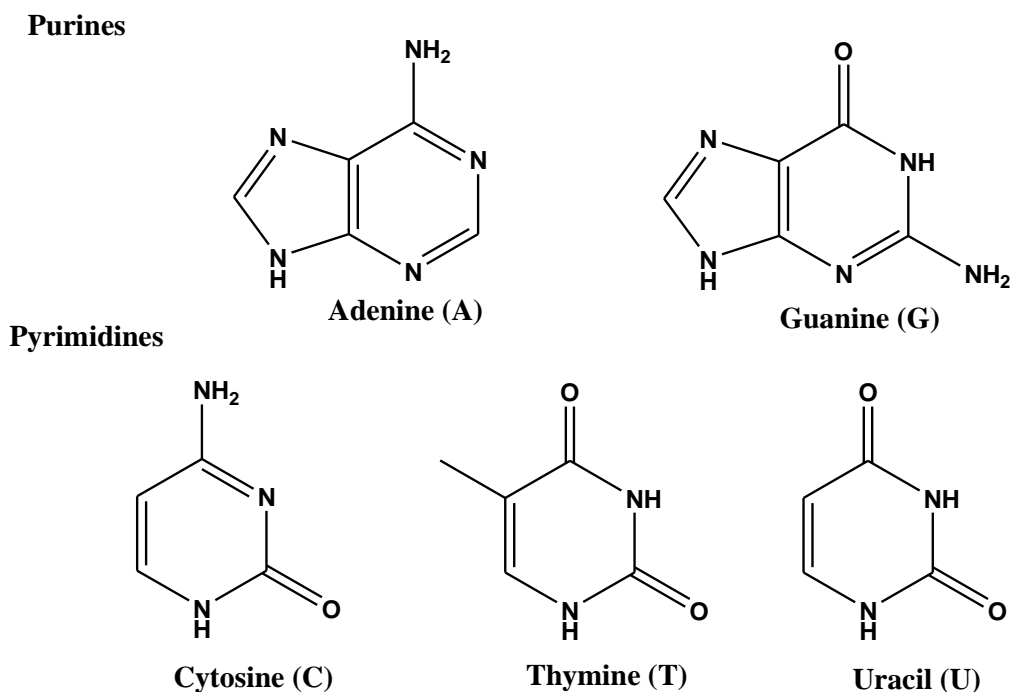
Pyrimidines

Fig. 1.13. Nitrogenous bases corresponding to purines and pyrimidines of DNA and RNA.

The cross linking of *cis*-platin to two strands of double helix of DNA *via* N7 nitrogen atoms of the guanine bases and/or adjacent N7 atoms of guanines in a single strand, gave us the idea of analogical mechanism may occur in other metal-based compounds, as reported by few other researchers. Few organotin(IV) derivatives of guanine and guanosine and guanosine-5'-monophosphate were reported [37, 38, 39]. By introducing N-donor, 1,10-phenanthroline in to the structure, there is a chance to improve the antitumor activity. Hence, guanosine is selected as ideal choice.

The other nucleic acid moiety is the inosinic acid or 5'-inosine monophosphate (5'-IMP) a nucleoside monophosphate (a ribonucleotide of nucleic acids), which is the first nucleotide formed during the synthesis of purine. Deamination of adenosine-5'-monophosphate followed by hydrolysis leads to the formation of inosine monophosphate. It is also an intermediate ribonucleotide monophosphate in purine metabolism. Derivatives of

inosinic acid are found in nucleic acids and adenosine triphosphate, chemical energy storage in muscle and other tissues. Solid state synthesis of inosine with organotin(IV)s were not available in the literature, thus, entrusted as a judicious choice.

1.4.2. Solution Studies of Organotin Compounds

Early days, total quantification of an element was alone sufficient to determine potential health hazards or benefits, but lately, many research groups have acknowledged that the elemental quantification is not enough, particularly for arsenic and tin, where the bioavailability, transportation ability and toxicity are extremely species dependent. To acquire the knowledge of function, toxicity and distribution of elements of interest, not only its determination of presence and concentration of the elements is needed, but also their speciation, identification and characterization is incumbent. An analysis performed to identify and/or quantify one or more distinct chemical species in a sample of interest is known as speciation analysis.

Speciation analysis is becoming increasingly important in the applications in the field of environmental chemistry, where the identification of toxic metal- and metalloid-containing species in contaminated industrial sites or natural sources as well as successful clean-up strategies determination is a requisite. Further, advances in speciation analysis will indisputably have a tremendous impact in bioinorganic chemistry, as the entry of a species in an organism leads to chemical transformation altering radically its properties. Determination of chemical species throughout the metabolic pathway and within various bodily tissues and fluids can provide information about the biological mechanisms for cellular uptake, transport, storage and excretion. A number of drugs administered are in solution phase; hence, the concerted efforts should be made to study the structures of tested compounds in solution (especially in aqueous media).

Despite the extensive investigations reported on the structures of organotins and their derivatives in the solid and solution states, relatively a few aqueous solution studies have been performed. The wide distribution of organotins in environment especially marine, and the hydrolytic behavior in biological fluids resulting in numerous varieties of species grew interest in its aqueous chemistry over the last few years. To understand the species distribution in the systems studied or in the environment, measurement of equilibrium data must be undertaken. The chemistry of several organotins in different ionic media with wide

range of ionic strengths was reported in the literature [78–83]. Organotins in biological systems interact with a variety of biomolecules, e.g. to proteins (especially to the heteroatoms located in their side chains (N, O and S) or to the amide bond), to nucleic acids (in many different ways: to phosphates, to base N-donor atoms, or to sugar O-atoms), and to carbohydrates or lipids (C–O and P–O groups). Hence, discussion of formation equilibria of biologically active ligands is of considerable interest. Some studies on hydrolysis and complex formation equilibria in solution and the coordination chemistry of organotin(IV)$^{n+}$ moieties with amino acids, peptides and DNA constituents are exemplified as follows:

The interaction of dimethyltin(IV) and diethyltin(IV) cations with water and some amino acids and related compounds at 25 °C, I = 0.1 M NaNO$_3$ were potentiometrically studied by Shoukry [82], and the results reveal that the amino group of the amino acid is not free and is involved in the complex formation with diorganotin(IV). It was proposed that the dimethyltin(IV) complexes are more stable than the corresponding diethyltin(IV) complexes due to the steric crowding between ethyl group and the incoming ligand.

Potentiometric titration of dimethyltin(IV), diethyltin(IV) and trimethyltin(IV) with the selected peptides in aqueous medium demonstrated that all peptides except glycinamide coordinate either to amino group nitrogen or carboxylate oxygen atom, where as in case of glycinamide, the coordination occurs only *via* amino group of the peptide. Further, the stability constant values of trimethyltin(IV) are less than that of dialkyltin(IV) which indicate that tin(IV) binds to peptides in monodentate fashion in trimethyltin(IV) complexes and bidentate fashion in dialkyltin(IV) complexes [83].

The coordination of dimethyltin(IV) to 5'-AMP and the related compounds, D-ribose-5-phosphate (R5P), D-glucose-1-phosphate (G1P) and D-glucose-6-phosphate (G6P) in aqueous solution studied by potentiometric titration, showed the exclusion of coordination of metal to {N}, where as the bidentate coordination of phosphate group is presumed by comparing the pK values (in the absence and presence of metal ion) and stability constants. Further, the bidentate coordination of phosphate group was confirmed by ^{1}H, ^{31}P and ^{119}Sn mössbauer (in glassy state) spectroscopic studies. With the increase in pH, the phosphate groups are replaced by the deprotonated alcoholic {O} atoms of the sugar moiety [84].

Nagy et al. [85] prepared complexes of adenosine and related compounds (adenosine-5'-monophosphate, adenosine-5'-triphosphate and pyridoxal-5-phosphate) with Bu$_2$SnO and/or Bu$_2$SnCl$_2$ in solid state. It was stated that Bu$_2$SnO reacts with the D-ribose moiety (–

OH) of the ligands, where as Bu_2SnCl_2 to that of deprotonated phosphate group and the base of the ligands was not involved directly in complex formation. Comparing experimental ^{119}Sn mössbauer, Δ (quadrupole splitting) values with the *pqs* concept based calculated values, the organotin(IV) moiety was revealed to be trigonal bipyramidal (Tbp) and in some cases tetrahedral (T_h) geometry, therefore, the organotin(IV)-adenosine complex was suggested to have Sn(IV) cation in two different surroundings (Tbp and T_h).

Potentiometric titration, and ^1H and ^{31}P spectroscopic studies of dimethyltin(IV) to DNA fragments containing phosphate group (5'-GMP, 5'-AMP), DNA oligomer (5'-d(CGCGCG)$_2$) and their sugar constituents (D-ribose and 2-deoxy-D-ribose) in aqueous medium revealed the suitable sites for metal coordination *viz.* phosphate groups in acidic media, hydroxyl groups of the sugars or sugar moieties at higher pH. It was proposed that the base moieties of 5'-GMP and 5'-AMP were not coordinated to dimethyltin(IV) at any pH [86].

Barbieri et al. studied the aqueous systems of di-/trimethyltins with phosphate, D-ribose 5'-phosphate, dimethylphosphinate (mimick the phosphodiester residue of nucleic acids), 3',5'-cyclic adenosine monophosphate (cAMP) and native DNA [87] at pH 7.4 by ^{119}Sn mössbauer spectroscopy and the configuration of organotin moieties in the model systems and the nature of the complexes possibly formed were interpreted by applying point-charge model formalism. Consistent results were obtained for the phosphate and D-ribose 5-phosphate with respect to di-/trimethyltins. The effect due to dimethylphosphinate and cAMP is limited only to $SnMe_3(OH)(OH_2)$, and the native DNA was not involved in any interaction.

1.4.3. DNA Binding Studies

In recent years, many researchers focussed on interaction of small molecules with DNA, as DNA is the primary cellular target responsible for anticancer activity. The small molecules are stabilized in binding to DNA through a series of weak interactions, such as π-stacking interactions associated with intercalation of aromatic heterocyclic groups between the base pairs, hydrogen bonding and van der Waal's interactions of functionalities bound along the groove of the DNA helix. Further, to find out the extent of binding, determination of binding constant of the complex to the DNA is necessary. To quantitatively measure nucleic acid concentration and protein contamination and determination of binding constant, UV-Visible spectroscopy technique is a method to be opted. Nucleic acids strongly absorb at

260 nm and less strongly at 280 nm while proteins do the opposite. DNA, RNA, and protein strongly absorb ultraviolet light in the 260 to 280 nm range [88–91].

The other alternative method to find the interaction of the complexes with DNA is through fluorescence studies. The widely used fluorescence probe in recent years to detect the structures of nucleic acids is the ethidium bromide (EB), which is very sensitive to the change in molecular micro environment. The binding modes and ratios of EB to different nucleic acid molecules will vary according to their conformations, and then result in the changes in fluorescence intensity and other corresponding parameters (such as quantum yield, polarization degree etc.). Additionally, few studies pointed out that the ancillary binding energy and stabilization of nucleic acids under the physiological condition is provided by EB. Thus, it can be used to discriminate different DNA molecules [88, 89], to learn more characteristics about their conformations as well as to detect the formation of multi-stranded structures and other factors affecting their stabilities. The transfer of energy from DNA to EB can be measured from the excitation spectra and corresponding absorption spectra of the DNA/ethidium complex in the wavelength range of 220–320 nm [88, 89].

Few metal complexes have the tendency to partially or completely cleave the double helix. Agarose gel electrophoresis is a technique where the fragmented DNA can be separated.

Few examples where the binding studies and cleavage experiments reported are illustrated as follows:

Triorganotin(IV) dithiocarboxylates interaction with DNA resulted in blue shift and hypochromism with the addition of DNA which is attributed to the intercalation of the drugs into the DNA base pairs [72].

The cleavage experiments of supercoiled pBR322 DNA was conducted by Tabassum et al. on newly synthesized heterobimetallic Ni^{II}–Sn_2^{IV}, Cu^{II}–Sn_2^{IV} and Zn^{II}–Sn_2^{IV} complexes of containing D-glucosamine, 1,8-diamino-3,6-diazaoctane and imidazole, out of which Cu^{II}–Sn_2^{IV} exhibited effective cleavage activity [88]. UV–Vis binding studies of new glycosyl derived ligand (glycoconjugate) and its complexes, with $SnCl_4.5H_2O$ and $(CH_3)_2SnCl_2$ with CT DNA showed high binding affinity of $(CH_3)_2SnCl_2$ with CT DNA. The distribution of supercoiled and nicked forms of DNA in the agarose gel electrophoresis provides a measure of the extent of hydrolysis of the phosphodiester bond which suggested the more binding propensity of methyltin complex as compared to tin(IV) chloride complex [89].
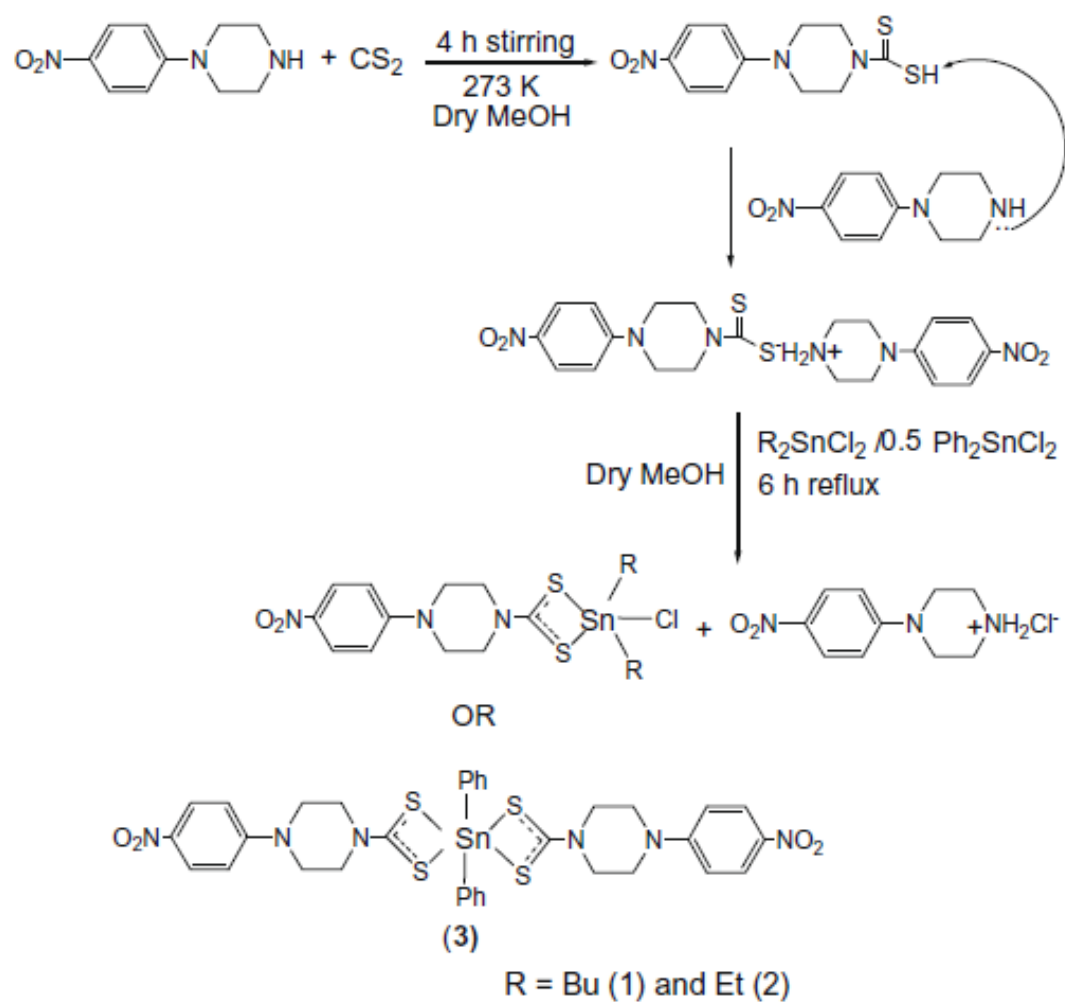
Fig. 1.14. Reaction scheme of organotin(IV) dithiocarboxylates [72].
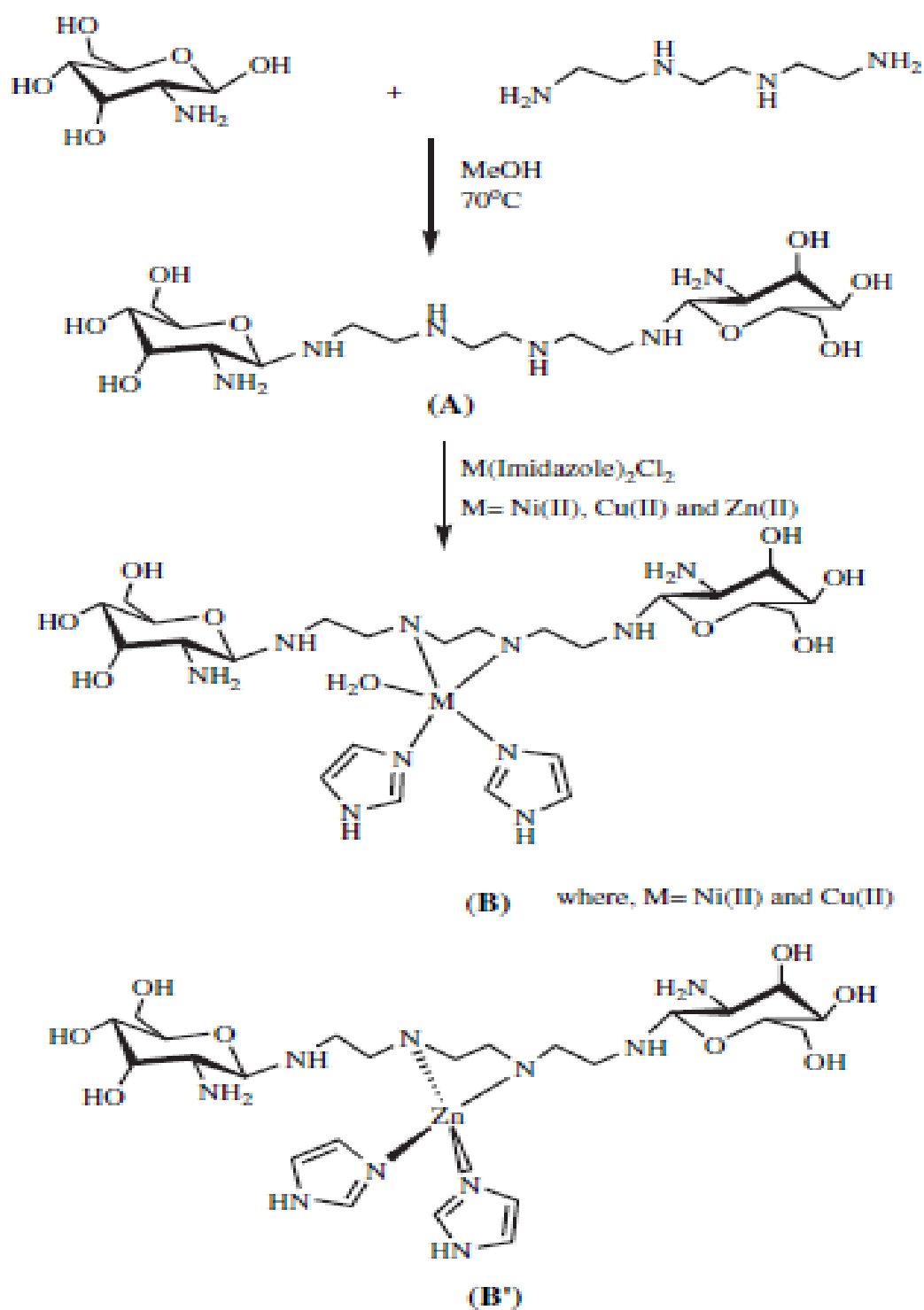
Fig. 1.15. Reaction scheme of heterobimetallic Ni^{II}–Sn$_2$^{IV}, Cu^{II}–Sn$_2$^{IV} and Zn^{II}–Sn$_2$^{IV} complexes with D-glucosamine, 1,8-diamino-3,6-diazaoctane and imidazole ligands [88].
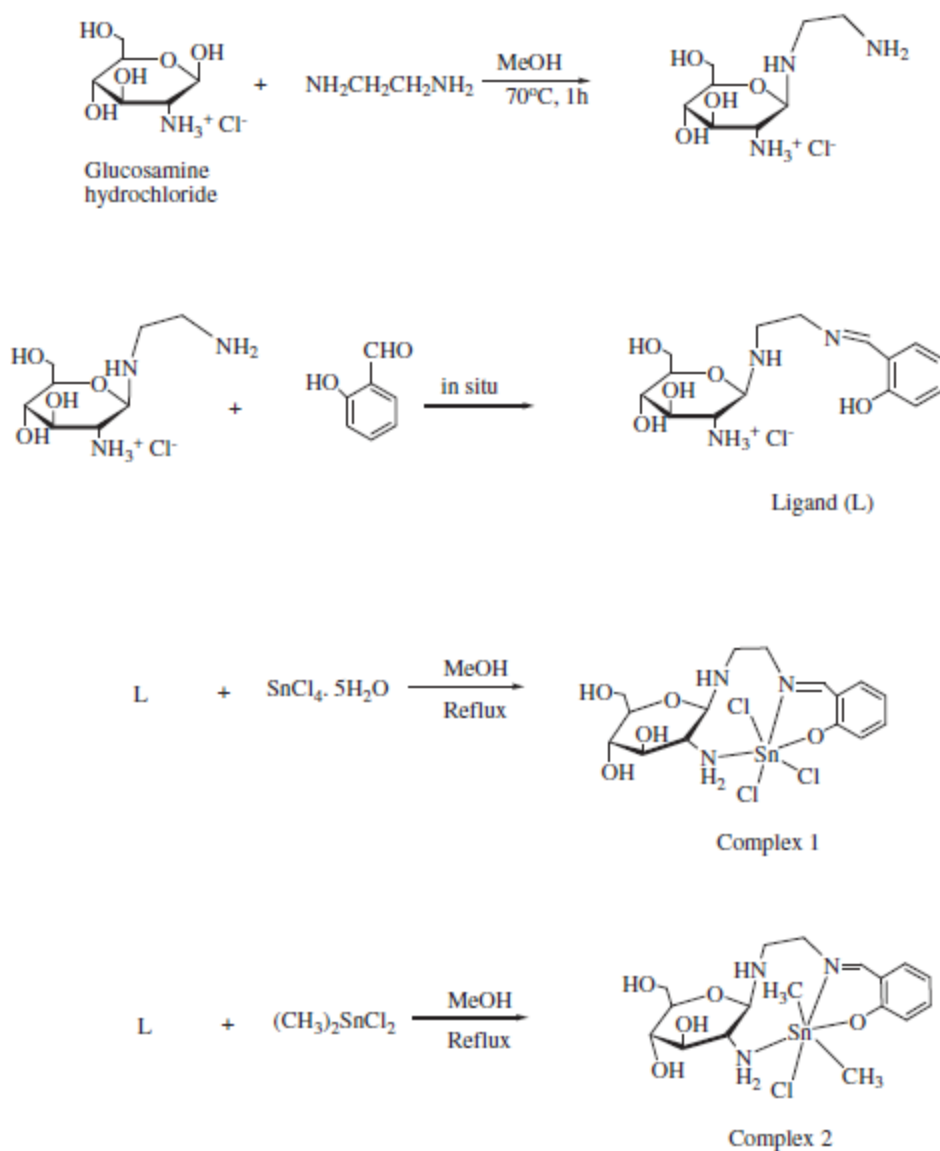
Fig. 1.16. Reaction scheme of organotin complexes with glycol-conjugate ligands [89].

Dimethyltin(IV) complexes of Schiff base ligand, *viz.* 2-(2-hydroxybenzylideneamino)isoindoline-1,3-dione (L$_1$), and 4-(4-hydroxy-3-methoxybenzylideneamino-*N*-(pyrimidin-2-yl)benzenesulfonamide (L$_2$) with or without 1,10-phenanthroline were synthesized and the DNA binding of the complexes without phenanthroline moiety by UV showed avid binding with CT DNA. The nuclease activity of complexes without phenanthroline moiety with plasmid DNA (pUC19) using agarose gel
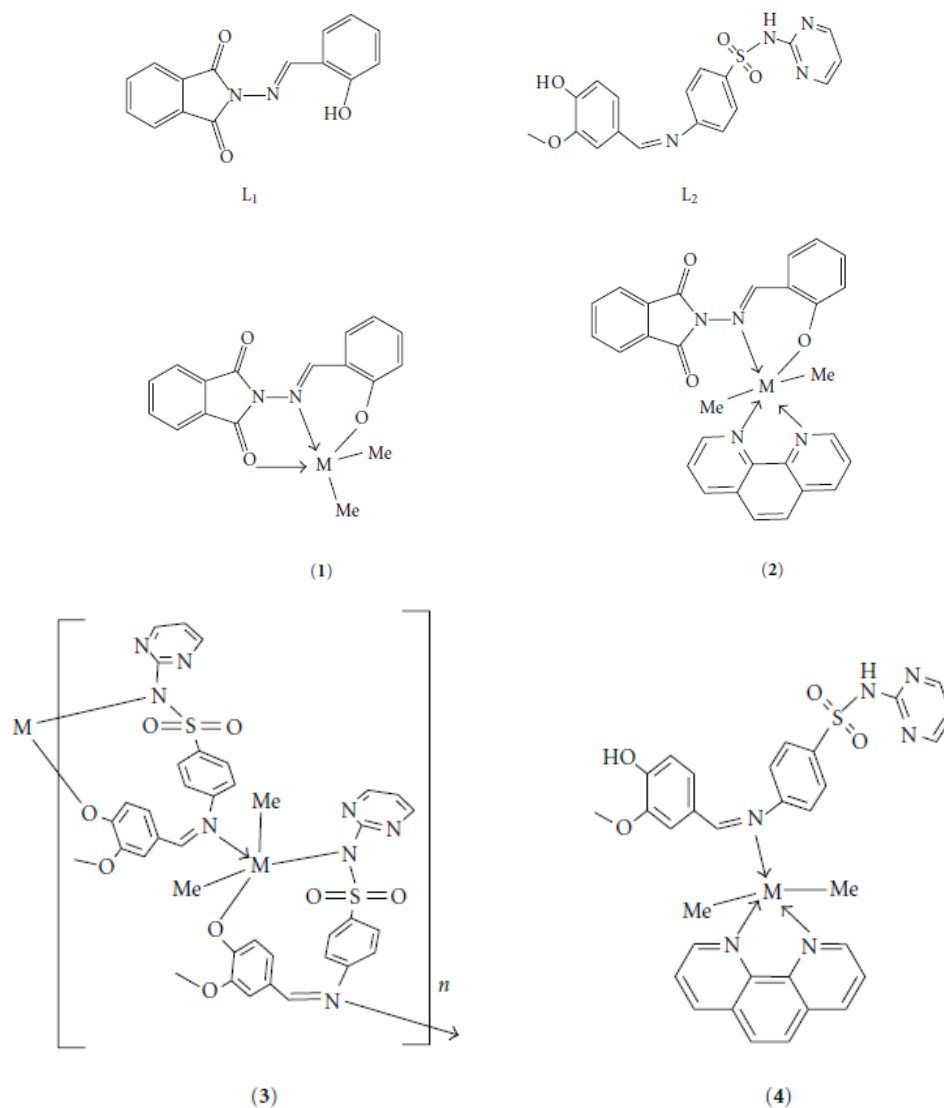
Fig. 1.17. Reaction scheme of dimethyltin(IV)-Schiff bases of ligands: 2-(2-hydroxybenzylideneamino)isoindoline-1,3-dione (L₁), and 4-(4-hydroxy-3-methoxybenzylideneamino-*N*-(pyrimidin-2-yl)benzenesulfonamide (L₂) [90].

electrophoresis showed that the complex with L_1 can act as effective DNA cleaving agent when compared to complex with L_2 resulting in the nicked form of DNA under physiological conditions [90].

De novo design strategy by applying by the condensation reaction of (R-/S-)2-amino-2-phenylethanol and dibromoethane with dimethyltin dichloride resulted in two enantiomers

of N,N-bis[(R-/S-)-1-benzyl-2-ethoxyethane] tin(IV) complexes. Intense absorption bands arising from the intraligand transition located at 263 nm and 328–332 nm were observed in the absorption spectra. With increasing DNA concentration, a considerable increase in the absorptivity (hyperchromism) with no apparent red or blue shift was observed. This can be correlated to non-classical electrostatic binding mode, aroused due to the preferential binding of the Sn(IV) to dinegative phosphate group of DNA backbone by virtue of Sn having hard Lewis acidic property, hence, any pronounced sequence or base preference when interacting with DNA cannot be feasible. Both the complexes are not planar, but the presence of two phenyl groups induces steric effect, which promote a partial intercalative binding of complexes to DNA. Intrinsic binding constant indicate pronounced enantiopreferential binding of R-enantiomer over S-enantiomer with CTDNA in a complementary fashion against the right handed groove of DNA [91].
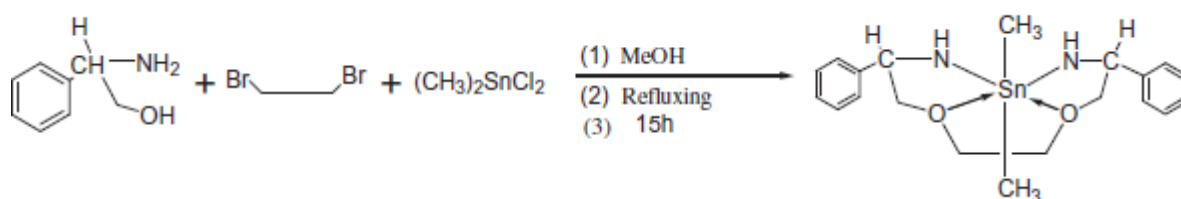
Fig. 1.18. Schematic representation of N,N-bis[(R-/S-)-1-benzyl-2-ethoxyethane] tin(IV) complex [91].

1.5. FORMULATION OF PROBLEM

From the colossal literature survey reported above, the following significances stood out.

1. From the consideration of environmental and equilibrium measurement aspects, the speciation of organotin(IV) species in water is very important to understand their reactivities. Since the biological and chemical behaviour of alkyltin(IV) compounds is strictly related to the form in which they are present in the environment, speciation in natural waters represents the basis of understanding their biochemistry. Though extensive work on solution studies of organotins(IV) have been done, their effect on nucleic acids and DNA are sparse. These studies can be useful for making predictions about the aqueous chemistry of similar homologous systems, such as $(C_4H_9)_nSn^{(4-n)+}$, $Ph_nSn^{(4-n)+}$ with very low solubility.

2. Solution studies of dimethyltin and 5'-guanosine monophosphate has been available in literature [86], but the trimethyltin 5'-guanosine monophosphate has not been performed. Di-/trimethyltin guanosine solid state studies were reported [37] but, speciation studies at physiological pH have not been studied till now.

3. Several organotin complexes of biological origin, namely carbohyrates, amino acids, nucleic acids etc. were synthesised and reported, but the mixed ligand complexes incorporating two or more ligands with good activities were not reported till now. After coordination with Sn, these bio-ligands may possess favourable properties which may possibly act as carriers in body fluids. Information relating to the complexation and the structure of the resulting complex species by spectral studies can further be explored.

4. Synthesis organotin(IV)-ionosine derivatives were also not reported till now in literature, also, mixed ligands synthesis with ionosine as one of the ligands is not reported.

5. Evaluation, designing and development of new metal-based anticancer drugs that may provide the basis for target-specific therapeutics is a trend at present. Now-a-days, a lot of work on cancer and to develop chemotherapeutic agents which inhibit the cancer growth and to identify the structure/ property relationships is being done but significant efforts on *in vitro* cytotoxic studies of organotin derivatives of nucleic acid moieties is relatively limited, almost considerably rare.

6.   Few mechanistic studies of simple organotins and their derivatives insinuated and accepted, however the mode of action of organotins(IV) and their derivatives is still a debate, and is to be further explored.

1.6. ORGANISATION OF WORK

In order to meet the desired objectives, the present work has been planned and compiled in this thesis in hierarchy and their detailed studies are described in successive chapters. The strategy selected is as follows:

1.   In order to understand the species distribution of di- and trimethyltin(IV) systems with biologically active ligands such as guanosine-5'-monophosphate and guanosine in the environment, measurement of equilibrium data and their characterization is a necessary tool. Hence, their quantitative and qualitative aqueous solution chemistry by means of potentiometry and spectroscopic studies (^{1}H, ^{13}C, ^{119}Sn NMR) has been studied.

2.   New mixed ligand complexes of organotin(IV) moieties with fragments of biological systems or biologically relevant ligand namely guanosine, and a nitrogen containing ligand (1,10-phenanthroline) were selected, and a series of complexes have been synthesized and characterized by elemental studies, IR, far-IR, ^{1}H, ^{13}C, ^{119}Sn NMR.

3.   Similar insightful studies have been carried out on organotin(IV) derivatives of inosine and their mixed derivatives of 1,10-phenanthroline along with their structural -property relationships.

4.   Significant efforts have been made to evaluate the cytotoxic activities of the developed compounds which inhibit the cancer growth (*in vitro*) against a panel of cell lines of human origin, *viz.* MCF7, HepG2, HEK293, PC3, DU125.

5.   Various bio assays such as enzyme assays *viz.* lactate dehydrogenase, lipid peroxidation assay, and DNA fragmentation assay, acridine orange test and comet assay on selected complexes with good IC_{50} values were conducted in order to elucidate their possible modes of their cytotoxicity.

2.1. MATERIALS

2.1.1. Solvents

Solvent, viz. absolute methanol (specially dried, Rankem chemicals) was used for synthesis work. Other solvents (Merck) such as chloroform, DMSO, acetone, ethanol, *n*-hexane, petroleum ether (b.p. 40–60 °C), acetonitrile, benzene were used as received.

2.1.2. Organotin Compounds

Dimethyltin(IV) dichloride (Sigma Aldrich, 97%), trimethyltin(IV) chloride (Sigma Aldrich, 97%), diphenyltin(IV) dichloride (Sigma Aldrich, 96%), triphenyltin(IV) chloride (Merck, 99%), *n*-dibutyltin(IV) dichloride (Sigma Aldrich), tributyltin(IV) chloride (Sigma Aldrich, 96%), *n*-dioctyltin(IV) oxide (Sigma Aldrich) were used as received. Diphenyltin(IV) dichloride was synthesized by reported method [92] by using tetraphenyltin and tin(IV) tetrachloride.

2.1.3. Nucleosides and Nucleotides

Guanosine (Fluka, 99.5%), guanosine-5'-monophosphate disodium (Fluka, >99.5%) were used for solution studies and guanosine (M.P. Biomedicals), inosine-5'-monophosphate disodium salt hydrate (Sigma Aldrich, HPLC grade, $\geq$ 98% and M.P. Biomedicals) were used for synthesis and were used as received without further purification.

2.1.4. Chemicals for Biological Activities

3-(4,5-Dimethylthiazol-2-yl)-2,5-diphenyltetrazolium bromide (MTT) (Hi-media), phosphate buffer saline (Hi-media), agarose (Hi-media, for molecular biology suitable for the biological processing of DNA < 1000 bp), tris(hydroxymethyl)aminomethane (GeNei), EDTA disodium salt (Thomas baker, 99%), glycerol (Merck, 98%), bromophenol blue (Hi-media, pH range 3.0–4.6), ethidium bromide (Hi-media, 95%), boric acid (Glaxo laboratories (India) Ltd., 99.5%), sodium chloride cryst. pure (Merck, 99%) were used as received. pBR322 supercoiled plasmid DNA (GeNei), calf thymus DNA (CT DNA) sodium salt (extrapure) (Sisco Research Laboratories (SRL)) were used as received. CT DNA stock

solution prepared in Tris–HCl/NaCl buffer (0.01 M, pH 7.2, 5:50 mM) gave the UV absorbance at 260 and 280 nm of 1.9:1 indicating that DNA was free from proteins. The DNA concentration per nucleotide was determined by the UV absorbance at 260 nm [93] using extinction coefficients 6600 dm^3 mol^{-1} cm^{-1}.

2.1.5. Other Chemicals

Potassium bromide (Sigma Aldrich, for IR), sodium hydroxide pellets (Thomas baker, purified, 97.5%), 1,10-phenanthroline (Qualigens fine chemicals), potassium nitrate (Samirtech chemicals), buffer tablets of pH 4.0, 7.0 and 9.2 (Qualigen fine chemicals) and all other chemicals, and solvents used for physio–chemical and spectral studies were of analytical reagent grade.

2.2. TECHNIQUES

The details of specifications of the instruments and experimental procedures applied are illustrated as below. The melting points of the synthesized complexes were determined on a Toshniwal capillary melting point apparatus and were uncorrected. Molar conductance was measured at room temperature on a Eutech con 510 electronic conductivity bridge.

2.2.1. Potentiometric (pH-metric) Studies

2.2.1.1. Experimental determination of stability constants by pH-metric method

Orion 960 plus autotitroprocessor equipped with a combined glass Orion Ross flow electrode was used to carry out the pH measurements in the aqueous media at 298.15 ± 0.1 K, ionic strength (*I*) adjusted to 0.1 M of KNO_3. Standard buffer solutions (Qualigens Fine chemicals) of pH 4.0 ± 0.05, 7.0 ± 0.05 and 9.2 ± 0.05 were used to calibrate the electrode and Orion 960 autotitroprocessor. Atmospheric CO_2 was excluded from the titration cell with a purging steam of purified nitrogen gas. All the solutions were prepared in double distilled water. The details of the experiments are mentioned in Chapter **3**.

2.2.1.2. Calculation of the stability constants using SCOGS program

The calculations of the stability constants of the complex species formed were performed by using a computer program, SCOGS (Stability Constants of Generalized Species) and the functional aspects of the software were best described in detail in the references [94–96]. pH-metric data between pH 2.0–11.0 were used for the evaluation. Tentative values of the constants, ionic product of water, activity coefficients of hydrogen ion at the experimental temperature (298.15 ± 0.1 K) and ionic strength (0.1 M KNO_3) were given as inputs. The refinement of values of the constants was done by several cycles of the operation, and values corresponding to the minimum standard deviation were accepted.

2.2.1.3. Illustration of species distribution curves

The computer output files obtained from the SCOGS program for a given system was inputted in Origin 6.1 software to draw the speciation curves by placing the pH on X-axis and the % distribution of species on Y-axis. With the help of the speciation curves, the complex formation equilibriums were further elucidated.

2.2.2. Elemental Analyses

Elemental analyses (C, H and N) of the synthesized complexes were obtained on a Vario EL III CHNOS elemental analyzer, at the Department of Chemistry, Indian Institute of Technology Roorkee (IITR), Roorkee (India).

Estimation of tin content in the synthesized complexes was determined gravimetrically as mentioned in the literature [35–39].

2.2.3. Spectral Studies

2.2.3.1. Infrared and far-infrared spectral studies

Thermo Scientific Nicolet 6700 FT-IR spectrometer was used for recording Infrared spectra (KBr pellets) of the ligands and their solid complexes in the range of 400–4000 cm^{-1} and also for recording Far-Infrared spectra (CsI pellets) in the range of 600–190 cm^{-1}, at the Department of Chemistry, IITR, Roorkee.

2.2.3.2. Nuclear magnetic resonance (NMR) spectral studies

Multinuclear (^{1}H, ^{13}C and ^{119}Sn) NMR spectra were recorded on a Bruker Avance-500 (500 MHz) NMR spectrometer in DMSO-*d6* at 298 ± 0.1 K, at the Institute Instrumentation Centre (IIC), IITR, Roorkee, using TMS as an internal reference for ^{1}H and ^{13}C NMR experiments, and tetraphenyltin(IV) as an external reference for ^{119}Sn NMR experiments. DMSO-*d$_6$* was used as solvent. For recording solid state ^{13}C NMR, JOEL Delta NMR 400 MHz instrument at Department of Chemistry, IITR, Roorkee was used.

The solution NMR studies were performed in a $H_2O:D_2O$ (9:1) mixture. For ^{1}H NMR, a suitable signal-to-noise ratio was obtained after the collection of ~ 64 transients and water resonance was suppressed as much as possible during the recycling delay. The ligand, guanosine has a limited solubility in water. Hence, their solution studies were performed at slightly increased temperature 313.10 ± 0.1 K.

2.2.3.3. Electronic spectral studies

Electronic spectra were recorded on a Shimadzu UV-1800 UV-VIS spectrophotometer in a cell of 1 cm path length in Tris–HCl/NaCl buffer, at Department of Chemistry, IITR, Roorkee. The concentration of stock solutions of DNA and complexes were mentioned in the respective Chapters.

2.2.3.4. Fluorescence studies

Emission spectra were determined with a Shimadzu RF5301 (2006) fluorescence spectrophotometer at Department of Chemistry, IITR, Roorkee, in Tris–HCl/NaCl buffer, excited at a wavelength 263 nm and the total fluorescence emission monitored at 603 nm. The measured fluorescence was normalized to 100% relative fluorescence. The concentration of stock solutions of DNA and complexes were mentioned in respective Chapters.

2.3. BIOLOGICAL STUDIES

2.3.1. Gel Electrophoresis

DNA cleavage experiments were performed with the help of GeNei submarine electrophoresis supported by GeNei power supply with a potential range of 50–250 V, visualized and photographed by Gel documentation system (Bio Rad, USA). The concentration of stock solutions of DNA and complexes were mentioned in respective Chapters.

2.3.2. Antitumor Screening

2.3.2.1. Cytotoxicity assay (MTT assay)

The synthesized complexes were evaluated *in vitro* against three cancer cell lines (purchased from National Center for Cell Science (NCCS) Pune, India) of human origin, *viz.* MCF7 (mammary cancer), HepG2 (liver cancer), DU145 (prostate cancer) cell lines along with human embryonic kidney cell line used as a standard. Cell viability was determined through a colorimetric method based on the tetrazonium salt MTT (Mosmann, 1983), which yielded purple formazan crystals on reduction in the cells. Stock solutions were prepared by dissolving the complexes in DMSO (HPLC Grade). On first day of experiment, approximately 5×10^3 cells per well in 200 μL of culture medium were seeded into 96-well flat bottom microtitre culture plates (Corning, New York, USA) and were allowed to preincubate at 37 °C, for the cells to adhere. Following day, serial dilutions of the test compounds ranging from 0−200 mM in DMSO were prepared. On day 3, vehicle control (or negative control) (with same concentration of DMSO as used for preparing dilutions) and 50 μL of each dilution (test and reference) were added in triplicate to three consecutive wells. The cell cultures were then incubated at 37 °C with 5% CO_2 for 24 h. On day 4, cultures were assayed by adding 10 μL of 5 mg/mL MTT and again incubating the plates for 4 h at 37 °C. Later, the MTT containing media was aspirated and 200 μL DMSO and 25 μL sorensen glycine buffer (0.1 M of glycine and 0.1 M of NaCl, at pH 10.5) were added to lyse the cells and solubilise the water insoluble purple formazon. The absorbance values of the cell lysates were measured on a Dynatech MR 5000 microplate reader at 584 nm.

The vehicle control or negative control (here in this case DMSO) was added to ensure that the cytotoxicity observed was only due to the activity of the compounds and not that of

the solvent. *Cis*-platin and 5-fluorouracil which are normally employed as standard chemo agents for comparison.

The % inhibition was calculated as given below:

$$\% \text{ Inhibition} = \frac{\text{Mean OD of negative control} - \text{Mean OD of treated cells}}{\text{Mean OD of negative control}} \times 100$$

2.3.2.2. Enzymatic assays

Few complexes showing good activities in MTT assay were selected and performed enzyme assays such as lipid peroxidase, lactate dehydrogenase assays and were compared with a groups of control cells (non treated) of cancerous cell lines. Tissue lysate in PBS (pH 7.4), containing 2 mM PMSF followed by sonication (3 bursts per 20 second) was prepared. Equal amount of protein sample was taken for each enzyme assay.

2.3.2.2.1. *Lipid peroxidase*

To estimate lipid peroxidase, 8.1% SDS, 20% acetic acid (pH 3.5) and thiobarbituric acid was added to the protein sample followed by incubation for 2 h at 95 °C. Later, the incubated contents were cooled at room temperature and 15:1 *n*-butanol: pyridine mixture was added. The OD was recorded at 532 nm after the centrifugation.

2.3.2.2.2. *Lactate dehydrogenase*

To measure lactate dehydrogenase (LDH) assay, Bergmeyer and Bent method, was used. To the protein sample, 0.1 M of sodium phosphate buffer along with 20 mM NADH and 10 mM sodium pyruvate were added. The absorbance of NADH produced was measured at 340 nM.

2.3.2.3. Acridine orange assay

Acridine orange staining is one of the assays performed to evaluate the apoptosis by analyzing the plasma-membrane permeability, nuclear morphology as well as the chromatin condensation. The method described by Takahashi et al. is used and the cells were stained

with acridine orange (AO)/ethidium bromide (EB) dye mixture (100 μg/mL of AO and 100 μg/mL of EB). 0.5×10^6 cells were seeded in a 6-well plate and incubated by adding the test compounds at their respective IC_{50} values and *cis*-platin (positive control) for 24 h. The resultant was washed with PBS and 500 μL of AO/EB dye mixture dissolved in PBS was added to the plate and the cells were observed under fluorescent microscope (Ziess, Axiovert 25, Germany).

2.3.2.4. Comet assay

A simple yet highly sensitive technique like comet assay is very useful in detecting the DNA damage in individual cells. Cytotoxic effect of the test compounds leads to DNA damage can also be validated by the comet assay (single cell gel electrophoresis). 5×10^5 cells were treated with the test compound and incubated for 24 h at 37 °C and thoroughly washed with PBS. Later fresh media was added and the cells were harvested after 24 h. Slides were prepared with 1% normal melting agarose, where, 0.3×10^6 cells were mixed with 50 μL of 1% low melting agarose at 37 °C in PBS and sandwiched between the previously prepared slide with 1% normal melting agarose. The prepared slides were stored at 4 °C for 10 min before incubating them in lysis buffer (2.5 M NaCl, 100 mM EDTA (pH 10), 10 mM tris-base, 1% sodium lauryl sarcosinate and 1% triton X-100) for 2 h at 4 °C. Electrophoresis was carried out for 5 min at 25 V in 300 mM NaOH and 1 mM EDTA. Later the cells were neutralized with tris base at pH 7.5. The nuclei stained with ethidium bromide were visualized under fluorescent microscope.

3.1. INTRODUCTION

The wide distribution of organotin(IV) compounds in the environment [97] and the high solubility of Me_3SnCl and Me_2SnCl_2 in aqueous medium leading to hydrolyzed species which are very toxic to aquatic living organisms, and their subsequent accumulation in the biota [98–102] are very concerning issues. In view of this, the speciation studies of organotins in aqueous media are indispensable. Several research groups studied their hydrolysis using different techniques [103–111]. Another reason to focus the attention on solution studies of organotins is due to their potential pharmaceutical application in oncology as an alternative for platinum drugs. The dialkyltin derivatives are known to exhibit efficient antitumor activity [69] as compared to mono-, tri-, and tetraalkyl analogues. Several mechanisms were proposed to explain the cytotoxicity [18, 20] and one of the hypothesis that $R_nSn^{(4-n)+}$ moiety might be the active species responsible for the activity is universally accepted. A good antitumoral agent should be easily dissociable following administration. Further, the cytotoxicity activity of the organotin compounds are controlled by the nature of the organotin moiety [103], nature of X or coordinated ligands which favor the transportation of the active species $R_nSn^{(4-n)+}$ to the site of action. The active species $R_nSn^{(4-n)+}$ ($n = 2$ or 3) may be bound to proteins and glycoproteins of cell membranes and nucleic acids [109], or with DNA *via* phosphate backbone [110]. Low molecular weight compounds such as amino acids, oligopeptides and nucleic acid constituents, present in biological fluids may also bind to organotin(IV) cations, significantly altering their speciation [111–117].

Model anticancer drug, *cis*-platin crosslinks the two strands of double helix of DNA *via* N7 nitrogen atoms of guanine base and/or the adjacent N7 atoms of guanine of a single strand of DNA [118]. The coordination behavior of a few di- and triorganotin(IV) derivatives of nucleic acid residues, particularly guanine [36], guanosine [37] and 5'-guanosine monophosphate [38] are recently reported in the solid state and are known to exhibit potential biological activity. In this chapter, the potentiometric studies of the interaction of $Me_nSn^{(4-n)+}$ (where $n = 2$ or 3) with 5'-guanosine monophosphate $(5'\text{-HGMP})^{2-}$ abbreviated as $(HL-1)^{2-}$ and guanosine (HGUO) abbreviated as (HL-2) (Fig. 3.1) in aqueous solution at 298.15 ± 0.1 K and at an ionic strength of 0.1 M of KNO_3 have been discussed.
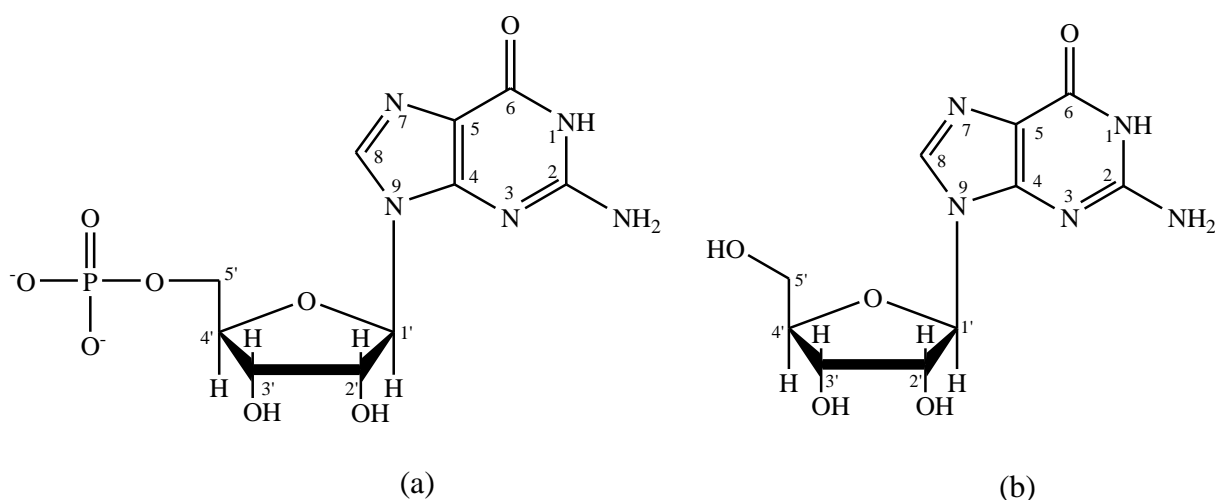
Fig. 3.1. Numbering scheme of: (a) [5'-guanosine monophosphate]$^{2-}$ ((5'-HGMP)$^{2-}$ or (HL-1)$^{2-}$) and (b) guanosine (HGUO) or (HL-2).

3.2. EXPERIMENTAL SECTION

3.2.1. Potentiometric Measurements

The potentiometric measurements were performed by using an Orion 960 plus autotitroprocessor equipped with a combined glass Orion Ross flow electrode at 298.15 ± 0.1 K. The autotitroprocessor and electrode were calibrated with standard buffer solutions of pH 4.0 ± 0.05, 7.0 ± 0.05 and 9.2 ± 0.05. Atmospheric CO_2 and O_2 were excluded from the titration vessel by bubbling purified nitrogen gas through the solution. The ionic strength was adjusted to 0.1 M by KNO_3 solution.

The following sets of solution (total volume 50 mL) (A)–(C) were titrated potentiometrically with carbonated free standardized NaOH solution (0.1M) up to pH 11.0–11.5 (60–80 data points) in aqueous media:

(A) 2.0×10^{-3} M (HL-1)$^{2-}$/(HL-2) and 0.1 M KNO_3

(B) 2.0×10^{-3} M Me$_3$SnCl/Me$_2$SnCl$_2$ and 0.1 M KNO_3

(C) 2.0×10^{-3} M (HL-1)$^{2-}$/(HL-2), 2.0×10^{-3} M Me$_3$SnCl/Me$_2$SnCl$_2$ and 0.1 M KNO_3.

Under the applied concentration range, no precipitation was observed in presence of Me$_2$Sn^{2+}/Me$_3$Sn$^+$. Each of the above set of solutions was titrated twice to check

reproducibility of the results. The pH-metric data obtained from titrating mixtures (A) and (B) were employed to calculate the protonation constants of $(HL-1)^{2-}$/(HL-2) under study and the hydrolysis constants of the organotin(IV) species, respectively, whereas the formation constants of the various complex species formed in dimethyltin(IV)-/trimethyltin(IV)-(HL-1)$^{2-}$/(HL-2) systems were determined by utilizing the data from titrating mixture (C). Further, the organotin(IV)-to-(HL-1)$^{2-}$ratio in mixture (C) was varied from 1:1 to 1:2 and organotin(IV)-to-(HL-2) varied from 1:1 to 1:3.

The following general equilibrium 3.1 was used to characterize the species formed in these systems, while the formation constants for these generalized species are given by Eq. (3.1a):

$$p\text{M} + q\text{L} + r\text{H} \rightleftharpoons \text{M}_p\text{L}_q\text{H}_r \tag{3.1}$$

$$\beta_{pqr} = \text{M}_p\text{L}_q\text{H}_r/[\text{M}]^p[\text{L}]^q[\text{H}]^r \tag{3.1a}$$

The formation of the hydroxo species is characterized by the equilibrium 3.2a/3.2b, and the formation constants are given by Eq. (3.3).

$$p\text{M} + q\text{L} \rightleftharpoons \text{M}_p\text{L}_q\text{H}_{-r} + r\text{H} \tag{3.2a}$$

$$p\text{M} + q\text{L} + r\text{OH} \rightleftharpoons \text{M}_p\text{L}_q(\text{OH})_r \tag{3.2b}$$
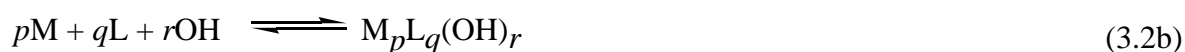
$$\beta_{\text{M}_p\text{L}_q\text{H}_{-r}} = \frac{[\text{M}_p\text{L}_q\text{H}_{-r}][\text{H}]^r}{[\text{M}]^p[\text{L}]^q} = \frac{[\text{M}_p\text{L}_q(\text{OH})_r](\text{K}_W)^r}{[\text{M}]^p[\text{L}]^q[\text{OH}]^r} = \beta_{\text{M}_p\text{L}_q(\text{OH})_r}(\text{K}_W)^r \tag{3.3}$$

Where, M = $[\text{Me}_2\text{Sn}]^{2+}$or $[\text{Me}_3\text{Sn}]^+$, L = non-protonated ligand or deprotonated ligand and H = proton, and p and q are positive integers or zero; r is positive for a protonated species and negative for hydroxo species. Charges are omitted for the sake of simplicity, but can be easily calculated by considering the notation $(HL-1)^{2-}$/HL-2 for the protonated ligands especially at N1.

The calculations for the protonation constants of $(HL-1)^{2-}$/(HL-2) and the formation constants of the complex species formed in aqueous solution at different pHs were performed using the computer program, SCOGS [94–96]. pH-metric data between pH 2.0–11.0 were used for the evaluation. Tentative values of the constants, ionic product of water, activity

coefficients of hydrogen ion at the experimental temperature (298.15 ± 0.1 K) and ionic strength (0.1 M KNO$_3$) were given as inputs [32]. The refinement of values of the constants was done by several cycles of the operation, and values corresponding to the minimum standard deviation were accepted. The output files obtained from the SCOGS program for a given system was employed in Origin 6.1 software to draw the speciation curves [32]. With the help of the speciation curves the complex formation equilibriums were elucidated.

3.2.2. NMR Measurements

Multinuclear (^{1}H, ^{13}C and ^{119}Sn) NMR measurements at different pHs were recorded in H$_2$O–D$_2$O (9:1) mixture. The ligand, guanosine has a limited solubility in water. Hence, the studies were performed at slightly increased temperature 313.10 ± 0.1 K. For ^{1}H NMR, a suitable signal-to-noise ratio was achieved after the collection of ~ 64 transients. During the recycling delay, the water resonance was suppressed as much as possible. 1024 transients were collected for each spectrum.

3.3. RESULTS AND DISCUSSION

3.3.1. Potentiometric Studies

The deprotonation and protonation sites of ligands, 5'-guanosine monophosphate (5'-HGMP)$^{2-}$ and guanosine (HGUO), abbreviated as (HL-1)$^{2-}$ and (HL-2) respectively, are considered to be N1-H (deprotonation site) and N7 (protonation site), respectively, and in case of (HL-1)$^{2-}$ phosphate oxygen (P = O) is considered as a protonation site (as shown in Fig. 3.1). The solution studies were carried out and the calculated protonation constants of the ligands, formation constants of organotin hydroxo species and formation constants of the various complex species together with their standard deviations from the program SCOGS are listed in Table 3.1 and the speciation curves are represented in Figs. 3.2 to 3.9. The literature values [119] were in fairly good agreement with the observed protonation constants of the ligands and hydrolysis constants of organotins. The probable structures of the formed complex species in aqueous solution have been determined from multinuclear NMR studies.

Table 3.1. Protonation Constants ($\log_{10} K$) of the Ligands, Formation Constants ($\log_{10} \beta$) of the Organotin(IV) Complexes and Hydrolysis Constants of the Dimethyltin(IV) and Trimethyltin(IV) Cations at 298.15 ± 0.1 K, $I = 0.1$ mol·dm^{-3} KNO$_3$; $\beta_{pqr} = $ M$_p$L$_q$H$_r$/[M]^p[L]^q[H]^r; Standard Deviations Shown in Parentheses

Species	$\log_{10} K$/ $\log_{10} \beta$
(5'-HGMP)$^{2-}$ or (HL-1)$^{2-}$	
p q r	N1, H$^+$ + (L-1)$^{3-}$ = (HL-1)$^{2-}$
011 $\log_{10} \beta$ (HL-1)$^{2-}$	9.30 (1), 9.36$^{(c)}$
	Phosphate, H$^+$ + (HL-1)$^{2-}$ = (H$_2$L-1)$^-$
012 $\log_{10} \beta$ (H$_2$L-1)$^-$	15.28 (1), 15.28$^{(c)}$
	N7, H$^+$ + (H$_2$L-1)$^-$ = (H$_3$L-1)
013 $\log_{10} \beta$ (H$_3$L-1)	17.70 (1), 17.58$^{(c)}$
	Phosphate (?), H$^+$ + (H$_3$L-1) = (H$_4$L-1)$^+$
014 $\log_{10} \beta$ (H$_4$L-1)$^+$	n.d., 18.287$^{(c)}$
pK_1 (HL-1)$^{2-}$ = $\log_{10} \beta_{011}$	9.30 (9.36)$^{(c)}$
pK_2 (H$_2$L-1)$^-$ = $\log_{10} \beta_{012} - \log_{10} \beta_{011}$	5.98 (5.92)$^{(c)}$
pK_3 (H$_3$L-1) = $\log_{10} \beta_{013} - \log_{10} \beta_{012}$	2.42 (2.30)$^{(c)}$
pK_4 (H$_4$L-1)$^+$ = $\log_{10} \beta_{014} - \log_{10} \beta_{013}$	n.d. (0.70)$^{(c)}$
For Me$_2$Sn(IV)-(HL-1)$^{2-}$ (1:1) and (1:2)	
110 $\log_{10} \beta$ Me$_2$Sn(HL-1)	14.99 (1), 14.81(3)$^{(d)}$
111 $\log_{10} \beta$ [Me$_2$Sn(HL-1)(OH)]$^-$	6.50 (1), 10.13(2)$^{(d)}$
11 −1 $\log_{10} \beta$ [Me$_2$Sn(HL-1H$_{-1}$)]	21.00 (1)
$\log_{10} K_{Me2Sn(HL-1)} = \log_{10} \beta_{Me2Sn(HL-1)} - \text{p}K_{(HL-1)}{}^{2-}$	5.69 (5.31)$^{(d)}$
For Me$_3$Sn(IV)-(HL-1)$^{2-}$ (1:1) and (1:2)	
110 $\log_{10} \beta$ [Me$_3$Sn(HL-1)]$^-$	11.98(2)
111 $\log_{10} \beta$ [Me$_3$Sn(HL-1)(OH)]$^{2-}$	2.52 (2)
(HGUO) or (HL-2)	

Contd.

		N1, $H^+ + (HL\text{-}2)^- = H_2L\text{-}2$
011	$\log_{10}\beta$ (H$_2$L-2)	9.22 (9.25)[c]
		N7, $H^+ + (H_2L\text{-}2) = (H_3L\text{-}2)^+$
012	$\log_{10}\beta$ (H$_3$L-2)$^+$	11.33, 11.15[c]

pK_1 (H$_2$L-2) $= \log_{10}\beta_{011}$		9.22 (1) (9.25)[c]
pK_2 (H$_3$L-2)$^+$ $= \log_{10}\beta_{012} - \log_{10}\beta_{011}$		2.11 (1) (1.90)[c]

For Me$_2$Sn(IV)-(HL-2) (1:1), (1:2) and (1:3)

11 –1	$\log_{10}\beta$ [Me$_2$Sn(HL-2H$_{-1}$)]$^{2+}$	20.69(2)
110	$\log_{10}\beta$ [Me$_2$Sn(HL-2)]$^{2+}$	15.24(2)
111	$\log_{10}\beta$ [Me$_2$Sn(HL-2)(OH)]$^+$	6.00 (2)

For Me$_3$Sn(IV)-(HL-2) (1:1), (1:2) and (1:3)

111	$\log_{10}\beta$ [Me$_3$Sn(HL-2)(OH)]	2.25(2)
110	$\log_{10}\beta$ [Me$_3$Sn(HL-2)]$^+$	13.88(2)

Hydrolysis Constants of		Me$_2$Sn(IV)$^{2+}$	Me$_3$Sn(IV)$^+$	
10 –1	β [Me$_2$Sn(OH)]$^+$	–3.16 (1)[a]	β [Me$_3$Sn(OH)]	–6.16 (0.1)[a]
		(–3.16)[b]		(–6.18)[b]
10 –2	β [Me$_2$Sn(OH)$_2$]	–8.42 (1)[a]	β [Me$_3$Sn(OH)$_2$]$^-$	–17.88 (0.1)[a]
		(–8.42)[b]		(–17.80)[b]
10 –3	β [Me$_2$Sn(OH)$_3$]$^-$	–19.40 (1)[a]		
		(–19.46)[b]		
20 –2	β [(Me$_2$Sn)$_2$(OH)$_2$]$^{2+}$	–4.96 (1)[a]		
		(–4.95)[b]		
20 –3	β [(Me$_2$Sn)$_2$(OH)$_3$]$^+$	–9.79 (1)[a]		
		(–9.79)[b]		

[a] This work; [b] Ref. [32]; [c] Ref. [119]; [d] Ref. [86]; with standard deviation (3)

3.3.1.1. Dimethyltin(IV)-(HL-1)$^{2-}$ system

The cation, dimethyltin(IV) was reported [111] to be hydrolyzed to form a series of mono- and polynuclear hydroxo species according to general equilibrium 3.4 and the compiled literature results of the hydrolysis of Me_2Sn^{2+} in different media are presented in reference [109].

$$x Me_2Sn^{2+} + y H_2O \rightleftharpoons \{(Me_2Sn)_x(OH)_y\}^{(2x-y)+} + y H^+ \qquad (3.4)$$
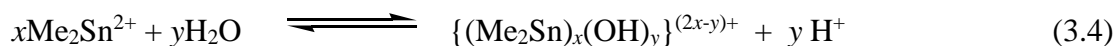
(Where $x = 1$, $y = 1, 2, 3$; $x = 2$, $y = 2, 3$; $x = 3$, $y = 4$; $x = 4$, $y = 6$).

The hydroxo species, ($[Me_2Sn(OH)]^+$, $[Me_2Sn(OH)_2]$, $[Me_2Sn(OH)_3]^-$, $[(Me_2Sn)_2(OH)_2]^{2+}$ and $[(Me_2Sn)_2(OH)_3]^+$) and their hydrolysis constants [94] as reported by Arena et al. have been taken into consideration in the present study, and the observed $\log_{10} \beta$ values (Table 3.1) are in close agreement with the reported values. Inclusion of formation constants of polynuclear organotin-hydroxo species such as $(Me_2Sn)_2(OH)_4$, $[(Me_2Sn)_3(OH)_4]^{2+}$, $[(Me_2Sn)_4(OH)_5]^{3+}$ and $[(Me_2Sn)_4(OH)_6]^{2+}$ (as reported [107] by Natsume et al.) in the SCOGS program resulted in high standard deviation, hence they were rejected. This is due to the fact that the formation of organotin(IV) polymeric species is strictly concentration dependent and the experimental concentration under the present study is too low to allow their formation.

The following species, *viz.* $[SnMe_2(HL-1)]$, $[SnMe_2(HL-1)(OH)]^-$, $[SnMe_2(OH)]^+$, $[SnMe_2(OH)_2]$, $[SnMe_2(OH)_3]^-$, $[SnMe_2(HL-1H_{-1})]$, $[SnMe_2(HL-1H_{-2})(OH)]^{2-}$, $[SnMe_2(HL-1)(OH)_2]^{2-}$, $[SnMe_2(HL-1)_2]^{2-}$, $[SnMe_2(HL-1)_2(OH)]^{3-}$ and $[SnMe_2(HL-1)_2(OH)_2]^{4-}$ are considered for dimethyltin(IV)-(HL-1)$^{2-}$ systems studied with metal:ligand ratio of 1:1 to 1:2, but inclusion of the last five species in species matrix resulted negative values and a very high standard deviation, hence, they were ruled out.

At pH ~ 3.0, the complexation of Me_2Sn^{2+} with (HL-1)$^{2-}$ in 1:1 molar ratio starts yielding neutral complex, $Me_2Sn(HL-1)$ (87.3% at pH 7.12) according to Eq. (3.5). In this complex species, Me_2Sn^{2+} binds with the anionic oxygen present in the phosphate group of (HL-1)$^{2-}$ as the $Me_2Sn(IV)$ moiety has stronger tendency to bind with oxygen than nitrogen [120]. At pH = 7.01, a significant upfield shift observed in proton resonance signals of the ligand in the equilibrium mixture, provides an evidence for the coordination of the ligand *via* phosphate group to the dimethyltin(IV) moiety. The calculated stability constant (5.69) of this

complex species [$\log_{10} K_{\text{Me2Sn(HL-1)}} = \log_{10} \beta_{\text{Me2Sn(HL-1)}} - pK_{\text{(HL-1)}}^{2-}$] is in close agreement with the reported value (5.31), and clearly supports the strong affinity of dimethyltin(IV) towards the phosphate group [86]. Due to the low solubility of this complex, a white precipitate is formed if the concentration of dimethyltin dichloride in the titration mixture C is greater than 1.0×10^{-2} M above pH 3.0, whereas the hydrolysis products of dimethyltin dichloride are soluble at this concentration, and there was no precipitation during titration of (HL-1)^{2-} below this concentration.

With an increase in the pH of the solution on the addition of alkali, after pH 5.91, the conversion of Me$_2$Sn(HL-1) into a mixed-ligand hydroxo complex species (Eq. (3.6)), *viz.* [Me$_2$Sn(HL-1)(OH)]$^-$ (89.3% at pH 9.96) takes place by deprotonation from one of the H$_2$O molecules coordinated to Me$_2$Sn^{2+}. However, the formation of Me$_2$Sn(OH)$_2$ after pH 7.0 (14.37% at pH 11.05) (Eq. (3.7a)) also takes place slowly with the release of the (HL-1)^{2-} (0.1−2.29%) as indicated in the species distribution diagram (Fig. 3.2). It means that the hydrolysis of Me$_2$Sn^{2+} is shifted to higher pH by ~ 1.5 pH units upon coordination to (HL-1)$^{2-}$. Further, the negligible shift observed in NMR resonances of the ligand in the equilibrium mixture at pH 9.0 also supported the release of the (HL-1)^{2-}. Above pH 9.53, further hydrolysis takes place resulting [Me$_2$Sn(OH)$_3$]$^-$ (16.1% at pH 11.05) according to Eq. (3.8). Due to the base proton H8, and protons of the sugar moiety, H1', H2', H3', H4', H5' of (HL-1)$^{2-}$, six sets of the ^{1}H signals have been observed in the sequence of descending δ values. Due to deprotonation of N7, the upfield shift of the proton H8 is observed in the presence of dimethyltin(IV) at pH ~ 3.0. At lower pH, the formation of [Me$_2$Sn(HL-1H$_{-1}$)] (99.9% at pH 3.0) may be due to the interaction of organotin(IV) moiety with the base part (N7) of the ligand (Eq. (3.9)).

$$\text{Me}_2\text{Sn}^{2+} + \text{(HL-1)}^{2-} \rightleftharpoons \text{Me}_2\text{Sn(HL-1)} \qquad (3.5)$$

$$\text{Me}_2\text{Sn(HL-1)} + \text{OH}^- \rightleftharpoons [\text{Me}_2\text{Sn(HL-1)(OH)}]^- + \text{H}_2\text{O} \qquad (3.6)$$

$$[\text{Me}_2\text{Sn(HL-1)(OH)}]^- + \text{OH}^- \rightleftharpoons \text{Me}_2\text{Sn(OH)}_2 + \text{(HL-1)}^{2-} \qquad (3.7a)$$

$$\text{Me}_2\text{Sn}^{2+} + n\text{OH}^- \rightleftharpoons [\text{Me}_2\text{Sn(OH)}_n]^{(2-n)+} \qquad (3.7b)$$

(n =1 or 2)

$$Me_2Sn(OH)_2 + OH^- \quad \rightleftharpoons \quad [Me_2Sn(OH)_3]^- \qquad (3.8)$$

$$Me_2Sn^{2+} + (HL\text{-}1H_{-1})^{2-} \quad \rightleftharpoons \quad [Me_2Sn(HL\text{-}1H_{-1})] \qquad (3.9)$$
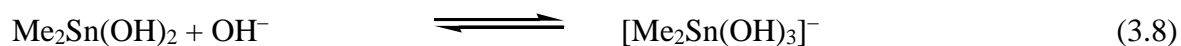
The initial pH in the titration mixture for $Me_2Sn(IV)$-$(HL\text{-}1)^{2-}$ system with 1:2 (Metal:Ligand) molar ratio, starts from 5.12 and at this pH, $Me_2Sn(HL\text{-}1)$ (5.71%), $[Me_2Sn(HL\text{-}1H_{-1})]$ (44.3%), $[Me_2Sn(OH)]^+$ (29.1%) and $Me_2Sn(OH)_2$ (16.0%) (Eq. (3.7b)) along with little amount of dimethyltin(IV) (4.61%) exist. This is probably due to the formation of double amount of NaOH in the titration mixture containing $[Me_2SnCl_2{:}2Na_2(HL\text{-}1)]$, which results the formation of hydroxo species at this pH, whereas in 1:1 system it starts after pH 7.0. As pH increases, $Me_2Sn(HL\text{-}1)$ (44.8% at pH 7.18) and $Me_2Sn(OH)_2$ (49.9% at pH 8.4) go on increasing with simultaneous formation of $[Me_2Sn(HL\text{-}1)(OH)]^-$ (48.6% at pH 10.4), and the species $[Me_2Sn(HL\text{-}1H_{-1})]$ and $[Me_2Sn(OH)]^+$ go on decreasing as indicated by the species distribution diagram (Fig. 3.3). Further on increasing pH, $[Me_2Sn(OH)_3]^-$ (28.4% at pH 11.03) is also formed (Eq. (3.8)). At pH ~ 7.0, both $Me_2Sn(HL\text{-}1)$ and $Me_2Sn(OH)_2$ species are competitive.
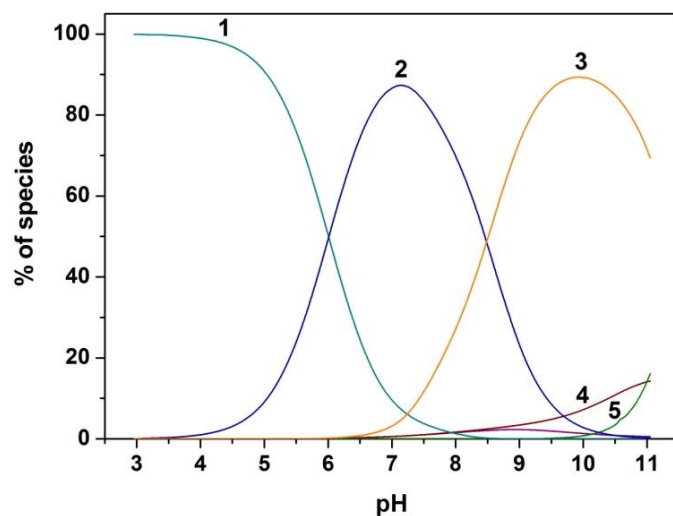
Fig. 3.2. Speciation curves for 1:1 dimethyltin-(HL-1)$^{2-}$: 1 = [Me$_2$Sn(HL-1H$_{-1}$)]; 2 = Me$_2$Sn(HL-1); 3 = [Me$_2$Sn(HL-1)(OH)]$^-$; 4 = Me$_2$Sn(OH)$_2$; 5 = [Me$_2$Sn(OH)$_3$]$^-$; 6 = (HL-1)$^{2-}$ (where (HL-1)$^{2-}$ = (5'-HGMP)$^{2-}$).
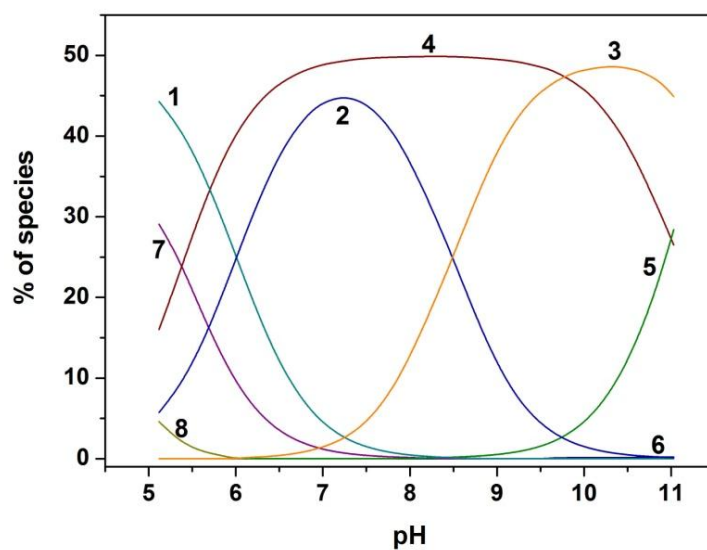
Fig. 3.3. Speciation curves for 1:2 dimethyltin-(HL-1)$^{2-}$: 1 = [Me$_2$Sn(HL-1H$_{-1}$)]; 2 = Me$_2$Sn(HL-1); 3 = [Me$_2$Sn(HL-1)(OH)]$^-$; 4 = Me$_2$Sn(OH)$_2$; 5 = [Me$_2$Sn(OH)$_3$]$^-$; 6 = (HL-1)$^{2-}$; 7 = [Me$_2$Sn(OH)]$^+$; 8 = Me$_2$Sn^{2+} (where (HL-1)$^{2-}$ = (5'-HGMP)$^{2-}$).

3.3.1.2. Trimethyltin(IV)-(HL-1)$^{2-}$ system

The hydrolysis of trimethyltin(IV) ion was previously investigated in dilute and fairly concentrated aqueous solution where the dinuclear species is also formed [32, 121, 122]. The formation of Me$_3$Sn(OH), [Me$_3$Sn(OH)$_2$]$^-$ and [(Me$_3$Sn)$_2$(OH)]$^+$ species [32, 122] was found to be consistent with the fitted model. For trimethyltin(IV) system, [Sn(CH$_3$)$_3$(H$_2$O)$_2$]$^+$ undergoes hydrolysis according to equilibrium 3.10.

$$[Sn(CH_3)_3(H_2O)_2]^+ + H_2O \; \rightleftharpoons \; [Sn(CH_3)_3(H_2O)(OH)] + H_3O^+ \qquad (3.10)$$
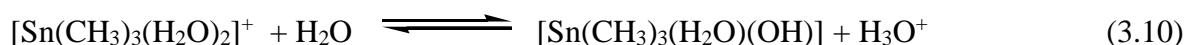
The hydrolysis of trimethyltin(IV) chloride has been investigated in the present study in the pH range 2.0−11.0 at 298.15 ± 0.1 K and I = 0.1 M KNO$_3$ and the observed $\log_{10} \beta_{10\,-1}$ value (−6.16) is in fair agreement with the previously reported value (−6.18) (Table 3.1) obtained in 0.1 M KNO$_3$. The formation constant of [Sn(CH$_3$)$_3$(OH)$_2$]$^-$ ($\log_{10} \beta_{10\,-2}$ = −17.88) has also been determined and given in the Table 3.1, but no polymeric species has been observed in this concentration range. Furthermore, the degree of hydrolysis of trimethyltin chloride has been observed considerably less than that of its dimethyltin counterpart ($\log_{10} \beta_{10\,-1}$ = −3.16; $\log_{10} \beta_{10\,-2}$ = −8.42 (Table 3.1)).

At pH 6.18, in Me$_3$Sn(IV)-(HL-1)$^{2-}$ system (1:1 Metal:Ligand molar ratio), [Me$_3$Sn(HL-1)]$^-$ exists almost 100% in solution according to Eq. (3.11), whose concentration starts decreasing with the addition of alkali. [Me$_3$Sn(HL-1)]$^-$ gets converted into [Me$_3$Sn(HL-1)(OH)]$^{2-}$ as pH increases beyond 6.61, according to Eq. (3.12), which goes up to maximum level of 97.2% as pH reaches to 11.0, as shown in the species distribution curve (Fig. 3.4). No evidence for the formation of organotin hydroxide species in the present system was found. But in case of 1:2 system, the formation of Me$_3$Sn(OH) (49.3% at pH 9.61) and [Me$_3$Sn(OH)$_2$]$^-$ (8.97% at pH 11.06) was also observed (Eq. (3.13) and Eq. (3.14)) in addition to [Me$_3$Sn(HL-1)]$^-$ (49.9% at pH 6.66) and [Me$_3$Sn(HL-1)(OH)]$^{2-}$ (48.8% at pH 11.06) as indicated in Fig. 3.5. This is due to the greater amount of NaOH in the 1:2 titration mixture.
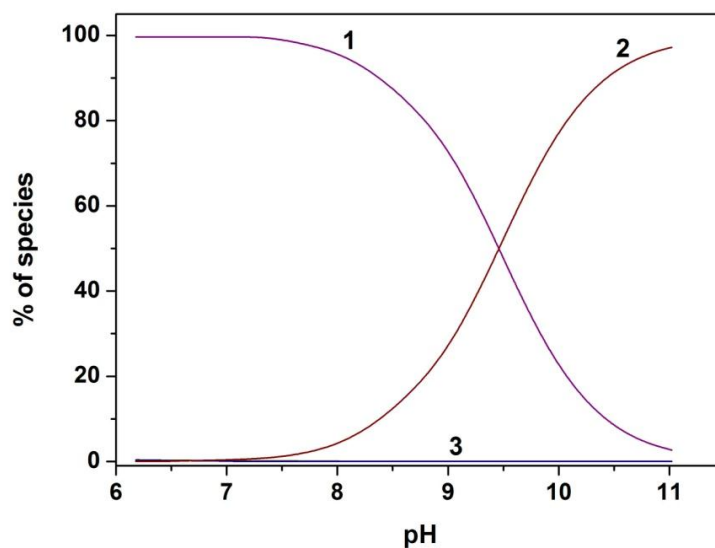
Fig. 3.4. Speciation curves for 1:1 trimethyltin-(HL-1)$^{2-}$: 1 = [Me$_3$Sn(HL-1)]$^-$; 2 = [Me$_3$Sn(HL-1)(OH)]$^{2-}$; 3 = (HL-1)$^{2-}$ (where (HL-1)$^{2-}$ = (5'-HGMP)$^{2-}$).

Fig. 3.5. Speciation curves for 1:2 trimethyltin-(HL-1)$^{2-}$: 1 = [Me$_3$Sn(HL-1)]$^-$; 2 = [Me$_3$Sn(HL-1)(OH)]$^{2-}$; 3 = Me$_3$Sn(OH); 4 = [Me$_3$Sn(OH)$_2$]$^-$; 5 = Me$_3$Sn$^+$ (where (HL-1)$^{2-}$ = (5'-HGMP)$^{2-}$).

$(Me_3Sn)^+ + (HL\text{-}1)^{2-} \quad \rightleftharpoons \quad [Me_3Sn(HL\text{-}1)]^- \qquad\qquad (3.11)$

$[Me_3Sn(HL\text{-}1)]^- + OH^- \quad \rightleftharpoons \quad [Me_3Sn(HL\text{-}1)(OH)]^{2-} \qquad (3.12)$

$(Me_3Sn)^+ + OH^- \quad \rightleftharpoons \quad [Me_3Sn(OH)] \qquad\qquad (3.13)$

$[Me_3Sn(OH)] + OH^- \quad \rightleftharpoons \quad [Me_3Sn(OH)_2]^- \qquad\qquad (3.14)$
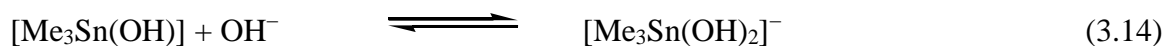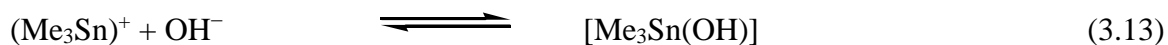
3.3.1.3. Dimethyltin(IV)-(HL-2) system

During the early stages of the reaction (pH < 4.0), there is a possibility of protonation at N7 position, and the species $[Me_2Sn(HL\text{-}2H_{-1})]^{2+}$ is formed (98.6% at pH 3.6) with the deprotonation of N7-H (Eq. (3.15)). As the pH of the solution increases with the addition of the alkali, formation of $[Me_2Sn(HL\text{-}2)]^{2+}$ starts (Eq. (3.16)) resulting in 88.9% of it at pH 7.04 as shown in Fig. 3.6. Almost negligible conversion of $[Me_2Sn(HL\text{-}2)]^{2+}$ into $[Me_2Sn\text{-}(HL\text{-}2)(OH)]^+$ takes place (0.70% at pH 10.1) (Eq. (3.17)) after pH 6.5, by deprotonation from one of the H_2O molecules associated with dimethyltin(IV) moiety. After pH 7.5, the formation of $Me_2Sn(OH)_2$ (31.5% at pH 11.04) and $[Me_2Sn(OH)_3]^-$ (34.0% at pH 11.04) increases (Eq. (3.18) and Eq. (3.19)). No change in the concentration of the species formed in 1:2 (as shown in Fig. 3.7) and 1:3 systems, at lower pH, but at physiological pH ~ 7.0 there is a slight increase in the formation of $[Me_2Sn(HL\text{-}2)]^{2+}$ (91.2% in 1:2 and 92.3% in 1:3 systems). At higher pH (~ 10.3), further, significant amount of $[Me_2Sn(HL\text{-}2)(OH)]^+$ (84.3% in 1:2 and 88.1% in 1:3 systems) is formed with the simultaneous reduction in the formation of $Me_2Sn(OH)_2$ (20.7% and 16.4% at pH 11.2 in 1:2 and 1:3 systems, respectively) and $[Me_2Sn(OH)_3]^-$ (29.2% and 24.8% at pH 11.2 in 1:2 and 1:3 systems, respectively).

$(Me_2Sn)^{2+} + (HL\text{-}2H_{-1}) \quad \rightleftharpoons \quad [Me_2Sn((HL\text{-}2H_{-1})]^{2+} \qquad (3.15)$

$(Me_2Sn)^{2+} + (HL\text{-}2) \quad \rightleftharpoons \quad [Me_2Sn(HL\text{-}2)]^{2+} \qquad\qquad (3.16)$

$[Me_2Sn(HL\text{-}2)]^{2+} + OH^- \quad \rightleftharpoons \quad [Me_2Sn(HL\text{-}2)(OH)]^+ \qquad (3.17)$

$[Me_2Sn(HL\text{-}2)]^{2+} + 2OH^- \quad \rightleftharpoons \quad Me_2Sn(OH)_2 + (HL\text{-}2) \qquad (3.18)$

$Me_2Sn(OH)_2 + OH^- \quad \rightleftharpoons \quad [Me_2Sn(OH)_3]^- \qquad\qquad (3.19)$

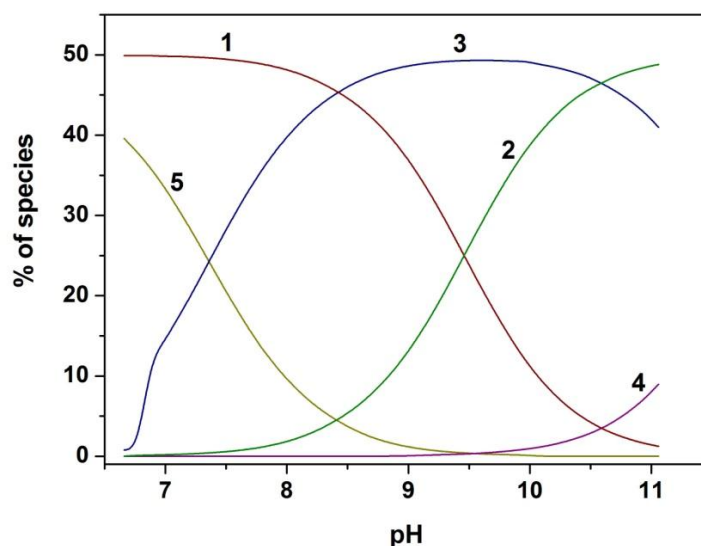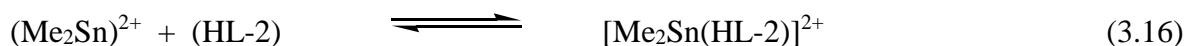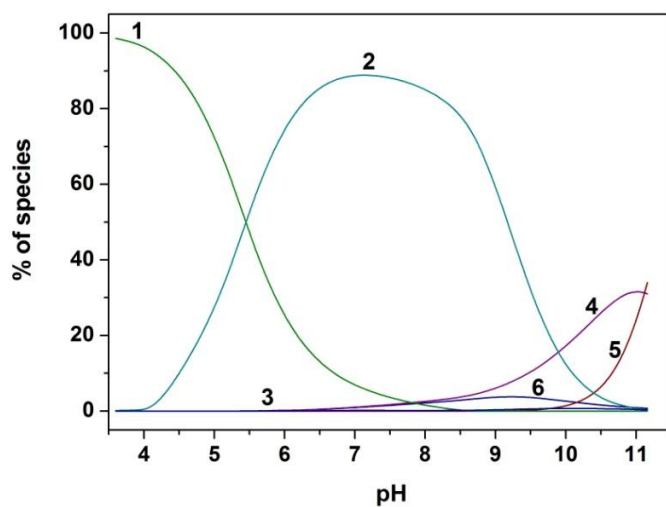**Fig. 3.6.** Speciation curves for 1:1 dimethyltin-(HL-2): 1 = $[Me_2Sn(HL-2H_{-1})]^{2+}$; 2 = $[Me_2Sn(HL-2)]^{2+}$; 3 = $[Me_2Sn(HL-2)(OH)]^+$; 4 = $Me_2Sn(OH)_2$; 5 = $[Me_2Sn(OH)_3]^-$; 6 = (HL-2) (where (HL-2) = (HGUO)).
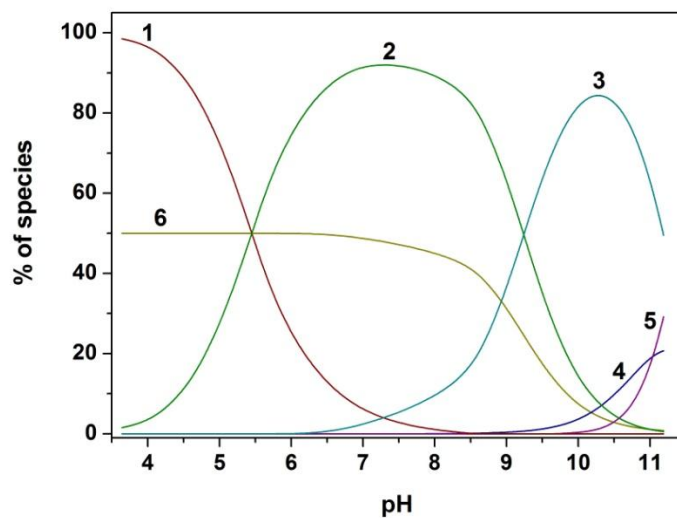
Fig. 3.7. Speciation curves for 1:2 dimethyltin-(HL-2): 1 = $[Me_2Sn(HL-2H_{-1})]^{2+}$; 2 = $[Me_2Sn(HL-2)]^{2+}$; 3 = $[Me_2Sn(HL-2)(OH)]^+$; 4 = $Me_2Sn(OH)_2$; 5 = $[Me_2Sn(OH)_3]^-$; 6 = (HL-2) (where (HL-2) = (HGUO)).
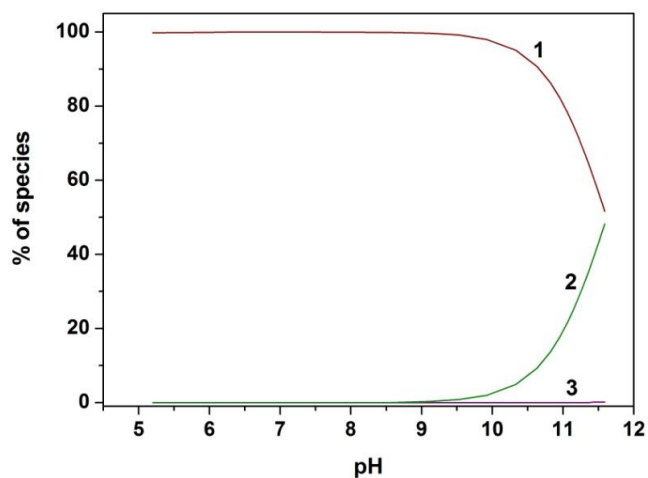
Fig. 3.8. Speciation curves for 1:1 trimethyltin-(HL-2): 1 = [Me₃Sn(HL-2)]⁺; 2 = Me₃Sn(HL-2)(OH); 3 = Me₃Sn(OH) (where (HL-2) = (HGUO)).
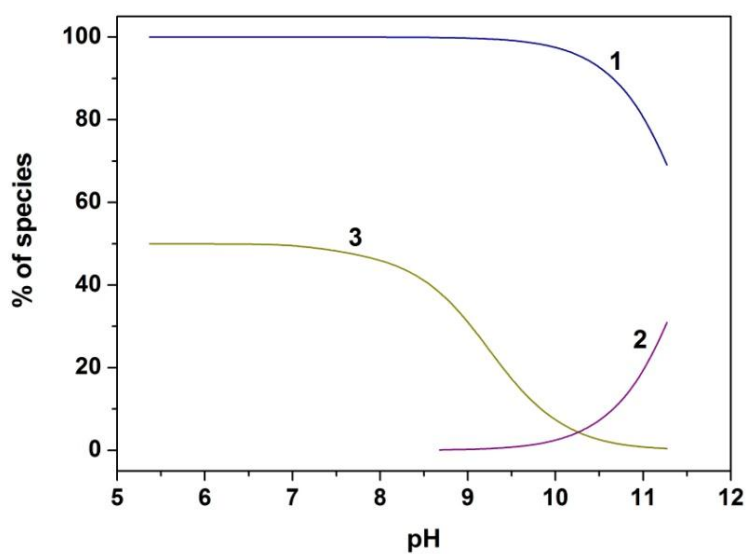
Fig. 3.9. Speciation curves for 1:2 trimethyltin-(HL-2): 1 = [Me₃Sn(HL-2)]⁺; 2 = Me₃Sn(HL-2)(OH); 3 = (HL-2) (where (HL-2) = (HGUO)).

3.3.1.4. Trimethyltin(IV)-(HL-2) system

The initial pH for $Me_3Sn(IV)$-(HL-2) 1:1 system in the titration mixture starts from 5.2, and at this pH, almost 100% of $[Me_3Sn(HL-2)]^+$ in solution exists and continues to be 100% up to pH ~ 9.0 according to Eq. (3.20). Thereafter, the concentration of $[Me_3Sn(HL-2)]^+$ starts decreasing as pH increases because of its conversion into $[Me_3Sn(HL-2)(OH)]$ (Eq. (3.21)), which goes up to a maximum level (48.2%) as pH reached to 11, as shown in the species distribution curve (Fig. 3.8). There is not much significant increment of hydrolyzed species at pH 5.0 to 9.0 in 1:2 (as shown in Fig. 3.9) and 1:3 systems, but a significant change in the concentration of $[Me_3Sn(HL-2)(OH)]$ (30.9% in 1:2 and 46.6% in 1:3 systems) is observed at pH ~ 11, and the unreacted (HL-2) remains in the solution (49.4% in 1:2 and 66.4% in 1:3 systems at pH 7.0).

$$(Me_3Sn)^+ + (HL-2) \rightleftharpoons [Me_3Sn(HL-2)]^+ \qquad (3.20)$$

$$[Me_3Sn(HL-2)]^+ + OH^- \rightleftharpoons [Me_3Sn(HL-2)(OH)] \qquad (3.21)$$

3.3.2. Multinuclear NMR Studies

The multinuclear (^1H, ^{13}C and ^{119}Sn) NMR experiments of the reaction mixtures at different pHs were carried out to propose the possible geometry of the existing complex species in aqueous medium. Table 3.2 presents the ^1H NMR data, *i.e.* chemical shifts and two-bond coupling constants $^2J(^1H-^{117/119}Sn)$ of (Me_2Sn^{2+}/Me_3Sn^+ + Ligand) systems, together with the $\angle C-Sn-C$ bond angles calculated by employing the Lockhart and Manders equation [123]. The ^{13}C and ^{119}Sn NMR data of di-/trimethyltin(IV) + (HL-1)$^{2-}$ and di-/trimethyltin(IV) + (HL-2) systems are presented in Tables 3.3–3.6. Some representative ^1H and ^{119}Sn NMR spectra of di-/trimethyltin(IV) + (HL-1)$^{2-}$/(HL-2) systems at pH 7.0–7.4 are presented in Figs. 3.10, 3.12, 3.14 and 3.16. The calculated values of individual chemical shifts and coupling constants $^2J(^1H-^{117/119}Sn)$ as well as their geometry of the resulting hydrolyzed species of dimethyltin cation were compared with the values reported earlier [32, 124].

Table 3.2. ^{1}H NMR Spectral Data[a] of Di- and Trimethyltin(IV)-(HL-1)[2−] Mixtures at Different pHs

pH	Species (%)[b]	H_α[c]	Line Width[d]	∠C–Sn–C[e]	H8	NH₂	H1'	2'-OH/ 3'-OH	H2'	H3'	H4'	H5'
	[Me₂Sn(H₂O)₄][2+]	0.84 [102]	5.66	166								
For Me₂Sn(IV) + (HL-1)[2−] Mixture 1:1 system												
3.2	Me₂Sn(HL-1H₋₁) (99.8), Me₂Sn(HL-1) (0.27)	0.86 [92]	6.27	148	8.19	-	5.95	-	4.46	4.33	4.10	3.35
4.5	Me₂Sn(HL-1H₋₁) (96.9), Me₂Sn(HL-1) (3.3)	0.79 [86]	5.18	139	8.10	6.35	5.93	-	4.47	4.32	4.08	3.35
7.1	Me₂Sn(HL-1) (87), Me₂Sn(HL-1H₋₁) (9.6), [Me₂Sn(HL-1)(OH)]⁻ (3.4), Me₂Sn(OH)₂ (0.7)	0.79 [86]	6.06	139	8.13	6.34	5.92	-	4.46	4.31	4.03	2.71
9.3	[Me₂Sn(HL-1)(OH)]⁻ (82.9), Me₂Sn(HL-1) (12.9), Me₂Sn(OH)₂ (4.3)	0.67 [80]	5.57	131	8.18	-	5.91	-	4.47	4.38	4.29	3.96
For Me₂Sn(IV) + (HL-1)[2−] Mixture 1:2 system												
5.0	Me₂Sn(HL-1H₋₁) (44.4), [Me₂Sn(OH)]⁺ (29.0), Me₂Sn(OH)₂ (16.0), Me₂Sn(HL-1) (5.7),	0.72 [82]	3.92	133	8.12	6.35	5.93	-	4.47	4.32	4.07	3.35

Contd.

pH	Species (%)												
	[Me₂Sn(H₂O)₄]²⁺ (4.6)												
7.2	Me₂Sn(OH)₂ (49.3), Me₂Sn(HL-1) (44.6), [Me₂Sn(HL-1)(OH)]⁻ (2.3), Me₂Sn(HL-1H₋₁) (2.9), [Me₂Sn(OH)]⁺ (0.8)	0.70 [80]	3.27	131	8.19	6.35	5.93	-		4.49	4.40	4.31	3.99
9.2	Me₂Sn(OH)₂ (49.2), [Me₂Sn(HL-1)(OH)]⁻ (41.7), Me₂Sn(HL-1) (8.2), [Me₂Sn(OH)₃]⁻ (0.7)	0.69 [80]	3.84	131	8.20	-	5.93	-	-	-	-		3.35
	Me₃Sn(H₂O)₂⁺	0.57 [66]	5.60	116									
For Me₃Sn(IV) + (HL-1)²⁻ Mixture 1:1 system													
6.9	[Me₃Sn(HL-1)]⁻ (99.9), [Me₃Sn(HL-1)(OH)]²⁻ (0.2), (HL-1)²⁻ (0.2)	0.42 [64]	4.99	115	8.18	-	5.93	-		4.48	4.31	3.99	-
9.3	[Me₃Sn(HL-1)]⁻ (58.8), [Me₃Sn(HL-1)(OH)]²⁻ (41.3)	0.40 [64]	4.01	115	8.19	-	5.92	-		4.48	4.31	3.97	3.35
For Me₃Sn(IV) + (HL-1)²⁻ Mixture 1:2 system													
6.9	[Me₃Sn(HL-1)]⁻ (49.9), Me₃Sn(H₂O)₂⁺ (35.5),	0.49 [66]	6.25	117	8.20	6.38	5.97	-		4.48	4.39	4.04	3.40

59

	Me$_3$Sn(OH) (11.5),											
	[Me$_3$Sn(HL-1)(OH)]$^{2-}$ (0.14)											
8.9	Me$_3$Sn(OH) (48.3),	0.45	5.63	115	8.23	-	5.97	-	4.48	4.35	4.02	3.40
	[Me$_3$Sn(HL-1)]$^-$ (38.8),	[64]										
	[Me$_3$Sn(HL-1)(OH)]$^{2-}$ (11.2),											
	Me$_3$Sn(H$_2$O)$_2{}^+$(1.5)											

[a] Solvent: H$_2$O:D$_2$O (9:1); Atom numbers mentioned as in Fig. 3.1; α_{CH_3-Sn} [b] Percentage of species from speciation diagram; [c] Values in square bracket [ ] are $^2J(^{119}Sn-^1H)$ in Hz; [d] Line width = the half line-width of the methyl protons; [e] Calculated using Eq.: θ ($\angle$C–Sn–C) = $0.0161|^2J(^1H-^{119}Sn)|^2 - 1.32|^2J(^1H-^{119}Sn)| + 133.4$, taken from Ref. [123].

High quality ^{1}H NMR spectra were obtained by performing the measurements using the concentrations [Me$_2$Sn(IV)] = 2.0 × 10^{-3} M, [(HL-1)$^{2-}$] = (2.0 − 4.0) × 10^{-3} M for Me$_2$Sn(IV)-(HL-1)$^{2-}$ system and by using [Me$_3$Sn(IV)] = 1.5 × 10^{-3} M, [(HL-1)$^{2-}$] = (2.0 − 4.0) × 10^{-3} M for Me$_3$Sn(IV)-(HL-1)$^{2-}$ system. For ^{13}C and ^{119}Sn NMR experiments, [Me$_2$Sn(IV)] = 8.0 × 10^{-2} M, [(HL-1)$^{2-}$] = (8.0 − 16.0) × 10^{-2} M for Me$_2$Sn(IV)-(HL-1)$^{2-}$ system and [Me$_3$Sn(IV)] = 5.0 × 10^{-2} M, [(HL-1)$^{2-}$] = (5.0 − 10.0) × 10^{-2} M for Me$_3$Sn(IV)-(HL-1)$^{2-}$ system have been employed. For ^{13}C and ^{119}Sn NMR experiments of Me$_2$Sn(IV)-/Me$_3$Sn(IV)-(HL-2), the concentrations employed are [Me$_2$Sn(IV)]/[Me$_3$Sn(IV)] = 5.0 × 10^{-2} M, [HL-2] = (5.0 − 10.0) × 10^{-2} M. These concentration limits of organotin(IV) moiety and ligands were optimized in order to avoid the precipitation during and after the NMR experiments. Further, limited solubility of guanosine in water at room temperature imposed to carry out the measurement at a slightly increased temperature 313.10 ± 0.1 K. Unfortunately, the suppression of water resonance during recycling delay in ^{1}H NMR at this temperature could not be achieved as expected. Hence, the evidence from ^{13}C and ^{119}Sn were used for interpretation.

3.3.2.1. NMR of Dimethyltin(IV)-(HL-1)$^{2-}$ system

In ^{1}H NMR spectra of both 1:1 and 1:2 Me$_2$Sn-(HL-1)$^{2-}$ systems, the methyl proton (bound to tin) resonance shifts to higher field and the $^{2}J(^{1}H-^{119}Sn)$ coupling constant value decreases upon increasing the pH of the solution, which are similar to Me$_2$Sn^{2+}, Me$_2$Sn-captopril/dipeptide systems [24, 84, 124] and Me$_2$Sn-heterocyclic thiones [32]. Only one sharp methyl proton (bound to tin) resonance with well resolved satellites and half line-width (in the range 3.27−6.27 Hz) was observed in all the systems (Table 3.2), indicating that various complex species formed at a given pH are in fast mutual exchange relative to the NMR timescale. The coupling constant, $^{2}J(^{1}H-^{119}Sn)$ provides information on the average ∠C–Sn–C bond angle of all the possible complex species at a given pH, there by indicating the possible coordination and geometry around the tin atom. Similarly, single set of resonances of methyl carbon bound to tin was observed in ^{13}C NMR spectra, but $^{1}J(^{13}C-^{119}Sn)$ values could not be determined with sufficient certainty in most of the systems, due to the broad CH$_3$–Sn signals, except a few (Table 3.3). Furthermore, in comparison to ^{1}H and ^{13}C, the ^{119}Sn chemical shifts are more diagnostic,

and provide invaluable information regarding the coordination number around tin, as well as the existence of more than one tin-containing species [32]. The ^{119}Sn chemical shifts in the ranges δ 200 to -60, -90 to -190 and -210 to -400 ppm [125] have been reported for the complexes having four-, five- and six-coordinate tin centers, respectively.

In Me$_2$Sn(IV)-(HL-1)$^{2-}$ 1:1 system, at pH 3.2/at pH 4.5, the predominant tin containing species is [Me$_2$Sn(HL-1H$_{-1}$)] (99.8/96.7 %). The methyl proton resonance observed at δ 0.86/0.79 ppm has a $^2J(^1H-^{119}Sn)$ of 92.0/86.0 Hz with C–Sn–C bond angle 148$°$/139$°$, suggesting a distorted *cis*-octahedral geometry around tin [123]. The proposed geometry is also supported by ^{13}C NMR data at pH 4.7 (δ 13.6 ppm, $^1J(^{13}C-^{119}Sn)$ 696.8 Hz, $\angle$C–Sn–C 137.9$°$) and ^{119}Sn resonance at -215.31, -272.42 ppm at pH 4.7 (as shown in (b1/b2) in Fig. 3.11). The major species Me$_2$Sn(HL-1) (87.0%) existing at physiological pH 7.0 has a chemical shift δ 0.79 ppm, $^2J(^1H-^{119}Sn)$ 86.0 Hz and $\angle$C–Sn–C 139$°$. The ^{13}C NMR data (at pH 7.4, δ 11.0 ppm, $^1J(^{13}C-^{119}Sn)$ 637.47 Hz and $\angle$C–Sn–C 132.67$°$) also suggests the existence of a distorted octahedral species Me$_2$Sn(HL-1). In ^{119}Sn NMR at pH 7.4, a chemical shift of δ -280.68 ppm is observed, assigned to major species Me$_2$Sn(HL-1) (87.5%) exhibiting six coordination around Sn (as shown in (b1/b2) in Fig. 3.11). The major species [Me$_2$Sn(HL-1)(OH)]$^-$ (84.6%) (together with a minor species Me$_2$Sn(OH)$_2$ (4.8%)) observed at pH 9.4 exhibits ^{13}C chemical shift at δ 12.3 ppm with $^1J(^{13}C-^{119}Sn)$ 540.7 Hz and $\angle$Me–Sn–Me 124.18$°$, suggesting a distorted trigonal bipyramidal geometry for [Me$_2$Sn(HL-1)(OH)]$^-$ species with equatorial methyl groups (as shown in (c) in Fig. 3.11). But in ^{119}Sn NMR, resonances at δ 94.52, -117.73 and -233.4 ppm may be attributed to four coordinated Me$_2$Sn(OH)$_2$ (as shown in (d) in Fig. 3.11), five coordinated [Me$_2$Sn(HL-1)(OH)]$^-$ and six coordinated Me$_2$Sn(HL-1), respectively.

Similarly, ^{1}H NMR spectra of Me$_2$Sn-(HL-1)$^{2-}$ 1:2 system at different pHs lie closely exhibiting δ 0.72−0.69 ppm, $^2J(^1H-^{119}Sn)$ 82−80 Hz and $\angle$C–Sn–C angle 133.0−131.0$°$, and the half line width of methyl protons (H$_\alpha$) bound to tin slightly varies (at pH 5.0, 3.92 Hz; at 7.2, 3.27 Hz; at 9.2, 3.84 Hz), indicating that more than one tin-containing species may be present, which undergo fast mutual exchange in NMR timescale in solution. Three ^{13}C resonances at δ 16.2 ppm ($^1J(^{13}C-^{119}Sn)$ = 591.1 Hz), 16.0 ppm ($^1J(^{13}C-^{119}Sn)$ = 646.5 Hz) and 4.1 ppm

Table 3.3. ^{13}C NMR Spectral Data[a] of Di- and Trimethyltin(IV)-(HL-1)$^{2-}$ Mixtures at Different pHs

pH	Species (%)[b]	C_α[c]	∠C–Sn–C[d]	C6	C2	C4	C8	C5	C1'	C4'	C2'	C3'	C5'
	Na₂GMP (Na₂(HL-1))	-		156.7	153.6	151.3	135.6	116.6	86.3	85.2	73.6	70.3	61.3

For Me₂Sn(IV) + (HL-1)$^{2-}$ Mixture 1:1 system

pH	Species (%)[b]	C_α[c]	∠C–Sn–C[d]	C6	C2	C4	C8	C5	C1'	C4'	C2'	C3'	C5'
	[Me₂Sn(H₂O)₄]$^{2+}$	16.7, 12.9 [494.4]	120.1										
4.7	Me₂Sn(HL-1H₋₁) (95.1), Me₂Sn(HL-1) (4.9)	13.6 [696.8]	137.9	155.96	-	142.32	136.63	116.51	83.26	79.61	-	66.07	54.13
5.8	Me₂Sn(HL-1H₋₁) (61.2), Me₂Sn(HL-1) (38.8)	16.5 [707.9]	138.8	-	-	140.49	128.8	115.81	-	75.66	-	-	-
7.4	Me₂Sn(HL-1) (85.4), [Me₂Sn(HL-1)(OH)]⁻ (9.4), Me₂Sn(HL-1H₋₁) (4.5), Me₂Sn(OH)₂ (0.79)	11.0 [637.5]	132.67	154.39	150.75	148.13	121.08	-	86.26	80.74	72.24	63.16	60.75
9.4	[Me₂Sn(HL-1)(OH)]⁻ (84.6), Me₂Sn(HL-1) (10.7), Me₂Sn(OH)₂ (4.8)	12.3 [540.7]	124.18	-	-	142.29	132.9	117.86	-	80.45	-	-	56.72

Contd.

For Me₂Sn(IV) + (HL-1)²⁻ Mixture 1:2 System

pH	Species (%)												
7.2	$Me_2Sn(OH)_2$ (49.2), $Me_2Sn(HL-1)$ (44.6), $Me_2Sn(HL-1H_{-1})$ (3.0), $[Me_2Sn(HL-1)(OH)]^-$ (2.4), $[Me_2Sn(OH)]^+$ (0.82)	16.2 [591.1], 16.0 [646.5], 4.1 [200.4]	128.60 133.47 94.33	160.63	153.15	149.95	135.51	117.77	85.65	-	70.48	66.49	54.65
9.4	$Me_2Sn(OH)_2$ (48.8), $[Me_2Sn(HL-1)(OH)]^-$ (44.5), $Me_2Sn(HL-1)$ (5.6), $[Me_2Sn(OH)_3]^-$ (1.4)	9.6 [213.8], −7.8 [375.6]	95.50 109.7	154.04	149.12	143.87	133.75	120.17	-	-	69.67	64.32	-
10.3	$[Me_2Sn(HL-1)(OH)]^-$ (48.6), $Me_2Sn(OH)_2$ (42.2), $[Me_2Sn(OH)_3]^-$ (8.5), $Me_2Sn(HL-1)$ (0.74)	−7.0 [528.2], −15.4	123.09	162.98	153.79	143.98	139.21	113.5	86.03	81.49	74.55	65.79	61.31

For Me₃Sn(IV) + (HL-1)²⁻ Mixture 1:1 system

	$Me_3Sn(H_2O)_2^+$	−1.57 [475]f											

pH	Species[b]	δ / [|^1J|][c]										
7.2	[Me₃Sn(HL-1)]⁻ (99.9), [Me₃Sn(HL-1)(OH)]²⁻ (0.88), (HL-1)²⁻ (0.05)	−15.15 [425.8]	114.1	159.0	154.0	143.65	129.69	-	87.00	85.00	74.00	71.00	65.00
10.8	[Me₃Sn(HL-1)(OH)]²⁻ (95.5), [Me₃Sn(HL-1)]⁻(4.4)	−2.99 [445.2]	115.8	160.82	-	151.72	135.83	117.36	85.94	84.48	73.92	70.83	63.56

For Me₃Sn(IV) + (HL-1)²⁻ Mixture 1:2 system

pH	Species	δ / [J]											
7.2	[Me₃Sn(HL-1)]⁻ (49.8), Me₃Sn(H₂O)₂⁺ (28.3), Me₃Sn(OH) (19.8), [Me₃Sn(HL-1)(OH)]²⁻ (0.35)	−12.86 [529.2]	123.2	160.75	155.32	-	130.46	118.83	-	-	-	-	58.67
10.4	Me₃Sn(OH) (47.7), [Me₃Sn(HL-1)(OH)]²⁻(44.8), [Me₃Sn(HL-1)]⁻ (5.2), Me₃Sn(OH)₂]⁻ (2.3)	−2.99 [444.6]	115.7	156.22	-	147.47	130.53	116.65	-	-	-	68.22	-

[a] Solvent: H₂O:D₂O (9:1); Atom numbers mentioned as in Fig. 3.1; α_{CH_3-Sn} ; [b] Percentage of species from speciation diagram; [c] Values in square bracket [ ] are |^1J($^{13}C-^{119}Sn$)|in Hz; [d] Line width = the half line-width of the methyl protons; [e] Calculated using Eq.: |^1J| = 11.4θ − 875, taken from Ref. [123]; [f] Data taken from Ref. [32]
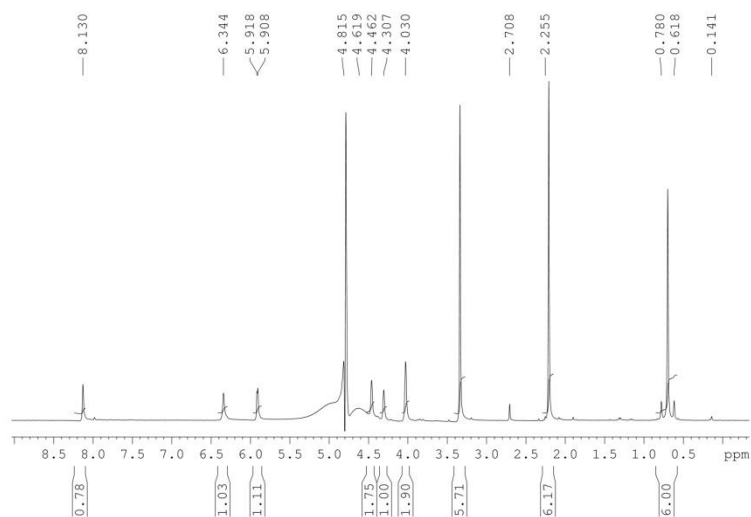
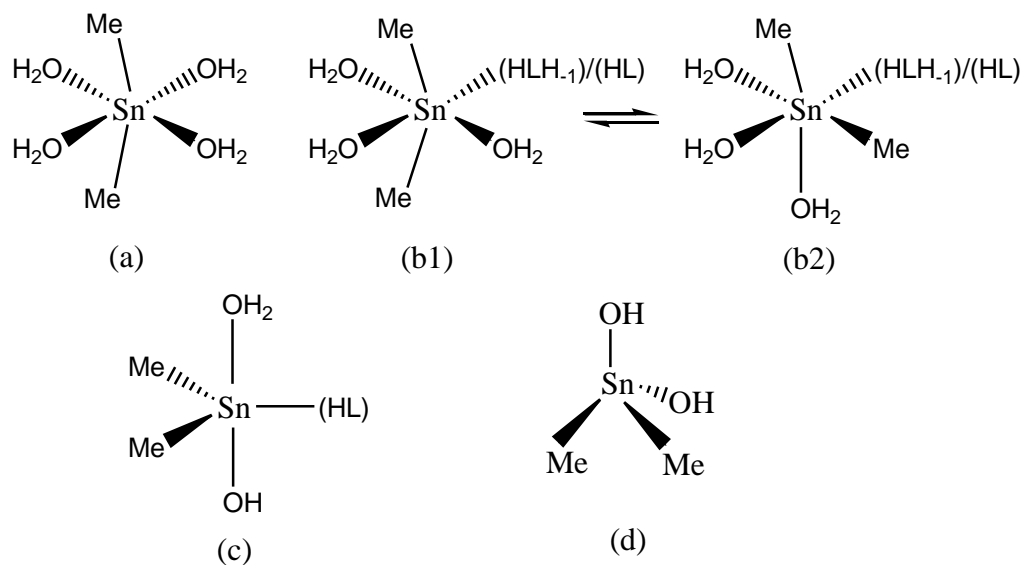**Fig. 3.10.** ^{1}H NMR spectrum of (Me$_2$Sn(IV) + HL-1) 1:1 system at pH 7.17.

Fig. 3.11. Possible geometrical structures of dimethyltin(IV)-(HL-1)$^{2-}$ complex species: (a) [Me$_2$Sn(H$_2$O)$_4$]$^{2+}$, (b1/b2) isomers of [Me$_2$Sn(HL-1H$_{-1}$)]/Me$_2$Sn(HL-1), (c) [Me$_2$Sn(HL-1)(OH)]$^-$, and (d) Me$_2$Sn(OH)$_2$ (For the sake of simplicity, the charges on the species are omitted).

($^1J(^{13}C-^{119}Sn)$ = 200.4 Hz), at pH 7.2 are observed which may be attributed to Me$_2$Sn(HL-1), [Me$_2$Sn(HL-1H$_{-1}$)] and Me$_2$Sn(OH)$_2$, respectively. As the pH reaches 9.4, two ^{13}C resonances at δ 9.6 ppm ($^1J(^{13}C-^{119}Sn)$ = 213.8 Hz), and δ –7.75 ppm ($^1J(^{13}C-^{119}Sn)$ = 375.6 Hz) are observed corresponding to Me$_2$Sn(OH)$_2$ and [Me$_2$Sn(HL-1)(OH)]$^-$, respectively. Same results have been observed at pH 10.3 (Table 3.3). At pH 7.2/9.4, three ^{119}Sn resonances at δ 27.00/163.20, –187.28/–164.26, –294.43/–246.84 ppm are attributed to tetrahedral Me$_2$Sn(OH)$_2$, trigonal bipyramidal [Me$_2$Sn(HL-1)(OH)]$^-$ and octahedral Me$_2$Sn(HL-1), respectively, whereas at pH 10.3, [Me$_2$Sn(HL-1)(OH)]$^-$ (δ –131.51 ppm) and Me$_2$Sn(OH)$_2$ (δ 101.22 ppm) are formed in considerable amount.

3.3.2.2. NMR of Trimethyltin(IV)-(HL-1)$^{2-}$ system

The chemical shifts of the methyl protons decreased with the increase in pH (range δ 0.49−0.40 ppm) and $^2J(^1H-^{119}Sn)$ coupling constants (66−64 Hz) and $\angle$C–Sn–C 115–117° are observed in both 1:1 and 1:2 systems (Table 3.2). In aqueous solution, [(CH$_3$)$_3$Sn]$^+$ is reported [32] to have a trigonal bipyramidal geometry with three methyl groups in equatorial positions and two water molecules in axial positions, and complex formation may occur by substitution of one water molecule with ligand/OH$^-$. However, various penta-coordinated trimethyltin(IV) species are expected to undergo fast mutual exchange on the NMR time scale, therefore, only one set of methyl proton/methyl carbon resonances with $^2J/^1J$ values are observed [32] corresponding to five coordinated [Me$_3$Sn(HL-1)]$^-$ and [Me$_3$Sn(HL-1)(OH)]$^{2-}$ species in both 1:1/1:2 systems (Tables 3.2 and 3.3). Further, in both 1:1 and 1:2 systems, penta-coordinated [Me$_3$Sn(HL-1)]$^-$ and [Me$_3$Sn(HL-1)(OH)]$^{2-}$ species are also observed at pH 7.3 ± 0.1/10.61 ± 0.2 as revealed by the ^{119}Sn NMR spectra (Table 3.5) (as shown in (f1/f2/f3) in Fig. 3.13). Tetrahedral Me$_3$Sn(OH) has also been observed at δ 76.23 ppm at pH 10.41 in 1:2 system (as shown in Fig. 3.13), but same resonance at δ 76.07 ppm at pH 10.81 in 1:1 system is also observed whereas no tetrahedral/Me$_3$Sn(OH) species is present in species distribution curve of 1:1 system (Fig. 3.4) . Probably Me$_3$Sn(OH) may form on keeping the mixture at pH 10.81 for a little longer because the ^{119}Sn NMR was recorded after 5−10 minutes of mixing the contents.
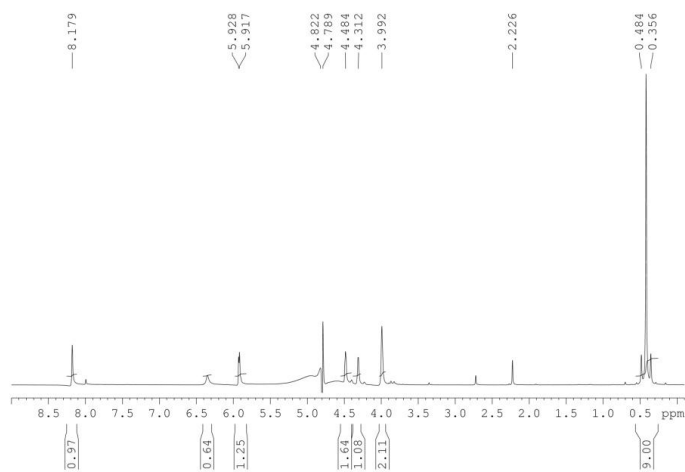
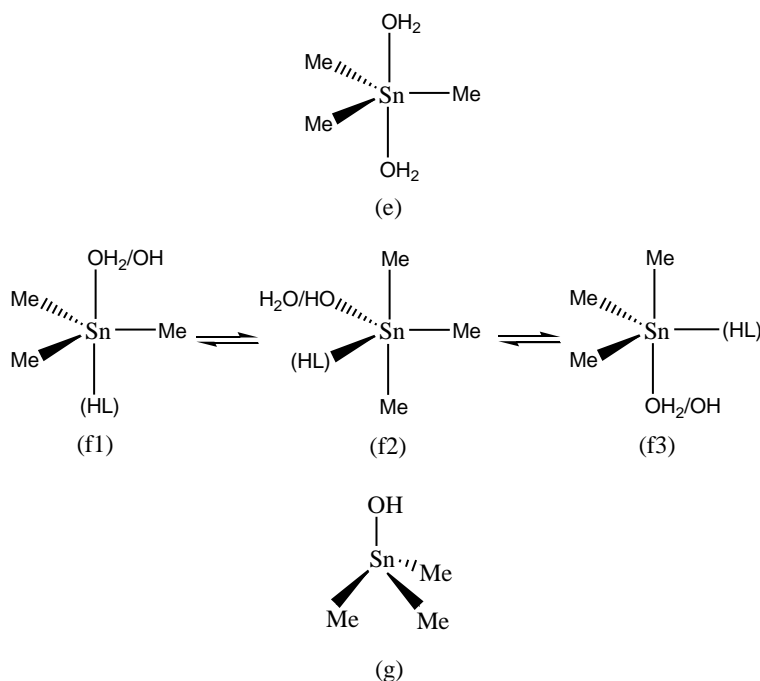**Fig. 3.12.** ^{1}H NMR spectrum of (Me$_3$Sn(IV) + HL-1) 1:1 system at pH 6.92; solvent: H$_2$O : D$_2$O (9:1) mixture.

Fig. 3.13. Possible geometrical structures of trimethyltin(IV)-(HL-1)$^{2-}$ complex species: (e) [Me$_3$Sn(H$_2$O)$_2$]$^+$, (f1/f2/f3) isomers of [Me$_3$Sn(HL-1)]$^-$/[Me$_3$Sn(HL-1)(OH)]$^{2-}$, and (g) Me$_3$Sn(OH) (For the sake of simplicity, the charges on the species are omitted).

68

3.3.2.3. NMR of Dimethyltin(IV)-(HL-2) system

The ^{1}H NMR of Me$_2$Sn(IV)-HL-2 system at 313.0 ± 0.1 K (because guanosine has a limited solubility at room temperature) could not be recorded satisfactorily because, during recycling delay, suppression of the water resonance could not be achieved simultaneously with rise in temperature. Further, ^{13}C NMR spectra are also not good and some resonances of guanosine are not observed in such a dilute solution. In ^{13}C NMR, the $|^1J|$ coupling constants could not be determined due to the unresolved satellites. At pH 4.0, ^{119}Sn resonance observed (Table 3.6) at δ −162.89 ppm may be assigned to the major species [Me$_2$Sn(HL-2H$_{-1}$)]$^{2+}$ (89%) having a distorted trigonal bipyramidal geometry (as shown in (b) in Fig. 3.15). With raise in pH up to 7.4, a resonance at δ −276.17 ppm becomes prominent, which may be assigned to a distorted octahedral [Me$_2$Sn(HL-2)]$^{2+}$ (94.6%) species (as shown in (c1/c2) in Fig. 3.15), and a very small amount of Me$_2$Sn(OH)$_2$(H$_2$O)$_2$ gives a resonance at δ −280.31 ppm. As the pH further increased to 11.0, two resonances at δ −104.47 and −186.73 ppm may be attributed to [Me$_2$Sn(HL-2)(OH)]$^+$ (2.5%) (as shown in (d) in Fig. 3.15) and Me$_2$Sn(OH)$_2$(H$_2$O)$_2$ (48.56%) (as shown in (e) in Fig. 3.15), respectively. For 1:2 system, similar results are obtained (Table 3.6).

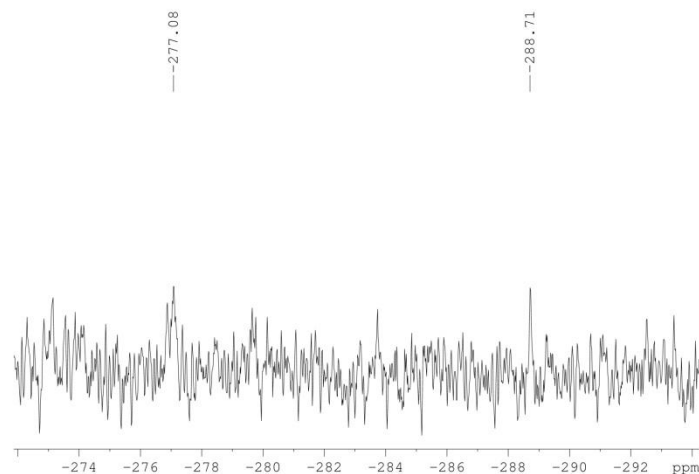**Fig. 3.14.** ^{119}Sn NMR spectrum of (Me$_2$Sn(IV) + HL-2) 1:2 system at pH 7.4.

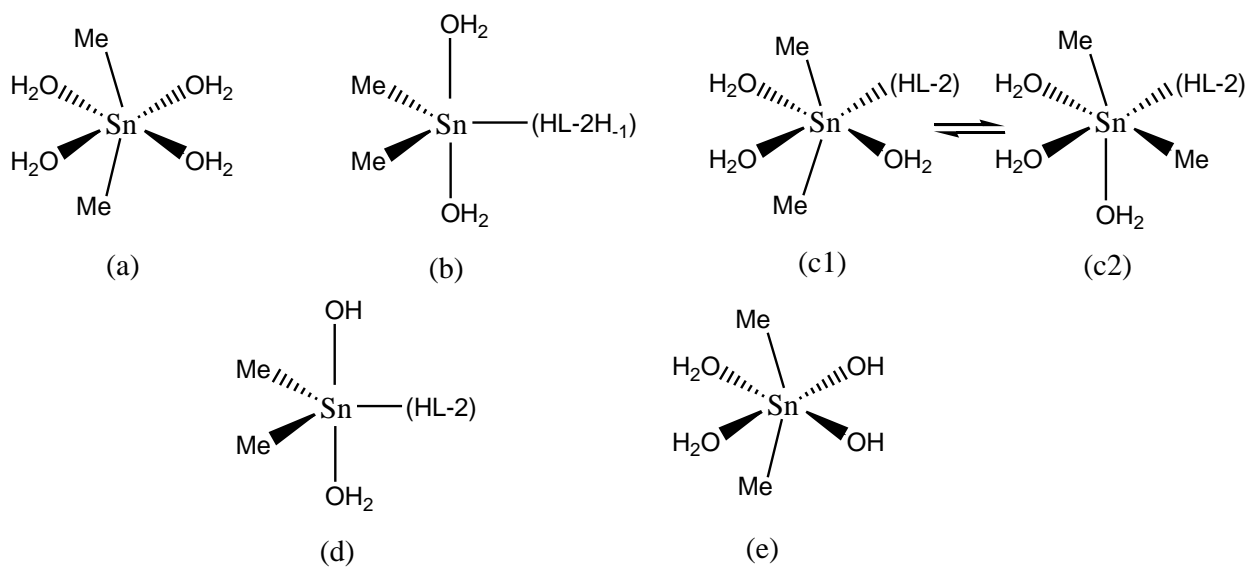**Fig. 3.15. Possible geometrical structures of dimethyltin(IV)-(HL-2) complex species: (a) [Me$_2$Sn(H$_2$O)$_4$]$^{2+}$, (b) [Me$_2$Sn(HL-2H$_{-1}$)]$^{2+}$, (c1/c2) isomers of [Me$_2$Sn(HL-2)]$^{2+}$, (d) [Me$_2$Sn(HL-2)(OH)]$^+$, and (e) Me$_2$Sn(H$_2$O)$_2$(OH)$_2$ (For the sake of simplicity, the charges on the species are omitted).**

3.3.2.4. NMR of Trimethyltin(IV)-(HL-2) system

Trimethyltin(IV) is reported [112] to form a penta-coordinated hydrolysed species with trigonal bipyramidal geometry in aqueous medium. However, after complexation the geometry is no longer trigonal bipyramidal but changes to distorted tetrahedral/distorted trigonal bipyramidal (as shown in (g)/(h1)/(h2)/(h3) in Fig. 3.17). At pH 7.3, ^{119}Sn NMR chemical shift observed (Table 3.6) at −61.21 δ ppm is attributed to [Me$_3$Sn(HL-2)]$^+$ (99.89%). As the pH is increased to 9.4, two resonances at −163.52 and −84.03 ppm are attributed to distorted trigonal bipyramidal Me$_3$Sn(HL-2)(OH) (9.46%) (as shown in (h1)/(h2)/(h3) in Fig. 3.17) and [Me$_3$Sn(HL-2)]$^+$ (99.28 %), respectively. Whereas in 1:2 system, the observed ^{119}Sn NMR chemical shifts suggest the presence of a distorted tetrahedral/a highly distorted trigonal bipyramidal [Me$_3$Sn(HL-2)]$^+$ at pH 7.03 and 10.47.
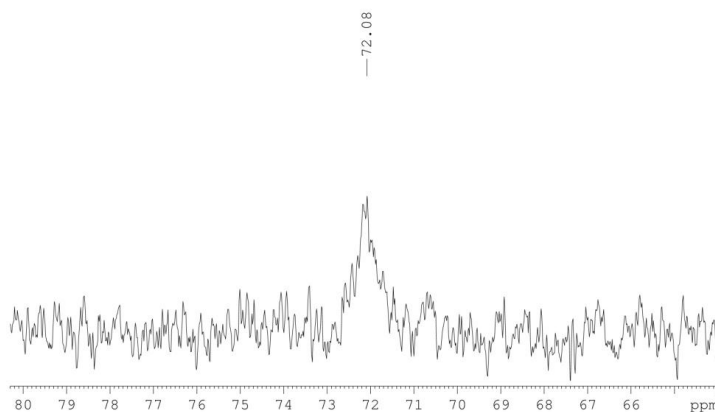
Fig. 3.16. ^{119}Sn NMR spectrum of (Me$_3$Sn(IV) + HL-2) 1:2 system at pH 7.0; H$_2$O : D$_2$O (9:1) mixture.
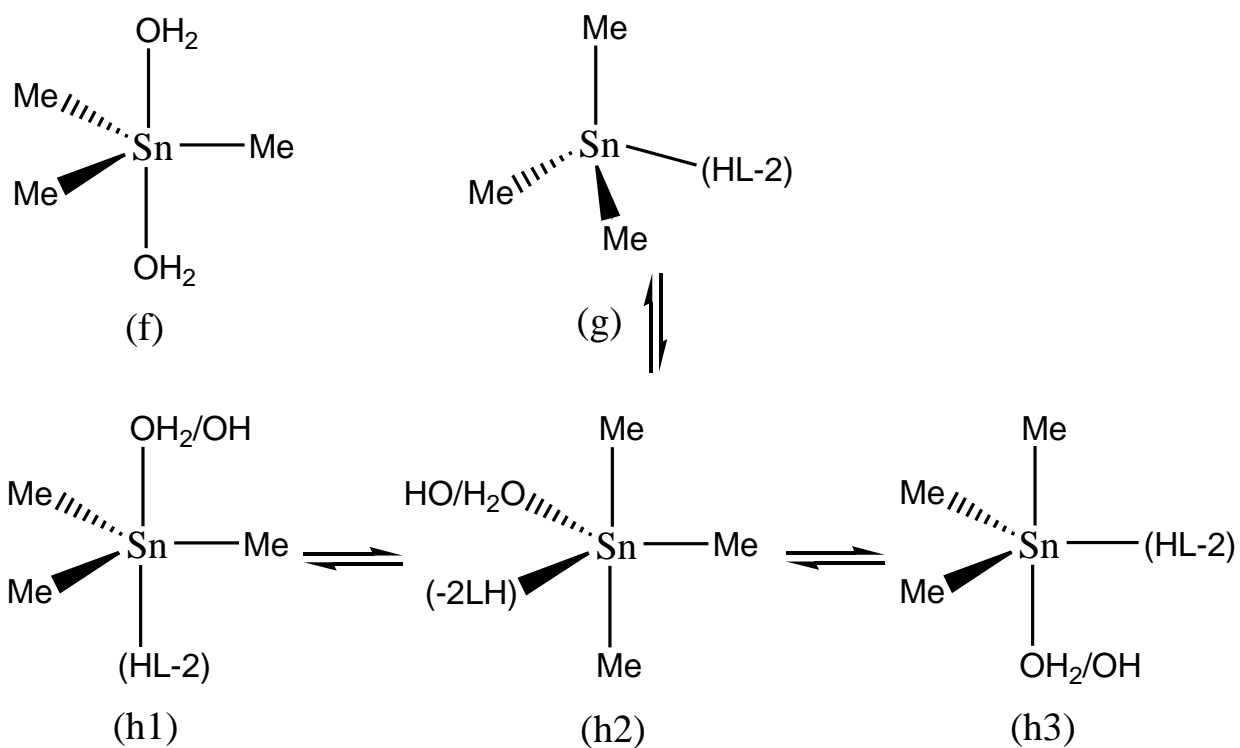
Fig. 3.17. Possible geometrical structures of trimethyltin(IV)-(HL-2) complex species: (f)
[Me₃Sn(H₂O)₂]⁺, (g) [Me₃Sn(HL-2)]⁺, and (h1/h2/h3) isomers of [Me₃Sn(HL-
2)]⁺/Me₃Sn(HL-2)(OH) (For the sake of simplicity, the charges on the species are
omitted).

Table 3.4. ^{13}C NMR Spectral Data[a] of Di- and Trimethyltin(IV)-(HL-2) Mixtures at Different pHs

pH	Species (%)[b]	C_α	C6	C2	C4	C8	C5	C1'	C4'	C2'	C3'	C5'
	Guanosine (HGUO) or (HL-2)	-	156.7	153.5	151.1	135.5	116.4	86.2	85.1	73.5	70.2	61.2
For Me₂Sn(IV) + (HL-2) Mixture 1:1 system												
4.0	[Me₂Sn(HL-2H₋₁)]²⁺ (96.5), [Me₂Sn(HL-2)]²⁺ (0.6)	6.00	159.18	152.67	148.42	133.12	114.25	88.28	-	71.45	70.91	61.98
7.4	Me₂Sn(HL-2)]²⁺ (88.6), Me₂Sn(OH)₂ (1.56) [Me₂Sn(HL-2)(OH)]⁺ (0.027)	4.15	-	-	-	137.28	109.19	-	80.33	-	-	56.28
11.2	[Me₂Sn(OH)₃]⁻ (34.2), Me₂Sn(OH)₂ (31), [Me₂Sn(HL-2)(OH)]⁺ (0.39)	19.98, 9.89	167.52	160.92	151.07	136.67	118.05	-	-	72.35	68.21	62.52
For Me₂Sn(IV) + (HL-2) Mixture 1:2 System												
4.0	[Me₂Sn(HL-2H₋₁)]²⁺ (96.45), (HL-2) (49.9), Me₂Sn(HL-2)]²⁺ (3.77)	6.82	159.16	154.68	151.68	138.30	122.62	88.29	86.38	74.06	70.96	61.96

Contd.

pH	Species (%)											
7.4	Me$_2$Sn(HL-2)]$^{2+}$ (91.8), (HL-2) (47.7), [Me$_2$Sn(HL-2)(OH)]$^+$ (4.3), [Me$_2$Sn(HL-2H$_{-1}$)]$^{2+}$ (3.5)	–0.71	-	-	146.78	138.34	-	-	85.69	-	70.48	62.02
9.2	Me$_2$Sn(HL-2)]$^{2+}$ (57.5), [Me$_2$Sn(HL-2)(OH)]$^+$ (42.0), (HL-2) (28.5), Me$_2$Sn(OH)$_2$ (0.46)	-	-	-	-	132.05	116.45	-	-	75.76	67.35	-
11.2	[Me$_2$Sn(HL-2)(OH)]$^+$ (50.0), [Me$_2$Sn(OH)$_3$]$^-$ (29.0), Me$_2$Sn(OH)$_2$ (20.6), Me$_2$Sn(HL-2)]$^{2+}$ (0.77), (HL-2) (0.77)	10.16, 0.46	156.18	-	145.48	136.61	120.7	-	83.32	-	-	61.75
For Me$_3$Sn(IV) + (HL-2) Mixture 1:1 system												
7.3	[Me$_3$Sn(HL-2)]$^+$ (100.0)	–2.96	-	-	144.84	-	118.82	89.6	-	-	71.81	64.67
9.5	[Me$_3$Sn(HL-2)]$^+$ (98.8), Me$_3$Sn(HL-2)(OH) (0.62)	–2.96	-	153.72	151.76	136.39	-	86.98	81.25	74.29	69.6	-
For Me$_3$Sn(IV) + (HL-2) Mixture 1:2 system												

pH	Species										
7.0	[Me$_3$Sn(HL-2)]$^+$ (100.3), (HL-2) (49.7)	−2.81	158.8	-	151.87	132.75	123.45	-	-	-	67.16	60.31
10.8	[Me$_3$Sn(HL-2)]$^+$ (86.8), Me$_3$Sn(HL-2)(OH) (13.5), (HL-2) (1.56)	−2.98	156.22	-	147.47	130.53	116.65	-	-	-	68.22	-

^{a} Solvent: H$_2$O:D$_2$O (9:1); Atom numbers mentioned as in Fig. 3.1; α_{CH_3-Sn} ; ^{b} Percentage of species from speciation diagram

Table 3.5. ^{119}Sn NMR Spectral Data[a] of Di- and Trimethyltin(IV)-(HL-1)[2−] Mixtures at Different pHs

pH	[119]Sn δ/ppm
For Me$_2$Sn(IV) + (HL-1)[2−] Mixture 1:1 system	
4.69	−215.31, −272.42
7.45	−179.93, −280.68
9.41	94.52, −117.73, −233.47
For Me$_2$Sn(IV) + (HL-1)[2−] Mixture 1:2 system	
7.21	27.00, −187.28, −294.43
9.40	163.20, −164.26, −246.84,
10.30	101.22, −131.51
For Me$_3$Sn(IV) + (HL-1)[2−] Mixture 1:1 system	
7.36	−199.19, −227.96
10.81	76.07, −178.84, −237.58
For Me$_3$Sn(IV) + (HL-1)[2−] Mixture 1:2 system	
7.20	32.67, −170.32
10.41	76.23, −126.06, −256.04

[a] Solvent: H$_2$O:D$_2$O (9:1)

Table 3.6. ^{119}Sn NMR Spectral Data[a] of Di- and Trimethyltin(IV)-(HL-2) Mixtures at Different pHs

pH	^{119}Sn δ/ppm
For Me$_2$Sn(IV) + (HL-2) Mixture 1:1 system	
4.06	−162.89
7.40	−276.17, −280.31
11.04	−104.47, −186.73
For Me$_2$Sn(IV) + (HL-2) Mixture 1:2 system	
4.07	−153.46
7.45	−277.08, −288.71
11.22	−103.14, −215.15
For Me$_3$Sn(IV) + (HL-2) Mixture 1:1 system	
7.33	−61.21
9.46	−84.05, −163.52
For Me$_3$Sn(IV) + (HL-2) Mixture 1:2 system	
7.03	72.08
10.47	76.43

[a] Solvent: H_2O:D_2O (9:1)